

# **Dynamics of Cell Metabolism and Enzymopathies in *Chromobacterium violaceum*: A Systems Approach**

Thesis Submitted to AcSIR For the Award of  
the Degree of  
DOCTOR OF PHILOSOPHY  
In Biological Sciences



By  
DEEPANWITA BANERJEE  
10EB11A26061

UNDER THE GUIDANCE OF  
DR. ANU RAGHUNATHAN

CSIR – NATIONAL CHEMICAL LABORATORY  
DR. HOMI BHABHA ROAD  
PUNE – 411008, INDIA

## *Dear Thesis*

*When I used to teach my students*

*I felt a deficiency that needed to be treated,*

*I wanted to learn, I wanted to be sufficient,*

*Give me any problem I just want to be efficient.*

*I jumped off the cliff thought I would grow wings*

*I did not fall as I had guardian angels*

*Yes, you were not a single point optimization*

*I needed more than one, I needed motivation.*

*I saw the tunnel, I had to fly low*

*They helped me stay afloat, just went with the flow*

*Yes, I did defy gravity and held my head high*

*Travelling through the tunnel, understanding the how's and whys*

*Then came a point I forgot where I was*

*I knew my purpose but had forgotten the cause*

*You were going away; I was losing fuel and time*

*But no, I didn't give up and pushed forward one last time*

*There you were, I could see you at the end*

*I just had to keep hope and follow across the bend*

*Patience and perseverance fueled my last lap*

*I glided through smoothly and finally it's a wrap.*

*Deepanwita Banerjee*

*November 27, 2017, 2 am*

“In the Ganges during pilgrimage season, there are levels of antibiotics in the river that we try to achieve in the bloodstream of patients,”

Sally Davies, England’s chief medical officer, The Guardian 2017.



# सीएसआयआर-राष्ट्रीय रासायनिक प्रयोगशाला

(वैज्ञानिक तथा औद्योगिक अनुसंधान परिषद)

डॉ. होमी भाभा मार्ग, पुणे - 411 008. भारत



## CSIR-NATIONAL CHEMICAL LABORATORY

(Council of Scientific & Industrial Research)

Dr. Homi Bhabha Road, Pune - 411008. India

### Certificate

This is to certify that the work incorporated in this Ph.D. thesis entitled **Dynamics of Cell Metabolism and Enzymopathies in Chromobacterium violaceum: A Systems Approach** submitted by Ms. **Deepanwita Banerjee** to Academy of Scientific and Innovative Research (AcSIR) in fulfillment of the requirements for the award of the Degree of **Doctor of Philosophy**, embodies original research work under my supervision. I further certify that this work has not been submitted to any other University or Institution in part or full for the award of any degree or diploma. Research material obtained from other sources has been duly acknowledged in the thesis. Any text, illustration, table etc., used in the thesis from other sources, have been duly cited and acknowledged.

*Deepanwita Banerjee*

Deepanwita Banerjee  
(Student)

*Anu Raghunathan*

Dr. Anu Raghunathan  
(Supervisor)

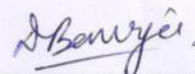
Place: PUNE  
Date: 7/5/18



# Declaration of Authorship

I hereby declare that this Ph. D. thesis entitled “**Dynamics of Cell Metabolism and Enzymopathies in *Chromobacterium violaceum*: A Systems Approach**” was carried out by me for the degree of **Doctor of Philosophy** in Biological Sciences under the guidance and supervision of Dr. Anu Raghunathan, Senior Scientist, CSIR-National Chemical Laboratory, Pune, India. I confirm that this work was done wholly by me while in candidature for a research degree at this institution. I also affirm that no part of this thesis has previously been submitted for a degree or any other qualification at this institution or any other institution. Also, the interpretations put forth are based on my knowledge and understanding of the original research articles and all resources and researchers have been duly cited and acknowledged as and when appropriate.

Place: PUNE  
Date: 7/5/18



Deepanwita Banerjee  
Metabolic Inquiry and Cellular Engineering (MICE) Lab  
Chemical Engineering Division  
CSIR-National Chemical Laboratory

# Acknowledgement

When I look back at the path I travelled to make this thesis a success, I see numerous people to thank and acknowledge. Although like in any reputed journal I will try to be concise and humble at the same time. From the “lab manager” to the “student involved in all projects” took me six years but I definitely leveled up my game and accomplished a lot.

I am privileged to express my deep sense of gratitude and profound regards to my supervisor **Dr. Anu Raghunathan**. Her apt guidance and supervision was available during the hours when I needed it the most irrespective of what hour of the day that was. I would also like to thank her for helping me and inspiring me towards inculcating a scientific temperament and keeping me motivated all through. Her empathetic attention and sometimes personal care made me balance at times when my patience and faith started dwindling. Her continuous inputs and interactions made me well versed in the field of Systems Biology and Cellular Engineering. Thanks to her I was actively involved in all the lab projects from Biolog to Biomodeling and many others in between. She had faith in me, whether it was to represent lab work at IIT Bombay when I was new to the lab philosophy or when it was a last minute talk at IISER Pune meeting on antibiotic resistance. I hope she continues to have the same faith in future for any kind of research collaborations or contributions.

My Doctoral Advisory Committee (DAC) guided me through all these years. Thank you to **Dr. Mugdha Gadgil**, **Dr. Dhiman Sarkar** for their periodical assessment, valuable guidance, recommendations and critical feedback to shape my doctoral work better. I am also thankful to **Dr. Rajnish Kumar** and **Dr. A.P. Giri** for their continuous encouragement as the chairperson of the DAC committee. I would also like to thank **Dr. Venkateswaralu Panchagnula** for valuable collaborations for generating metabolomics data using Mass spectrometry without which the systems biology approach on my thesis title would remain incomplete.

I am also thankful to **Prof. David A. Fell** and **Prof. Mark Poolman** from Oxford Brookes University along with **Prof. Stefan Schuster** for their timely visits to our laboratory that inculcated healthy interactions, inspiration and exposure to the know how's in the global systems biology community. I would like to thank **Dr. Ashish Orpe**, **Dr. Guruswamy Kumaraswamy**, **Dr. Chetan Gadgil** and **Dr. Rajnish Kumar** who made me well versed in courses crucial for my thesis work. I would also like to thank **Dr. C G Suresh**, **Dr. Asmita Prabhune** among

others in the biological sciences division who kept me up to date with the courses in the biology front required for my thesis work. I am also thankful to the **Directors** during my tenure in this prestigious institute along with **Dr. Vivek Ranade**, former HOD, Chemical Engineering Department. I would also like to thank **DST** for providing me with INSPIRE Ph.D. fellowship that was definitely inspiring in the literal meaning. I would also like to acknowledge **SERB (DBT)** for sanctioning the travel grant for attending an international conference in United States to present the work conducted as a part of this thesis. A special thanks to **Mrs. Sujaya Ingale** who helped with flow cytometry using BD LSR Fortessa SORP cell analyzer available at the Cell Studio, Venture center.

This thesis would not have materialized in this laboratory if it wasn't for my lab mates and interns who kept improving my perspective towards this work. I would like to thank **Selva Rupa Christinal I.**, my colleague without whom this journey would have next to been impossible to tread. I would also like to thank **Sudeepa Nandi**, **Abhishek Gupta** for helping me when I was in the initial phase of this work. My special thanks to **Priyanka Buddhiwant**, **Deepika Dhaware**, **Nivedita Bhattacharya**, **Dharmesh Parmar** and **Avinash Ghanate**. Although from another lab, they were always a phone call away for any kind of assistance. I am also thankful to **Vishwanathgouda Maralingannavar** for his late night presence that saved me from being spooked in the lab premise during wee hours. I also acknowledge the efforts of **Riya Uthup**, **Mridula Prasad**, **Dipali Kale**, **Bhalchandra Vaidya**, **Newton Bissoyi**, **Shreya Bandopadhyay**, **Priyanka Deshmukh** and **Mayooreshwar Rajankar** for their timely help and support.

Finally I would like to express my love and gratitude to my father in law and parents. Baba, **Mr. Asis Kumar Banerjee**, has always been supportive of my thesis work. Ma, **Mrs. Bharati Das** and Dad, **Mr. Jawahar Lal Das** always made this seem a work of utmost honor. Their sincere blessings and wishes have enabled me to complete my work successfully. Most of all I thank my husband **Amitrajit Banerjee** who energized me whenever I felt exhausted or demotivated. His encouragement and endless support has helped me through every step of my life including this Ph.D.

# Abstract

The leading edge of the global problem of antibiotic resistance necessitates novel therapeutic strategies. Herein is described a systems biology approach to study antibiotic resistance in *Chromobacterium violaceum*. Differential features of genotype and metabolic phenotype in response to antibiotics and antibiotic selection pressures were identified. This novel model integrated/ driven approach identified metabolic supplementation strategies for killing antibiotic resistant pathogens using benign metabolites. Controlled laboratory evolutions established chloramphenicol and streptomycin resistant pathogens of *Chromobacterium*. These resistant pathogens showed high growth rates and required high lethal doses of antibiotic. Growth and viability testing identified malate, succinate, pyruvate and oxoadipate as re-sensitising agents for antibiotic therapy. Resistant genes were catalogued through whole genome sequencing. Intracellular metabolomic profiling identified violacein as a potential biomarker for resistance. The temporal variance of metabolites captured the linearized dynamics around the steady state and correlated to growth rate. Genome-scale models provide a comprehensive yet concise representation of biochemical reaction networks and their functional states. ATP maintenance, substrate uptake and growth yields were used as constraints and allowed definition of susceptible and resistant populations *in silico*. Such a constraints-based flux balance model was used to identify changes in metabolic flux distributions and synthetic lethality of susceptible and resistant *in silico* strains. The resistant pathogen rewired its metabolic networks to compensate for disruption of redox homeostasis. We foresee the utility of such scalable workflows in identifying metabolites for clinical isolates as inevitable solutions to mitigate antibiotic resistance.

# Table of Contents

<b>Certificate</b>	<b>i</b>
<b>Declaration</b>	<b>ii</b>
<b>Acknowledgement</b>	<b>iii</b>
<b>Abstract</b>	<b>v</b>
<b>Table of Contents</b>	<b>vi</b>
<b>Abbreviations</b>	<b>xii</b>
<b>List of Figures</b>	<b>xiv</b>
<b>List of Tables</b>	<b>xviii</b>

## **Chapter 1 Introduction**

1.1. Motivation .....	2
1.2. Overall objective and specific aims .....	4
1.3. Systems biology paradigm .....	5
1.4. <i>Chromobacterium violaceum</i> .....	6
1.5. Antibiotics chloramphenicol and streptomycin .....	9
1.6. Antibiotic resistance .....	10
1.7. Dynamics of cell metabolism .....	11
1.8. Resistance phenotypes not always predictable from genotypes alone .....	12
1.9. Constraints based modeling and Flux balance analysis .....	14
1.10. Overall methodology .....	18
1.11. Summary of work .....	19

## **Chapter 2 Towards a Genetic Basis for Antibiotic Resistance in *Chromobacterium violaceum***

2.1. Introduction .....	21
2.2. Materials and methods.....	24
2.2.1. Adaptive laboratory evolution .....	24

2.2.2. Confirm and characterize genetic changes using whole genome sequencing on Ion torrent platform .....	24
2.2.3. Capillary sequencing for confirmation of variants .....	25
2.2.4. <i>In silico</i> structure - function analysis of the mutations acquired .....	25
2.3. Results and discussion .....	25
2.3.1. Evolved population ChlR and StrpR .....	26
2.3.2. Genome sequencing of ChlR and StrpR .....	26
2.3.3. Altered genotypes and <i>in silico</i> protein function .....	27
2.4. Conclusion .....	33

### **Chapter 3 Metabolic Dynamics and Phenotypic Profiling of Antibiotic Resistant Population**

3.1. Introduction .....	35
3.2. Materials and methods .....	37
3.2.1. Minimum inhibitory concentration estimation .....	37
3.2.2. Effect of varying concentration of antibiotics on growth profiles and growth rate estimation .....	37
3.2.3. Preparation of intracellular metabolite extracts .....	37
3.2.4. Spectrophotometric analysis .....	38
3.2.5. LC-MS analysis of intracellular metabolites .....	38
3.2.6. LC-MS data analysis .....	39
3.2.7. AP-MALDI of intracellular metabolites .....	39
3.2.8. AP-MALDI data analysis .....	40
3.2.9. Growth profiling on different exogenous carbon and nitrogen sources .....	40
3.2.10. Effect of acyl homoserine lactones on growth profiles and violacein .....	40
3.2.11. Effect of antibiotic resistance on heterologous violacein phenotype .....	41
3.2.12. NADH and NAD measurements .....	44

3.2.13. Membrane potential measurement .....	44
3.3. Results and discussion .....	45
3.3.1. Evolution of antibiotic resistance and fitness .....	45
3.3.2. Effect of exogenous metabolites and antibiotics on growth .....	46
3.3.3. The metabolic phenotype of resistant populations .....	48
3.3.3.1. Differential violacein levels in resistant populations .....	48
3.3.3.2. Differential metabolic dynamics: LC-MS analysis .....	49
3.3.3.3. Differential metabolic dynamics: API-MALDI analysis .....	55
3.3.3.4. Effect of acyl homoserine lactones on violacein and growth.....	56
3.3.3.5. Effect of antibiotic resistance on heterologous violacein phenotype .....	58
3.3.3.6. Effect of different metabolites on redox capacity of <i>C. violaceum</i> .....	58
3.3.3.7. Effect of different metabolites on membrane potential .....	62
3.4. Conclusion .....	63

**Chapter 4 Understanding Emergence of Antibiotic Resistance by Modeling Central Metabolism**

4.1. Introduction .....	65
4.2. Materials and methods .....	69
4.2.1. Constraints based modeling of <i>C. violaceum</i> central metabolism: network reconstruction .....	69
4.2.2. Flux balance analysis and associated sensitivity parameters .....	70
4.2.3. Flux variability analysis .....	71
4.2.4. Dynamic flux balance analysis .....	72
4.2.5. Pareto front analysis using NADPH and NADH oxidases .....	72
4.3. Results and discussion .....	73

4.3.1. Network reconstruction of central metabolism of <i>C. violaceum</i> .....	73
4.3.2. Flux balance analysis and associated sensitivity parameters .....	75
4.3.3. Differential metabolic dynamics prediction using flux variability analysis .....	77
4.3.4. <i>In silico</i> prediction of NAD/NADH balance and redox homeostasis .....	79
4.4. Conclusion .....	80

## **Chapter 5 Genome Scale Metabolic Modeling of *C. violaceum***

5.1. Introduction .....	81
5.2. Materials and methods .....	83
5.2.1. Genome annotation .....	83
5.2.2. Reconstruction of <i>C. violaceum</i> metabolic network .....	84
5.2.3. Initial draft reconstruction .....	84
5.2.4. Manual curation for accurate biomass prediction .....	84
5.2.5. Translation to BiGG database format and consistency check .....	85
5.2.6. Biomass composition .....	85
5.2.7. Flux balance analysis .....	86
5.2.8. Validation of the metabolic model .....	86
5.2.9. Metabolic model of WT, ChlR and StrpR population .....	86
5.2.10. Flux variability analysis .....	86
5.2.11. NADH oxidase simulations to understand redox homeostasis.....	87
5.2.12. Lethal and synthetic lethal genes in <i>C. violaceum</i> .....	87
5.3. Results and discussion .....	88
5.3.1. Genome scale reconstruction and model statistics .....	88
5.3.2. <i>In silico</i> representation of metabolic genome features of <i>Chromobacterium violaceum</i> .....	90
5.3.2.1. Central carbon metabolism .....	93
5.3.2.2. Cyanide formation .....	94
5.3.2.3. Violacein biosynthesis .....	95



5.3.2.4. Macromolecular biosynthesis .....	97
5.3.3. SEED draft model limitations .....	99
5.3.4. Metabolic capacity validation of iDB858 based on BIOLOG GN2 plate phenotype .....	101
5.3.5. Growth prediction accuracy using iDB858 based on in house carbon nitrogen source utilization phenotype .....	103
5.3.6. Representing antibiotic resistant populations of <i>C. violaceum</i> .....	104
5.3.7. Redox coupled metabolic flux redistribution a function of antibiotic perturbation .....	107
5.3.7.1. Effect of antibiotic on <i>C. violaceum</i> metabolic network .....	108
5.3.7.2. Compensatory metabolic reprogramming as a survival strategy in resistant population: Rebalance redox cofactors .....	111
5.3.8. Redox homeostasis critical for survival against antibiotics: NADH oxidase .....	114
5.3.9. Gene essentiality and synthetic lethality .....	117
5.4. Conclusion .....	120

## **Chapter 6 Antibiotic Resistance – A Public Health Perspective**

6.1. Introduction .....	123
6.2. Materials and methods .....	128
6.2.1. Study design and population .....	128
6.2.2. Study questionnaire .....	129
6.2.3. Statistical analysis .....	130
6.3. Results and discussion .....	131
6.3.1. Demographics .....	131
6.3.2. Knowledge .....	132
6.3.3. Attitude .....	134
6.3.4. Practice .....	135

6.4. Conclusion .....	141
<b>Chapter 7 Conclusion and Future Scope</b>	
7.1. Recapitulation .....	144
7.2 Unknown frontiers of antibiotic resistance .....	145
7.3. Future scope and prospects .....	147
<b>References .....</b>	<b>149</b>
<b>List of Publications .....</b>	<b>173</b>
<b>Appendices .....</b>	<b>174</b>
<b>Curriculum Vitae .....</b>	<b>203</b>

# Abbreviations

2,5-DHB	2,5-Dihydroxybenzoic acid
2OXOADP	2-oxoadipate
ACALD	Acetaldehyde dehydrogenase
AGC	Automated gain control
AHL	Acyl homoserine lactone
AKGDH	2-Oxoglutarate dehydrogenase
ALCD2x	Alcohol dehydrogenase
ALE	Adaptive Laboratory Evolutions
AM-XIC	Accurate mass - extracted ion chromatogram
AP-MALDI	Atmospheric pressure - matrix-assisted laser desorption/ionization
ATCC	American Type Culture Collection
ATP	Adenosine triphosphate
ATP4Sr	ATP synthase
ATV	Atorvastatin
bp	Base pairs
cat	Category
CBM	Constraint based modeling
CFU/mL	Colony-forming units per milliliter
CHCA	2-Cyano-4-hydroxycinnamic acid
chl	Chloramphenicol
ChlR	Chloramphenicol resistant population of <i>Chromobacterium violaceum</i>
COBRA	Constraints Based Reconstruction and Analysis Toolbox
DNA	Deoxyribose nucleic acid
ER	Emergency room
ETC	Electron Transport Chain
EX_ etoh(e)	Ethanol exchange
FBA	Flux balance analysis
FDA	Food and Drug Administration
FORTi	Formate transport via diffusion
FVA	Flux Variability Analysis
FWHM	Full width at half maximum
g3p	Glyceraldehyde-3-phosphate
gDW	Grams Dry Weight
GPR	Gene protein relationships
HDAC	Histone deacetylase
HESI	Heated electrospray ion source
HPLC	High performance liquid chromatography
HRMS	High-resolution mass spectrometry
KAP	Knowledge attitude practice
LB	Luria Bertani
LBA	Luria Bertani Agar
LC-MS	Liquid chromatography–mass spectrometry
LP	Linear Programming
m/z	Mass by charge ratio

mal	L-malate or L-malic acid
MDH	Malate dehydrogenase
MEW	Mass extraction window
MIC	Minimum Inhibitory Concentration
MS/MS	Tandem mass spectrometry
MUT	Mutated
NAD <sup>+</sup>	Nicotinamide adenine dinucleotide (oxidised form)
NADH	Nicotinamide adenine dinucleotide (reduced form)
NADP <sup>+</sup>	Nicotinamide adenine dinucleotide phosphate (oxidised form)
NADPH	Nicotinamide adenine dinucleotide phosphate (reduced form)
NADTRHD	NAD transhydrogenase
NGS	Next generation Sequencing
Nt CDS	Non coding sequence
OD600	Optical density at 600 nanometer
ORF	Open reading frame
OTC	Over the counter
PABA	Para-amino benzoate or 4-Aminobenzoate
PCA	Principal component analysis
PCR	Polymerase chain reaction
PDF	Pulse dynamic focusing
PDH	Pyruvate dehydrogenase
PFL	Pyruvate formate lyase
PGM	Personal Genome Machine
PHA	Polyhydroxyalkanoates
Plt2r	Phosphate reversible transport via symport
PLP	Pyridoxal phosphate
PMF	Proton Motive Force
PPC	Phosphoenolpyruvate carboxylase
ppm	Parts per million
PTZ	Piperacillin/Tazobactam
Pyr	Pyruvate or Pyruvic acid
QC	Quality control
QS	Quorum sensing
SAM	S-adenosyl methionine
SAH	S-adenosyl homocysteine
strep	Streptomycin
StrpR	Streptomycin resistant population of <i>Chromobacterium violaceum</i>
Succ	Succinate or Succinic acid
SUCOAS	Succinyl-CoA synthetase (ADP-forming)
TCA	Tricarboxylic acid cycle
TCS	Two-component system
THD2	NAD(P) transhydrogenase
TV	Temporal variance
WT	Wild type <i>Chromobacterium violaceum</i>
ZIC-HILIC	Zwitterionic hydrophilic interaction liquid chromatography
γredox	Gamma redox

# List of Figures

<b>Figure 1.1:</b>	Antibiotic resistance a multifactorial societal issue .....	3
<b>Figure 1.2:</b>	Systems Biology paradigm .....	5
<b>Figure 1.3:</b>	<i>Chromobacterium violaceum</i> .....	6
<b>Figure 1.4:</b>	Antibiotics used in this study and their mechanism of action .....	9
<b>Figure 1.5:</b>	Mechanisms of antibiotic resistance .....	10
<b>Figure 1.6:</b>	Dynamics of Energy Metabolism .....	11
<b>Figure 1.7:</b>	Research time line related to this thesis work .....	12
<b>Figure 1.8:</b>	Overall methodology followed in this thesis work .....	18
<b>Figure 2.1:</b>	Graphical abstract of this chapter .....	22
<b>Figure 2.2:</b>	Overall methodology followed in the genomic profiling .....	25
<b>Figure 2.3:</b>	MIC estimation using E-strips or liquid broth dilution method .....	26
<b>Figure 2.4:</b>	Ab initio model of AcrR for wild type (WT) and mutated (MUT) protein .....	28
<b>Figure 2.5:</b>	Homology model of RpsL for wild type (WT) and mutated (MUT) protein .....	29
<b>Figure 2.6:</b>	3DLigandSite representation of the ligand binding residues (blue) including Ser238 .....	30
<b>Figure 2.7:</b>	Ab initio model of PabC for wild type (WT) and mutated (MUT) protein .....	30
<b>Figure 2.8:</b>	Schematic representation of the hypothesis, dark arrows represents higher flux towards violacein synthesis .....	31
<b>Figure 2.9:</b>	Ab initio model of KdpD for wild type (WT) and mutated (MUT) protein .....	32
<b>Figure 2.10</b>	The $\Delta$ C499-894 protein functioned as a K <sup>+</sup> .....	32
<b>Figure 3.1:</b>	Growth rate estimation for <i>C. violaceum</i> populations .....	45
<b>Figure 3.2:</b>	MIC for Piperacillin/Tazobactam (PTZ) .....	45

<b>Figure 3.3:</b>	Heat map showing effect of different metabolites on biomass, growth and viability for the three populations – WT, ChlR and StrpR .....	48
<b>Figure 3.4:</b>	Violacein quantitation for the three populations across time .....	48
<b>Figure 3.5:</b>	LC-MS time profiles of metabolites showing significant differences (a-f) as well as negligible changes (g-h) among the three populations .....	49
<b>Figure 3.6a:</b>	Box and whiskers plot explained using guanosine .....	50
<b>Figure 3.6b:</b>	Box and whiskers plot for metabolites showing significant differences (a-f) as well as negligible changes (g-h) among the three populations .....	50
<b>Figure 3.7:</b>	PCA plots of PC1 versus PC3 for both biological replicates for all three population shows differential features of ChlR compared to WT and StrpR for 12 hr fractions and onwards .....	51
<b>Figure 3.8:</b>	PCA score trends for PC1 (a and b) and PC3 (c and d) for both biological replicates for all three population .....	51
<b>Figure 3.9:</b>	PCA plots showing metabolites with higher loading values for PC1 show higher variance across time points .....	52
<b>Figure 3.10:</b>	LC-MS time profiles of metabolites showing phase lag (Leu, Lys, Pro) or negligible changes (Gln, Arg, Lact, Adenosine) .....	52
<b>Figure 3.11:</b>	Differential LC-MS time profiles of metabolites .....	53
<b>Figure 3.12:</b>	LC-MS time profiles of metabolites representing nucleotides .....	53
<b>Figure 3.13:</b>	Heat map for relative abundance and temporal variation for all three populations .....	54
<b>Figure 3.14:</b>	3D plots correlating growth, relative abundance and temporal variance of metabolites .....	54
<b>Figure 3.15:</b>	AP-MALDI time profiles of metabolites representing violacein pathway Intermediates (a - d and f) along with the Violacein biosynthetic pathway (g) adapted from Duran et. al., 2012.....	55
<b>Figure 3.16:</b>	AP-MALDI time profiles of other metabolites .....	55
<b>Figure 3.17:</b>	Total violacein produced by WT normalized to amount of violacein in the absence of AHL .....	56
<b>Figure 3.18:</b>	Total violacein produced by ChlR and StrpR normalized to WT and normalized to that in absence of AHL in presence or absence of antibiotic .....	56

<b>Figure 3.19:</b>	Heat Map of a) WT normalized, b) double normalized data for violacein (mmol/gDCW, violet), c) growth rate (grayscale, hr-1) and d) biomass formation (yellow to green, grams) .....	57
<b>Figure 3.20:</b>	Violacein estimation in different <i>E. coli</i> strains with the violacein operon.....	58
<b>Figure 3.21:</b>	Culture of different <i>E. coli</i> strains with the violacein operon .....	58
<b>Figure 3.22:</b>	NAD and NADH estimation for the different population of <i>C. violaceum</i> in the presence of glucose .....	59
<b>Figure 3.23:</b>	NAD and NADH estimation for the different population of <i>C. violaceum</i> in the presence of pyruvate .....	59
<b>Figure 3.24:</b>	NAD and NADH estimation for the different population of <i>C. violaceum</i> in the presence of succinate .....	60
<b>Figure 3.25:</b>	NAD and NADH estimation for the different population of <i>C. violaceum</i> in the presence of 2-Oxoadipate .....	60
<b>Figure 3.26:</b>	NADH and NAD experimental values attained for the three different strains using four different metabolites – Glucose, Pyruvate and Succinate .....	61
<b>Figure 3.27:</b>	Membrane potential (PMF) estimation for the different population of <i>C. violaceum</i> in the presence of glucose .....	62
<b>Figure 3.28:</b>	Membrane potential (PMF) estimation for the different population of <i>C. violaceum</i> in the presence of three substrates – pyruvate, succinate and Maleate .....	63
<b>Figure 3.29:</b>	Membrane potential (PMF) estimation for the different population of <i>C. violaceum</i> in the presence of 2-Oxoadipate .....	63
<b>Figure 4.1:</b>	The core model iDB149 visualization using Escher .....	74
<b>Figure 4.2:</b>	Model statistics and subsystem wise classification for iDB149 .....	74
<b>Figure 4.3:</b>	Dynamic FBA results for the three different populations of <i>C. violaceum</i> .....	78
<b>Figure 4.4:</b>	Robustness analysis for ChlR and StrpR of the NADH or NADPH oxidase versus ATP maintenance flux .....	79
<b>Figure 5.1:</b>	Reconstruction of genome scale metabolic model .....	82
<b>Figure 5.2:</b>	Job submitted to RAST Server .....	83

<b>Figure 5.3:</b>	Literature mining for manual curation .....	89
<b>Figure 5.4:</b>	The Model SEED server showing the initial draft reconstruction .....	89
<b>Figure 5.5:</b>	Stoichiometric matrix for iDB858 .....	91
<b>Figure 5.6:</b>	Model statistics and subsystem wise classification for iDB858 .....	92
<b>Figure 5.7:</b>	Robustness analysis to understand metabolite limitation on biomass and violacein formation in iDB858 in glucose .....	96
<b>Figure 5.8:</b>	Missing chorismate mutase (red circle) as in Model SEED server .....	100
<b>Figure 5.9:</b>	Gene, enzyme and reaction information of chorismate mutase as in KEGG database .....	101
<b>Figure 5.10:</b>	Subsystems wise classification of essential genes common to all the substrates	117
<b>Figure 5.11:</b>	Single Gene deletion (SGD) analysis .....	118
<b>Figure 5.12:</b>	Heat map showing double gene deletion analysis on glucose under aerobic condition.....	119
<b>Figure 5.13:</b>	Double Gene deletion (DGD) analysis .....	120
<b>Figure 6.1:</b>	Interventions needed against antibiotic resistance, a multifactorial problem, in India .....	124
<b>Figure 6.2:</b>	Causes of antibiotic resistance, a multifactorial problem, in India .....	125
<b>Figure 6.3:</b>	Trends in antibiotic consumption in India, 2000 – 2010 .....	127
<b>Figure 6.4:</b>	Methodology followed in this study .....	130
<b>Figure 6.5:</b>	Overall KAP score and response to the first question of the knowledge section of the KAP survey .....	132
<b>Figure 6.6:</b>	Responses to the attitude section of the KAP survey .....	135
<b>Figure 6.7:</b>	Responses to the practice section question 1 of the KAP survey .....	136
<b>Figure 6.8:</b>	Responses to the practice section questions 2 to 5 of the KAP survey .....	137
<b>Figure 6.9:</b>	Handout distributed to the respondents post KAP study .....	140
<b>Figure 7.1:</b>	Schematic representation of the conclusions attained in this thesis work .....	146



# List of Tables

<b>Table 2.1:</b>	Coverage details .....	27
<b>Table 2.2:</b>	Amino acid sequence information for AcrR protein .....	28
<b>Table 3.1:</b>	Strains used to study the effect of antibiotic resistance on heterologous violacein phenotype .....	41
<b>Table 3.2:</b>	MIC estimation for 11 different antibiotics for <i>C. violaceum</i> .....	45
<b>Table 3.3:</b>	Altered kinetic parameters represented as Growth Rates and Time lag of <i>C. violaceum</i> (WT, ChlR and StrpR) on multiple micro-environment metabolites.....	47
<b>Table 4.1:</b>	Nine Categories defined for FVA analysis .....	72
<b>Table 4.2:</b>	Constraints used in this study for simulation of growth for the three different populations of <i>C. violaceum</i> using iDB149 .....	76
<b>Table 4.3:</b>	Sensitivity parameters assessed using FBA - Scaled shadow prices, Logarithmic sensitivity and Maximum reduced costs .....	76
<b>Table 4.4:</b>	FVA results showing category change in resistant strains as a function of antibiotic that involve redox cofactor balancing .....	77
<b>Table 4.5:</b>	Gamma Redox .....	78
<b>Table 5.1:</b>	Confidence score assigned during manual curation of the reconstruction obtained from SEED server .....	85
<b>Table 5.2:</b>	Biomass composition of <i>C. violaceum</i> .....	90
<b>Table 5.3:</b>	Model characteristics .....	91

<b>Table 5.4:</b>	Physiological characteristics successfully predicted by iDB858 .....	93
<b>Table 5.5:</b>	Reaction information for the cyanide biosynthesis module .....	95
<b>Table 5.6:</b>	Reaction information for the violacein biosynthesis module .....	97
<b>Table 5.7:</b>	BIOLOG in silico prediction accuracy .....	101
<b>Table 5.8:</b>	<i>In silico</i> prediction for the 57 BIOLOG GN2 plate substrates .....	102
<b>Table 5.9:</b>	Overall in silico prediction accuracy of iDB858 for Ex-mets .....	104
<b>Table 5.10:</b>	In silico prediction accuracy of iDB858 for the 29 Ex-mets .....	104
<b>Table 5.11:</b>	Experimental conditions used to define the three different population of <i>C. violaceum</i> .....	106
<b>Table 5.12:</b>	Experimental condition used to define wild type growth on different substrates .....	106
<b>Table 5.13:</b>	Experimental condition used to define resistant population growth on different substrates .....	106
<b>Table 5.14:</b>	FVA analysis results to show the effect of chloramphenicol on WT .....	109
<b>Table 5.15:</b>	FVA analysis results to show the effect of streptomycin on WT .....	110
<b>Table 5.16:</b>	FVA analysis results to show compensation in case of ChlR .....	113
<b>Table 5.17:</b>	FVA analysis results to show compensation in case of StrpR .....	113
<b>Table 5.18:</b>	Constraints used for NADH oxidase simulations for ChlR and StrpR .....	116
<b>Table 5.19:</b>	Effect of NADH oxidase on the resistant models of <i>C. violaceum</i> .....	116
<b>Table 5.20:</b>	Single gene deletion analysis for glucose under aerobic condition .....	117
<b>Table 5.21:</b>	Selected genes from single gene deletion analysis for six metabolites including glucose and candidate metabolites that re-sensitize ChlR and StrpR .....	119
<b>Table 5.22:</b>	Double gene deletion analysis for glucose under aerobic condition .....	119
<b>Table 6.1:</b>	National Policies and Campaigns against Antibiotic misuse and Resistance ....	127
<b>Table 6.2:</b>	Demographic details of all 504 respondents .....	131
<b>Table 6.3:</b>	Correlational Statistics for all 504 respondents .....	139

# Chapter 1

## Introduction

*“This is the book I never intended to write.”*

*- Kevin Brown, Penicillin Man*

*“The thoughtless person playing with penicillin is morally responsible for the death of the man who finally succumbs to infection with the penicillin-resistant organism. I hope this evil can be averted”*

*- Sir Alexander Fleming, 1945*

*“If we are not careful, we will be soon in a post-antibiotic era”*

*-Tom Rieden, CDC director, 2013*

Revolutions cause paradigm shifts. The discovery of Penicillin by Alexander Fleming in 1928 qualified as a revolution (Thomas Kuhn) as it changed the world-view on the treatment of infection. It changed the way the medical profession viewed infectious disease in that humanity was considered no longer vulnerable to death by bacterial pathogens. However, Fleming in his Nobel lecture predicted the emergence of penicillin resistant microbes when exposed to sub lethal concentrations. Today, almost a century later, we are dangerously at its helm.

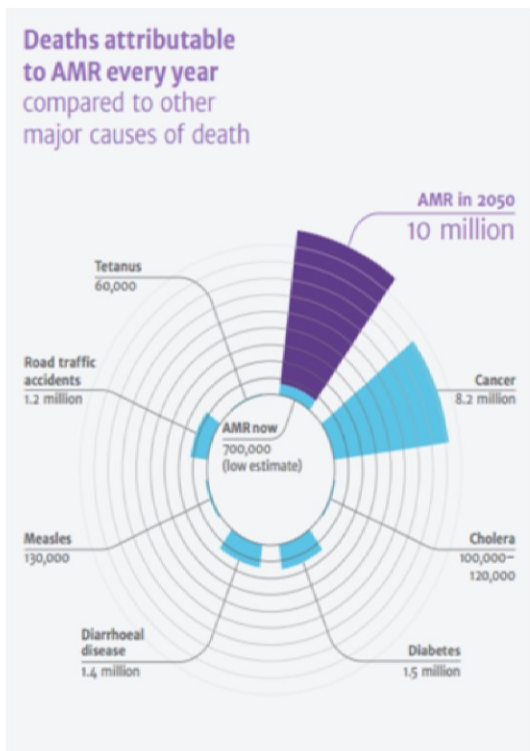
## 1.1. Motivation

10 million deaths by 2050 will be attributed to antimicrobial resistance alone, far more than that of diseases including cancer. At present about 700,000 die from drug resistant infections as stated in a review led by Jim O’Neill, formerly chief economist at Goldman Sachs, on behalf of the British government and the Wellcome Trust. Antibiotics, once considered miracle drugs, are now undervalued by our society, receiving only a fraction of yearly revenue compared to that of next generation anti-cancer drugs hence as a consequence major pharmaceutical companies are exiting from the antibiotic research and development sector hindering novel antibiotic development. The Food and Drug Administration (FDA) approved drugs in the market are exponential decreasing, so the shelf life of existing antibiotics needs to be extended. Adding up is another complication of self-prescribing and Over the counter (OTC) sale in country like ours which adds up to the ineffectiveness of antibiotics and development of resistance. One in five does not believe antibiotic resistance is a serious issue, one in four do not complete the prescribed dosage and one in ten self-medicate. National awareness of the potential threat posed by the loss of effective therapies to treat bacterial infections has increased significantly due to well-publicized reports from the World Health Organization (WHO, 2014), and national governments of countries including the UK, the USA, Canada and Australia, among others (Butler et al., 2017). We are being pushed into a human health era where we will face the same risks as before Alexander Fleming discovered penicillin in 1928, a “post-antibiotic” era, common infections would be able to kill again.

Albert Alexander, a British policeman in 1941 was scratched by a rose thorn and succumbed to *Staphylococcus aureus* and *Streptococci* sepsis. In 2017, Gennifer Gonzales of California spent around USD 2,50,000 in the emergency room (ER) for cellulitis treatment that is supposed to be uncomplicated and be treated in the outpatient setting with oral antibiotics. A question that arises is can post genomic era subvert the onset of a “post-antibiotic era” or the “antibiotic apocalypse”?

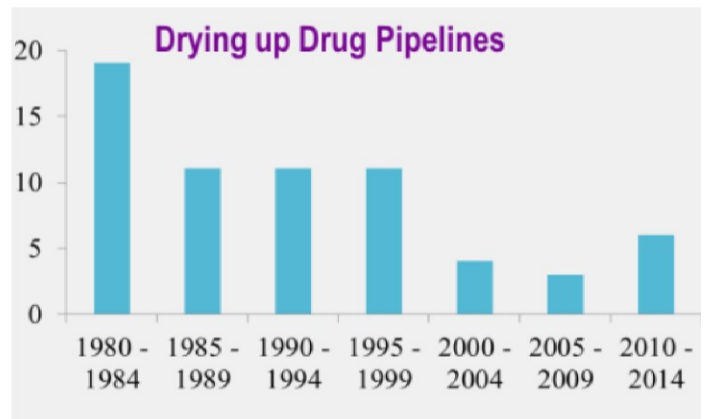
Till date only a handful of research articles have looked at systemic level changes as a function of antibiotic resistance. High throughput technologies such as next generation genome sequencing (NGS) of antibiotic-sensitive and -resistant isolates are powerful tools to understand the mode of action of antimicrobial drugs and delineate the link between genotype, dynamics of metabolism, antibiotic resistance and growth phenotype. These generate catalogues of virulence and pathogenic genes yet, antibiotic resistance remains a serious health concern. There is thus an urgent need for novel approaches to

understand survival strategies and integrated predictive models for hypothesis generation and discovery of how to re-sensitize antibiotic resistant populations.



Review on Antimicrobial Resistance 2014

**1** in five - antibiotic resistance is not a serious issue  
 in four - stop antibiotics once they feel better  
 in 10 - self-medicate\*



Data from CDC 2013



Antibiotics can be bought without a prescription in many countries, and overuse of the drugs is fueling the evolution of resistant microbes.

**Antibiotic resistance sweeping developing world**  
 Nature 509, 141-142, 2014

**Figure 1.1:** Antibiotic resistance a multifactorial societal issue. \*as per KAP study discussed in Chapter 6 of this thesis.

## 1.2. Overall objective and specific aims

The main objective of this thesis is to delineate the systems level changes and metabolic dynamics of a zoonotic pathogen *Chromobacterium violaceum* under antibiotic selection pressures. To satisfy this objective, certain specific aims were put forth in the context of the systems biology paradigm to study antibiotic resistance (Figure 1.2) and include:

- Development of a controlled model system through laboratory evolution
- Delineating the genetic basis through whole genome sequencing
- Delineating the metabolic basis through metabolite profiling
- Building genome-scale models flux balance models to integrate acquired data
- Delineating compensatory mechanisms in resistant populations

The thesis aims to understand how interaction between genome sequence changes, enzymopathies, growth and metabolism of a pathogen shapes death and survival of the pathogen in various antibiotic scenarios.

The underlying hypothesis is that identifying compensatory mechanisms of antibiotic resistant pathogens through metabolic reprogramming will set the stage for upcoming metabolite based treatment strategies to mitigate antibiotic resistance.

### 1.3. Systems Biology Paradigm

In this post genomics era huge “omics” datasets are generated and each gene is assigned a biological function and the information is used to generate hypothesis and elucidate the metabolic networks. Further the huge information generated is translated into a mathematical representation using constraints based modeling (CBM), one of several approaches published in literature so far. CBM helps in modeling large scale data using flux balance analysis.

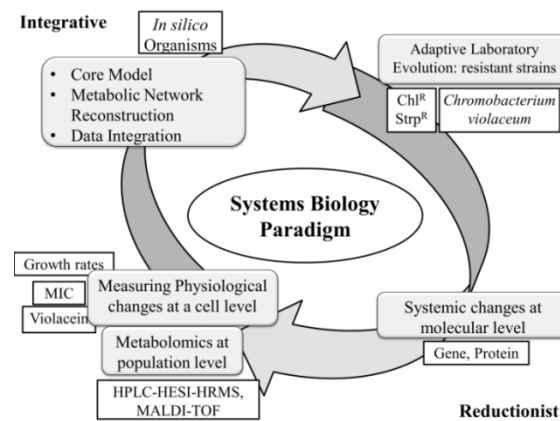


**Figure 1.2:** Systems Biology paradigm

In this thesis I explore the paradigm of systems biology in the context of antibiotic resistance. The methods developed herein help us not only to understand mechanism of resistance but also provide solutions in terms of metabolic environment designs to re-sensitize resistant population of *C. violaceum*. The antibiotic resistant strains of *Chromobacterium violaceum* were developed under controlled laboratory environment using adaptive laboratory evolution (ALE) followed by investigation of systemic changes at molecular level in the bacterium. The molecular components under focus were the enzymopathies as an effect of changes in gene or DNA sequence. Out of 4.75 Mega bases of the genome 13 variations resulted in changes in only 6 open reading frames (ORF). To understand genotype phenotype relationship as a result of these genetic variations growth rates, violacein synthesis and other phenotypic changes were investigated which were correlated to increased growth related to antibiotic resistance. Systemic changes at metabolomic level were also investigated to understand the impact of genotype-phenotype relationship and the associated metabolic reprogramming. The data generated was integrated into a core model representing central metabolism and further into a genome-scale model, that were used to predict growth phenotype observed. This iterative experimentation comprising (reductionist approach) and integration of heterogenous data types into flux balance models (systems based approach) predicted physiological changes resulting in the emergent antibiotic resistance phenotype.

## 1.4. *Chromobacterium violaceum*

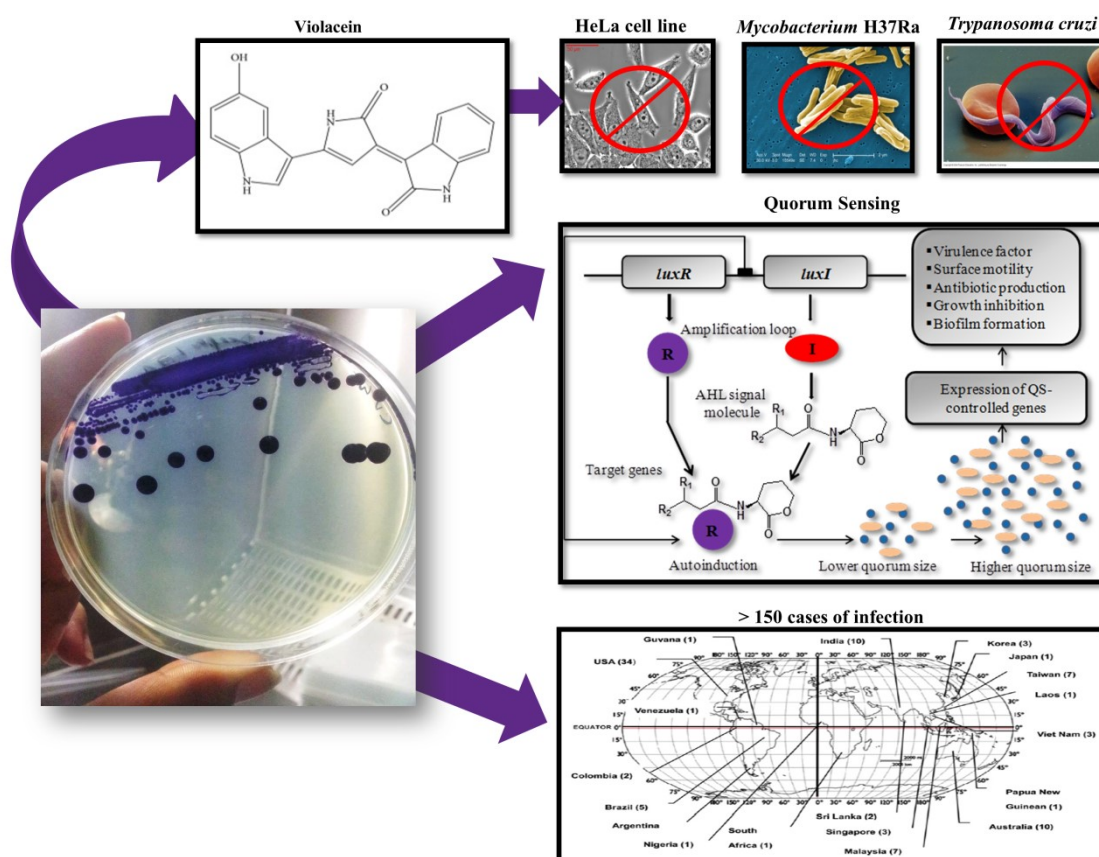


**Figure 1.3:** *Chromobacterium violaceum* a model organism

*Chromobacterium violaceum* is a gram-negative  $\beta$ -proteobacterium discovered in 1881. Primarily a zoonotic neglected pathogen, opportunistic in humans can convert the essential amino acid tryptophan to violacein, a blue-violet, non-diffusible pigment of interest with a wide range of well documented antibiotic properties (Durán and Menck, 2001). *C. violaceum* is found in water and soil of tropical and sub-tropical regions of the world and is incompetent in surviving in cold temperature. *C. violaceum* is also considered a good candidate for polyhydroxyalkanoates (PHA) production (Bhubalan et al., 2010; Kolibachuk et al., 1999; Steinbüchel and Schmack, 1995) and bioleaching of gold (Campbell et al., 2001) due to cyanogenic property. It can also be used for environmental remediation along with other bacteria for decontamination of sites contaminated with toxic metals such as arsenic and uranium and also for removal of Gold and Copper from electronic scrapped wastes. *C. violaceum* is also known for the production of a new class of anti-cancer drugs, histone deacetylases (HDACs)inhibitors, Romidepsin, several antibiotics and anti-blood coagulant currently being used in pharmaceutical industry. *C. violaceum* tightly regulates the production of secondary



metabolites through quorum sensing (QS) including violacein biosynthesis, cyanide biosynthesis and degradation, elastase production, chitinase production and biofilm formation. But, the regulatory pathway is not completely understood. Quorum sensing is a process of bacterial cell to cell communication in which cells produce, detect, and respond to extracellular signal molecules called autoinducers. Using quorum sensing, bacteria modulate their gene expression and respond to changes in cell density and environment. The quorum sensing system of *C. violaceum* comprises five components: the LuxI and LuxR homologue, CviI and CviR, Acyl homoserine lactones (AHLs) that are the autoinducers in gram negative bacteria and some target genes like chitinases, exoproteases, virulence factors along with an upstream CviR binding site for promoter recognition as reported upstream of *vioA* (Stauff and Bassler, 2011). CviI synthesizes the AHLs and CviR is the quorum sensing receptor. It has also been reported that a 20-bp Lux box-like palindromic sequence, Cvi box sequence in the *VioA*- promoter region represents the binding site of the CviR/AHL complex and regulates violacein biosynthesis (Morohoshi et al., 2010). Another striking observation was that the regulation of violacein by AHLs was different for different strains of *C. violaceum*. *C. violaceum* ATCC 12472 produces several AHLs, but violacein production in strain VIR07 (*cviI* knockout strain of ATCC 12472) is induced by long chain (C10- C16) AHLs and particularly enhanced by C10-AHL whereas it was lower or negligible in the presence of short-chain (C4–C8) AHLs (Morohoshi et al., 2010, 2008). In case of *C. violaceum* ATCC 31532 violacein biosynthesis was induced by short chain (C4–C8) AHLs in the mutant CV026 (*cviI* Tn5 mutant of ATCC 31532) and inhibited by (C10–C14) long chain AHLs (McClellan et al., 1997). Although, CviR/C6-HSL and CviR/C10-HSL complexes can equally activate transcription of *vioA* independently in *E. coli* (Morohoshi et al., 2010). It has been reported that the affinity of AHL for the CviR protein to form CviR-AHL complex was almost independent of N-acyl chain length, but played a crucial role in binding with RNA polymerase (Swem et al., 2009).

*C. violaceum* also presents itself as an emerging opportunistic pathogen, with around 150 cases worldwide (Yang and Li, 2011) of which 20 cases have been reported in India (Appendix 1.2). Cases of infection with high mortality rate worldwide could be due to various survival strategies of *C. violaceum* against antibiotics along with superoxide dismutase and catalase activities to escape phagocytic attack of the host defense. Horizontal gene transfer has endowed genes to different strains of *Chromobacterium violaceum* which helps it in environmental adaptation. Thus with the genome sequencing

of *C. violaceum* in 2003 (Haselkorn et al., 2003), there is a need to develop a functional genome scale model as has been developed for multiple pathogens (Chavali et al., 2008; Jamshidi and Palsson, 2007; Raghunathan et al., 2010, 2009a). This would enable the understanding of this organism not only for metabolic engineering of violacein but also for its pathogenic implications, interaction with host/environment and design potential treatment strategies.

*Chromobacterium violaceum* is known to have beta lactamases activity (Farrar and O'dell, 1976) that is primarily active against first – generation cephalosporins, ampicillin and penicillin. It is also resistant to p-chloromercuribenzoate, vancomycin, rifampin and ceftriaxone (Fantinatti-Garboggini et al., 2004; Farrar and O'dell, 1976; Lima-Bittencourt et al., 2011, 2007, Aldridge et. al., 1988; Berkowitz and Metchock, 1995; Martinez et al., 2000).

*C. violaceum* has been reported sensitive to aminoglycosides including streptomycin, chloramphenicol, doxycycline, trimethoprim-sulfamethoxazole, cloxacillin, gentamicin, imipenem (Taylor, 2009, Berkowitz and Metchock, 1995, Midani and Rathore 1998) and only cefotetan among the cephalosporins (Durán and Menck, 2001). *C. violaceum* infection can also be cured by tetracyclines (Moss and Ryall, 1981) as well as ciprofloxacin, norfloxacin and perfloxacin (Aldridge et al., 1988).

Resistance to a variety of antibiotics makes the treatment of *C. violaceum* infections difficult. Minimum inhibitory concentrations (MICs) of different antibiotics against *Chromobacterium violaceum* reported in literature have been tabulated in Appendix 1.1. More than 150 medical cases of *C. violaceum* infection have been reported across the globe. Some of these cases become fatal due to incorrect treatment, nature of infection or delay in the identification of cause of infection.

### **1.5. Antibiotics chloramphenicol and streptomycin**

As discussed in previous section, *C. violaceum* is known to be susceptible to chloramphenicol and streptomycin and no resistant isolates have been reported in literature so far. Both the antibiotics act on the translational ribosomal machinery of the cell yet chloramphenicol is a bacteriostatic antibiotic whereas streptomycin is bactericidal in nature. These antibiotics provide selection pressure for adaptation of growth and evolution of resistance.

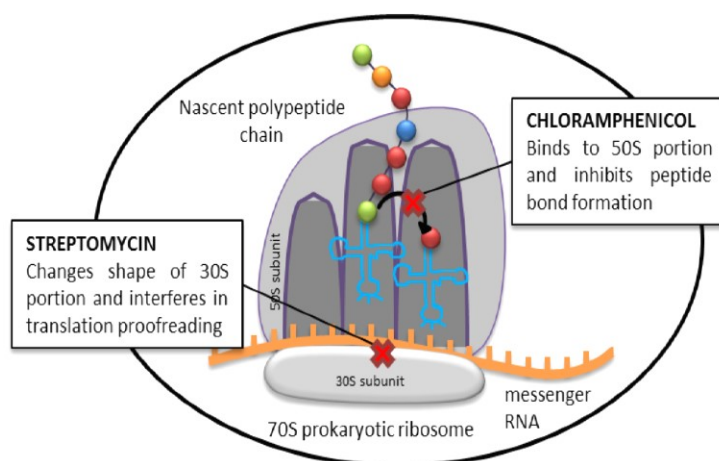


**Figure 1.4:** Antibiotics used in this study and their mechanism of action

The p-nitroaromatic broad spectrum antibiotic Chloramphenicol (chl) has been used extensively to treat life-threatening infections due to *Haemophilus influenzae* and *Neisseria meningitidis*; its mechanism of action is the inhibition of protein biosynthesis. It is naturally produced by *Streptomyces*. After decades of limited use, it has been the focus of renewed interest due to the lack of new antibiotic agents and the appearance of resistance caused by the indiscriminate use of current antibiotics. In fact, at present a number of multi-resistant clinical isolates from pathogenic bacteria are still sensitive to chloramphenicol, a fact that could be attributed to the limited use of this antibiotic in developed countries. Thus, chloramphenicol is being reconsidered as an option for treatment of certain infections in critically ill patients. The most common mechanism of resistance to chloramphenicol in bacteria is its enzymatic inactivation by acetylation mainly via acetyltransferases (Schwarz et al., 2004) or, in some cases, by chloramphenicol phosphotransferases (Mosher et al., 1995) or nitroreductase (Smith et al., 2007). Resistance to chloramphenicol may also be due to target site mutation/modification (Montero et al., 2007), decreased outer membrane permeability (Burns et al., 1989), and the presence of efflux pumps that often act as multidrug extrusion transporters, thereby reducing the effective intracellular drug concentration (Daniels and Ramos, 2009; Fernández et al., 2012).

Streptomycin (strep), an aminoglycoside antibiotic, has been shown to interact directly with the small ribosomal subunit (Carter et al., 2000). The mechanism of action involves irreversible binding to the ribosomal protein S12 and 16S rRNA domain, which are the constituents of the 30S subunit of the bacterial ribosome and play a vital role at the ribosome accuracy center (Carter et al., 2000). Through this interaction, streptomycin

interferes with translational proofreading and thereby inhibits protein synthesis. A number of mutations in the *rpsL* gene encoding the S12 polypeptide generate resistance to streptomycin (Agarwal et al., 2011; Barnard et al., 2010; Han et al., 2003; Kenney and Churchward, 1994; Levin et al., 2000; Paulander et al., 2009; Springer et al., 2001; Sreevatsan et al., 1996).

## 1.6. Antibiotic resistance

There are many ways of defining antibiotic resistance. The one used in this thesis is the uncontrolled growth of pathogens even in the presence of drugs, especially at concentrations of drugs that are generally therapeutic. So as a result, antibiotic resistance occurs when the drug has lost its ability to kill or retard pathogen growth in other words uncontrolled growth of pathogens in the presence of therapeutic levels of antibiotic.

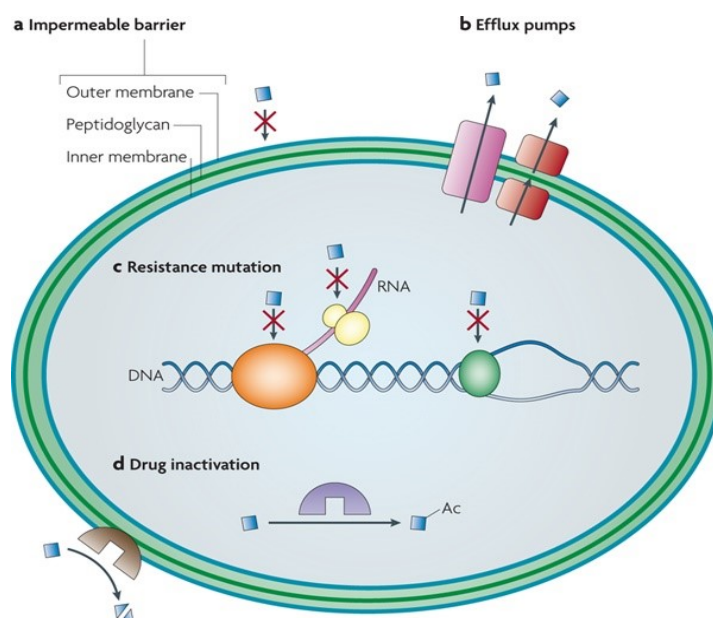


**Figure 1.5:** Mechanisms of antibiotic resistance adapted from Allen et al., 2010

Bacteria have been developing resistance to antibiotics from the time they have been in use; even Alexander Fleming, warned about the possibility when he accepted his Nobel Prize in 1945. Antibiotics are characterized by their chemical composition and mode of action. The main targets for action in bacteria include the bacterial cell wall, cell membrane, DNA, RNA and protein biosynthesis and enzymatic pathways (Brooks et al., 2001). There are several mechanisms (Figure 1.5) well documented (Allen et al., 2010; Andersson, 2003; Davies, 1994; Livermore, 2003) for development of antibiotic

resistance in bacteria which include decrease in antibiotic permeability due to changes in outer membrane proteins, RND or other efflux pumps, resistance mutation in the antibiotic target, drug inactivation by different mechanisms such as enzyme hydrolysis of antibiotics (beta-lactamases), antibiotic-binding proteins (penicillin binding proteins) or enzymes modifying an antibiotic (acetyltransferases), expression of metabolic pathways that bypass the reaction inhibited by the drug, or expression of altered enzymes that are less affected by the drug. The resistance phenotypes are not always predictable from genotypes alone i.e. the origin of drug resistance may be genetic or non-genetic. The acquisition of drug resistance is a complex phenomenon that involves changes in various cellular hierarchical layer including the genome, transcripts and metabolites. The possible strategy to understand the complex dynamics is to analyze various “omics” data and then to integrate them into a network model to predict essential phenotypes for drug resistance.

### 1.7. Dynamics of cell metabolism

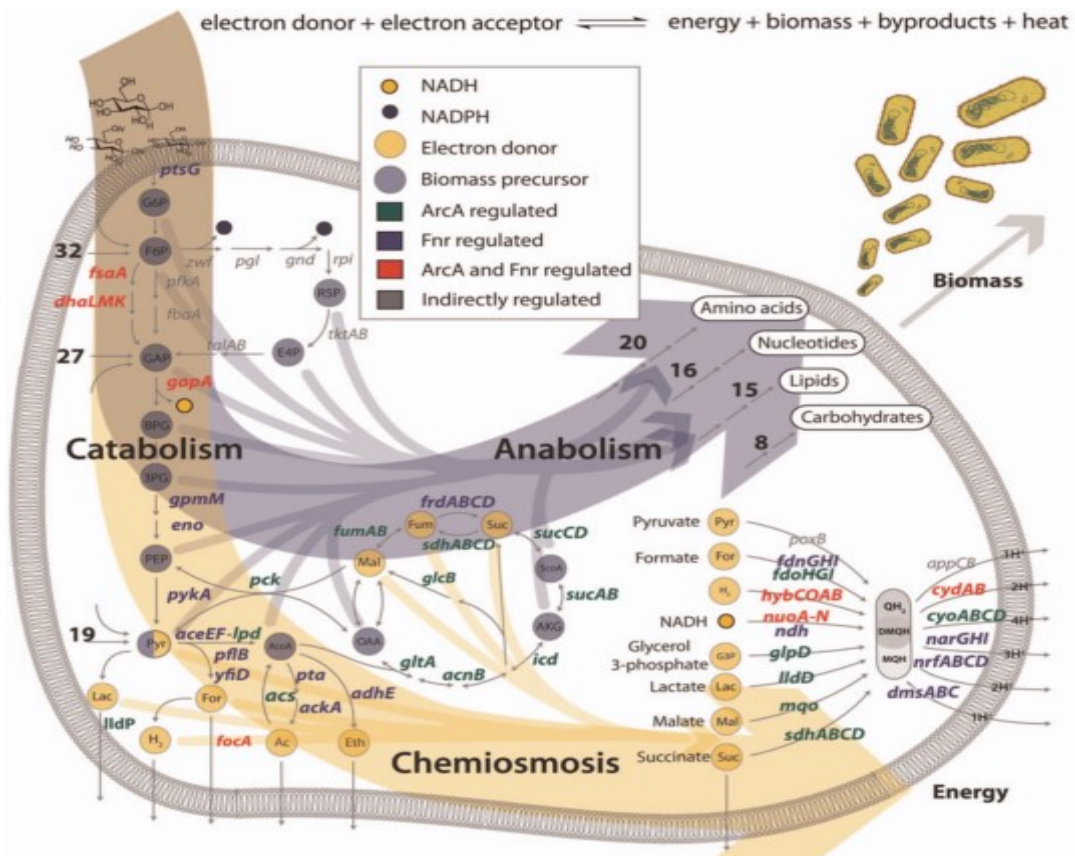


**Figure 1.6:** Dynamics of Energy Metabolism adapted from Federowicz et al., 2014

Antibiotics inhibit major consumers of cellular energy output, so may have important consequences on bacterial metabolism (Lobritz et al., 2015). Metabolism is the sum total of all reactions occurring in a cell including catabolism and anabolism. Growth and energy generation are two principal (competing) dimensions of cell function and proliferation (Federowicz et al., 2014; Fuhrer and Sauer, 2009; Schuetz et al., 2012). One is to convert sources of energy in the environment into forms of energy useful for the organism. The second principal is to synthesize small molecules needed for cell growth or biomass generation from nutrients present in the environment. This duality of cell function, orchestrated by metabolic networks, is critical for survival and governs resistance. For most carbon substrates, nearly 60 reactions of the central carbon metabolism provide the building blocks and energy at appropriate rates and stoichiometry's to fuel around 300 anabolic reactions (Fuhrer and Sauer, 2009). Redox homeostasis is important to effectively harness reducing power produced through the catabolism of various substrates and to utilize this power in the anabolism of cellular components such as DNA, lipids and proteins. Under aerobic condition, the primary role of the redox cofactor NADH is respiratory ATP generation via oxidative phosphorylation whereas the role of NADPH drives anabolic reductions. Oxidative phosphorylation is oxidation of electron donors to transfer electrons to NAD<sup>+</sup> or NADP<sup>+</sup> that are further passed through ETC to terminal acceptor and generate ATP through the process of chemiosmosis. Anabolism utilizes ATP to drive reactions for production of biomass.

### 1.8. Resistance phenotypes not always predictable from genotypes alone: Antibiotic resistance and cell metabolism

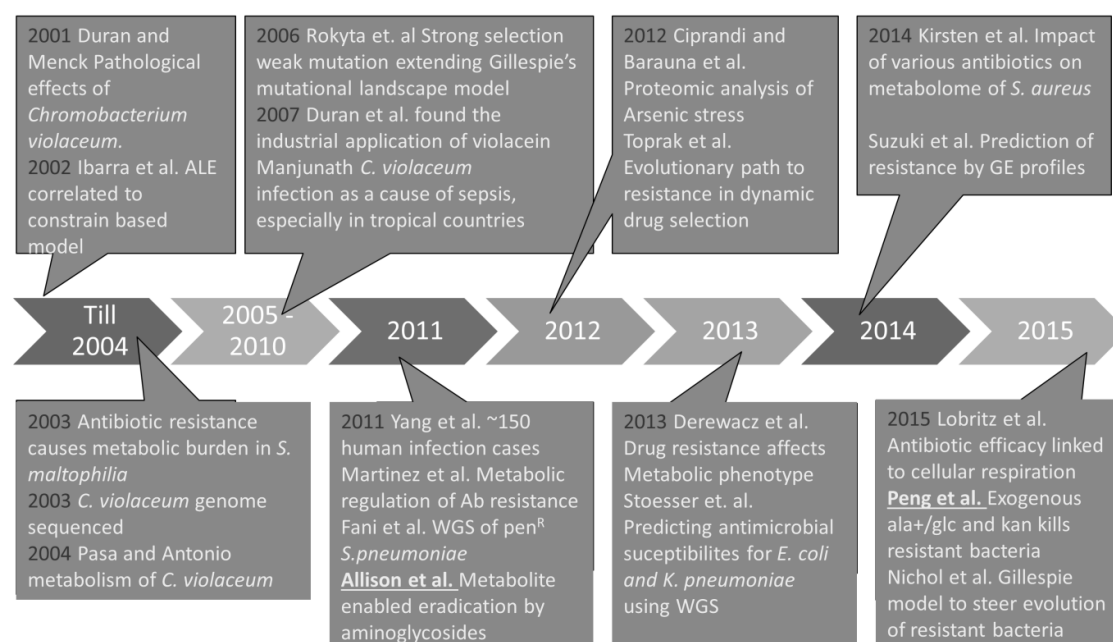


**Figure 1.7:** Research time line related to this thesis work

Significant amount of literature is available that links antibiotic resistance to specific genes (Fani et al., 2011; Renzoni et al., 2011; Stoesser et al., 2013), gene expression (Suzuki et al., 2014), respiration (Lobritz et al., 2015), and even metabolome (Dörries et al., 2014). Metabolic regulation and gene expression modulation are now recognized as major players in antibiotic resistance (Derewacz et al., 2013; Dörries et al., 2014; Martínez and Rojo, 2011; Suzuki et al., 2014). Specific metabolites have been associated with varying degrees of killing antibiotic tolerant pathogens (persisters) by stimulating proton motive force (PMF) and increasing antibiotic uptake (Allison et al., 2011; Peng et al., 2015; Su et al., 2015). Promoting tricarboxylic acid cycle (TCA)/Krebs cycle by glucose/alanine activation that subsequently also increase PMF stimulating uptake of antibiotic have initiated death in multi-drug resistant *Edwardisiella tarda* (Peng et al., 2015). Research elucidating killing mechanisms for such resistance strains are upcoming wherein researchers have worked to increase the PMF and hence drug uptake (Allison et al., 2011) or increase TCA which in turn increases PMF (Peng et al., 2015).

Before 2011 majority of the research reported the differential substrate utilization patterns observed as a function of antibiotic resistance but there wasn't any focus towards studying or investigating complex relationship between genetic and metabolic pathways and antibiotic resistance. Rather overall gene expression, transcriptomic or proteomic analysis was used to investigate bacterial response to environmental perturbation by antibiotics but its downstream effect on the cell phenotype or metabolism was not fully looked at. Rifampin resistant mutant of *Bacillus subtilis*, mutant in *rpoB*, better utilized beta-glucosides (Perkins and Nicholson, 2008) whereas fosfomycin was reported to be useful for treating *Listeria* infections as it was hyper-susceptible *in vivo* due to metabolic adaptation for using nutrients inside its host cell (Chico-Calero et al., 2002; Scotti et al., 2006). *Stenotrophomonas maltophilia* mutant overexpressing MDR efflux pump SmeDEF were reported to be more proficient in utilizing gentibiose, dextrin, mannose and formic acid whereas utilization of amino acids such as alanine, serine or proline was impaired (Alonso and Martinez, 2000).

Michael A. Kohanski, Daniel J. Dwyer and James J. Collins were one of the pioneers to investigate more than the drug-target relationship of antibiotics and investigate downstream cellular response and effected biochemical pathways in response to antibiotic stress/resistance (Kohanski et al., 2007, 2010). In the following years (post 2011) more emphasis and attention was paid to understand the complex relationship between metabolism and antibiotic resistance. Fructose or alanine and/or glucose

restored susceptibility of Multidrug-Resistant *E. tarda* to kanamycin (Bhargava and Collins, 2015; Peng et al., 2015; Su et al., 2015) activation of tricarboxylic acid cycle (TCA) was reported to produce NADH that generates PMF and increased uptake of the antibiotics. *S. aureus* was treated with several antibiotics and the metabolome was studied and it was reported that each antibiotic affected intracellular levels of TCA intermediates (Dörries et al., 2014). Ciprofloxacin altered the pool of nucleotides and peptidoglycan precursors whereas erythromycin increased intermediates of the pentose phosphate pathway and lysine and vancomycin and ampicillin resulted in overall decrease in central metabolite levels. Researchers also linked antibiotic efficacy to cellular respiration (Lobritz et al., 2015) and reactive oxygen species (ROS) generation (Dwyer et al., 2014) among other investigations.

### **1.9. Constraints based modeling and Flux balance analysis**

Metabolism is the most conserved cellular process in a living organism. It is defined as the sum total of biochemical reactions mostly catalyzed by enzymes, involved in sustenance of life in any living organism. It may have many alternative routes to reach a particular metabolic goal. Systems level mathematical representation of metabolism is based on the assumption of metabolism as a network. In other words metabolic network is a cascade of biochemical reactions which involves biotransformation of an initial molecule into a product. Such representations of living organisms with respect to their metabolism have been a prominent tool to analyze and predict the cellular phenotype of a biological system and to ultimately apply engineering principles to design cellular metabolic processes that achieve a desired objective (i.e. cellular engineering). Such mathematical representations make use of the widely available genomic data along with high throughput “omics data” to predict a particular phenotype.

Since 1995, when the first genome was sequenced, rapid sequencing technologies along with detailed biochemical, enzymatic and omics data in electronic databases on microbial metabolism have led to reconstruction of metabolic networks at the genome scale (Feist et al., 2009; Price et al., 2004; Thiele, Ines; Palsson, 2010). This advancement have also led to combining various cellular components along with their biochemical interactions to formulate a mathematical description of the sum total of such interactions, identify and apply constraints that the resulting network operates under, and apply optimization principles to evaluate and predict a particular phenotype under a particular environment (Orth et al., 2010). Therefore, in order to accurately predict such



physiological characteristics the mathematical representations of metabolic models also need refinement and validation using such advanced data. By comparing the in silico phenotype with the in vivo or in vitro results, the quality and accuracy of the metabolic model can be improved. In other terms recent advances in omics and genetic engineering technologies have resulted in novel techniques to interrogate and manipulate biological processes at a systems level for cellular engineering and allied fields (Mahadevan and Henson, 2012). Since the first genome scale metabolic model was published (Edwards and Palsson, 1999), numerous mathematical models of metabolism have been developed for prokaryotes and eukaryotes (Kim et al., 2012). These models have been used for a range of applications starting from cellular engineering for production of value added products like itaconate, lovastatin (Liu et al., 2013) and polyhydroxyalkanoates (Puchałka et al., 2008), investigating biofilm formation (Xu et al., 2013), predicting drug targets and biomarkers for cancer (Jerby and Ruppin, 2012) and quite recently linking virulence factors to metabolism (Bartell et al., 2017). These models, systems biologists can also apply to (1) Reannotation of genes, (2) generate and test new hypotheses, (3) assess the nutritional requirements of the organism and approximate its environmental niche, (5) identify missing enzymatic functions in the annotated genome, (6) engineer desired metabolic capabilities in model organisms, (7) growth profile followed by adaptive evolution and on different media and (8) symptoms of different enzymopathologies, etc.

All of the biological information available in a metabolic network can be translated into mathematical terms through stoichiometric matrix. All genome-scale metabolic network models published till date are structural and stoichiometric models, which incorporate reaction stoichiometry but do not require any knowledge of kinetic parameters. While they do not allow the analysis of non-equilibrium dynamics, stoichiometric models have been found very useful for predicting the metabolic capabilities in steady state (Oberhardt et al., 2008; Reed et al., 2003; Riemer et al., 2013).

The earliest mathematical representation of microbial metabolism utilized Monod kinetics and involved only substrate, product and biomass concentrations. Structured mathematical representation of metabolism that only considered cellular compartments was in early 1980s when one of the first intracellular models of *Escherichia coli* was developed by Domach. The concept of a cellular objective was first proposed in the context of linear programming in *E. coli* for acetate production and overflow metabolism

(Majewski and Domach, 1990) which was later extended to the central metabolic network of *E. coli* by Varma and Palsson (Varma and Palsson, 1994), who first developed the flux balance analysis approach where the cellular objective was assumed to be maximization of growth rate. The advancement in genome sequencing technologies and bioinformatics made biology a data rich field which emphasized the need for systems level analysis and a change in the mathematical representation approach of metabolism. Traditional approaches for mathematical representation included kinetic (dynamic approach required detailed information about kinetic constants along with detailed information about enzymes rates and metabolites), stochastic and cybernetic approaches but these cannot be extended to genome scale networks due to large number of parameters and computation complexities. So for such large mathematical representations, constraint based modeling is used (Price et al., 2004).

A range of methods to interrogate the large-scale metabolic networks using linear optimization techniques collectively known as constraint-based modeling (CBM) were developed (Price et al., 2004). It is an approach to analyze a metabolic system under quasi steady state condition (Wodke et al., 2013). We assume that metabolic dynamics are under a quasi-steady state, as metabolism occurs in a much faster rate compared to regulation and cell division. The stoichiometric coefficients of the metabolites or compounds in the associated reactions are typically represented in a stoichiometric matrix,  $S$  with its rows corresponding to the metabolites and the columns representing the chemical transformations that the gene products (enzymes) catalyze. This is how the biochemistry and the genetics of a cell are interpreted into a mathematical form for model development and further assessment. So we reach a homogenous system of linear equations, where consumption of a metabolite equals production and the solution lies in the null space of  $S$ . In CBM approach, constraints are applied on the various metabolic pathways to characterize the cellular behavior or phenotype of the living system. The constraints are based on enzyme capacity, reaction stoichiometry and thermodynamics feasibility associated with directionality of reactions. Methods based on this approach include Flux Balance Analysis (FBA), Flux Variability Analysis (FVA), Minimization of Metabolic Adjustment (MOMA) and the toolbox developed under constraint based approaches includes COBRA. Constraint-based reconstruction and analysis (COBRA) toolbox is for quantitative prediction of cellular behavior using a constraint-based approach (Becker et al., 2007). It allows predictive computations of both steady-state and dynamic optimal growth behavior, the effects of gene deletions; and robustness analyses.

The initial step of CBM approach involving FBA is a mathematical method for analyzing the metabolic capacity of a cell. The objective of FBA is to find out the set of metabolic fluxes that maximizes (or minimizes) the growth rate of a target metabolite (or any other objective function), given some known available nutrients (Varma and Palsson, 1994; Wodke et al., 2013). The success of FBA can be seen in the ability to accurately predict the growth rate of the prokaryote *E. coli* when cultured in different growth media (Edwards et al., 2002), define precise minimal media for the culture of *S. typhimurium* (Raghunathan et al., 2009b) and accurate prediction of essential genes in minimal and rich media for *A. terreus* (Liu et al., 2013).

This approach and the related computational developments allowed the construction of the first genome-scale models of *Escherichia coli* (Edwards and Palsson, 2000) and *Saccharomyces cerevisiae* (Forster, 2003) in the early 2000s. Subsequently, experimental results from chemostats validated many predictions of the *E. coli* genome-scale model, including the optimal growth rate (Ibarra et al., 2002). These results suggested that the use of a suitably chosen cellular objective might be sufficient to overcome the lack of metabolic regulation represented in genome-scale models. However, recently it has been shown that a combination of growth maximization and minimization of adjustment from a reference metabolic state might be a more appropriate objective function for capturing the intracellular flux distribution (Cheung et al., 2013). Recent genome scale metabolic model for *E. coli* (Riemer et al., 2013) and yeast (Österlund et al., 2013) have also been reconstructed based on the same approach after which the yeast model was used as a framework for integration of transcriptome and fluxomic data for four different conditions whereas in the *E. coli* model reaction centric view of flux distribution was replaced by metabolite centric view for a number of currency metabolites to fully characterize the energy metabolism and identify model refinement potential with respect to NADPH metabolism.

## 1.10. Overall methodology

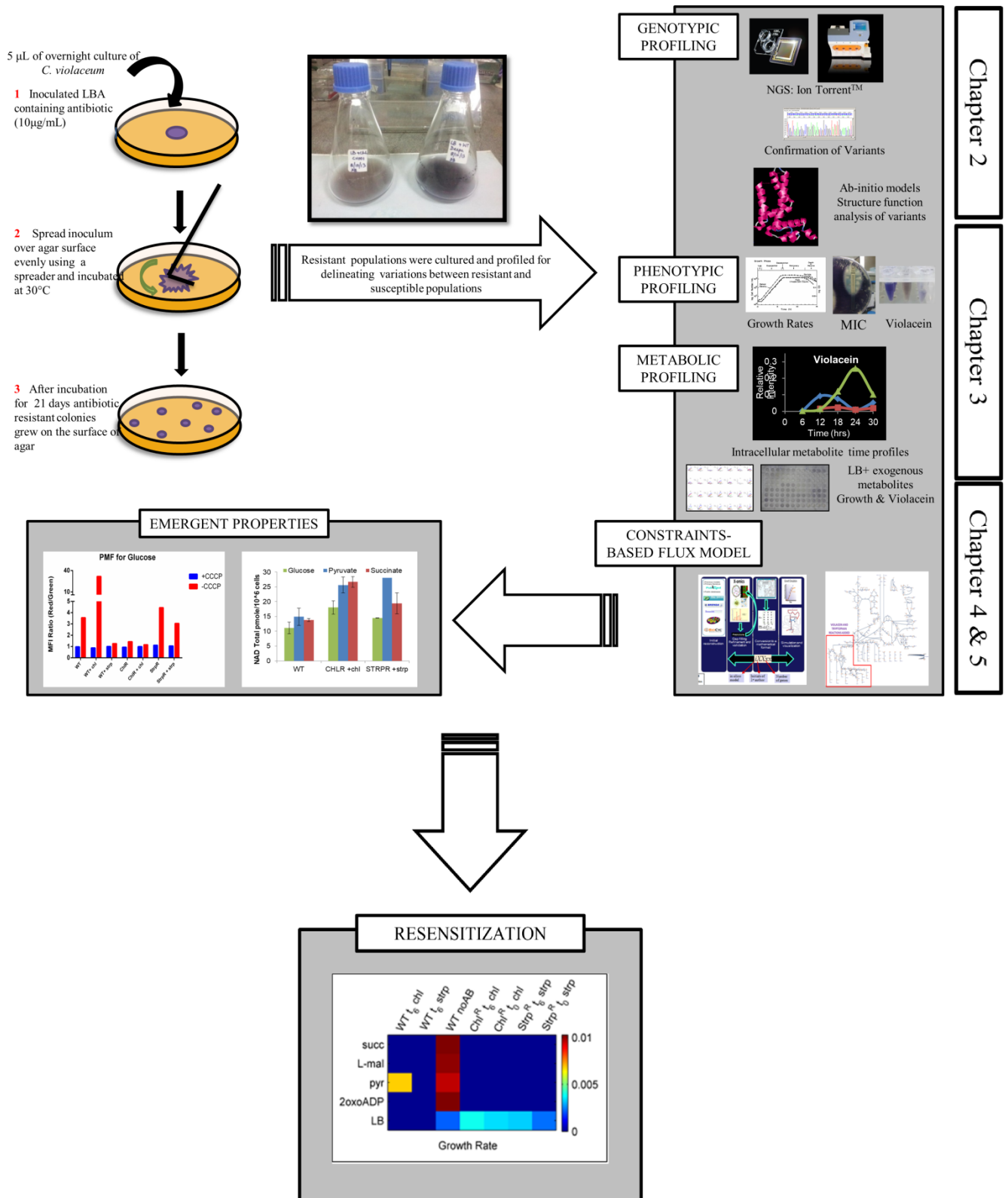


**Figure 1.9:** Overall methodology followed in this doctoral thesis work

### 1.11. Summary of work

In this work, metabolites have been identified that stimulate antibiotic action and death of streptomycin and chloramphenicol resistant population of the pathogen *Chromobacterium violaceum*. Primarily a zoonotic pathogen, it is opportunistic in humans and converts the essential amino acid tryptophan to violacein, a blue-violet pigment. *Chromobacterium violaceum* is sensitive to aminoglycosides, chloramphenicol, and tetracycline and resistant to ampicillin, penicillin, and first-generation cephalosporins. The overall objective is to understand the compensatory mechanisms of antibiotic resistant populations of *C. violaceum* against the imbalance created due to antibiotic as a selection pressure using systems biology approach. The specific aims in order to reach the objectives are to understand the genetic basis of antibiotic resistance, changes in dynamics of metabolism and other phenotypes in order to delineate the link between genotype, dynamics of metabolism, antibiotic resistance and growth (Phenotype). The work has been divided into seven chapters.

As a fundamental basis for systems biology approach the **first chapter** of thesis provides an introduction to the system under study along with the global scenario of antibiotic resistance in addition to literature evidence that emphasizes on the fact that there is lack of research relating already available content of antibiotic resistance genes/virulence factor catalogues to set the stage for upcoming strategies to mitigate antibiotic resistance.

**Second chapter** provides the detailed description of how the antibiotic resistant *C. violaceum* (ChlR and StrpR) were generated followed by the genotypic profiling by Ion Torrent PGM Platform. The variants confirmed after whole genome sequencing have also been discussed in this chapter. Out of 4431 open reading frames (ORFs), variation in only 6 ORFs resulted in acquisition of resistance against the two different antibiotics. Conventional mutations were observed in ChlR in the repressor of a multidrug efflux pump, *acrR* whereas variation in different levels of hierarchy were observed in case of StrpR pointing towards a systemic change in the two resistant populations. Sequence to structure to function to phenotype correlations were made for the variants using ab-initio models generated by ROBETTA software and visualized using PyMol.

**Third chapter** focusses on phenotypic and metabolomics profiling using various methods including API-MALDI and HR-MS for the intracellular metabolites in the three

different population of *C. violaceum*. It also includes violacein estimation, minimum inhibitory concentration (MIC) estimation and kinetic profiling of growth parameters. Further, growth profiling of the three different strains, in the presence and absence of antibiotics with 30 different added carbon or nitrogen sources were assessed for the effect on growth kinetic parameters. The results include differential phenotype identified in the evolved strains ChIR and StrpR with 30% increase and 35% decrease in the violacein amounts. Differential temporal variation of metabolites provided in this chapter suggests metabolic reprogramming as a survival strategy against antibiotics. Out of the 30 substrates, maleate, succinate, 2-oxoadipate and pyruvate resulted in re-sensitization of the resistant strains.

**Chapter 4** discusses the central carbon metabolism model *iDB147*, developed in this work that has prediction accuracy of 90%. Flux Balance Analysis (FBA) was used to make several predictions and various sensitivity parameters pointed towards the importance of NADH and NADPH in the biomass yield (growth). Also, flux variability results are included which show that forced flux through reactions such as alpha ketoglutarate dehydrogenase (AKGDH) and malate dehydrogenase (MDH) is critical for survival of the pathogen.

The whole genome scale model (GSM) of *C. violaceum*, *iDB858* is discussed in **fifth chapter**. The overall methodology of developing a functional GSM model from an initial automated draft reconstruction is described along with the extensive manual curation done for the refinement and increase prediction accuracy and applicability of the model. *iDB858* was used to predict phenotype after being validated using existing BIOLOG legacy data. The methods used included FBA, FVA and single gene/reaction deletion analysis among others. *iDB858* had a prediction accuracy of 86%. As it is an opportunistic pathogen, gene lethality was used to identify potential drug targets.

**Sixth chapter** discusses a public health perspective towards the serious problem of antibiotic resistance using a knowledge attitude practice (KAP) study in the Indian setup. An analysis of 504 respondents confirmed the need for a multi-pronged intervention to combat antibiotic resistance.

**Chapter seven** concludes the thesis with significant findings and future scope.

# Chapter 2

## Towards a Genetic Basis for Antibiotic Resistance in *Chromobacterium violaceum*

*“Evolution is a tinkerer”*

*-Francois Jacob*

*“Our genomes are catalogues of instructions from all kinds of sources in nature, filed for all kinds of contingencies”*

*- Lewis Thomas*

### 2.1. Introduction

Evolution drives the diversity and unity of life. Evolution works across all hierarchies and scales of living systems: Molecular, Cellular, Organismal, Population and Ecological. The ability to maintain a particular state can be altered by evolutionary processes, and the interactions can lead to emergent properties. Evolution shapes our understanding not just of where we come from and where we are going, but also how we interact with the environment. For instance, can wild species adapt in time to cope with the changes we have imposed on the climate? And can we keep up with the 'evolutionary arms race' between superbugs and antibiotics?

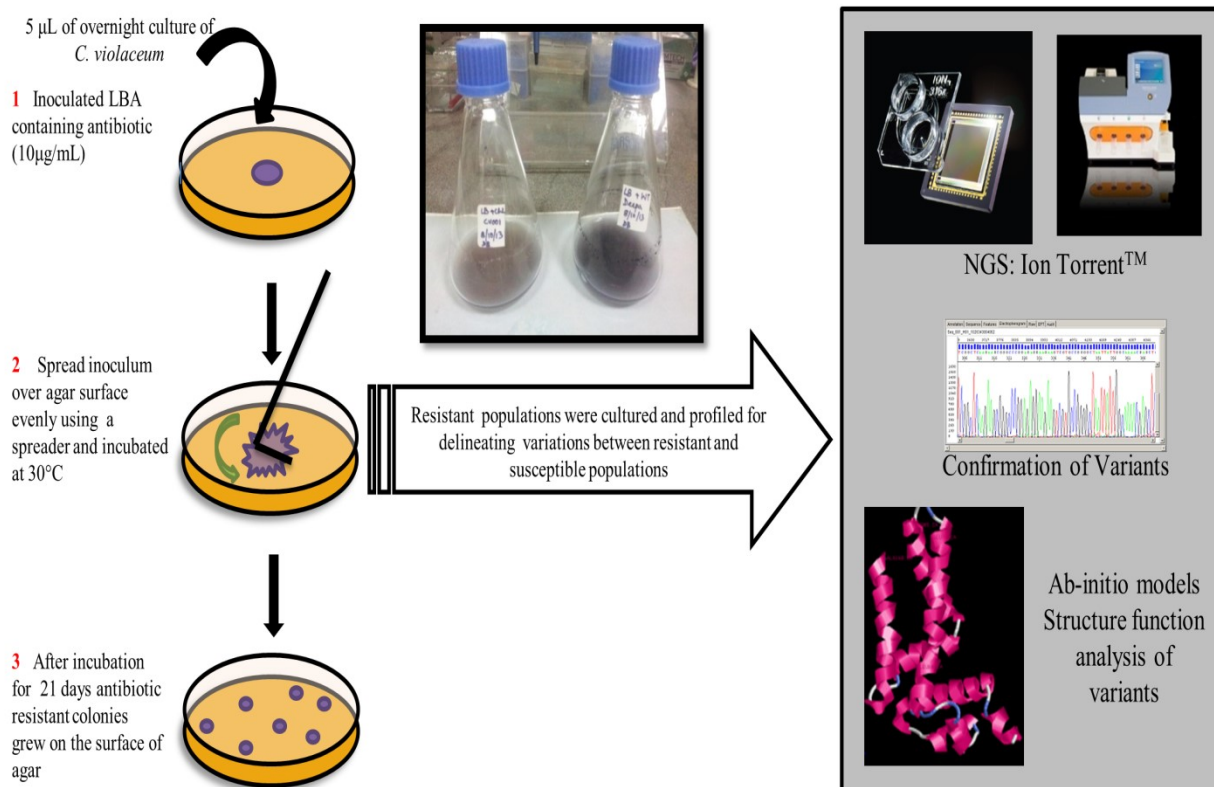


**Figure 2.1:** Graphical abstract of this chapter

Antibiotics and their resistance genes are the task forces in a biological warfare. As described in the previous chapter, there are several mechanisms for development of antibiotic resistance in bacteria that have been well documented in literature. All these mechanisms more or less involve genetic modification or variation at different levels of cellular proteins ranging from outer membrane proteins, efflux pumps or other associated antibiotic targets to metabolic bypass proteins or alternative enzymes less affected by the antibiotic. The emergence of such genetic mutations in the bacterial genome is one of the major factors underlying evolution of bacteria under the selection pressure of antibiotic in the environment. Also, the literature suggests that *C. violaceum* is naturally susceptible to many antibiotics including chloramphenicol, streptomycin, ciprofloxacin, etc. and resistant to ampicillin, penicillin, cephalosporins as discussed in **Chapter 1**. In this study two antibiotics chloramphenicol and streptomycin were used for adaptive laboratory evolution (ALE) of *C. violaceum* under controlled conditions.



Adaptive laboratory evolution (ALE) has been widely used, more so in last 25 years to gain insights into the basic mechanisms of molecular evolution and adaptive changes that accumulate in microbial populations during long term selection under specific growth conditions, in this case presence of an antibiotic. This adaptive potential of microorganisms is increasingly explored in biotechnology by adaptive laboratory evolution experiments (Blum et al., 2016). Post genomic era having advanced in transcripts and economical next-generation sequencing technologies has resulted in many recent studies, which successfully applied this technique in order to engineer microbial cells for biotechnological applications. ALE has been utilized to make production strains more efficient by making them tolerant to the metabolic product (Hu et al., 2016) by activating cryptic gene or inactive pathways (Wang et al., 2016) or by enabling growth on non-native substrates (Lee and Palsson, 2010). In addition, ALE experiments can improve our understanding of fundamental evolutionary principles that might help us solve rising global challenges of undesirable adaptations like drug resistances in microbial pathogens (Jahn et al., 2017). One way to analyze the acquisition of de novo mutations conferring antibiotic resistance is adaptive laboratory evolution. Usually, ALE experiments focus on the adaptation to specific physical or chemical factors such as temperature (Sandberg et al., 2014) or antibiotic tolerance (Lázár et al., 2013; Toprak et al., 2012).

The advent of next generation sequencing (NGS) has been due to the need for high throughput whole genome sequences. NGS employs micro and nano technologies that allows massive parallel sequencing, reduce sample size and costs. NGS machines like the Ion Torrent Personal Genome Machine (PGM) or the Illumina MiSeq apparatus makes bacterial whole-genome sequencing (WGS) feasible (Quail et al., 2012). The Ion Torrent™ PGM utilizes a small chip for detection of released hydrogen ions emitted during DNA polymerization. The Ion Torrent instrument was first marketed in February 2010 by Life Technologies Incorporated (Thermo Scientific) and is capable of sequencing megabases of raw sequence reads on a single chip. It is a scalable, fast run analysis (less than 3 hours) approach with a rate of correct SNP calling higher (82%) than that of Illumina (68 – 76%) and is the fastest sequencing system on the market (Rothberg et al., 2011).

This chapter discusses the successful whole-genome sequencing of two independent *C. violaceum* mutant strains selected for in vitro resistance to chloramphenicol (ChlR) and streptomycin (StrpR) respectively. All genetic changes have been confirmed using Sanger sequencing and delineated during the evolution of antibiotic resistance after next

generation sequencing using Ion Torrent™ PGM platform. The objective of this chapter is to delineate the genetic basis that results in antibiotic resistance in *Chromobacterium violaceum* for the antibiotics chloramphenicol and streptomycin.

## **2.2. Materials and Methods**

### **2.2.1. Adaptive Laboratory Evolution**

The detailed Adaptive Laboratory Evolution (ALE) workflow is well described in Figure 2.1. *Chromobacterium violaceum* strain ATCC 12472<sup>T</sup> was obtained from the American Type Culture Collection Center (ATCC), USA. The wild type *C. violaceum* was routinely cultured on Luria-Broth (LB, Hi-Media-M575) and maintained at 30°C with continuous aeration in a shaker incubator set at 180 rpm. *C. violaceum* was tested to be susceptible to low concentrations of both antibiotics (Chloramphenicol: MIC 8 µg/mL and Streptomycin: MIC 10 µg/mL in liquid culture and 60 µg/mL in agar plates). Antibiotic resistant strains of *C. violaceum* were evolved separately under controlled laboratory environments using the two antibiotics, chloramphenicol (chl) and streptomycin (strep) at sub-lethal concentrations (10 µg/mL) on Luria Bertani agar (LBA) plates. Clonal purification by repeated sub-culturing of the colonies obtained on LBA plates with antibiotic (10 µg/mL) resulted in single colonies. These colonies were cultured in LB with antibiotic (10 µg/mL) and further cryopreserved in 50% glycerol and all further experiments including phenotypic profiling discussed in Chapter 3 were done by thawing the frozen vials and sub-culturing in LB with antibiotic (10 µg/mL) at 30°C with continuous aeration in a shaker incubator set at 180 rpm until mentioned otherwise.

### **2.2.2. Confirm and characterize genetic changes using whole genome sequencing using Ion torrent platform**

In order to extract genomic DNA for whole genome re-sequencing, ChlR and StrpR cultures were revived from previously cryopreserved glycerol stocks on LBA plates with respective antibiotic at 30°C. These cultures have been previously tested for all the phenotypic traits as described in the results section. A single colony from LBA was cultured in LB broth at 30°C, 180 rpm and mid – log phase cells were harvested for genomic DNA extraction using the DNeasy Blood and Tissue Kit (Qiagen, USA) according to the manufacturer's instructions. The quality of the genomic DNA was assessed for RNA contamination using A260/A280 ratio and visualized on agarose gel. The DNA was also quantitated using Qubit before library preparation.

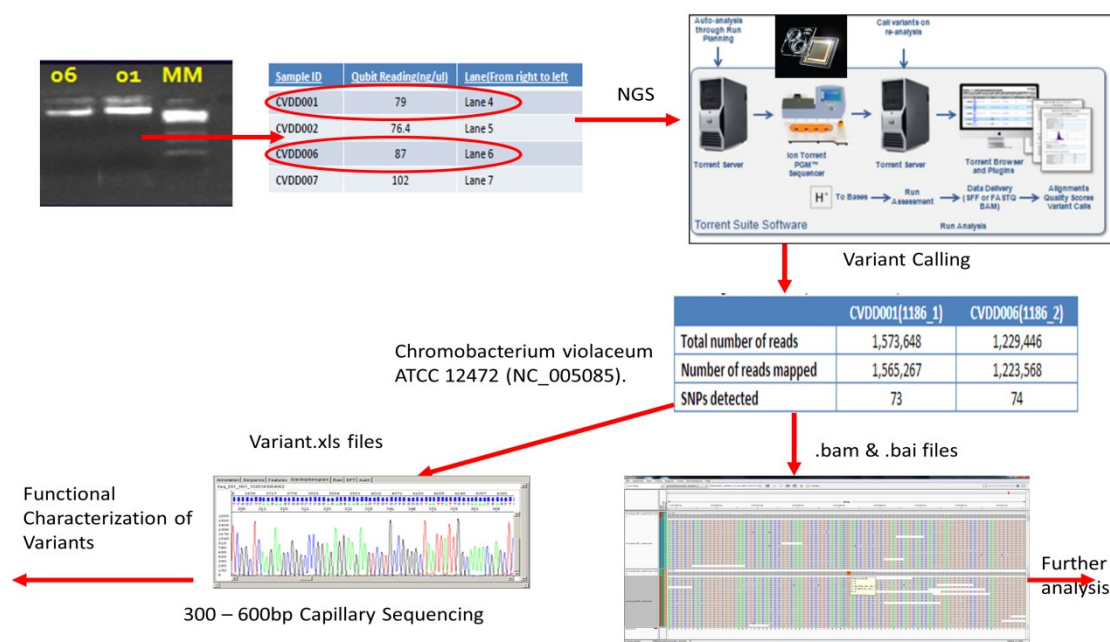


**Figure 2.2:** Overall methodology followed in the genomic profiling

### 2.2.3. Capillary sequencing for confirmation of variants

All NGS identified sequence variations were confirmed by Sanger sequencing. Primers (Appendix 2.2) were designed to amplify around 200 to 600 bp amplicons such that the nucleotide of interest (of the 121 variants) was at a position for easy read during Sanger sequencing. Amplification and sequencing was performed by Eurofins Genomics India Pvt. Ltd.

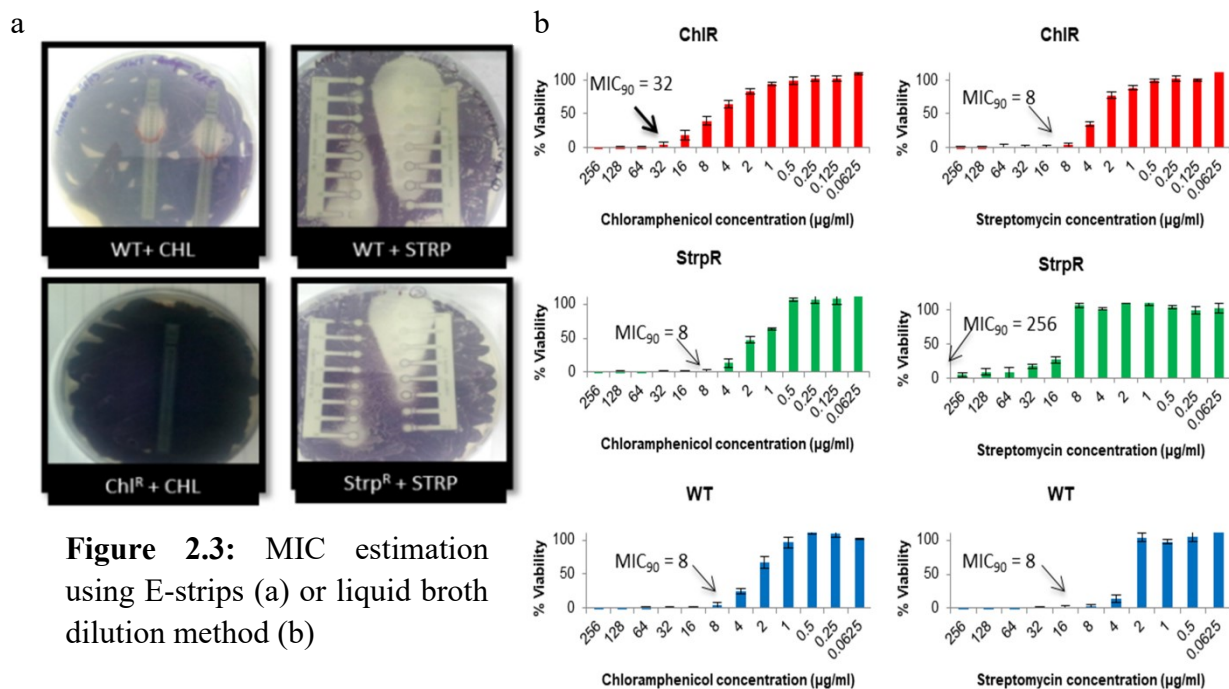
### 2.2.4. *In silico* Structure - Function analysis of the mutation acquired

Ab-initio models were made using ROBETTA server (Kim et al., 2004) (<http://robetta.bakerlab.org>) except for RpsL (homology modeling was used) and the models generated were checked for various parameters for model assessment, such as Ramachandran Plots using PROCHECK. Finally, visualization and manipulation of the three dimensional models were performed using the software PyMOL (Schrödinger, LLC, 2015). In addition 3DLigandSite (Wass et al., 2010) was used to get a better understanding of the structure-function change post mutation/variation.

## 2.3. Results and Discussion

### 2.3.1. Evolved population ChIR and StrpR

The schema for the workflow followed in this study (Figure 2.1) involved the evolution of *Chromobacterium violaceum* strain ATCC 12472<sup>T</sup> (*C. violaceum* or WT)



from a small inoculum onto Luria Bertani agar (LBA) plates chloramphenicol (chl) and streptomycin (strep), both targeting protein translation at the ribosomal subunit level. To provide strong evolutionary pressure while maintaining a sizeable population, the concentration of antibiotic was chosen such that no more than 60% of growth was inhibited. Once defined this sub-lethal concentration (SLC), of the antibiotic ( $10 \mu\text{g/mL}$ ) was not varied throughout the evolution as well as other experiments until specified. The adaptive evolution continued for about 3 weeks and when the first positive trait appeared, these colonies were cultured multiple times on LB agar plates with the respective antibiotics followed by colony purification. Multiple clones that were evolved in parallel were colony purified. Broth cultures of the respective antibiotic resistant population, ChlR resistant to chloramphenicol and StrpR resistant to streptomycin, were used for Minimum Inhibitory concentrations (MIC) calculations. One of the parallel lines of evolved clones resistant to antibiotics was further used in genotypic, phenotypic and metabolic profiling studies as will be discussed in this thesis in different chapters.

### 2.3.2. Genome sequencing of ChlR and StrpR

Genome sequences were obtained for the two evolved populations, ChlR and StrpR, using Ion Torrent PGM<sup>TM</sup> (Life Technologies) NGS using the 314<sup>TM</sup> chip with mean read length of 180 and 188 base pairs respectively. Coverage details for ChlR and StrpR samples are given in Table 2.1. The sequencing data analysis for ChlR and StrpR samples showed 86% and 84% of the bases read were of  $\geq Q20$  quality respectively. For

77.07% of ChlR and 71.3% of StrpR samples the genome base coverage was 20x and for 18.61% and 10.01% coverage was 100x. The assemblies and comparative analysis against NCBI sequence of *C. violaceum* (accession number NC\_005085) were also performed and variants were identified. A total of 121 variants, 64 for ChlR and 57 for StrpR were identified. Of these, 41 variants were common among both the populations and 23 and 16 unique variants. The genome sequence data generated for the current study is available in SRA repository (<http://www.ncbi.nlm.nih.gov/sra/?term=SRP072862>) and assigned the identifier SRP072862.

**Table 2.1:** Coverage details for whole genome sequencing

Samples	Total base reads	Mapped reads	Mean length	Average Base coverage depth (%)	Genome base coverage (%)		
					1x	20x	100x
ChlR	280780471	1565267	180bp	59.10	96.16	77.07	18.61
StrpR	229212916	1223568	188bp	48.24	95.3	71.30	10.01

In order to see how genotype was shaping the growth phenotype of the resistant populations, we re-sequenced the whole genome using capillary sequencing. All the variants present in the two resistant populations (ChlR and StrpR) were analyzed and primers were designed for all of them and PCR amplification followed by capillary sequencing was performed for the three strains (WT, ChlR and StrpR) using all of the 160 primers. Only 14 sequence variations were confirmed which belonged to 8 genes, as shown in Appendix 2.1. The sequence changes were seen to affect the protein structure and function *in silico*.

### 2.3.3. Altered genotypes and *in silico* protein function

In order to see how the altered genotype was shaping the growth phenotype of the resistant populations the sequence changes were analyzed to see the effect on the protein structure and function *in silico*.

As discussed above fourteen sequence changes were confirmed using capillary sequencing. The ChlR population acquired mutations in *marC* (Haselkorn et al., 2003) and the transcription repressor *acrR* of the tripartite AcrAB-TolC multidrug efflux pump (Elkins et al., 2010; Li et al., 2008; Okusu and Nikaido, 1996). Mutations in *marC* were silent substitutions.

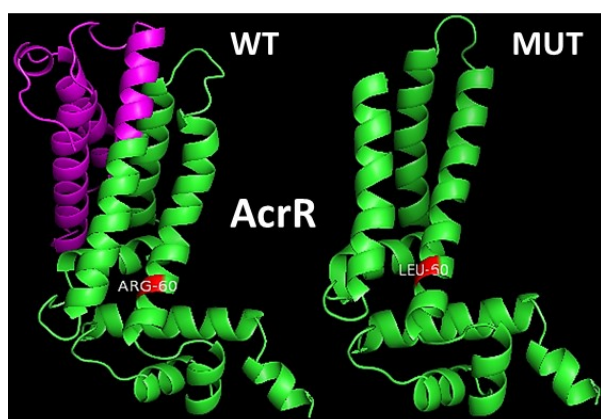


**Figure 2.4:** *Ab initio* model of AcrR for wild type (WT) and mutated (MUT) protein

**Table 2.2:** Amino acid sequence information for AcrR protein

Helix	Domain	Remarks	Amino acids
1	N-terminal		7 to 27
2		HTH DNA-binding motif	34 to 41
3			45 to 51
4	Ligand-binding domains		a - 55 to 65 b - 69 to 80
5		85 to 102	
6		104 to 115	
7		122 to 151	
8	C-terminal	Ligand binding domains – involved in dimer formation which bind to the operator site for repression	160 to 180
9			190 to 204

The repressor protein suffered premature truncation after translation of 141 amino acids and a non-synonymous substitution R60L resulting in altered domain that is involved in ligand binding for repression. *acrR* which codes for the local transcription repressor of the tripartite AcrAB-TolC multidrug efflux pump, had two mutations, a frameshift insertion and a SNP which resulted in amino acid change at 60th position from Arginine (R) to Leucine (L) and premature termination of the protein after 141 amino acid residues. The overexpression of this efflux pump has been well documented to be responsible for intrinsic antibiotic resistance to chloramphenicol in *E. aerogenes* (Ghisalberti et al., 2005), fluoroquinolone in *S. typhimurium* (Olliver et al., 2004) and *K. pneumoniae* (Schneiders et al., 2003) as well as multiple antibiotic resistance in *E. coli* (Okusu and Nikaido, 1996). Frameshift insertions in *acrR* in case of ampicillin resistant clinical isolates of *H. influenza*

have been reported (Kaczmarek et al., 2004) whereas mutation at 45th amino acid residue has been reported in case of clinical isolates resistant to ciprofloxacin in *E. coli* (Webber et al., 2005). Frameshift mutation in *acrR* has been reported in several cases resulting in antibiotic resistance (Dean et al., 2005; Pradel et al., 2002; Schneiders et al., 2003; Wang and Dzink-Fox, 2001). There are studies in *E. coli* isolates that reveal the role of *acrR* mutations in high-level fluoroquinolone resistance in the absence of *mar* mutations also (Wang and Dzink-Fox, 2001). Analysis of the crystal structure of AcrR of *E. coli* (PDB

ID – 2QOP:A) which has a 40% identity and 64% similarity to *C. violaceum acrR* (Li et al., 2008) suggests that on truncation of the protein after 141 amino acid residues, out of the 9 helices present in the protein, the eighth and ninth helix involved in dimer formation to bind to the operator site for repression, are deleted hence preventing repression of the efflux pump and hence efflux of the drug.

In case of the StrpR population, a non-synonymous substitution R86S was detected in *rpsL*, coding for the 30S ribosomal protein S12 (Agarwal et al., 2011; Carter et al., 2000; Demirci et al., 2013; Panecka et al., 2014) along with deleterious mutations in *kdpD*, encoding for the sensor kinase of the two-component signal transduction system (TCS) (Freeman et al., 2013) and *pabC*, encoding the pyridoxyl 5' phosphate (PLP)–dependent enzyme 4-amino-4-deoxychorismate lyase catalyzing 4-aminobenzoate or para-amino benzoate (PABA) biosynthesis (Green et al., 1992; Ye et al., 1990). *Ab initio* models built using ROBETTA and ligand binding analysis using 3DLigandSite (<http://www.sbg.bio.ic.ac.uk/3dligandsite>) showed that the mutated KdpD and PabC proteins truncated after 682 and 226 amino acids respectively resulting in loss of critical ligand binding or sensory domains.

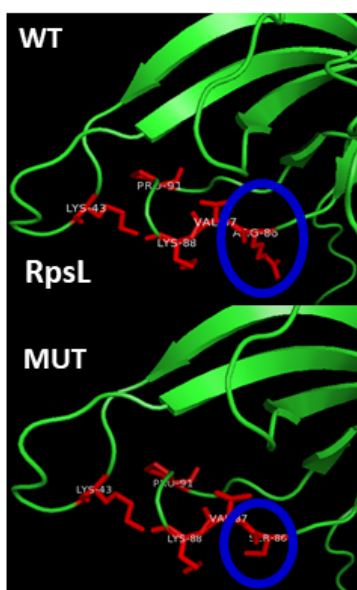


**Figure 2.5:** Homology model of RpsL for wild type (WT) and mutated (MUT) protein

The gene *rpsL* codes for a 30S ribosomal protein S12 which is known to have a critical role in the recognition of cognate tRNA (Agarwal et al., 2011) and contributes in the fidelity of mRNA decoding (Demirci et al., 2013) for maintaining translation accuracy and proper ribosomal function. As a result of mutation, the 86th amino acid residue Arginine (R) is replaced by Serine (S). Alignment of other *rpsL* homologues from *E. coli* and *S. typhimurium* indicate that the arginine at position 86 is highly conserved, further evidence that mutation at such a region is critical for alteration in the protein function. It is well documented that resistance to streptomycin is often conferred by mutations in this gene. *Escherichia coli* S12 protein is known to have around 20 different kinds of substitutions including R86S to confer either streptomycin resistance (SmR) or streptomycin dependence (SmD) (Edgar et al., 2012; Timms et al., 1992; Toivonen et al., 1999). The same mutation, R86S, has been reported, in case of *M. smegmatis* responsible for



chromosomally acquired streptomycin resistance (Kenney and Churchward, 1994). In *M. tuberculosis* as well, point mutations in *rpsL* have been reported to be responsible for streptomycin resistance in various geographical isolates (Sreevatsan et al., 1996). Also, there have been experiments reporting such above mentioned point mutations in the gene which are responsible for “error-restrictive” translation phenotype (Agarwal et al., 2011). It is presumed that the error prone translation or misreading as a result of streptomycin binding maybe “treated” by such hyper-accurate mutations in the S12 protein (Demirci et al., 2013).

The gene *pabC* encodes the pyridoxyl 5' phosphate (PLP) – dependent enzyme 4-amino-4-deoxychorismate lyase that catalyzes the second step in PABA biosynthesis (Green et al., 1992; Ye et al., 1990). The 270 amino acid long enzyme is responsible for the formation of 4-aminobenzoate (PABA) along with the release of pyruvate during folate biosynthesis (Figure 2.2). Frameshift deletion in this gene results in premature termination of the protein after 226 amino acid residues. This enzyme has been documented to be an essential enzyme for the growth of Gram-negative bacteria, including important pathogens such as *Pseudomonas*

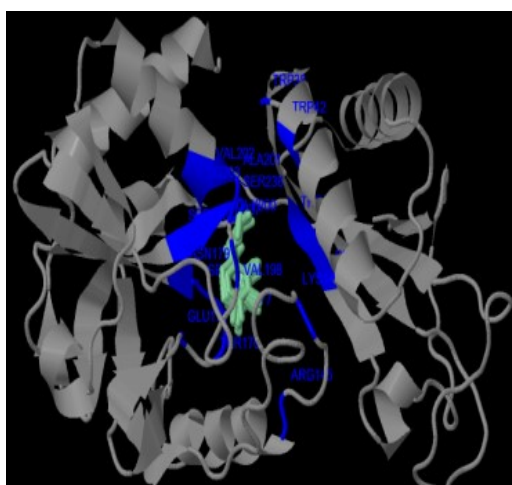


**Figure 2.6:** 3DLigandSite representation of the ligand binding residues (blue) including Ser238

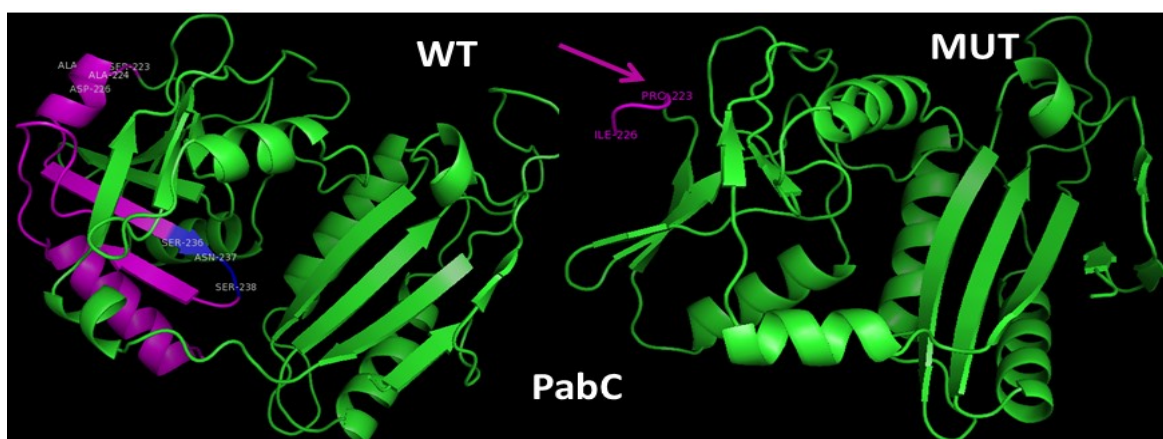


**Figure 2.7:** *Ab initio* model of PabC for wild type (WT) and mutated (MUT) protein *aeruginosa*. The absence of the enzyme in humans and its essentiality in various microbes suggests that inhibition of PabC offers the possibility of new therapies targeting a range



of microbial infections and structural studies provide useful data to assess the potential of this protein for such early stage drug discovery. On performing BLASTp against the PDB protein database, we found that the PabC protein of *C. violaceum* shares maximum homology with the PabC protein of *P. aeruginosa* PAO1, PDB ID 2Y4R (43% identity) (O'Rourke et al., 2011). On sequence comparison, out of the crucial 24 amino acid residues involved in the active site, 7 residues which are strictly conserved among PabC of *P. aeruginosa*, *E. coli*, *L. pneumophila* and *T. thermophilus* (Phe27, Thr29, His43, Arg46, Gly199, Lys140 and Arg202 in pabC\_P.aer) are also conserved in *C. violaceum* with the exception of His43. Ser237 and Asn236 which interact with the PLP phosphate using main chain and side chain groups are also conserved in *C. violaceum* protein. Other residues which interact directly or indirectly with the Lys140-PLP adduct include Phe92, Glu173, Val175, Phe176, Ser177, Asn178, Val197, Val200 and Met201 of which residues 175, 176, 200 and 201 are replaced with Threonine, Methionine, Alanine and Valine, respectively. Further, of those which contribute to the organization of the active site or that participate in solvent mediated interactions between the protein and the cofactor, Glu28, Leu139 and Gln147 are replaced by Arginine, Valine and Serine respectively whereas His141, Arg144, and Glu161 remain conserved. The sequence and structural analysis further shows that truncation as a result of deletion results in premature termination after 226 amino acids in case of *C. violaceum* which is homologous to the loss of amino acid from 225th residue in case of *P. aeruginosa* protein. This presumably shows at sequence level, the loss of two crucial amino acid residues important for the interaction of PLP cofactor with the enzyme. Also, at structural level it seems that there is partial loss of Domain II with 2 alpha helices ( $\alpha 7$  and  $\alpha 8$ ) and one beta sheet ( $\beta 8$ ) truncated. The PLP cofactor is covalently bound to Lys140 that is in domain II and also the active site is formed in a cleft formed between the two domains. So overall the truncation may result in deactivation of the enzyme.

We hypothesize that this loss of function mutation results in the carbon flux diversion towards aromatic amino acid biosynthesis instead of folate biosynthesis and hence directly increases violacein production in *C. violaceum*.

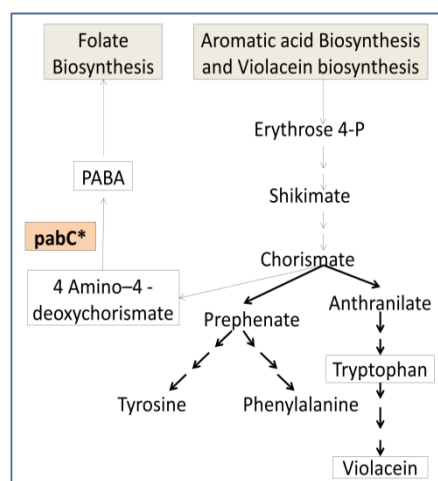


**Figure 2.8:** Schematic representation of the hypothesis, dark arrows represents higher flux towards violacein synthesis

The gene *kdpD* codes for the sensor kinase of the two-component signal transduction system (TCS). Mutation results in premature termination after 682 amino acids. The TCS regulatory protein functions in K<sup>+</sup> homeostasis and also plays a crucial role in virulence and intracellular survival of pathogenic bacteria, including *Staphylococcus aureus*, entero-haemorrhagic *Escherichia coli*, *Salmonella typhimurium*, *Yersinia pestis*, *Francisella species*, *Photorhabdus asymbiotica*, and mycobacteria. (Freeman et al., 2013; Parish et al., 2003).

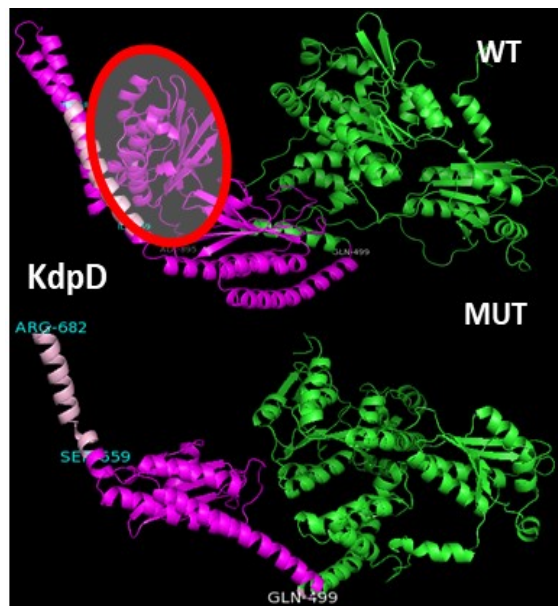


**Figure 2.9:** *Ab initio* model of KdpD for wild type (WT) and mutated (MUT) protein

among Gram-negative bacteria (e.g., *E. coli*, *Salmonella enterica serovar Typhimurium* LT2, and *Clostridium acetobutylicum*) and Gram-positive bacteria (e.g., *Bacillus cereus* E33L, *Alicyclobacillus acidocaldarius*, and *Mycobacterium tuberculosis*). Recently using whole genome sequencing, in case of *V. cholera*, resistant mutants against a particular antimicrobial active structure, vz0825, were reported to have SNP in the gene VC\_A0531 (GenBank: AE003853.1) which encodes for KdpD protein (Sergeev et al., 2014). Quite recently it was reported that streptomycin induces K<sup>+</sup> and glutamate efflux before decrease in viability of cells (Iscla et al., 2014) and also the cytoplasmic C-terminal domain of the *Escherichia coli* KdpD protein, that is found to be truncated in StrpR, functions as a K<sup>+</sup> sensor (Rothenbücher et al., 2006).

The KdpD protein, which has a cytosolic sensor domain and C-terminal histidine kinase activity, spans the bacterial cell membrane, while the other Kdp proteins have an exclusively cytosolic location (Puppe, 1995). In *Escherichia coli*, the Kdp-ATPase is a high-affinity K<sup>+</sup> uptake system and its expression is activated by the KdpDE two-component system in response to K<sup>+</sup> limitation or salt stress (Walderhaug et al., 1992). However, information about the role of this system in many bacteria still remains obscure. Homologue of Kdp protein sequences are found to be widely distributed

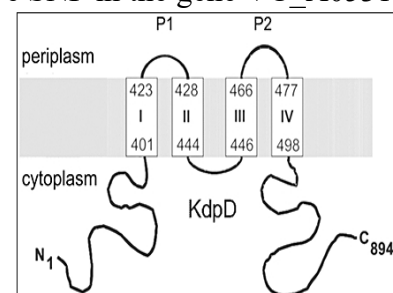


**Figure 2.10:** The  $\Delta$ C499-894 protein functioned as a K<sup>+</sup> Sensor adapted from Rothenbücher et al., 2006

## 2.4. Conclusion

Continuous exposure to the antibiotics at concentrations slightly lower than the MIC, resulted in resistance to the antibiotics. This adaptive evolutionary phenomenon allowed growth on agar plates at high antibiotic concentrations (MIC: 200 µg). Out of 4431 ORFs variation in only 6 ORFs resulted in acquisition of resistance. Classical mutation was observed in ChIR in the repressor of a multidrug efflux pump. Variations in genes that impact different levels of cellular or molecular hierarchy were observed in case of StrpR. In all eight genetic variations resulted in acquired antibiotic resistance against two antibiotics that had different mechanism of action. The resistance phenotypes are not always predictable from genotypes alone. Drug resistance is a function of genetic variation along with metabolic, regulatory and environmental perturbations. Also, acquisition of antibiotic resistance is a complex phenomenon that involved changes in different levels of cellular hierarchy including genome, transcripts and metabolites.



# Chapter 3

## Metabolic Dynamics and Phenotypic Profiling of Antibiotic Resistant Population

*“The essential thing in metabolism is that the organism succeeds in freeing itself from all the entropy it cannot help producing while alive”*

*- Erwin Schrödinger, What is Life?*

### 3.1. Introduction

Darwin’s Theory of Evolution combined with the recognition that the body chemistries of many disparate species were remarkably similar led Claude Bernard to develop his theory of the Milieu Intérieur: “The constancy of the internal environment is the condition of a free and independent existence”. This permanence is due to integrated regulatory mechanisms. This control was eventually termed homeostasis (by behaviorist Walter Cannon) to describe the physiologic processes that, in aggregate, maintain the constancy of the internal chemistries, as well as blood pressure, body temperature, and energy balance.

Metabolic plasticity is an evolutionary “save all ships” response to antibiotic challenge. This chapter discusses the differential metabolic dynamics and phenotypic profiles of ChlR and StrpR compared to WT population. The phenotypic characteristics investigated in this work include Minimum inhibitory concentrations (MICs), growth rate, violacein synthesis, NADH and Proton motive force (PMF). Differential metabolic dynamics is assayed using high resolution liquid chromatography techniques including LCHRMS with MS/MS and AP-MALDI. Different variants of LC-MS have been successfully used to study the effect of antibiotic on the metabolome of certain bacteria (Dörries *et al.*, 2014; Derewacz *et al.*, 2013; Nandakumar *et al.*, 2014).

Of the different phenotypic characteristics assessed in *C. violaceum* population the one used by clinicians as gold standards is Minimum inhibitory concentration (MIC) calculation (Riedel *et al.*, 2014; Andrews, 2001). One of the distinguishing phenotypic characteristics of *C. violaceum* is the violet pigment violacein. Violacein is known to have antibacterial, antitumoral, antiviral, trypanocidal and antiprotozoan properties (Durán *et al.*, 2016). Violacein biosynthesis in *C. violaceum* involves five genes, *vioA* to *vioE*, assembled in an operon (August *et al.*, 2000; Balibar and Walsh, 2006; Sánchez *et al.*, 2006; Shinoda *et al.*, 2007; Hoshino, 2011). The operon is positively regulated by the CviI/R quorum sensing system. The main precursor metabolite for the synthesis of violacein is the amino acid tryptophan (Demoss and Evans, 1959) and the amount of violacein produced is directly proportional to amount of L-tryptophan present when it is limiting (Demoss and Evans, 1959). Production of violacein is also used as microbiological assay for L-tryptophan (Sebek, 1965). In the presence of VioC, oxygen and NADPH, deoxyviolaceinic acid is formed from protodeoxyviolaceinic acid which is converted to deoxyviolacein in a non-enzymatic pathway in the presence of oxygen. If VioD acts on protodeoxyviolaceinic acid before VioC, in the presence of NADPH and molecular oxygen, then it forms protoviolaceinic acid. VioC synthesizes violaceinic acid which later gets converted into violacein by spontaneous oxidative decarboxylation. In the absence of VioC, VioD and NADPH, protodeoxyviolaceinic acid gets converted into prodeoxyviolacein in the presence of oxygen spontaneously. Therefore the two major bottlenecks that may modulate violacein biosynthesis are availability of the substrate tryptophan and the cofactor NADPH.

Promoting Tricarboxylic acid cycle (TCA)/Krebs cycle by glucose and/or alanine activation subsequently increases PMF and NADH stimulating higher antibiotic kanamycin induced death in multi-drug resistant *Edwardsiella tarda* (Peng *et al.*, 2015).

Additionally specific metabolites have been associated with varying degrees of killing antibiotic tolerant pathogens (persisters) by stimulating proton motive force (PMF) and increasing antibiotic uptake (Allison *et al.*, 2011; Peng *et al.*, 2015). In this Chapter we also discuss the NADH estimation and PMF for the different population of *C. violaceum*.

## **3.2. Materials and Methods**

### **3.2.1. Minimum Inhibitory Concentration (MIC) determination**

Antibiotic susceptibilities were determined with EzyMIC<sup>TM</sup> Strips (HiMedia Laboratories, India) on Müller-Hinton agar plates using the manufacturer's instructions. The MICs were further determined using broth micro-dilution method for *C. violaceum* (at 30°C, 180 rpm) according to the dilution method described previously (Wiegand *et al.*, 2008).

### **3.2.2. Effect of varying concentration of antibiotics on growth profiles and growth rate estimation**

All strains were profiled for growth by varying concentrations of antibiotics at 30°C, 180 rpm. Exponential-phase cultures were prepared at 30°C, 180 rpm using a shaker incubator and further used to inoculate 3 mL of LB to an initial OD<sub>600</sub> of 0.1. Antibiotic stock solutions were added to yield desired concentrations of the antibiotic ranging from 0 to 256 µg/mL. Cultures were incubated in a shaker incubator at 30°C, 180 rpm and bacterial cell densities were estimated hourly using a spectrophotometer. Growth profile assays for each *C. violaceum* strain were performed in triplicate using independent starter cultures and antibiotic stocks. Growth rate was estimated graphically from growth curves by plotting the natural log values of OD<sub>600</sub> for each time point and determining the slope by linear regression. A minimum of four time points were used to determine the growth rate.

### **3.2.3. Preparation of Intracellular Metabolite Extracts**

For performing metabolomics experiments, the three different populations of *C. violaceum* were inoculated (10% inoculum of overnight starter culture) and incubated in a shaker incubator at 30°C, 180 rpm for 30 hours (hr). 2 mL of cell cultures were harvested at the end of 0, 6, 12, 18, 24 and 30 hr by centrifugation at 12000g at 4°C for removal of extracellular media. The following steps were carried out on ice. The pellets were reconstituted with ice-cold ethanol for quenching as well as maximal extraction of

metabolite features as used in previous study (Meyer *et al.*, 2010; Letisse and Lindley, 2000). For collecting the extracts, the suspension was centrifuged at 14000 g at 4°C. The intracellular extracts were aliquoted (100 µL) and immediately stored at -80°C till further use.

#### **3.2.4. Spectrophotometric analysis**

The intracellular as well as extracellular extracts were used for violacein estimation with BioPhotometer (Eppendorf) by comparing to standard calibration graphs for quantitation purpose as previously described (Blosser and Gray, 2000).

#### **3.2.5. LC-MS analysis of Intracellular Metabolites**

The intracellular extracts were dried in centrivap (Labconco) at 4 °C, followed by reconstitution in 100 µL of 10% water in acetonitrile containing 4 µM atorvastatin (internal standard). 10 µL of each sample was pooled to prepare a technical quality control (QC) sample. Metabolic profiling of samples was carried out on HPLC-HESI-HRMS. The separation was achieved on Sequent ZIC-HILIC column (100 mm\*2.1 mm\*5 µm, Merck Millipore) column using HPLC consisting of Accela quaternary gradient pump, a degasser and Accela autosampler (Thermo Fisher). The column was maintained at 45 °C using column oven (PerkinElmer). The mobile phase for elution consisted of 0.1% formic acid in deionized water (Mobile phase 'A') and 0.08% formic acid in acetonitrile (Mobile phase 'B'). Gradient was set with 5% of mobile phase A (0-5.0 min, 300 µL/min), 13% A (15.0, 300 µl/min), 45% A (20.0 min, 300 µL/min), 90% A (23.0 min-25.0 min, 300 µL/min), 5%A (27.0-32.0 min, 700 µL/min). Heated electrospray ionization (HESI) source was used as an interface between LC and HRMS instruments. The spray voltage of the source was set at 3.7 kV with capillary temperature 300 °C, sheath gas 45 units, auxiliary gas 10 units, heater temperature 390 °C and S-lens RF at 50 units. The data was acquired in range of 70-1050 *m/z* at resolution of 70,000 FWHM with AGC target 1e6 and injection time of 120 ms. Two technical replicates, each of 5 µL sample volumes were injected during analysis in both positive and negative ion mode. A total of 7 quality control (QC) samples were run at beginning, intermittently and end of the run.



### 3.2.6. LC-MS Data analysis

For data analysis, the Qual browser module of Xcalibur (Thermo) was used for manual inspection of presence of metabolite of interest through accurate mass - extracted ion chromatogram (AM-XIC). A mass extraction window (MEW) of 20ppm around monoisotopic  $m/z$  of possible adduct was used to generate the XIC. After establishing the retention time (Rt) and peak width of respective metabolites as well as internal standard (IS), Tandem Mass Spectrometry (MS/MS) was carried out in respective ion modes to confirm their identities. The MS/MS data was analyzed using fragment search tool in METLIN (Smith CA, O'Maille G, Want EJ, Qin C, Trauger SA, Brandon TR, Custodio DE, Abagyan R, 2005) data base (<http://metlin.scripps.edu>) and Mass frontier 7.0. A data processing method from processing setup module of Xcalibur software was prepared to integrate and generate area under peak data. The peak areas of metabolites were normalized to the area response of uniformly spiked internal standard, atorvastatin (ATV). This ratio is representative of the intracellular metabolite concentration (abundance) after taking into consideration the dilution factor for each sample extract. Principal component analysis (PCA) was used to get an overview of the data and to reduce the high dimension of the data set. For each metabolite, we calculated the temporal variation, using the coefficient of variation (CV):

$$CV = \sigma/\mu \quad (\text{Equation 3.1})$$

where  $\sigma$  and  $\mu$  are the standard deviation and mean of the measurements across the time points respectively.

### 3.2.7. AP-MALDI of intracellular metabolites

It was also estimated on Thermo Q-Exactive mass spectrometer (MS) coupled with an atmospheric pressure - matrix-assisted laser desorption/ionization (AP-MALDI) source equipped with a solid state Nd:YAG laser operating at 355 nm. A mixture of 2,5-dihydroxybenzoic acid (2,5-DHB) and 2-cyano-4-hydroxycinnamic acid (CHCA) was used as a matrix for the analysis. Samples were mixed with internal standard (2,4-diamino-6-methyl-1,3,5-triazine) before spotting on MALDI target plate in 6 replicates. The instrument was operated in full MS scan mode within  $m/z$  50-750 at resolution 35,000 FWHM. Spray voltage at 2.5 kV, capillary temperature at 250 °C, AGC target of 1e6 and 500  $\mu$ s injection time were optimized before beginning analysis. Laser fluence was optimized at 70% and PDF value of 100  $\mu$ s was used with automated rastering motion chosen for data acquisition.

### 3.2.8. AP-MALDI Data Analysis

Data analysis was performed with Thermo XCalibur Qual Browser, mMass (Strohalm *et al.*, 2008) for qualification and in-house software MQ v 5.0 ([www.lidi-ms.com](http://www.lidi-ms.com)) for quantification (Bhattacharya *et al.*, 2014) with a chosen MEW of 20 ppm.

### 3.2.9. Growth profiling on different exogenous carbon and nitrogen sources

*C. violaceum* was cultured overnight, then diluted to a density of 0.002 (OD<sub>600</sub>), mixed with an equal volume of LB that contains different metabolites at a final concentration of 2 mg/mL, except for lactate which was at a concentration of 0.27 mg/mL. *C. violaceum* was cultured in 96-well flat-bottom plastic microplates at 30 °C for 30 hr with or without antibiotic pressure. 30 different metabolites were tested in biological triplicates. The plates were monitored for growth, biomass and violacein using iMark™ Microplate Absorbance Reader (BIO-RAD) at 550 nm and 655 nm at regular time intervals. The amount of violacein and dry cell weight were determined using 550 nm and 655 nm readings and compared to standard calibration graphs for quantitation purpose. Different conditions were tested wherein one set had the respective antibiotics, to which the strains were resistant, from zeroth time point (t<sub>0</sub>) and in the other set, antibiotic was added 6 hr (t<sub>6</sub>) post inoculation. After 30 hr the t<sub>6</sub> set of plates were used to plate fresh LBA plates without any antibiotic to analyze viable colonies after the 30 hr incubation period. Growth rates were measured for the overall 30 hr duration experiment in four different phases: pre-6 hr phase, post 6 hr phase, overall growth rate and a maximum growth rate. Same phase wise analysis for biomass and violacein was also performed. Curve fitting, visualization and analysis of the different plots for this experiment were done using GraphPad Prism Version 6.01 (GraphPad Software, San Diego California USA, [www.graphpad.com](http://www.graphpad.com)). Nonlinear curve fitting was done using Gompertz growth equation (Zwietering *et al.*, 1990) for the growth data points (Appendix 3.1). All the heat maps were generated using MATLAB platform (Figure 3.3).

### 3.2.10. Effect of acyl homo serine lactones on growth profiles and violacein

*C. violaceum* was cultured overnight, then diluted to a density of 0.002 (OD<sub>600</sub>), mixed with an equal volume of LB broth that contains different acyl homoserine lactones (AHLs) at a final concentration of 0.36 μM. *C. violaceum* was cultured in 96-well flat-bottom plastic microplates at 30 °C for 37 hr without shaking with or without antibiotic pressure. Nine different acyl homo serine lactones were tested in biological triplicates.

The AHLs included in this study were N-butanoyl-L-homoserine lactone (C4-HSL), N-hexanoyl-L-homoserine lactone (C6-HSL), N-heptanoyl-L-homoserine lactone (C7-HSL), N-octanoyl-L-homoserine lactone (C8-HSL), N-decanoyl-L-homoserine lactone (C10-HSL), N-dodecanoyl-L-homoserine lactone (C12-HSL), N-tetradecanoyl-L-homoserine lactone (C14-HSL), N-butyryl-L-homocysteine thiolactone (C4 cytl) and N-3-oxo-hexanoyl-L-homoserine lactone (3-0-c6). The plates were monitored for growth, biomass and violacein using iMark™ Microplate Absorbance Reader (BIO-RAD) at 550 nm and 655 nm at regular time intervals. Different conditions were tested where in one set the respective antibiotics to which the strains were resistant were added and in the other no antibiotic was added. After 37 hr of incubation the amount of violacein and dry cell weight were determined using 550 nm and 655 nm readings and compared to standard calibration graphs for quantitation purpose.

### 3.2.11. Effect of antibiotic resistance on heterologous violacein phenotype

Different *E. coli* strains with or without antibiotic resistance were transformed with recombinant plasmid with the violacein operon from *C. violaceum* (Accession number AF172851) inserted into pUC19 vector (Thermo Fisher scientific Cat. no. SD0061) double digested with KpnI/PstI with ampicillin resistance. The strains used included *E. coli* K12, *E. coli* K12  $\Delta trpR$  Kan<sup>R</sup>, *E. coli* K12  $\Delta trpR$  and *E. coli* Lemo21 (DE3). The *trpR* gene, responsible for regulating L-tryptophan expression is knocked out in  $\Delta trpR$  strains resulting in constitutive expression of L-tryptophan, one of them included kanamycin resistance while the other was cured of the kanamycin resistance from the genome. *E. coli* Lemo21 (DE3) contains the plasmid pLemo expression vector driven by T7 RNA polymerase and requires chloramphenicol (30 µg/mL) for maintenance.

**Table 3.1:** Strains used to study the effect of antibiotic resistance on heterologous violacein phenotype

Strain	Genotype	Remarks
<i>E. coli</i> K-12 MG1655	F- lambda- <i>ilvG- rfb 50 rph-1</i>	Wild type strain no antibiotic resistance
<i>E. coli</i> K-12 MG1655 $\Delta trpR$	F- lambda- <i>ilvG- rfb 50 rph-1</i>	Prevent feedback inhibition
<i>E. coli</i> K-12 MG1655 $\Delta trpR$ Kan <sup>R</sup>	F- lambda- <i>ilvG- rfb 50 rph-1</i>	Kanamycin resistance
<i>E. coli</i> limo21(DE3)	<i>fhuA2 [lon] ompT gal (λ DE3) [dcm] ΔhsdS/ pLemo(Cam<sup>R</sup>)</i>	Chloramphenicol resistance

Luria–Bertani (LB) medium was used for all the growth, knockout, transformation and violacein estimation experiments. Ampicillin at a final concentration of 100 µg/mL concentration was used for the transformation experiments for selection and growth of recombinant plasmid containing strains. Luria–Bertani agar (LBA) was used for colony selection and purification. Kanamycin at a final concentration of 15 µg/mL was used for in the knockout experiments for the selection of transformants. All experiments were performed in triplicates until mentioned otherwise. The starting strain for  $\Delta trpR$  knock out was *E. coli* K-12 MG1655. The knockout was constructed by homologous recombination with PCR amplified fragments using the lambda Red recombinase system (Datsenko and Wanner, 2000) using the Quick and Easy *E. coli* Gene Deletion Kit (Gene Bridges) as per the manufacturer's protocol. Primers ATATGCTATCGTACTCTTTAGCG and TGGCGCTGAGTCCGTTTCATAAT were designed containing sequences surrounding the ORF, and these were used to amplify a kanamycin resistance gene flanked by FRT sites. After the induction of pREDET protein synthesis, transformation of PCR product containing FRT cassette into *E. coli* was done using electroporation. The genomic ORF was replaced by the kanamycin gene through homologous recombination, and this gene insert was later removed with an FLP recombinase, using pFLP706, leaving a small scar region in place of the original ORF. The kanamycin resistance gene was not excised after the final gene replacement for *E. coli* K12  $\Delta trpR$  Kan<sup>R</sup>, making it kanamycin resistant. To confirm the genotypes of the knockout strains, primers flanking each knockout site were designed and used to amplify genomic DNA. Amplified fragments were run on a 2% agarose gel with EtBr, and the length of the fragments indicated whether the genes were knocked out (~600 bp), contained the kanamycin insert (~1800 bp), or remained as the wild-type gene.

Transformation of the *E. coli* strains with the recombinant plasmid was done by electroporation as per Eppendorf Eporator® protocol (Protocol No. 4308 915.514 – 04/2002). Briefly, 2.5 mL of fresh overnight culture of *E. coli* K12 and *E. coli* K12  $\Delta trpR$  was inoculated into 500 mL of LB medium. The culture was incubated at 37 °C with shaking to an O.D 600 of 0.5 to 0.6. The culture was then incubated on ice for 15 min and then transferred to pre-chilled sterile 50 mL centrifuge tubes. Cells were harvested by centrifugation at 5,000 g at 4°C for 20 min. The cell pellet was re-suspended in 5 mL sterile ice cold water. Cells were washed twice with original culture volume of ice cold water and centrifuged as above. Supernatant was discarded and cells were mixed in the remaining liquid. These cells were immediately used by aliquotting 100 µl cells into

sterile pre-chilled micro centrifuge tubes. (If freezing the cells for later use, add 40 mL of ice-cold 10% glycerol, mix and centrifuge for 10 min, at 5,000xg and 2-4 °C. Re-suspend the cells in ice-cold 10% glycerol to a final concentration of approximately,  $2 \times 10^{11}$  cells/mL. Aliquot 40-300  $\mu$ l cells into pre-chilled centrifuge tubes and quick freeze on dry ice and store at  $-80$  °C).

Briefly, 50 ng/mL of recombinant plasmid was added to 40  $\mu$ l of each electro competent cells of *E.coli* K12, *E.coli* K12  $\Delta trpR$ , *E.coli* Lemo21 (DE3) separately in sterile micro-centrifuge tubes and properly mixed. This mixture was transferred to a pre-chilled electroporation cuvette. The cells were electroporated at voltage of 1,700V. After electroporation they were immediately mixed with 1 mL medium and 200  $\mu$ l of tryptophan and transferred to a sterile micro- centrifuge tube with micropipette. Cells were incubated at 37°C with moderate shaking for 60 min and 100  $\mu$ l was plated on LBA plates containing ampicillin (100  $\mu$ g/mL) agar plates and were kept for overnight incubation at 37°C. Isolated violet transformed colonies were picked up and streaked on LBA plates containing ampicillin (100  $\mu$ g/mL) agar plates for colony purification. The transformed colonies were confirmed for presence of plasmid using PCR, restriction digestion and sequencing. Upon confirmation, transformants were cultured in LB with ampicillin and further cryopreserved in 25% glycerol.

Loop-full culture of the transformed cells from glycerol stock was streaked on LBA agar plate with respective antibiotics and incubated overnight to obtain isolated colonies of the cells. 5 mL fresh LB medium containing ampicillin (100  $\mu$ g/mL) in a sterile 50 mL tubes (in triplicates) was inoculated with single isolated colony from the LBA and incubated for 16 hr at 37°C on a rotary shaker incubator. This was used as an inoculum for the violacein estimation of the transformed strains. Fresh LB containing ampicillin was inoculated with 10% pre-inoculum (in triplicates) and incubated at 37°C on a rotary shaker incubator for 24 hr. 2 mL culture sample was harvested for spectrophotometric estimation of violacein as discussed in previous section of this chapter. The sample was centrifuged at 12000g at 4°C for removal of extracellular media. The supernatant was collected separately and the pellet was re-suspended in equal volumes of absolute cold ethanol to dissolve the violacein with frequent vortexing to dissolve the crude violacein in ethanol followed by centrifugation at 12,000 g for 10 min at 4°C. Supernatant was collected and the amount of violacein was estimated with BioPhotometer (Eppendorf) by comparing to standard calibration graphs for quantitation purpose as previously described (Blosser and Gray, 2000).

### 3.2.12. NADH and NAD Measurements

NAD/NADH levels of *C. violaceum* cultures (WT, ChlR and StrpR) were measured using a commercially available kit (MAK037, Sigma Chemical, St. Louis, MO, United States) according to the manufacturer's instructions. NAD total (NAD and NADH) or NADH levels are quantified in a colorimetric assay at 450 nm using iMark™ Microplate Absorbance Reader (BIO-RAD). The estimation was performed for four substrates - Glucose, Pyruvate, Succinate and 2-oxoadipate (2oxoADP).

### 3.2.13. Membrane potential measurements

BacLight Bacterial Membrane Potential Kit (B34950, Invitrogen) was used to measure changes in proton-motive force (PMF) induced by different metabolites according to the manufacturer's instructions. Stationary cells cultured in presence of different metabolites were diluted to  $10^6$  CFU/mL and stained with 10  $\mu$ L of 3 mM DiOC2 (3), followed by incubation for 30 min. Samples were analyzed using a BD LSRFortessa SORP cell analyzer flow cytometer (Becton Dickinson, San Jose, CA) with settings optimized according to the BacLight kit manual. Filters used to detect were FITC and Texas Red dye, FSC threshold, 1,000; recorded events, 100,000. FSC and SSC outliers were gated out by visual inspection before data acquisition. The green/red mean fluorescence intensity (MFI) was detected through a 488–530/610 nm bandwidth band-pass filter, respectively. The membrane potential was determined and normalized as the intensity ratio of the red fluorescence (a membrane potential- dependent signal) and the green fluorescence (a membrane potential-independent signal). Proton ionophore (CCCP) was used as a control as it eradicates the proton gradient, eliminating bacterial membrane potential. The measurements were performed for five substrates - Glucose, Pyruvate, 2oxoADP, Maleate and Succinate. Relative PMF was determined in test samples compared to positive control samples (with glucose) and negative control samples (+CCCP).

### 3.3. Results and Discussion

#### 3.3.1. Evolution of antibiotic resistance and fitness

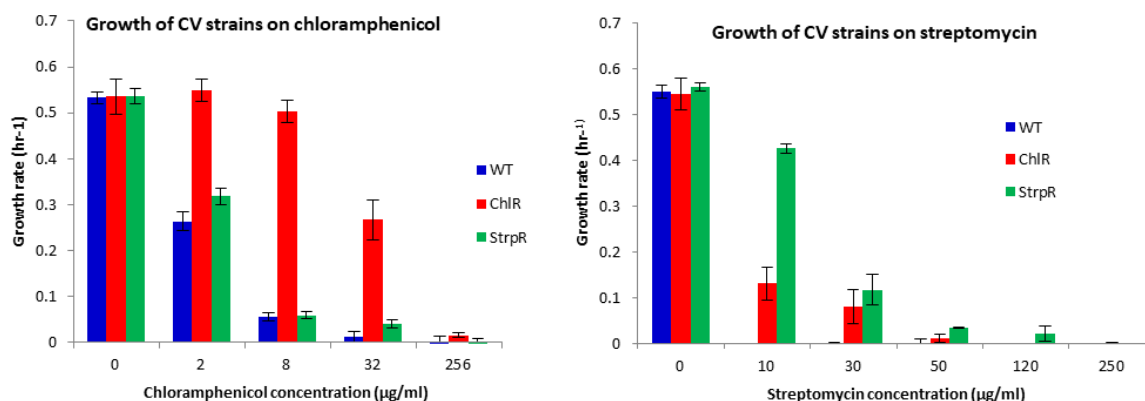


**Figure 3.1:** Growth rate estimation for *C. violaceum* populations

We first analyzed that growth rates and kinetic profiles of the resistant populations support evolution towards fitness on both antibiotics. The effect of varying antibiotic concentration on growth rate was studied (Figure 3.1). The growth rates of the chloramphenicol resistant (ChlR) population was reduced to 50% at 32 µg/mL chloramphenicol, while the streptomycin resistant population (StrpR) growth rate was lowered down to just 15% of that without antibiotic. At even 10 µg/mL of streptomycin the growth rate of the StrpR population was reduced by only 10%. The growth rate exponentially decreased with increasing concentration of the antibiotic in the wild type and evolved resistant populations (ChlR and StrpR). The resistant populations improved in growth rate and biomass yield substantially even in the presence of higher concentrations of antibiotic in contrast to the wild-type (WT). Surprisingly, no fitness costs associated with the acquired resistance were observed in the absence of antibiotics.

**Table 3.2:** MIC estimation for 11 different antibiotics for *C. violaceum*

Antibiotic (µg/mL)	Wild Type	Chl <sup>R</sup>	Strp <sup>R</sup>
Penicillin(Pen)	>256	>256	>256
Ampicillin(Amp)	>256	>256	>256
Ticarcillin(Ti)	240	240	240
Piperacillin/Tazobactam (PTZ)	32	>256	32
Ceftriaxone	>256	>256	>256
Amikacin	4	4	4
Gentamicin	1	1	1
Streptomycin	60	5	120
Chloramphenicol	8	>256	8
Ciprofloxacin	0.006	0.008	0.008
Co-trimoxazole	0.5	1	1



**Figure 3.2:** Differential MIC for WT, ChlR and StrpR for PTZ

Next, we assessed broad-spectrum antibiotic susceptibility for ChlR and StrpR populations via estimation of MIC on 11 different antibiotics (Table 3.2). The chloramphenicol evolved population, ChlR, had an MIC much greater than the wildtype, being able to resist high titers of 256  $\mu\text{g/mL}$  of chloramphenicol. The streptomycin evolved population, StrpR was able to resist twice the amount of antibiotic as the wildtype reaching a titer of 120  $\mu\text{g/mL}$ . StrpR populations showed low MICs for chloramphenicol indicating higher sensitivity. Only the ChlR population showed cross-resistance to Piperacillin/Tazobactam (PTZ) combination (Figure 3.2). Similar trends were observed when MIC values were estimated by broth dilution method (Figure 2.3) for chloramphenicol ( $>256 \mu\text{g/mL}$ ) and streptomycin (120  $\mu\text{g/mL}$ ) and were represented as percentage viability of the cells.

### 3.3.2. Effect of exogenous metabolites and antibiotics on growth

A systematic evaluation of benign microenvironment metabolites in excess of being limiting (Appendix 3.1) showed unique fitness landscapes and associated costs for the evolved and wild type populations (Figure 3.3). Wild type *C. violaceum* (WT) does not show capacity to utilize citrate, oxalate and glyceraldehyde-3-phosphate. Streptomycin (bactericidal) showed a more profound effect on growth, unable to support growth on 50% of the substrates tested while chloramphenicol (bacteriostatic) affected growth on only 7/30 (23%) of the substrates. The ChlR and StrpR populations showed fitness costs associated with growth on 13 and 17 substrates respectively. StrpR populations showed lag for extended period of times on many substrates (consistent with mutations discussed in the next section). Lowered fitness is observed on glycolytic intermediates like fructose-1,6-diphosphate and other TCA cycle intermediates. Strikingly, the ChlR population recorded almost no growth and viability on organic acids maleate (C3), pyruvate (C3), succinate (C4) and 2-oxoadipate (C6) even in the presence of chloramphenicol antibiotic (Figure 3.3d and 3e). The StrpR population exhibited similar growth patterns with the only exception of D-malate (C3) also being able to re-sensitize the resistant population. The null post treatment viability count (Figure 3.3c and 3f) make them ideal candidates for antibiotic therapy for resistant populations.



**Table 3.3:** Altered kinetic parameters represented as growth rates and time lag for *C. violaceum* (WT, ChlR and StrpR) on multiple micro-environment metabolites.

Metabolites	Growth Rates (hr <sup>-1</sup> )					Time Lag (hr)				
	WT+chl	WT+strep	WT	ChlR	StrpR	WT+chl	WT+strep	WT	ChlR	StrpR
Glucose	<b>0.00</b>	<b>0.00</b>	0.71	0.21	1.80			3	9.5	2
Glucose-6-phosphate	0.09	0.01	1.08	0.77	2.23	3	3	2	3.5	2
Glyceraldehyde 3-phosphate	<b>0.00</b>	<b>0.00</b>	<b>0.00</b>	<b>0.00</b>	<b>0.00</b>					
Fructose 1,6-bisphosphate	<b>0.00</b>	0.01	1.14	0.23	0.25		3	1.5	6	10
Fumarate	<b>0.00</b>	0.06	1.55	0.21	0.27		3	1.5	12	13.5
Maleic acid	<b>0<sup>d</sup></b>	<b>0.00</b>	0.60	<b>0<sup>a</sup></b>	<b>0<sup>c</sup></b>			1		
D-Malic acid	0.08	0.01	0.67	1.89	<b>0<sup>b</sup></b>	2.5	15.5	1.5	0	
Succinate	<b>0.00</b>	<b>0.00</b>	1.00	<b>0<sup>a</sup></b>	<b>0<sup>b</sup></b>			2.5		
Oxalic acid	<b>0.00</b>	<b>0.00</b>	<b>0.00</b>	<b>0.00</b>	<b>0.00</b>					
2-Oxoadipic acid	0.04	<b>0.00</b>	0.62	<b>0<sup>e</sup></b>	<b>0<sup>c</sup></b>	0		0		
Malonic acid	0.11	0.03	1.08	0.45	0.17	2.5	2.5	1.5	2	18
Pyruvate	0.41	<b>0.00</b>	0.58	<b>0<sup>e</sup></b>	<b>0<sup>b</sup></b>	4		2.5		
Citric acid	<b>0.00</b>	<b>0.00</b>	<b>0.00</b>	<b>0.00</b>	<b>0.00</b>					
Isocitric acid	0.46	<b>0.00</b>	1.31	0.32	0.32	10		3.5	3.5	12.5
L-Lactic acid	0.29	<b>0.00</b>	0.99	1.05	0.16	3		4.5	4.5	18
Ketoglutaric acid	0.15	0.09	0.19	0.24	0.04	0	0	3.5	0	21
L-Arabinose	<b>0.00</b>	<b>0.00</b>	0.88	0.54	0.29			3.5	3.5	13.5
Mannose 6-Phosphate	0.18	<b>0.00</b>	1.08	0.98	1.68	3		2.5	3.5	2.5
Ribose 5-phosphate	0.28	<b>0.00</b>	0.86	0.33	0.18	2.5		2.5	6	6
3-phosphoglyceric acid	0.29	0.26	0.28	0.40	0.18	2	2	0	6	6
L-Tryptophan	<b>0.00</b>	<b>0.00</b>	0.53	0.23	1.92			2	2	2
L-Alanine	0.21	<b>0.00</b>	0.96	0.28	0.36	2.5		2.5	6	3.5
L-Valine	0.28	<b>0.00</b>	0.74	0.33	0.14	2		2	6	6
L-Aspartate	0.27	0.20	0.19	0.41	0.18	2.5	2.5	0	6	10
L-Glutamine	<b>0.00</b>	<b>0.00</b>	0.83	1.15	0.26			2.5	3.5	13
L-Glutamate	0.52	0.16	1.28	1.12	0.23	3	3	3	3	12.5
Mannitol	0.24	<b>0.00</b>	1.00	0.98	0.20	3		2	3.5	8.5
D-Sorbitol	0.24	<b>0.00</b>	0.58	0.40	0.25	12.5		2.5	6	9.5
Glycerol	<b>0.00</b>	<b>0.00</b>	0.78	0.28	1.99			2.5	9.5	2.5
L-Ascorbic acid	<b>0.00</b>	0.18	0.81	0.23	0.27		3	3	6	12
Luria Bertani	<b>0.00</b>	<b>0.00</b>	0.47	0.37	1.69	3	3	1.5	3	3

Zero growth rates are represented in bold. a - t<sub>6</sub> initial till 180 min ; b - t<sub>0</sub> initial till 180 min ;

c - t<sub>0</sub> first 60 min ; d - 3 to 18 hr growth; e - growth after 24 hr.

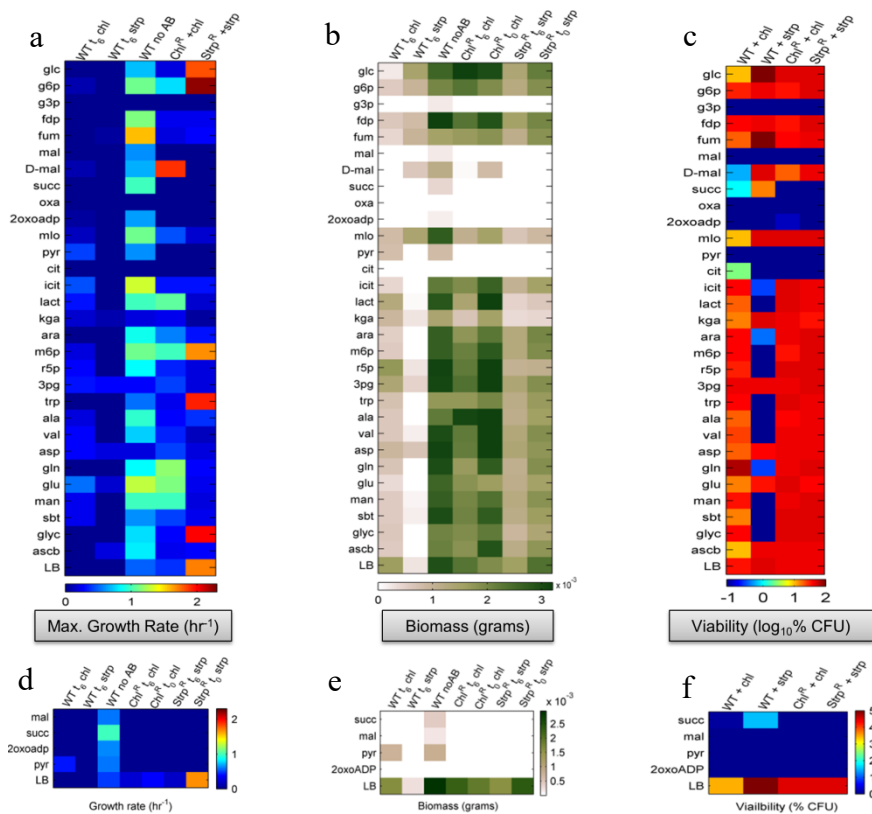


**Figure 3.3:** Heat map showing effect of different metabolites on biomass, growth and viability for the three populations – WT, ChlR and StrpR. a) Exponential growth rates b) Maximum biomass after 30 hr (as cell dry weight). c) Viability (log<sub>10</sub> CFU/mL) after 48 hr in the absence of antibiotics on rich LB media plates. d) to f) Inset showing effect of four metabolites maleate, succinate, pyruvate and 2-oxoadipate re-sensitizing ChlR and StrpR against antibiotics.

### 3.3.3. The metabolic phenotype of resistant populations

#### 3.3.3.1. Differential Violacein levels in resistant populations

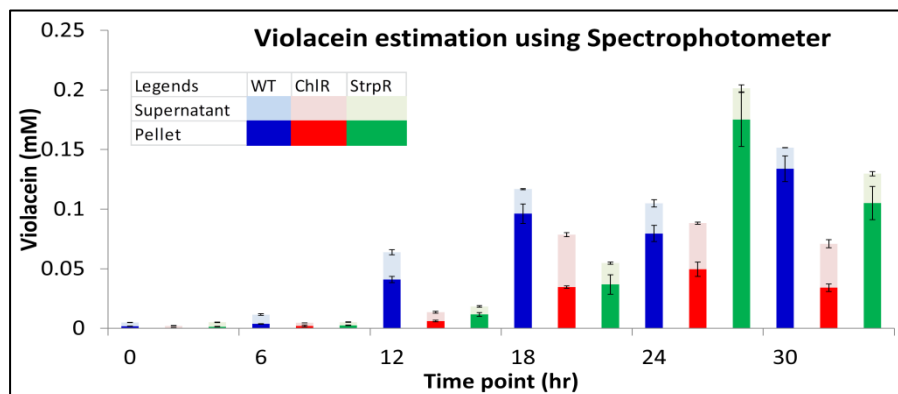


**Figure 3.4:** Violacein quantitation for the three populations across time

Accumulation of violacein was observed after 6 hr of growth. Violacein showed differential abundances in the three populations with >30% increase in StrpR and ~35% reduction in ChlR populations. Extracellular violacein (supernatant) was observed to be higher in case of ChlR.

### 3.3.3.2. Differential metabolic dynamics: LC-MS analysis

To determine the fundamental genotype-phenotype relationship and establish a metabolic basis for antibiotic resistance, intracellular metabolomics profiles were measured using mass spectrometry (LC-HRMS with MS/MS). Including both ion modes, total 126 metabolites were screened. At the end of the analysis, 59 metabolites were finally selected based upon qualification criteria of mass accuracy, MS/MS confirmation, elution profile, reproducibility of response of technical QC samples and biological relevance. Relative abundance was calculated by normalizing metabolite peak area response with that of internal standard (metabolite of interest peak area/internal standard peak area). This ratio is representative of the intracellular metabolite concentration (abundance) after taking into consideration the dilution factor for each sample extract across the three different populations of *C. violaceum*. All the LC-MS and AP-MALDI time profiles (Figure 3.5, 3.10 to 3.12, 3.15 and 3.16) were plotted as relative abundance on Y-axis and time point on X-axis.

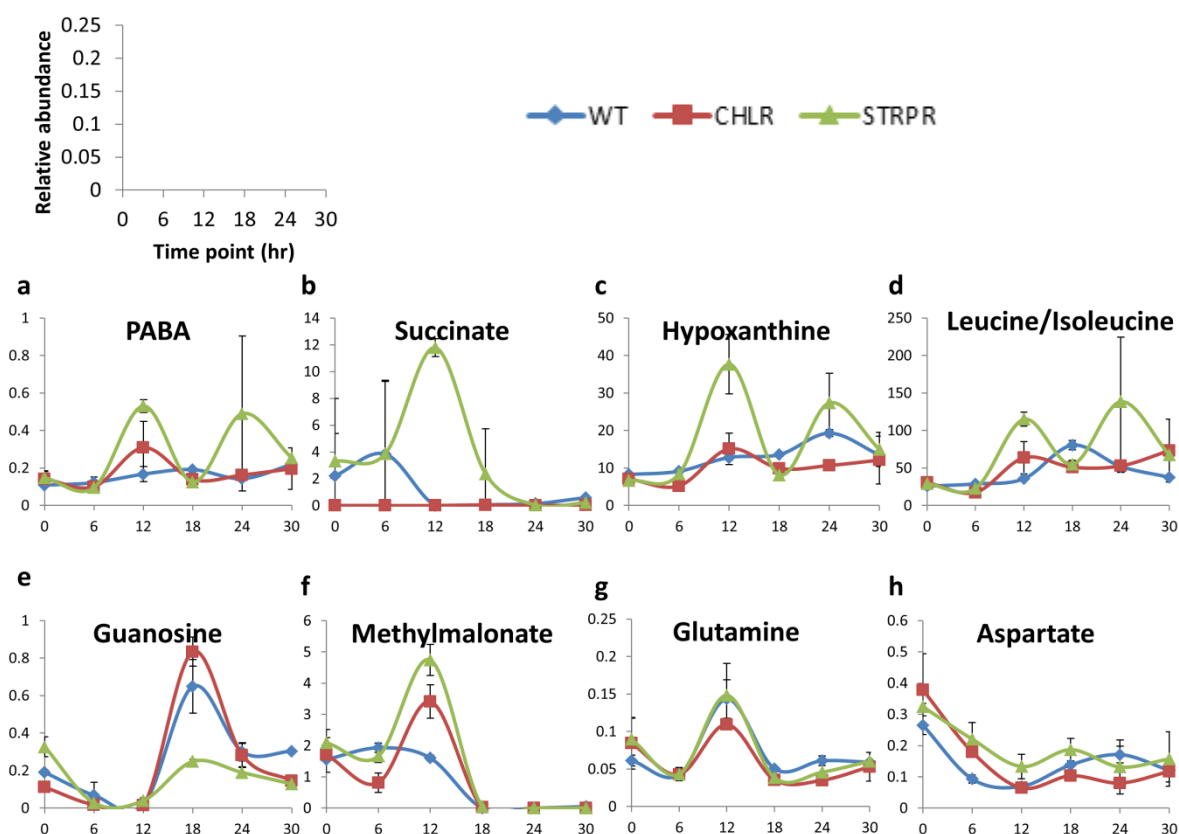


**Figure 3.5:** LC-MS time profiles of metabolites showing significant differences (a - f) as well as negligible changes (g - h) among the three populations

To understand the spread and skewness of the metabolomics data obtained for the three different populations (WT, ChIR and StrpR), the data was represented using box and whiskers plots as explained for Guanosine in Figure 3.6a. Such representation showed that the metabolite relative abundance levels in the three populations span three orders of magnitude intracellularly (Appendix 3.3). 4-aminobenzoate (PABA), succinate, hypoxanthine and leucine/isoleucine vary significantly in their magnitude whereas glutamine, aspartate, guanosine and methyl-malonate vary slightly.

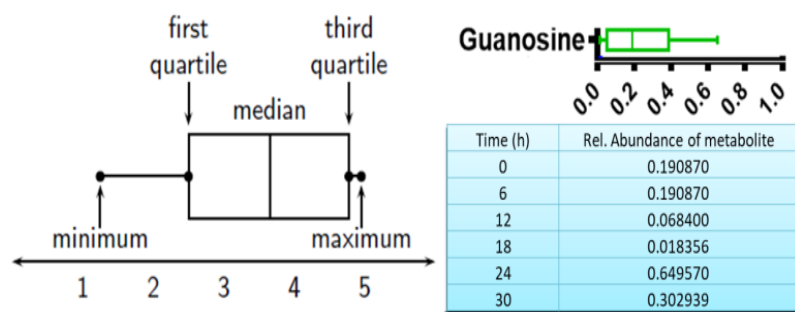


**Figure 3.6a:** Box and whiskers plot explained using guanosine as an example

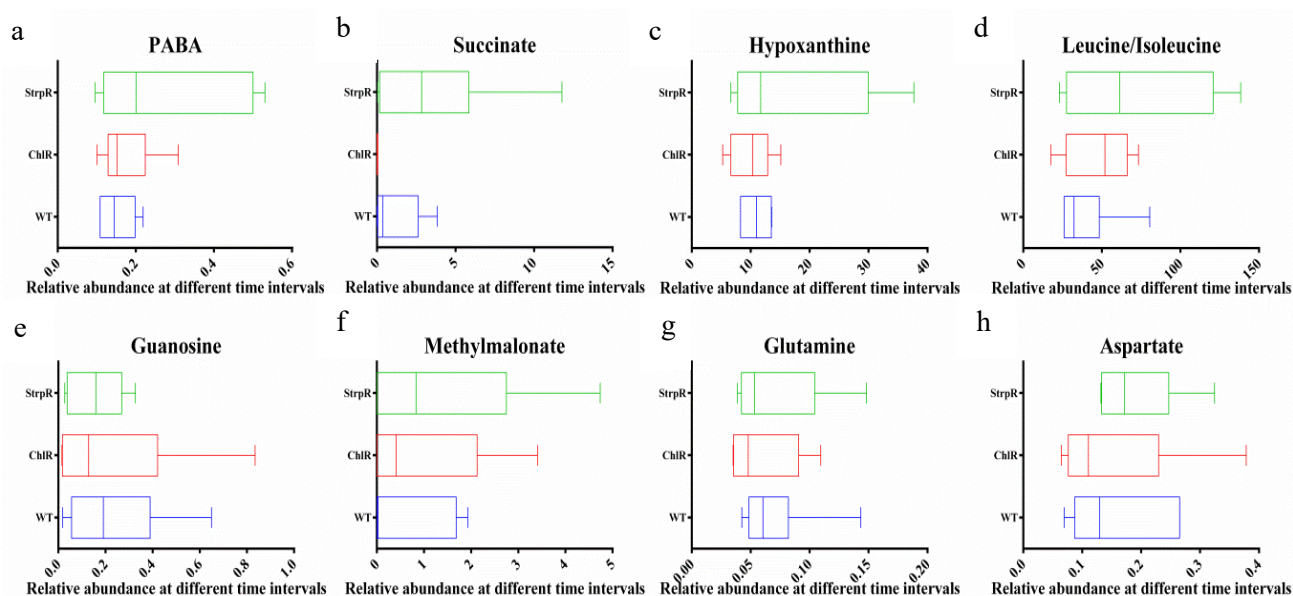


**Figure 3.6b:** Box and whiskers plot for metabolites showing significant differences (a - f) as well as negligible changes (g - h) among the three populations

To validate that the metabolism is different in the wild type (WT) and resistant strains (ChIR and StrpR), Principal Component Analysis (PCA) of quantitative features of metabolites of intermediary metabolism extracted from LC-HRMS data was performed. Score plots of principal components for both biological replicates, show trends that showcase maximum separation of data with respect to different time points (PC1) and also clustering of data points based on susceptibility or resistance to antibiotic (PC3).

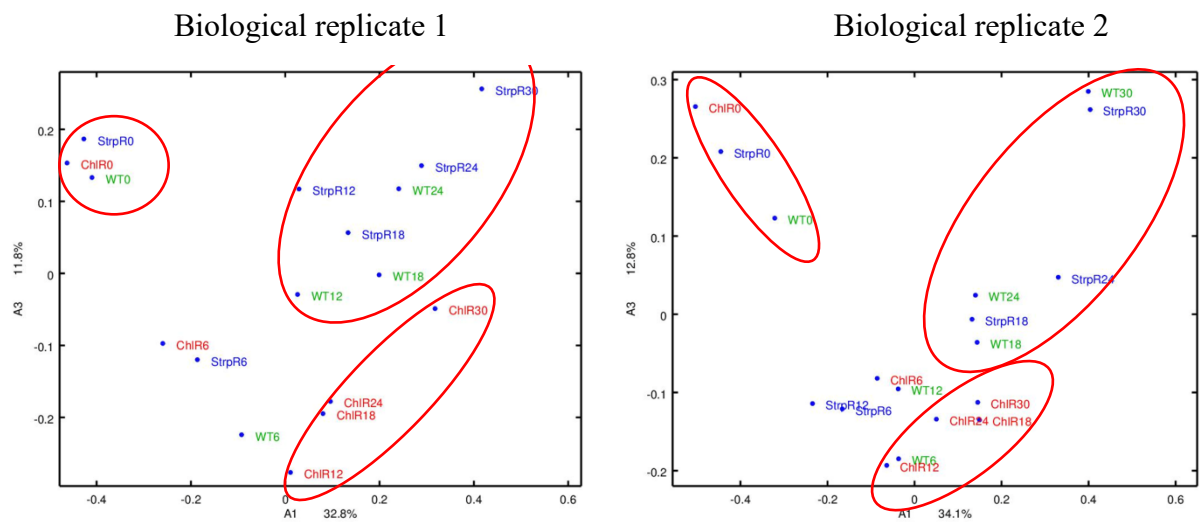


**Figure 3.7:** PCA plots of PC1 versus PC3 for both biological replicates for all three population shows differential features of ChIR compared to WT and StrpR for 12 hr fractions and onwards

Differential expression of features exhibited by ChIR was captured by PC3 in both the biological replicates (Figure 3.8). A significant difference after 6 hr time point in scores of ChIR shows a distinct deviation in metabolic behavior in comparison to the other two populations studied. The ChIR strain shows separation from the WT and the StrpR populations in terms of intermediary core metabolism on glucose as also identified through flux balance modeling that will be discussed in **Chapters 4 and 5**.

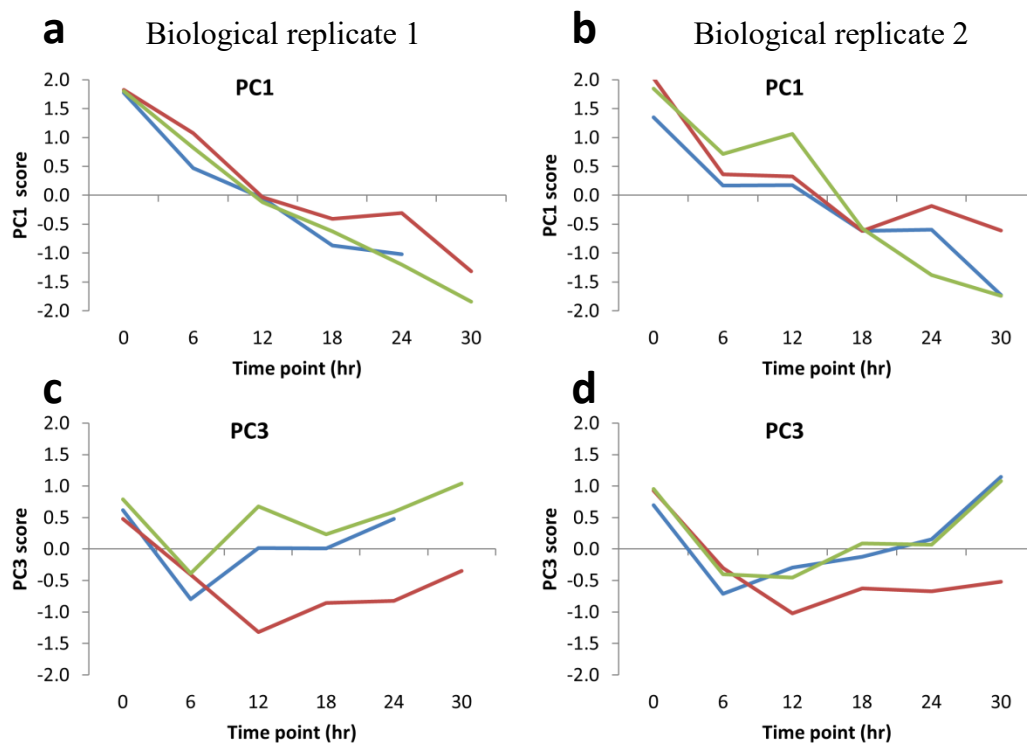
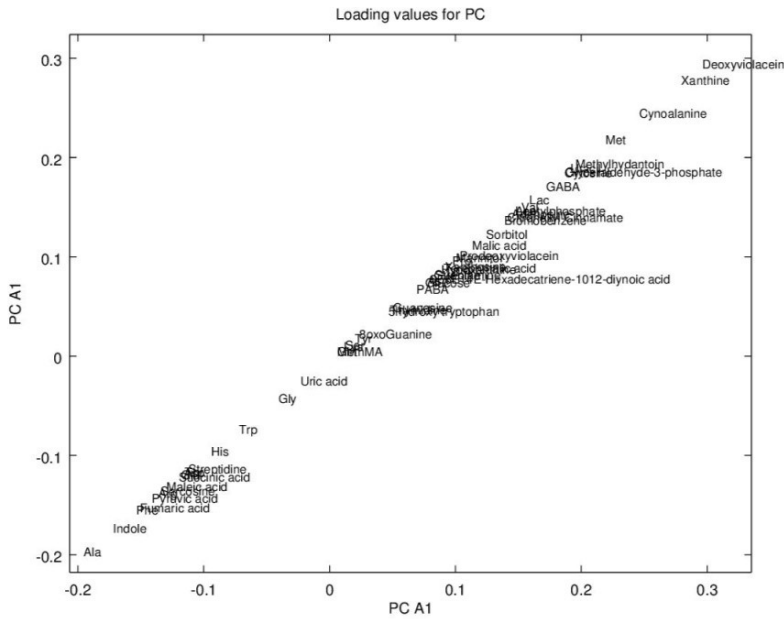


**Figure 3.8:** PCA score trends for PC1 (a and b) and PC3 (c and d) for both biological replicates for all three population



The significant metabolites after almost 30 hr of growth include deoxyviolacein, xanthine and  $\beta$ -cyanoalanine while the metabolites in the early hours of growth include core metabolite candidates like fumarate, maleate, malate, succinate and pyruvate (Figure 3.9).

**Figure 3.9:** PCA plots showing metabolites with higher loading values for PC1 show higher variance across time points

The metabolite abundances also show oscillatory behavior with varying amplitude, period and phase lag. Leucine (Figure 3.5d), lysine and proline (Figure 3.10a and d) had a characteristic oscillatory behavior with a period of 12 hr; also there is phase lag in WT compared to resistant populations. Certain metabolites such as arginine and adenosine (Figure 3.10b and e) showed negligible changes. Intermediate of violacein biosynthesis pathway, prodeoxyviolacein (Figure 3.10 c) was seen to increase linearly only in ChLR whereas it was very low for the other two i.e. WT and StrpR. The presence of prodeoxyviolacein, a precursor only in ChLR potentially explains the lowered violacein through limited availability of cofactor NADPH since tryptophan levels are similar (Figure 3.11e).

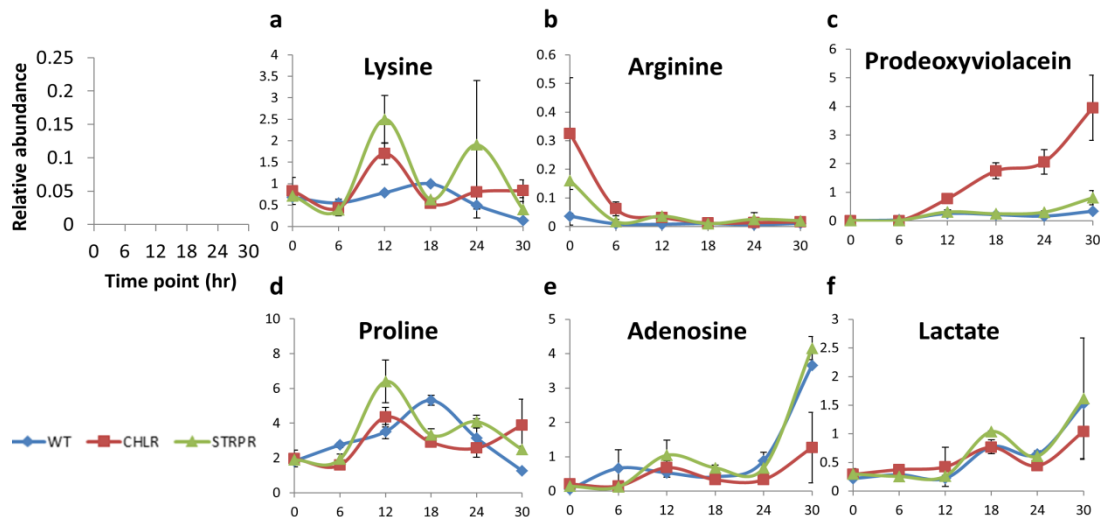
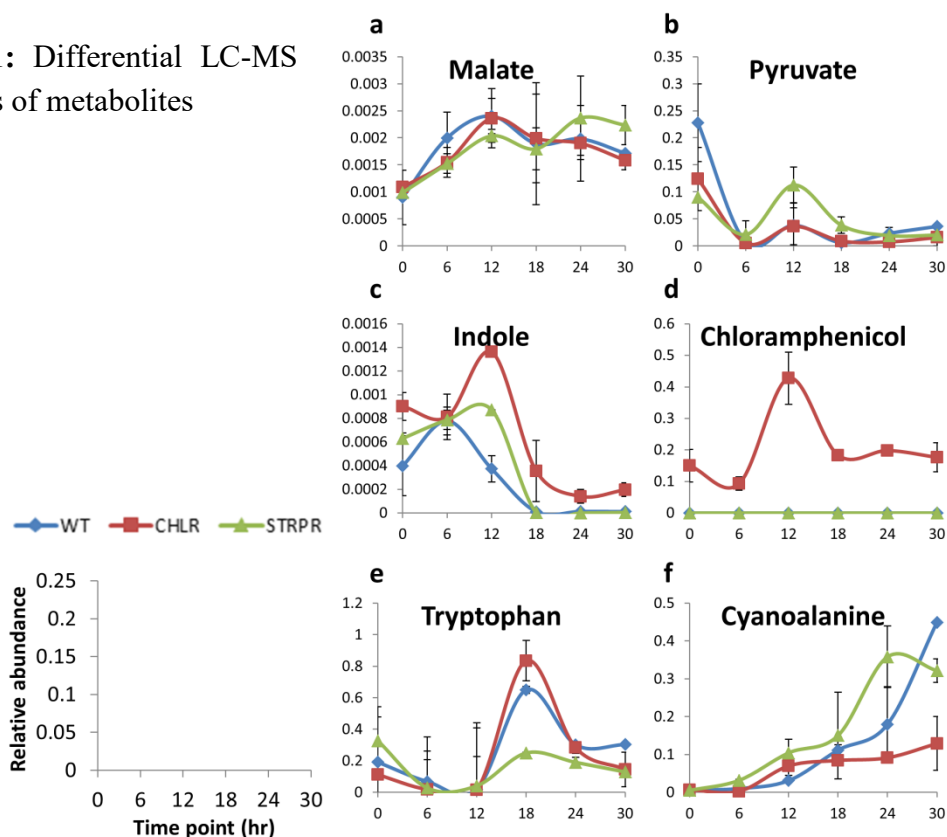


**Figure 3.10:** LC-MS time profiles of metabolites showing phase lag

Chloramphenicol was detected only in ChlR intracellular extracts confirming the uptake of the antibiotic by the resistant population. Additional metabolites that showed differential behavior in case of the three populations WT, ChlR and StrpR were malate, pyruvate, indole, tryptophan and cyanoalanine. Malate accumulated in case of StrpR from 24 hr whereas pyruvate showed significant accumulation in case of StrpR. Indole accumulation was observed to be significant in case of ChlR. Tryptophan accumulation was higher in case of WT and ChlR population when compared to StrpR.

**Figure 3.11:** Differential LC-MS time profiles of metabolites



Increased recycling of nucleotides through salvage pathways was reflected in high levels of adenosine, xanthine and hypoxanthine in the resistant populations (Figure 3.12). 8-oxoguanine, a major oxidized base lesion formed by reactive oxygen species, was higher in the StrpR population indicating potential oxygen radical effects.

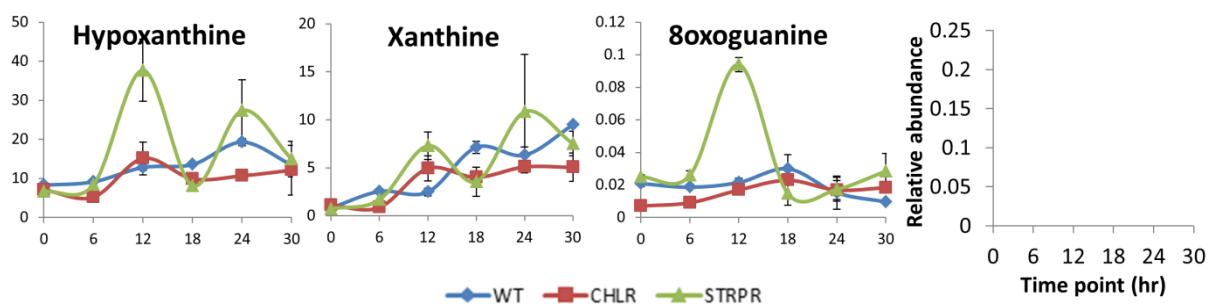


**Figure 3.12:** LC-MS time profiles of metabolites representing nucleotides



The linearized dynamics around the steady-state level of metabolites is captured by the temporal variation (TV, Figure 3.13). Low TV indicating potential growth limitation was observed in malate, glucose, glyceraldehyde-3-phosphate and uracil across all populations. Phenylalanine and methionine are potentially growth limiting (low TV) in ChlR while pyruvate only in StrpR. Tyrosine and serine are less growth limiting (high TV) in the resistant populations than the wild type. Pyruvate and malate showed low average intracellular abundance or had low TV in the resistant populations.

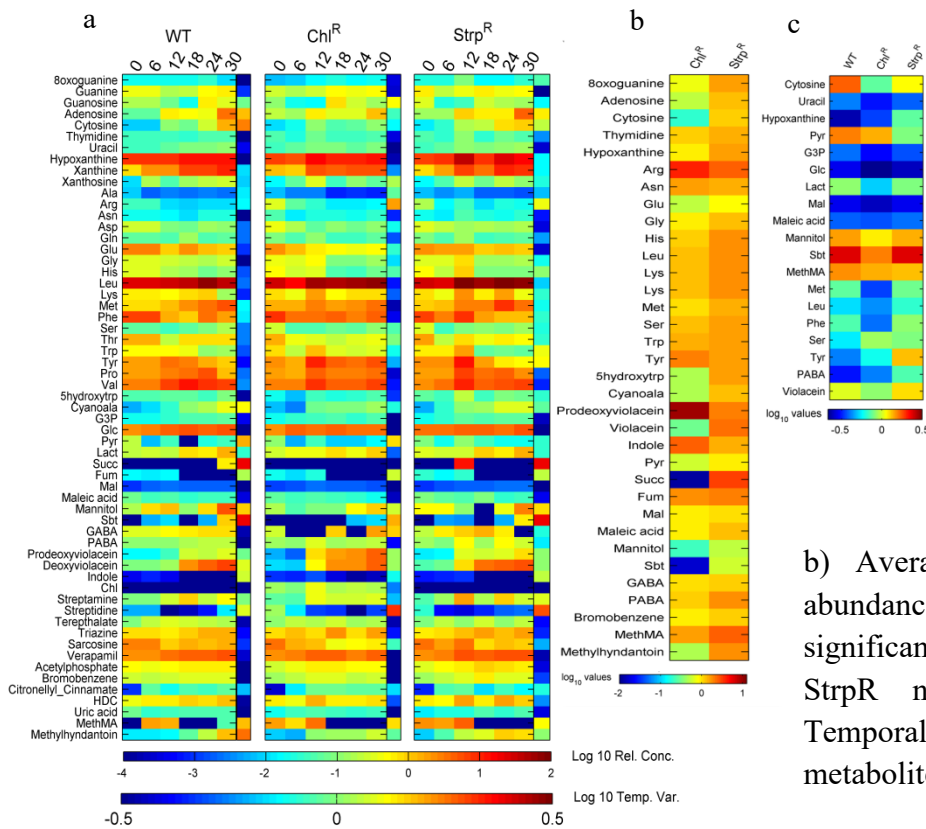


**Figure 3.13:** Heat map for relative abundance and temporal variation for all three populations. a) LC-MS time profiles of metabolites in Y axis and 6 time points on X axis followed by a column representing temporal variation.

b) Average intracellular relative abundance for metabolites showing significant changes in ChlR and StrpR normalized to WT. c) Temporal variation of selected metabolites.

As discussed above profiling various metabolic phenotypes for the three different *C. violaceum* populations we found certain differences and tried to correlate and reach certain trends (Figure 3.14) for the metabolites that showed promise in re-sensitization and killing. ChlR and StrpR have low relative abundance of pyruvate compared to WT in addition to low temporal variation in StrpR. Relative abundance of succinate was found to be low for ChlR compared to WT. Temporal variation for maleate was low for all three strains and relative abundance is low in ChlR.

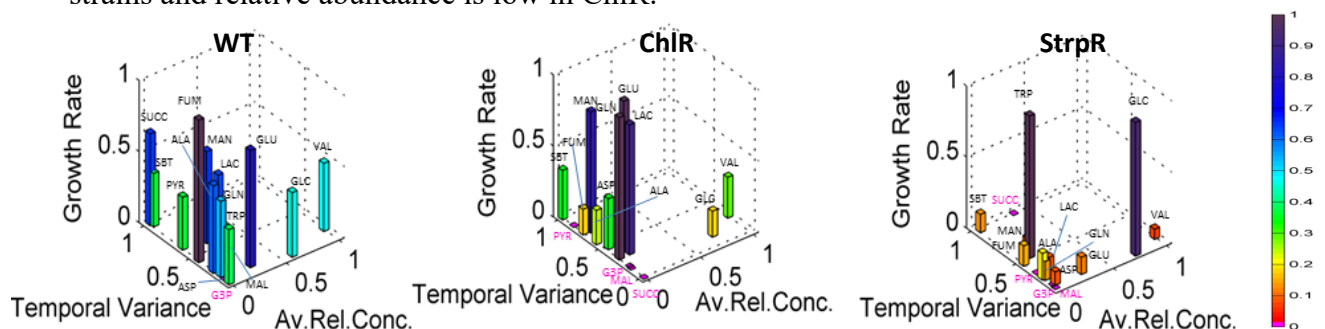


**Figure 3.14:** 3D plots correlating growth, relative abundance and temporal variance of metabolites



### 3.3.3.3. Differential metabolic dynamics: AP-MALDI analysis

Intracellular metabolic profiles were also determined at multiple time points using AP-MALDI Mass spectrometry. Tryptophan levels peaked at 12 hr and correlated to violacein dynamics. Differential time profiles of violacein were identified in ChlR and StrpR strains and Prodeoxyviolacein was detected only in ChlR population.

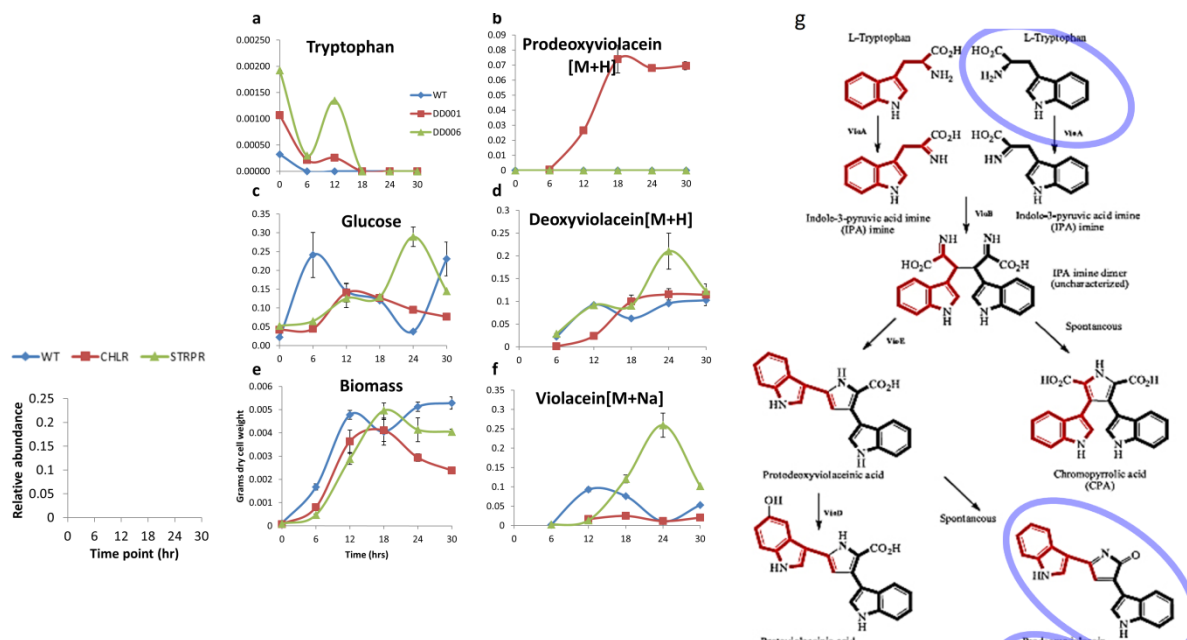


**Figure 3.15:** AP-MALDI time profiles of metabolites representing violacein pathway intermediates (a - d and f) along with the Violacein biosynthetic pathway (g) adapted from Duran et. al., 2012

Characteristic oscillatory profiles were detected in resistant populations for Lysine, Methionine, Phenylalanine and Glucose; concentrations lower in wild type. Wild type susceptible population showed highest levels of Valine and no accumulation of one carbon metabolites such as S-Adenosyl homocysteine (SAH), S-Adenosyl methionine (SAM) and Methionine.

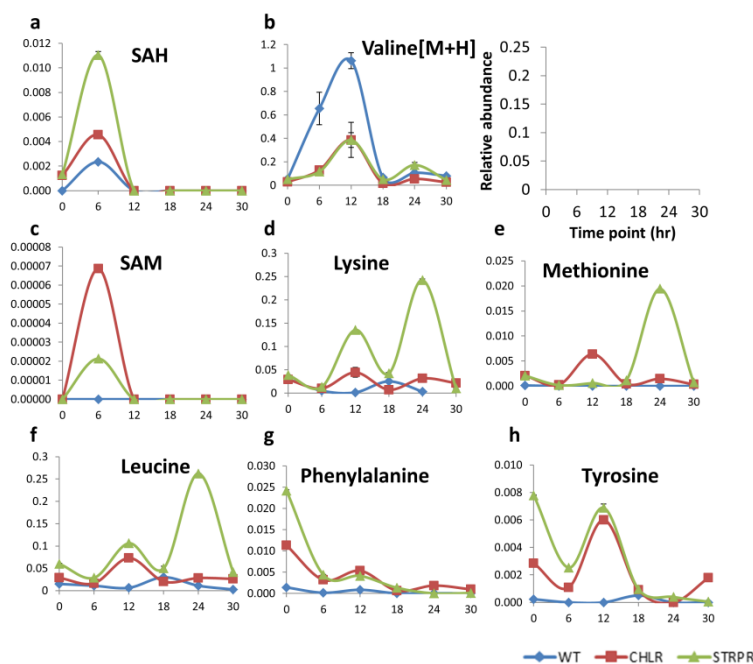


**Figure 3.16:** API-MALDI time profiles of other metabolites

### 3.3.3.4. Effect of acyl homo serine lactones on violacein and growth

As reported in literature WT *C. violaceum* ATCC 12472 showed a stimulatory response when long chain acyl homoserine lactones (AHL/HSL) (C10 – C14) were added to the media in comparison to short chain AHLs (C4 – C8).

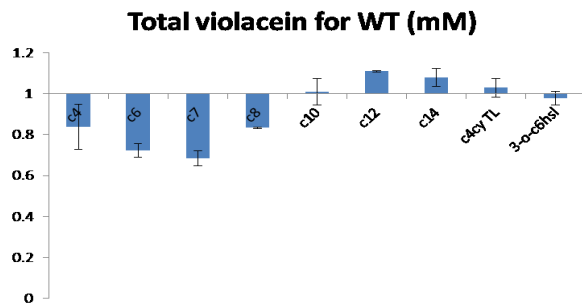


**Figure 3.17:** Total violacein produced by WT normalized to amount of violacein in the absence of AHL. X-axis shows the different AHLs used and Y- axis represents normalized violacein values.

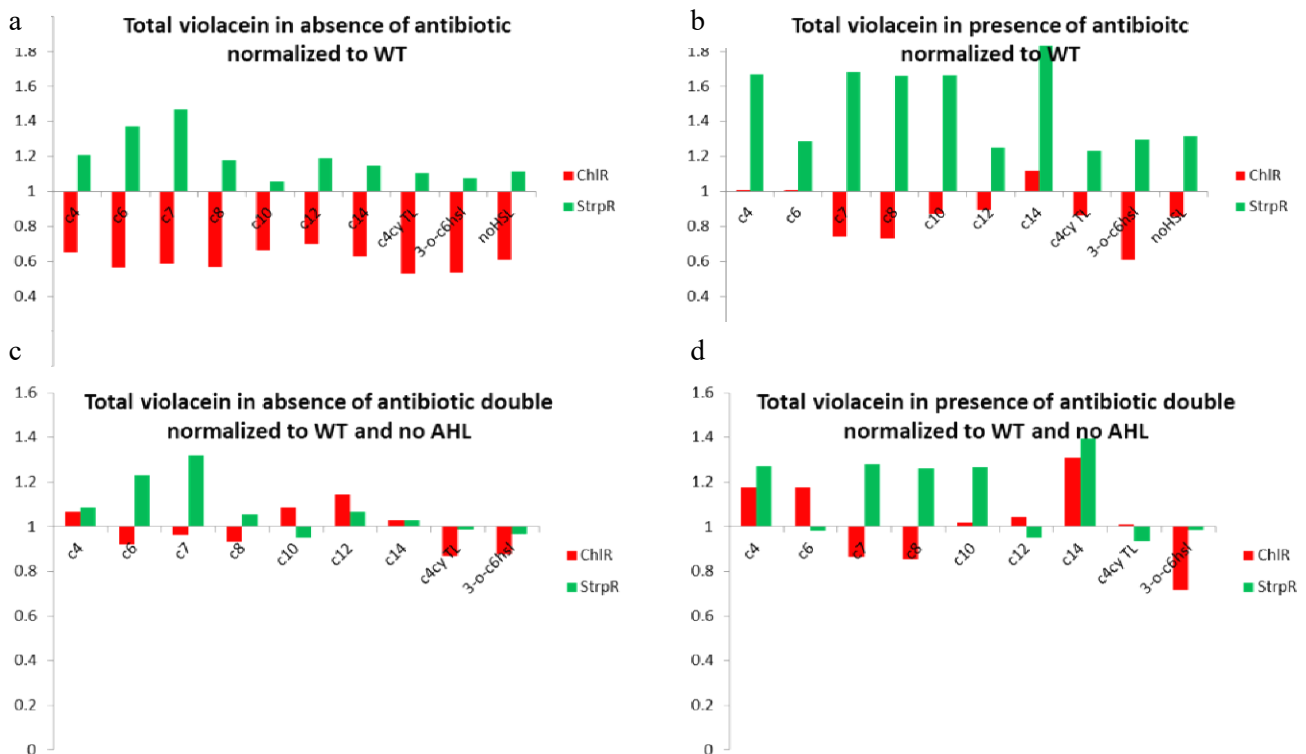


**Figure 3.18:** Total violacein produced by ChlR and StrpR normalized to WT (a,b) and normalized to that in absence of AHL (c,d) in presence (right) or absence (left) of antibiotic. X-axis shows the different AHLs used and Y- axis represents normalized violacein values.

ChlR and StrpR showed differential violacein secretion response towards the AHLs with ChlR showing the highest amounts of violacein in extracellular media in presence of C4 AHL (around 3.4 fold in the presence of chloramphenicol) whereas StrpR showed similar effect for C14 AHL (4 fold in presence of streptomycin). But on comparison of total violacein being produced C14 AHL induced maximum amount of violacein for both the

resistant strains (12% increase for ChIR and 83% for StrpR) and a trend for higher violacein for StrpR and lower for ChIR was observed independent of antibiotic being added in the media or the type of AHL except for C4, C6 and C14 AHLs. In case of C4 and C6 ChIR was capable of producing total violacein similar to WT. In case of C14 AHL ChIR produced 12% more than that of WT. For normalizing the strain specific violacein produced in the absence of any exogenous AHL a double normalization was performed (Figure 3.15) that highlighted the differential violacein features better for ChIR and StrpR. In the absence of antibiotic, we see differential violacein profiles in case of four AHL that include C6, C7, C8 and C10 acyl chains whereas in the presence of antibiotic we see differential violacein profiles in case of five AHL that include C6, C7, C8, C12 and C4cyTL acyl chains. These results definitely show differential behavior of the resistant population of ChIR and StrpR in comparison to WT and need to be further investigated. Similar trends were observed for growth rate and biomass.

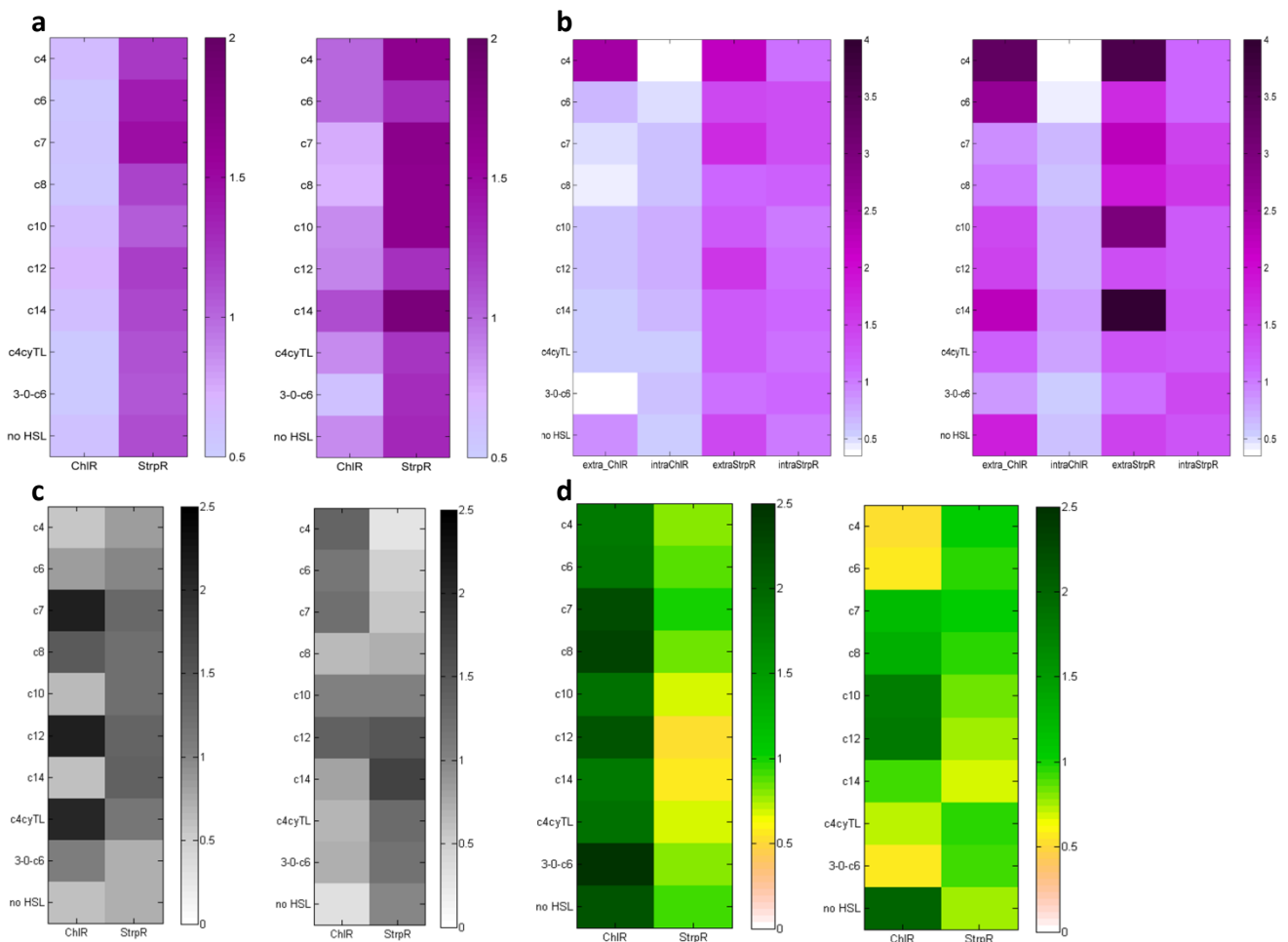


**Figure 3.19:** Heat Map of a) WT normalized, b) double normalized data for violacein (mmol/gDCW, violet) in intracellular (intra) and extracellular (extra) extracts, c) growth rate (grayscale, hr<sup>-1</sup>) and d) biomass formation (yellow to green, grams). In each pair experiment without antibiotic is represented on the left and with antibiotic on the right hand side.

### 3.3.3.5. Effect of antibiotic resistance on heterologous violacein phenotype

There have been two reports (Ahmetagic and Pemberton, 2010, 2011) suggesting the increased heterologous expression of violacein gene cluster along with alpha amylase (*amyA*) gene and urease gene cluster in antibiotic resistant mutants of *E.coli*. The antibiotics that resulted in selection of violacein overproducing strains belonged to the

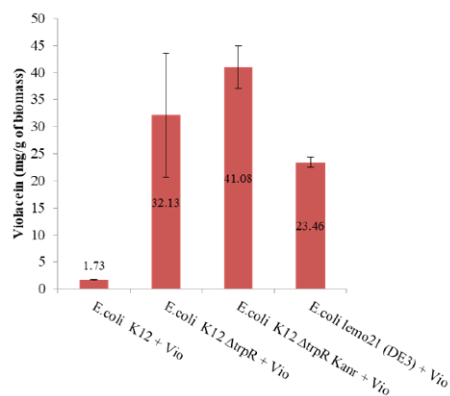


**Figure 3.20:** Violacein estimation in different *E. coli* strains with the violacein operon

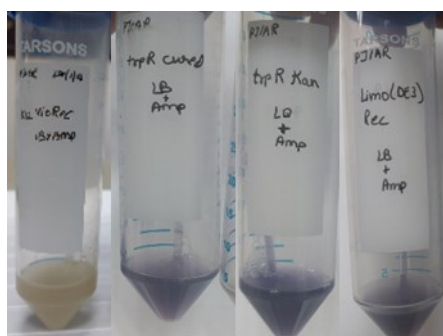


**Figure 3.21:** Culture of different *E. coli* strains with the violacein operon

group of aminoglycosides, rifamycin and lincosamides (Ahmetagic and Pemberton, 2011, 2010). Chloramphenicol was involved in the study yet did not yield in a violacein overproducing strain. To further test and confirm the hypothesis that chloramphenicol resistance reduces the violacein phenotype whereas aminoglycosides such as kanamycin and streptomycin increase the phenotype and put forth the theory as a potential drug resistance biomarker we successfully transformed all the strains with the violacein operon containing plasmid. *E.coli* K12  $\Delta$ trpR Kan<sup>R</sup> showed highest violacein production among all the strains. Kanamycin resistant strain, *E.coli* K12  $\Delta$ trpR Kan<sup>R</sup> showed around 30% higher violacein whereas chloramphenicol resistant, *E.coli* lemo21 (DE3) strain showed 30% lower violacein production. The amount of violacein could increase by two fold for *E.coli* K12  $\Delta$ trpR Kan<sup>R</sup> Rec in the presence of glucose.

### 3.3.3.6. Effect of different metabolites on redox capacity of *C. violaceum*

To establish experimental correlation of redox capacity to effect of antibiotics on *C. violaceum* we estimated the NADH/NAD levels in the presence of the candidate metabolites that showed promise in re-sensitizing antibiotic resistant population of *C. violaceum*. The metabolism of these substrates after their uptake, all involve the use of the cofactor couple NAD/NADH (Fuhrer and Sauer, 2009). By experimental quantitation of the NAD/NADH levels we found out that in the presence of glucose as the carbon source there was an increase in NAD levels (decrease in NADH) in the presence of the antibiotic

chloramphenicol whereas there was a decrease of NAD levels (increase in NADH) in the presence of streptomycin in the media in *C. violaceum* wild type population. The ChlR and StrpR population have evolved to counteract the effect of changes in NAD/NADH levels and hence maintain 3.5 fold higher NADH in ChlR and 2.5 fold higher NAD in StrpR respectively to grow “happily” on glucose in the presence of antibiotic. Therefore, the NAD/NADH ratio maintained in glucose for wild type is 0.25, for ChlR is 0.28 and for StrpR it is 2.47.

On the substrate pyruvate, WT maintains a NAD/NADH ratio of 0.73, i.e. the NADH is 1.5 fold more than NAD levels. Compared to levels in glucose it shows that there is an increase in NAD levels (in glucose NADH is four fold of NAD levels for WT). In case of ChlR (+/- antibiotic) NADH is around 8 fold of NAD levels that shows a disequilibrium in the ratio of NAD/NADH (0.13 on pyruvate as opposed to 0.28 on glucose) required for maintenance of redox homeostasis for the functioning of the cell. In case of StrpR, for functioning on glucose it maintained a NAD/NADH ratio of 2.472 which was not the case on pyruvate as the ratio went down to 0.833, where in NADH was only 1.2 fold of NAD levels compared to NAD being 3 fold of NADH levels in case of growth on glucose. In the absence of antibiotic streptomycin StrpR was still able to maintain a higher NAD level (NAD was 2 fold of NADH levels) similar to that in glucose but on addition of antibiotic in the presence of pyruvate creates a failure to maintain the redox homeostasis required for “happy” growth on pyruvate. The NAD/NADH ratio on pyruvate for wild type is 0.73, for ChlR is 0.131 and for StrpR is 0.833 compared to 0.25, 0.28 and 2.47 respectively in glucose on which they grow “happily” in the presence of antibiotic.

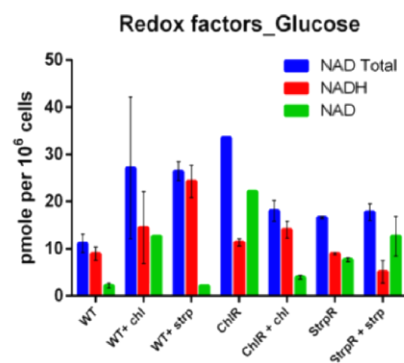


**Figure 3.22:** NAD and NADH estimation for the different population of *C. violaceum* in the presence of glucose

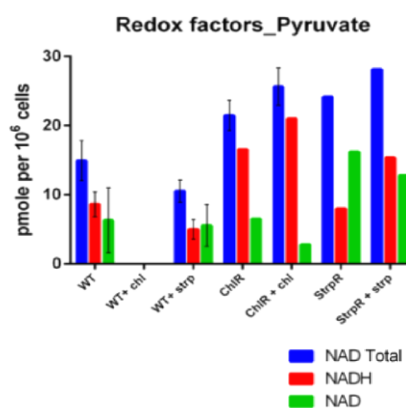


**Figure 3.23:** NAD and NADH estimation for the different population of *C. violaceum* in the presence of pyruvate

In case of substrate succinate, WT maintains a NAD/NADH ratio of 0.373, i.e. NADH is 3 fold more than NAD levels. Compared to levels in glucose it shows that there is an increase in NAD levels (in glucose NADH is four fold of NAD levels for WT). In case of ChlR in presence of chloramphenicol NADH is around 26 fold of NAD levels that shows a high disequilibrium in the ratio of NAD/NADH (0.04 on succinate as opposed to 0.28 on glucose) required for maintenance of redox homeostasis for the functioning of the cell. In the absence of antibiotic chloramphenicol ChlR was still able to maintain a higher NADH level (NADH was 4 fold of NAD levels) similar to that in glucose but on addition of the antibiotic in the presence of succinate creates a failure to maintain the redox homeostasis required for “happy” growth on succinate. In case of StrpR, for functioning on glucose it maintained a NAD/NADH ratio of 2.472 which was not the case on succinate as the ratio went down to 0.563, where in NADH was only 1.8 fold of NAD levels compared to NAD being 3 fold of NADH levels in case of growth on glucose. In the absence of antibiotic streptomycin StrpR had even higher NADH levels (NADH was 13 fold of NAD levels). Presence or absence of antibiotic in the presence of succinate creates a failure to maintain the redox homeostasis required for “happy” growth of StrpR on succinate. The NAD/NADH ratio on succinate for wild type is 0.37, for ChlR is 0.04 and for StrpR is 0.56 compared to 0.25, 0.28 and 2.47 respectively in glucose on which they grow “happily” in the presence of antibiotic.

In case of substrate 2-Oxoadipate (2oxoADP), we were not able to measure the redox capacity of WT. Commenting on the redox capacity of the evolved population of *C. violaceum* ChlR and StrpR we saw a similar trend of failure to maintain the required NAD/NADH ratios in the presence of 2oxoADP as a substrate for growth. In case of ChlR in presence of chloramphenicol NADH is around 3 fold of NAD levels that shows disequilibrium in the ratio of

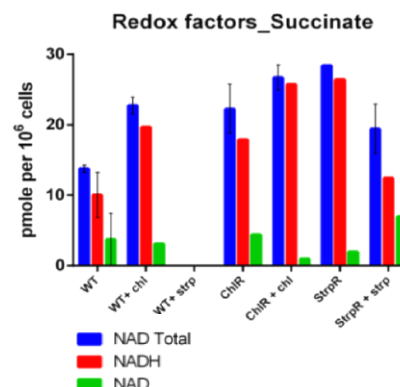


**Figure 3.24:** NAD and NADH estimation for the different population of *C. violaceum* in the presence of succinate

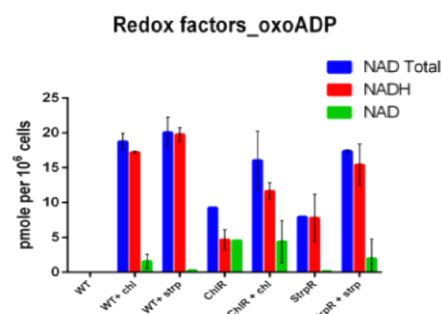


**Figure 3.25:** NAD and NADH estimation for the different population of *C. violaceum* in the presence of 2-Oxoadipate



NAD/NADH (0.38 on 2oxoADP as opposed to 0.28 on glucose) required for maintenance of redox homeostasis for the functioning of the cell. In the absence of antibiotic chloramphenicol ChlR the NAD/NADH ratio was equal but on addition of the antibiotic in the presence of 2oxoADP creates a failure to maintain the redox homeostasis required for “happy” growth on 2 oxoADP. In case of StrpR, for functioning on glucose it maintained a NAD/NADH ratio of 2.472 which was not the case on 2 oxoADP as the ratio went down to 0.128, where in NADH was 8 fold of NAD levels compared to NAD being 3 fold of NADH levels in case of growth on glucose. In the absence of antibiotic streptomycin, StrpR had very high NADH levels. Presence or absence of antibiotic in the presence of 2 oxoADP creates a failure to maintain the redox homeostasis required for “happy” growth of StrpR on 2 oxoADP. The NAD/NADH ratio on 2oxoADP for ChlR is 0.38 and for StrpR is 0.13 compared to 0.28 and 2.47 respectively in glucose on which they grow “happily” in the presence of antibiotic.

Overall the results suggest that in order to grow on pyruvate, succinate and 2-oxoadipate a critical NAD/NADH ratio has to be maintained and failure to maintain the critical NAD/NADH ratio in the evolved population of *C. violaceum* ChlR and StrpR on these substrates make them vulnerable to such antibiotic and substrate combinations. Another trend observed was that the total NAD/NADH pools were increased compared to WT in each of the substrates so definitely there was an effort towards changing the NAD/NADH ratios. Evolved population failed to reach the critical ratio needed to survive the added effect of introduction of antibiotic, candidate metabolites that modulate the redox capacity of the cell and the metabolic reprogramming as an effect of evolution to be resistant to the respective antibiotic.

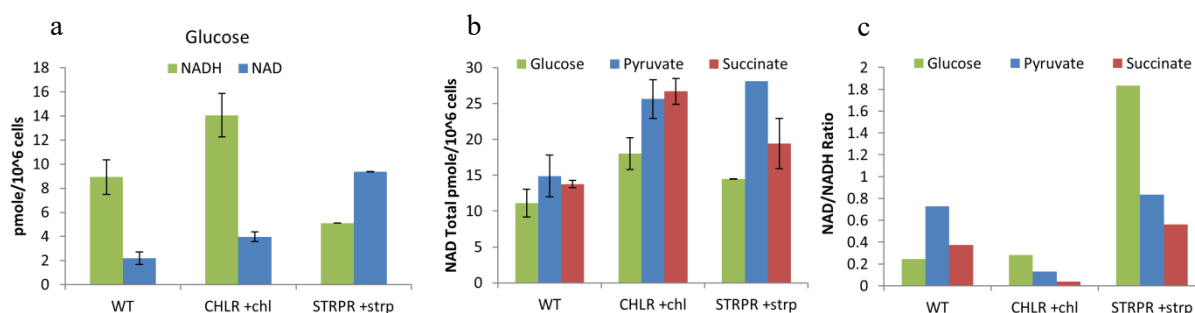


**Figure 3.26:** NADH and NAD experimental values attained for the three different strains using three different metabolites – Glucose, Pyruvate and Succinate. Mean  $\pm$  S.D. for triplicate samples represented.

### 3.3.3.7. Effect of different metabolites on membrane potential

To understand the correlation between redox capacity and proton motif force (PMF) in case of the three population of *C. violaceum* – WT, ChlR and StrpR under the influence of the candidate metabolites Glucose, Pyruvate, 2-oxoadipate, Maleate and Succinate we assessed the membrane potential under different conditions/combinations. In case of glucose we observed there was a significant increase in the membrane potential (10 fold of that without antibiotic) in the presence of the antibiotic chloramphenicol in case of WT population whereas in case of additional of streptomycin antibiotic to WT the membrane potential in the presence and absence of CCCP (proton ionophore) had only a difference of 26% (1/3<sup>rd</sup> of that without antibiotic). This shows a marked difference in the effect of the two antibiotics on membrane potential (PMF) of the cell, one increasing it by ten fold (chloramphenicol) and the other decreasing it by 3 fold (streptomycin) compared to that of wild type growing on glucose. As a coping/evolutionary mechanism for the resistant population we observed that there was a decrease in the PMF for ChlR in the presence of chloramphenicol compared to in the absence of chloramphenicol (1.15 compare to 1.43) which in turn were lower than that for WT (3.55). On the contrary in case of StrpR it tried to compensate for reduction in PMF as an effect of streptomycin by having higher PMF irrespective of presence or absence of the antibiotic for StrpR (3.04 or 4.43) around that of WT.

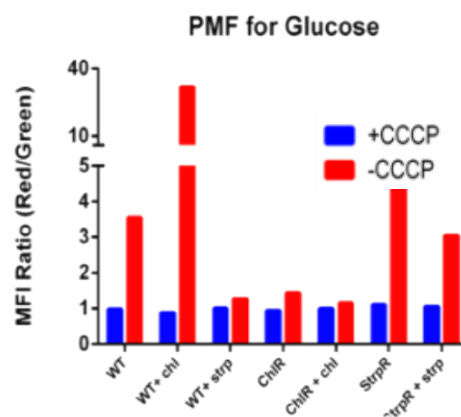


**Figure 3.27:** Membrane potential (PMF) estimation for the different population of *C. violaceum* in the presence of glucose

For three other substrates – Pyruvate, Succinate and Maleate we observed a similar trend wherein the ratio between the test samples (-CCCP) and the negative control (+CCCP) range between 0.73 to 1.26. In other words for these three substrates the variation of the PMF is merely  $\pm 30\%$  compared to depolarized membrane potential. In case of pyruvate the lowest and the highest changes in PMF were observed in case of WT in presence of chloramphenicol (0.74) and in presence of streptomycin (1.26). In case of succinate the lowest and the highest changes in PMF were observed in case of WT in absence of antibiotic (0.84) and ChlR in presence of chloramphenicol (1.22). In case of maleate the lowest and the highest changes in PMF were observed in case of WT in



presence of chloramphenicol (0.73) and StrpR in presence of streptomycin (1.16). These results suggest that the three substrates Pyruvate, Succinate and Maleate definitely do not show significant increase in PMF which may result in higher uptake of antibiotic and eventually killing the cell as reported earlier (Allison *et al.*, 2011; Su *et al.*, 2015; Peng *et al.*, 2015) but there is more to the killing mechanism than just merely changes in the PMF of the cell population.

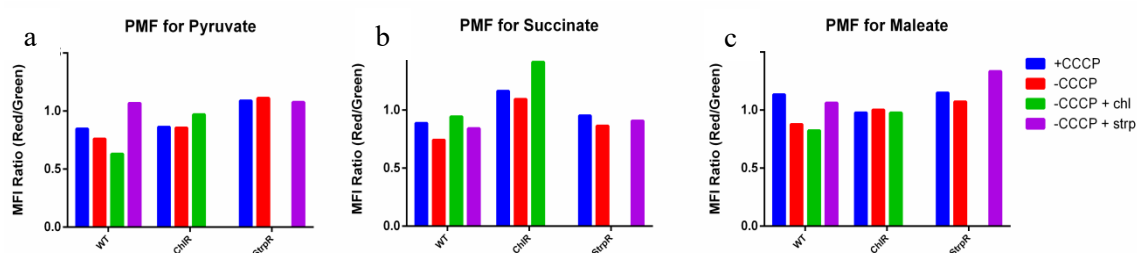


**Figure 3.28:** Membrane potential (PMF) estimation for the different population of *C. violaceum* in the presence of three substrates – pyruvate, succinate and maleate

In case of 2 oxoADP the observations regarding PMF were different compared to the other three substrates discussed above. For WT in the absence of antibiotic the PMF was lower compared to that in the presence of glucose (1.38 compared to 3.55). ChlR in presence of chloramphenicol had a PMF of 2.33 and StrpR in presence had a PMF of 1.8 compared to 1.38 for WT in absence of antibiotic. There was an increase in the PMF for ChlR and StrpR in the presence or absence of antibiotic compared to WT in the presence of 2 oxoADP which may be responsible for higher uptake of the antibiotic that eventually may lead to killing in addition to other causes for the re-sensitization in case of growth on 2 oxoADP for the resistant population of *C. violaceum*.

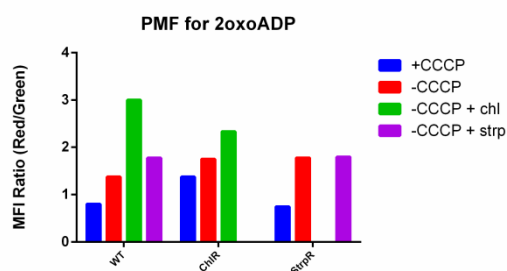


**Figure 3.29:** Membrane potential (PMF) estimation for the different population of *C. violaceum* in the presence of 2-Oxoadipate

### 3.4. Conclusion

Differential phenotype identified in the evolved strains – ChlR and StrpR. Differential temporal variation of metabolites suggests metabolic reprogramming as a survival strategy against antibiotics. Maleate, Succinate, 2-oxoadipate and Pyruvate result in re-sensitization of resistant strains. Phenotypic plasticity and metabolic reprogramming identified in the resistant populations.



# Chapter 4

## Understanding Emergence of Antibiotic Resistance through Integrated Model of Central Metabolism

*“The application of mathematics to natural phenomena is the aim of all science, because the expression of the laws of phenomena should always be mathematical”*

*-Claude Bernard, An introduction to the study of experimental medicine, 1865*

*“Pathology is physiology with obstacles”*

*- Rudolf Virchow*

### 4.1. Introduction

Evolution is a powerful optimizer especially in systems like bacteria with large populations and small generation times. An integral part of systems biology approach towards any problem is the analysis and interpretation of metabolic networks. The assumption being that metabolic network is a cascade of biochemical reactions that involve conversion of a reactant molecule into a product. Such metabolic network models have been extensively used to analyze and predict the cellular phenotype of a biological system and to ultimately apply engineering principles to design cellular metabolic

processes that achieve a desired objective like cellular engineering for production of polyhydroxyalkanoates (Puchałka et al., 2008), predicting drug targets for cancer (Jerby and Ruppin, 2012) or correlate virulence factors to metabolism (Bartell et al., 2017).

The model used in this chapter is a small model of central metabolism (159 reactions) that has been tailored to represent metabolism of *Chromobacterium violaceum*. Although there are advantages of using GSMs, small-scale models offer certain advantages. The main advantage of using a model of central metabolism is that it represents all the core processes that are required for growth and energy production, the two principle dimensions of life. Another advantage is that it can be tailored by addition of subsystems of reactions that are specific to the pathogen under consideration. Reactions are conserved across species like more prevalent pathogens like the ESKAPE pathogens (<http://www.who.int/mediacentre/news/releases/2017/bacteria-antibiotics-needed/en/>) but also more notorious ones like *Francisella*, *Neisseria* etc. This makes the concepts derived from such models potentially scalable and increases overall applicability of the study. Also, the indispensability of the metabolic core for growth makes it prone to several existing antibiotics. This makes select bacterial enzymes in the core attractive and critical targets in the research of antibiotic resistance and drug-target discovery (Almaas et al., 2005).

In this chapter, growth rate is used as a reasonable proxy for ‘fitness’ in bacterial populations being explored. We have assumed that the cell’s ability to survive and to grow has led to the evolutionary selection of its optimal growth in a particular set of conditions under antibiotic selection pressure. In our work we define fitness in terms of the absolute growth rate of the pathogen in a specific environment. On evolution of resistance the microbe clearly benefits in the presence of the antibiotic (increased growth rate). One would expect the resistant bacterium suffer a cost of resistance (i.e. a reduction in fitness) when the antibiotic is absent (reduced growth rates in the absence of antibiotic). We thus define fitness costs in this study as lowering in the growth rates seen in the absence of antibiotic on many carbon sources. Reduced growth rates could potentially arise due to complex changes in bacterial physiology, metabolic shifts, and differential metabolite utilization related to metabolic burden, changes in bacterial virulence, energetic burden to fitness gain (Martínez and Rojo, 2011; Perkins and Nicholson, 2008). We attempt to understand the metabolic basis for such a decrease in growth rates or fitness cost in silico by delineating the interplay between constraints and

objectives, in the context of stoichiometric growth optimality using constraints based modeling (CBM) and Flux balance analysis (FBA) as discussed in Chapter 1.

Evolutionary optimality has been linked to FBA in 2002 (Ibarra et al., 2002). If we want to predict the growth rate in a flux balance model, we have to specify the input rate. FBA simply finds the highest yield  $Y$  such that the growth rate is maximal at the specified input rate. So, even though a rate is maximized in FBA ( $\mu$  in Eq 1), it is through the yield  $Y$  that this is achieved. The underlying biological assumption is that metabolic efficiency (high yield) is the strategy through which the organism reaches its maximal growth rate. Also, growth is calculated in the flux balance model by optimizing an artificial reaction that represents biomass composition that essentially represents the drain on biosynthetic precursors in a stoichiometric amount needed to make 1g biomass.

$$\mu = Y \cdot V_{\text{in,substrate}} \quad (\text{Equation 4.1})$$

Where  $\mu$  is the specific growth rate (units  $\text{h}^{-1}$ ),  $V_{\text{in,substrate}}$  is the uptake rate of the growth substrate (units  $\text{mmol h}^{-1} \text{gDW}^{-1}$ ), and  $Y$  is the yield of biomass with respect to the substrate (units  $\text{gDW mmol}^{-1}$ ).

The sensitivity of an FBA solution is indicated by two parameters shadow prices and reduced costs (Schellenberger et al., 2011). They are assessed in order to understand the effects of changing biomass, ATPM, metabolites and reactions of the different populations of *C. violaceum*. Shadow prices are the derivative of the objective function with respect to the exchange flux of a metabolite. They indicate how much the addition of that metabolite will increase or decrease the objective. Reduced costs are the derivatives of the objective function with respect to an internal reaction with 0 fluxes, indicating how much each particular reaction affects the objective. In addition to the primal solution (optimal fluxes), the linear programming solver provides the corresponding dual solution i.e., shadow price and reduced cost for the FBA problem. Reduced costs assigned to nutrient uptake fluxes give us an indication of the growth-limiting compounds in the medium. To understand the stoichiometric optimality of growth we calculated the yields of biosynthetic precursors and cofactors that eventually constrain the biomass molar yield. Since yields are substrate specific, we calculate a shadow price scaled in terms of substrate units that tell the relative importance of the precursor intermediate in achieving that biomass yield. Three additional sensitivity parameters were also assessed for the core model that included scaled reduced costs, logarithmic sensitivity and gamma redox. Logarithmic sensitivity measures the percentage change in biomass yield in response to percentage change in precursor requirement. Gamma redox is the difference between the

shadow prices for the redox couplets (Acevedo et al., 2014). It is an index of available reducing capacity available to the cell and whether it is limiting or in excess for biomass formation. A positive value suggests available reducing capacity in excess of the optimal demand for growth whereas negative represents growth limitation. A positive value doesn't necessarily indicate accumulation but also suggests metabolic rewiring into overflow metabolism.

Within the optimality-preserving variability at one condition, evolution favors flux distributions that minimize adjustments to other environmental conditions (Schuetz et al., 2012). Pareto optimality analysis (Cheung et al., 2013; Heinken et al., 2013; Nagrath et al., 2007, 2005; Schuetz et al., 2012) was named after its proposer Vilfredo Federico Damaso Pareto (1848-1923), French-born Italian engineer and a founder of welfare economics. It is also called 80/20 principle, Pareto's Law, or principle of imbalance. In this analysis the assumption made involves the observation where a large number of factors or agents contribute to a result, the majority (80%) of the result is due to the contributions of a minority (20%) of factors or agents. It is however a heuristics principle, and has not been proved as a scientific law. Pareto optimality is a versatile tool for flux balance analysis (FBA), allowing exploration of competing objective functions (Schuetz et al., 2012) or competing constraints (Cheung et al., 2013). Biological systems have evolved to operate over a range of conditions that may require competing objectives or constraints, and such competition may be explored by using Pareto optimality analysis. Pareto surface formed from three objective functions (minimization of total flux, maximization of ATP yield and maximization of biomass yield) has been used to better describe  $^{13}\text{C}$ -MFA flux measurements (Schuetz et al., 2012) or to account for maintenance costs of NADPH and ATP in plant cell and better predict metabolic phenotypes under stress conditions (Cheung et al., 2013). Further it has also been used to explain *B. thetaiotaomicron* and mouse mutualistic growth (growth dependencies) using integrated models (Heinken et al., 2013) or to correlate growth rate, and virulence factor production capacities in *P. aeruginosa* during chronic cystic fibrosis lung infection (Oberhardt et al., 2010). Pareto front analysis was used to understand the sensitivity and trade off that exists between the cofactors NADH, NADPH, ATP in the context of growth optimality.

## 4.2. Materials and Methods

### 4.2.1. Constraints based modeling of *C. violaceum* central metabolism: Network reconstruction

Stoichiometric network analysis based on the constraint-based modeling framework has been proven to be a valuable tool to study cellular metabolism and phenotypic capabilities of many organisms (Varma and Palsson, 1994). In the small-scale central metabolic model of *C. violaceum* presented here, a manually curated stoichiometric network reconstruction and model that allows probing special characteristics of this bacterium. It was done using available literature data (Balibar and Walsh, 2006; Creczynski-pasa and Antônio, 2004; Demoss and Happel, 1959; Ryan et al., 2008) as well as information from databases such as KEGG, Biocyc, Metacyc. Further information from the in-house developed whole genome scale model of *C. violaceum* (discussed in Chapter 6) was also used to compile the violacein biosynthesis reaction list, including reaction stoichiometry, reversibility, sub-cellular localization, and gene locus/loci for each reaction comprising core metabolism. The biomass equation for the model was also modified in order to take into account for tryptophan contribution towards biomass production. For all simulations maximization of the biomass equation was fixed as the objective function until mentioned otherwise. The model was initially validated using a set of 10 substrate utilization BIOLOG GN2 plate data existing in literature (Lima-Bittencourt et al., 2011; Martin et al., 2007; Young et al., 2008).

Further a set of constraints that define the antibiotic susceptible WT and differentiated the evolved populations (ChlR and StrpR) were determined. The constraints used in different simulations included (i) Substrate (Glucose) uptake rates (ii) Growth yields (iii) Violacein secretion (iv) ATP maintenance costs associated with molar growth yields of each strain as discussed (Table 4.2). The specific growth rates were calculated using 1g biomass as the basis. The growth yields thus calculated were compared across the three strains. The goal of the simulations was to understand the flux distribution *in silico* and the sensitivity of growth yield to various precursors with specific reference to the cofactors NADH, NADPH and ATP. Constraints based flux balance analysis (FBA), as described in the following section, was used to simulate for growth (maximize biomass objective function) and violacein production. Constraints-based methods were used to perform a comparative analysis between the susceptible and resistant populations to understand the connections between metabolism and resistance.

Implementation of the central metabolic reconstruction for *C. violaceum* and constraints-based analysis was done using COBRA Toolbox 2.0.2 (Schellenberger et al., 2011) with MATLAB v 7.11, (R2010b) and TOMLAB/CPLEX v7.7 optimizer. MATLAB codes for all referenced COBRA functions are available at the COBRA's website (<https://opencobra.github.io/>).

#### 4.2.2. Flux Balance Analysis and Associated Sensitivity Parameters

Flux-balance analysis (FBA) is a method for assessing the systemic properties and cell behaviors of a metabolic genotype. In short the primal FBA problem, Equation 4.2 describes the steady-state mass balances of the biochemical reaction network (Orth et al., 2010; Price et al., 2004)

$$\begin{aligned} & \text{Maximize } Z = c^T v && \text{(Equation 4.2)} \\ & \text{Subject to } S \cdot v = 0 \\ & v_{LB} \leq v \leq v_{UB} \end{aligned}$$

where  $c$ ,  $v$ ,  $v_{LB}$ , and  $v_{UB}$  are vectors of length  $n$ , and  $S$  is the  $m \times n$  stoichiometric matrix. Mathematically, the  $S$  matrix acts as a linear transformation between the vector that defines fluxes through  $n$  reactions in the biochemical network and the vector of the time derivatives of the concentrations of  $m$  metabolites involved in these reactions. The fundamentals of FBA have been widely reviewed (Acevedo et al., 2014; Feist et al., 2009; Reed et al., 2006; Schellenberger et al., 2011).

The function `optimizeCbModel()`, in COBRA toolbox was used for maximization of pathogen growth or biomass by fixing the objective function to be the biomass equation in the model.

Shadow prices and reduced costs (Schellenberger et al., 2011) - were also assessed. In the COBRA Toolbox, shadow prices and reduced costs can be calculated by `FBA_solution.y`, the vector of  $m$  shadow prices and the vector of  $n$  reduced costs is `FBA_solution.w`.

Scaled reduced costs (Maarleveld et al., 2013) and Logarithmic sensitivity coefficient (Varma and Palsson, 1993) were also calculated as shown in Equation 4.3 and 4.4 which better assess the sensitivity taking into account the substrate and growth yield. The logarithmic sensitivity coefficient ( $D_i$ ) represents the sensitivity of each precursor yield to its biosynthetic demand whereas scaled reduced costs ( $W_i$ ) are used to assess the limiting reactions.



$$W_i = (v_i \cdot w_i) / Z \quad (\text{Equation 4.3})$$

$$D_i = dX/dM \cdot dM \quad (\text{Equation 4.4})$$

In Equation 4.3  $v_i$  is the flux through a particular reaction having a  $w_i$  reduced cost associated with it.  $Z$  is the objective function value, in this case being biomass. Similarly, in Equation 4.4  $dX/dM$  is the associated shadow price to a particular metabolite and  $dM$  is the coefficient of the metabolite in the objective function equation.

Another sensitivity parameter, gamma redox, the difference between the shadow prices for the redox couplets (NADH/NAD) and (NADPH/NADP) were calculated (Acevedo et al., 2014).

$$\gamma_{\text{redox(NADH/NAD)}} = \nu_{\text{NADH}} - \nu_{\text{NAD}} \quad (\text{Equation 4.5})$$

$$\gamma_{\text{redox(NADPH/NADP)}} = \nu_{\text{NADPH}} - \nu_{\text{NADP}} \quad (\text{Equation 4.6})$$

### 4.2.3. Flux Variability Analysis

Flux variability analysis (FVA) was utilized to investigate the resulting space of feasible flux distributions (Mahadevan and Schilling, 2003). FVA can be set up in COBRA toolbox using the function `fluxVariability()`. One can thus determine the minimum and maximum flux value that each reaction in the model can take up while satisfying all constraints on the system for a specific objective. The objectives under consideration for this study include optimal growth. These will be considered as forced or fixed fluxes. Differences in these unique forced fixed rates in resistant populations as compared to wild type indicate metabolic reprogramming. To highlight the differences between the antibiotic sensitive and resistant populations, we classified reactions in the network based on their minimum and maximum flux values and assigned categories that reflect their rigidity or flexibility. Nine categories can thus be mapped onto the flux variability map based on the magnitude and direction of the flux (Table 4.1) ranging from category 1 for forward direction (positive fixed) fixed flux, i.e. minimum and maximum flux values were same, a non-zero positive value to category 9 wherein the minimum and maximum flux was zero (blocked). Specific attention was paid to reaction rates that were uniquely determined (i.e. if upper and lower boundaries as computed by FVA coincide; Categories 1 and 4). Changes between such rigid fluxes (1 and 4) to more variable flux capabilities (2,3,5,6,7 and 8) would reprogram the metabolic network by either changing the direction of equilibrium or modulating magnitude and span of the reaction rates.

**Table 4.1:** Nine Categories defined for FVA analysis

Category	Flux through the reaction	Min	Max	Flexible/Rigid
1	Positive fixed	+a	+a	Rigid
2	Positive variable	+b	+a	Flexible
3	Zero to positive	0	+a	Flexible
4	Negative fixed	-a	-a	Rigid
5	Negative variable	-a	-b	Flexible
6	Negative to zero	-a	0	Flexible
7	Negligible	small <sup>†</sup>	small <sup>†</sup>	Flexible
8	Reversible	-a	+a	Flexible
9	Blocked	0	0	Rigid

a,b >0; -a, -b <0 and a > b, † -0.001 > small < 0.001

#### 4.2.4. Dynamic Flux Balance Analysis

Dynamic flux balance analysis (dFBA) was utilized to qualitatively predict the outcomes of growth in batch culture conditions matching our experimental condition (Varma and Palsson, 1994). The resistant populations ChlR and StrpR needed to be assessed for the onset of overflow metabolism and secretion patterns as observed in FVA simulations. The dFBA can be set up in COBRA toolbox using the function `dynamicFBA()` (S A Becker et al., 2007). It is an implicit iterative process wherein at each iteration; FBA is used to simulate for growth, nutrient uptake and by-product secretion rates using an initial concentration for nutrients, which are in turn used to calculate biomass and nutrient concentrations in the culture at the end of the step. The same values are used to calculate maximum uptake rates of nutrients for the next time step.

#### 4.2.5. Pareto front analysis using NADPH and NADH oxidases

The Pareto front, the set of Pareto optimal solutions identified by constraining the glucose consumption rate, violacein secretion rate and the biomass production rate to experimental values and maximizing the fluxes through the generic ATPase (ATPM), NADPH oxidase and NADH oxidase reactions. Analysis of Pareto fronts and trade-off between ATP, NADH and NADPH maintenance reactions (NADH oxidase and NADPH oxidase, not generally present in *C. violaceum*) was performed to understand the

modulation of NADH/NAD ratios or NADPH/NADP ratios in growth. A reaction representing each, the NADH oxidase and NADPH oxidase (water forming) with the right balance of protons and oxygen were added to the model based on a recent report that uses a NADH oxidase enzyme system to delineate the role of NADH imbalance and show decoupling of electron transfer via ETC and proton pumping for ATP synthesis (Titov et al., 2016). These reactions essentially act as drain reactions if there is excess NADH or NADPH in the system.

### **4.3. Results and Discussion**

#### **4.3.1. Network Reconstruction of central metabolism of *C. violaceum***

To delineate a metabolic basis for the emergent resistance, the heterogeneous components of resistant genomes and elucidated metabolic physiology were integrated into a constraints-based flux balance model. A central metabolic network reconstruction represented by the genotype of *C. violaceum* iDB149 was developed (Figure 4.1 and 4.2). The network reconstruction represents the core metabolism for the pathogen including glycolysis, pentose phosphate pathway, TCA cycle, electron transport and basic amino acid metabolism. Although, primarily a generic reconstruction of central metabolism, it includes the virulence factor metabolism, tailoring it to mirror *C. violaceum* metabolism. It includes detailed amino acid metabolism of specifically tryptophan, due to its direct connection with the production of violacein, a virulence factor specific to this pathogen. A biomass equation was defined as a drain on metabolites present in intermediary metabolism and macromolecules in the precursor biomass based on *E. coli* and *Chromobacterium* legacy data. This biomass composition is kept constant throughout the analysis and between strains.

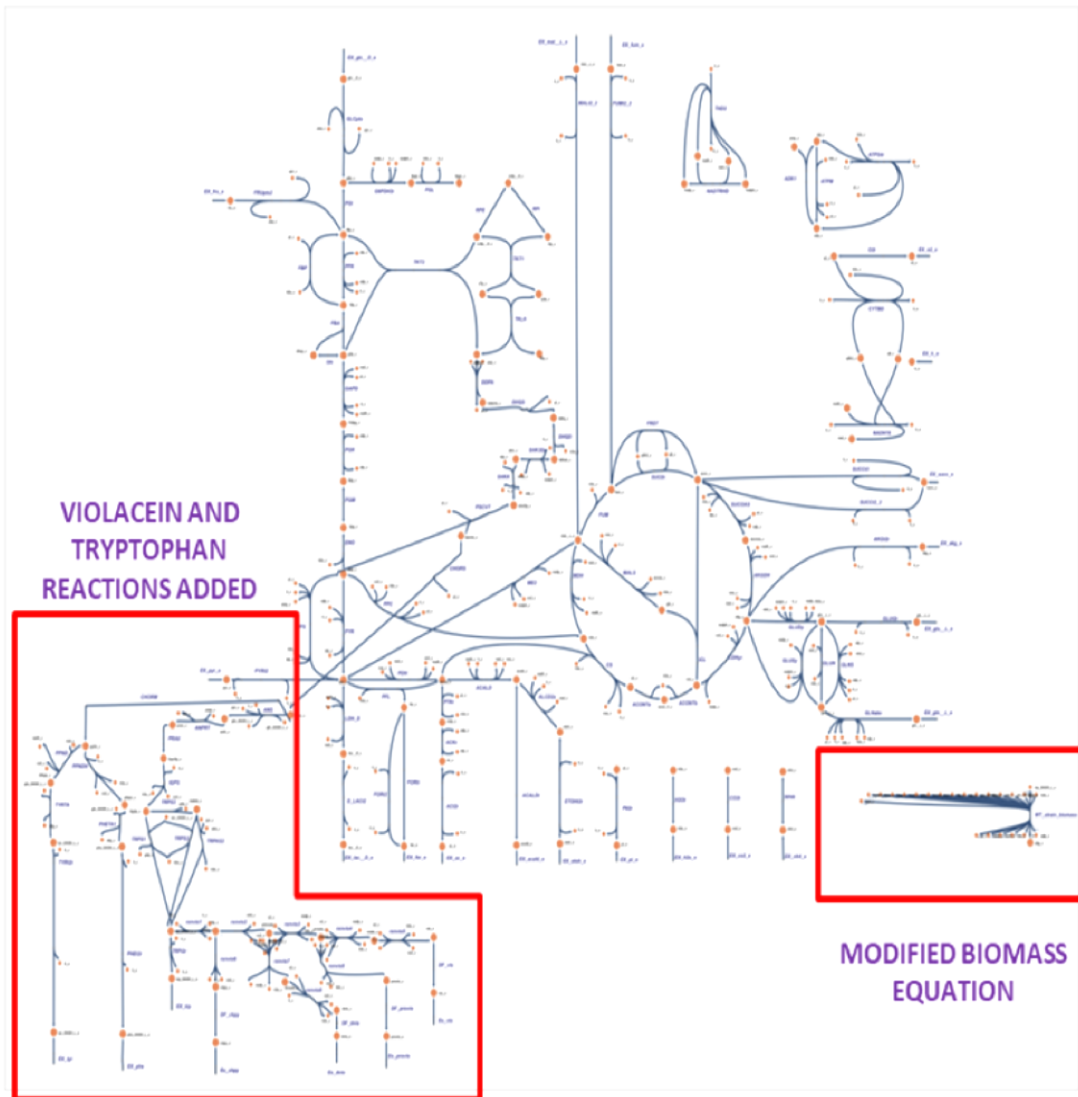


**Figure 4.1:** The core model *iDB149* visualization using Escher

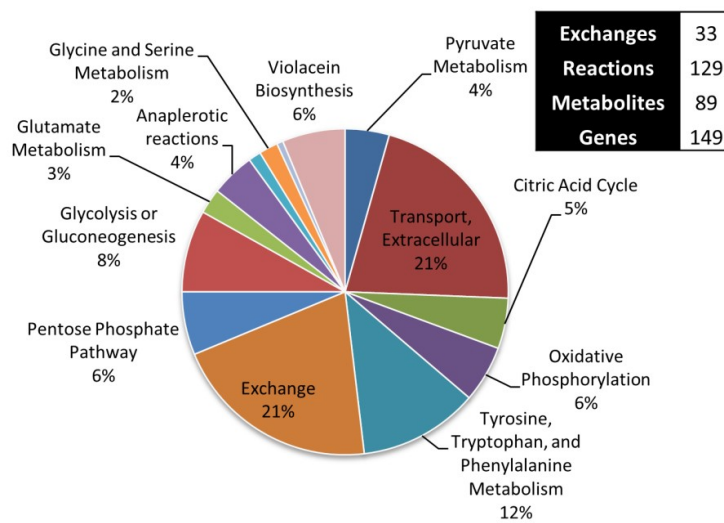


**Figure 4.2** Model statistics and subsystem wise classification for *iDB149*

### 4.3.2. Flux balance analysis and associated sensitivity parameters

Molar growth yields calculated based on experimental glucose utilization data and the maximum growth yield for *C. violaceum* (Table 4.2) was used to estimate the growth-rate independent energy ATP maintenance flux (Varma and Palsson, 1994) ( $v_{ATPM}$ ) that represents the energy required to sustain basal cellular activities. The value fitted from growth yield curves differed for the wild type and the resistant populations due to varying molar growth yields (Table 4.2). The differential violacein phenotype (represented as a production/secretion rate constraint) calculated from experimental data was used to define resistant populations in silico. Based on the sensitivity analysis of violacein production and growth yields, a trade-off exists between the production of violacein and biomass production. Fixing this biosynthetic demand as a critical constraint in the model, growth rates (via growth yields) predicted for both resistant ChlR, StrpR and WT populations were consistent with experimental data. The experimental rates used for the simulations were from the exponential growth phase of the three different populations of *C. violaceum*. With these constraints determined by experiments, the wild type model was tested for prediction of carbon source utilization patterns using experimental legacy data (Lima-Bittencourt et al., 2011; Martin et al., 2007; Young et al., 2008) of Biolog™. The model being a core metabolic model was validated for utilization of carbon sources that had transporters included and growth against a small subset of substrates was accurate. Further, the sensitivity of the yields to different biosynthetic demands, maintenance and changes in fluxes were probed. Shadow prices in the solution of the linear optimization problem of Flux balance analysis (FBA) define the sensitivity of the objective function with respect to each constraint indicating the utility of the metabolite in accelerating growth. Growth, as an objective in FBA, is defined as multiple simultaneous demands on precursors to make macromolecules related to biomass. In this context, a scaled shadow price for metabolites and scaled reduced costs for reactions that account for substrate and the growth yield are better sensitivity indicators (Table 4.3). In order to understand the effects of changing biomass composition, a logarithmic sensitivity coefficient (Varma and Palsson, 1993) that represents the sensitivity of each precursor yield to its biosynthetic demand was calculated for each of the 14 precursors of biomass. The logarithmic sensitivity for cofactor NADH is the lowest in the ChlR populations followed by StrpR and differ from wild type at molar yields. The 25% decrease in scaled shadow price values indicate that a compensation for that particular cofactor must have taken place during evolution resulting in a higher yield of that cofactor in the evolved strains for the

already achieved higher growth and biomass yield. The logarithmic coefficients show that NADH and NADPH as compared to ATP may potentially play a role in increase in biomass yields through changing biomass composition. The reduced costs of each reaction indicate their significance in increasing the objective (growth). The alpha-keto glutarate dehydrogenase (AKGDH) reaction in the ChlR strain while the isocitrate lyase (ICL) reaction in the StrpR strain have scaled reduced costs associated with them.

**Table 4.2:** Constraints used in this study for simulation of growth for the three different populations of *C. violaceum* using *iDB149*

Model	Glucose uptake rate	Violacein secretion rate	Molar growth yield	ATPM	Biomass
WT	9.99	1.49	0.0312	6.24	0.23
ChlR	10.532	0.673	0.0314	9.74	0.327
StrpR	12.777	0.702	0.0504	5.69	0.644

Units for Glucose uptake rate and Violacein secretion rate are mmol/gDW/hr whereas hr<sup>-1</sup> for Biomass and gDW/mmol of glucose for Molar growth yield

**Table 4.3:** Sensitivity parameters assessed using FBA - Scaled shadow prices, Logarithmic sensitivity and Maximum reduced costs

	Metabolite	Maximum Precursor Yield (M)	Shadow price in BOF (dX/dM)	Coefficient in BOF (dM)	Scaled shadow price (SSP)	Logarithmic sensitivity (LS)
WT	NADPH	0.004	-0.0079	13.028	-1.36E-04	-0.1024
	NADH	0.0061	-0.003	-3.547	-7.95E-05	0.0107
	ATP	0.0056	-0.0097	59.81	-2.37E-04	-0.5784
ChlR	NADPH	0.0034	-0.0054	13.028	-5.56E-05	-0.07
	NADH	0.0101	2.09E-18	-3.547	6.48E-20	-7.40E-18
	ATP	0.0034	-0.0108	59.81	-1.11E-04	-0.643
StrpR	NADPH	0.0009	-0.008	13.028	-1.11E-05	-0.1043
	NADH	0.0017	-0.0031	-3.547	-8.04E-06	0.0109
	ATP	0.0013	-0.0099	59.81	-1.93E-05	-0.5895
Maximum Scaled Reduced Cost	Reaction ID	Reaction Name		WT	CHLR	STRPR
		AKGDH	2-Oxoglutarate dehydrogenase	0	-8.11E-07	0
		EX_o2(e)	Oxygen Exchange	0	1.106	0.683
		ICL	Isocitrate lyase	0	0	-4.86E-07
		PGL	6 - Phosphogluconolactonase	0	-8.11E-07	-4.86E-07
		SUCc3	Succinate transporter	0	-8.11E-07	-4.86E-07
		PPNDH	Prephenate dehydratase	0	-8.11E-07	0
		GLCt2	Glucose Transporter	0	-8.11E-07	-4.86E-07
	Rxnvio8	Reaction 8 of Violacein Synthesis	0	-6.56E-08	-2.81E-08	

### 4.3.3. Differential metabolic dynamics prediction using Flux Variability analysis

Flux variability analysis (FVA) assesses the entire range of cellular function and the redundancy of optimal phenotypes. Applying FVA to identify reaction rates that can be uniquely determined allow us to explore the immutable or rigid metabolic state of the cell at maximal specific growth rate consistent with experimental data. Some reactions can be assigned fixed values, while the remaining calculable fluxes remain within the extreme bounds (Table 4.4). Uniquely computed reaction rates that are forced or fixed fluxes (coinciding upper and lower bounds) define metabolic rigidity and govern the plasticity of growth phenotype. Differences in these unique forced fixed rates in resistant and susceptible populations overall flux distribution indicate compensatory metabolic reprogramming as response to perturbations by the antibiotic. The constraints-based model identified two major features based on alternate optima predictions.

**Table 4.4:** FVA results showing category change in resistant strains as a function of antibiotic that involve redox cofactor balancing

Reaction ID	Reaction Formula	WT	ChlR	StrpR
HEX1	atp[c] + glc-D[c] -> adp[c] + g6p[c] + h[c]	1	7	7
PYK	adp[c] + h[c] + pep[c] -> atp[c] + pyr[c]	7	1	1
AKGDH	akg[c] + coa[c] + nad[c] -> co2[c] + nadh[c] + succoa[c]	1	7	1 <sup>a</sup>
MDH	mal-L[c] + nad[c] <=> h[c] + nadh[c] + oaa[c]	1	7	1 <sup>a</sup>
FUM	fum[c] + h2o[c] <=> mal-L[c]	1	7	1 <sup>a</sup>
SUCOAS	atp[c] + coa[c] + succ[c] <=> adp[c] + pi[c] + succoa[c]	4	7	4 <sup>a</sup>
ACKr	ac[c] + atp[c] <=> actp[c] + adp[c]	7	4	4
PFL	coa[c] + pyr[c] -> accoa[c] + for[c]	7	1	7 <sup>b</sup>
PTAr	accoa[c] + pi[c] <=> actp[c] + coa[c]	7	1	1
GLCt2	glc-D[e] + h[e] -> h[c] + glc-D[c]	1	7	7
ACT2r	ac[e] + h[e] <=> ac[c] + h[c]	7	4	4
FORti	for[c] -> for[e]	7	1	7 <sup>b</sup>
EX_ac(e)	ac[e] <=>	7	1	1
EX_for(e)	for[e] <=>	7	1	7 <sup>b</sup>

The color map indicates categories.

a – StrpR/WT flux fold is 0.52, b – StrpR/WT flux fold is 0.32)

Firstly, the resistant populations showed rigid flux distribution in secretion of overflow metabolites acetate and formate (Table 4.3). The onset of overflow metabolism and the details of secretion patterns were probed further using dynamic flux balance analysis (Figure 4.3). Both the resistant populations identified acetate as a common overflow metabolite. Dynamic FBA (dFBA) qualitatively identified secretion of acetate

and formate in that order in the ChIR population as indicated in the FVA and ethanol on lowering the oxygen uptake rates.

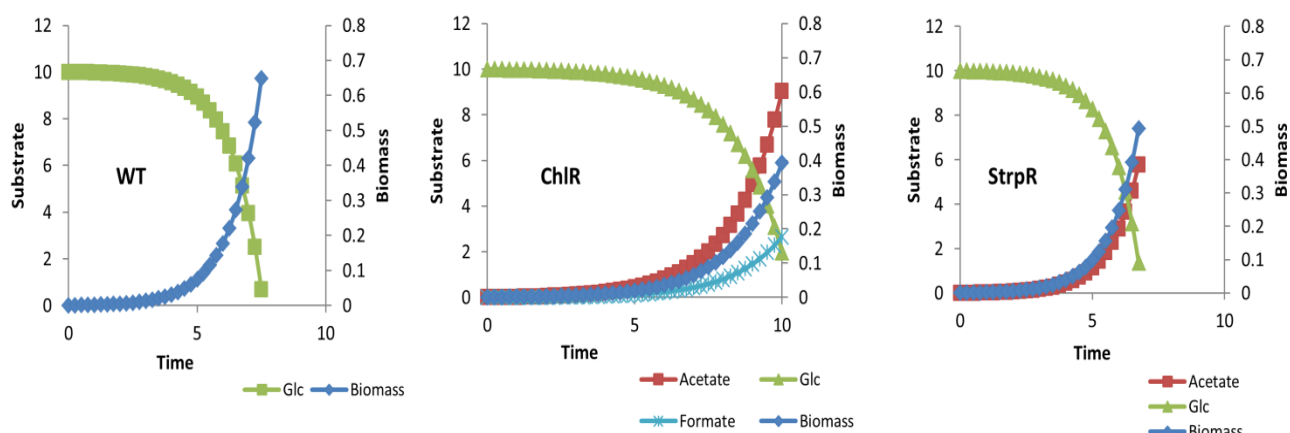


**Figure 4.3:** Dynamic FBA results for the three different populations of *C. violaceum*

The second major feature included reactions changing the rigid flux distribution in the wild type to a more flexible flux in the resistant populations. The reactions included alpha-keto glutarate dehydrogenase (AKGDH) and malate dehydrogenase (MDH) (Table 4.3). These change from a rigid flux configuration to more flexible one that potentially could modulate the direction and magnitude of flux involving NADH. The significance of alpha-keto glutarate (AKG) in the growth of the resistant populations is also supported by the high logarithmic sensitivity with respect to growth (Table 4.3). In order to probe this

**Table 4.5:** Gamma Redox

$\gamma$ redox(mets)	Glucose		
	WT	ChIR	StrpR
nad[c]	0	0.0014	-0.0031
nadh[c]	0	0	0
nadp[c]	-0.0054	-0.0041	-0.0080
nadph[c]	0	0	0
$\gamma$ redox (nadh/nad)	0	-0.0014	0.0031
$\gamma$ redox (nadph/nadp)	0.0054	0.0041	0.0080
	just right	limiting redox	excess redox

further, we looked at the Gamma redox,  $\gamma_{\text{redox}}$  and logarithmic sensitivity during experimental conditions (Table 4.5) and identified NADH and NADPH to limit growth in the ChIR strain while ATP was also growth limiting in the StrpR strain. Thus, disruption of redox homeostasis through NADH/NAD ratios and biomass precursor anabolism through NADPH/NADP ratios were identified as central to antibiotic action by FVA and sensitivity/shadow price analysis (Tobias Fuhrer and Sauer, 2009).



#### 4.3.4. *In silico* prediction of NAD/NADH balance and redox homeostasis

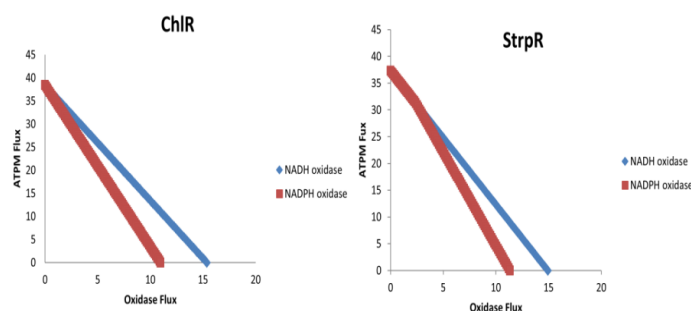


**Figure 4.4:** Robustness analysis for ChlR and StrpR of the NADH or NADPH oxidase versus ATP maintenance (ATPM) flux

FVA, as discussed in the previous section, showed metabolic flux redistribution associated with antibiotic resistance in reactions involving NADH. An experimental compartment-specific manipulation of the NAD<sup>+</sup>/NADH ratio has been reported wherein water forming NADH oxidase is introduced to investigate the redox imbalance in mammalian cells and decouple redox imbalance and ATP synthesis deficiency (Titov et al., 2016). We have included two pseudo reactions – a NADH oxidase and a NADPH oxidase reaction into the model and performed a Pareto front analysis of the relationship between the two oxidase and ATP maintenance in the system. We found that NADH oxidase is an essential constraint to lower the growth rates of the resistant populations to that of wild type. On probing the relation to ATPase (representing ATP maintenance, ATPM) by a Pareto front analysis, the differential relation for ChlR and StrpR was established. To reduce the growth of the ChlR strain to the wildtype molar yield we identified NADH oxidase as a critical constraint.

For StrpR, however, both NADH and NADPH oxidases were needed. This is also suggested by  $\gamma_{\text{redox}}$  analysis (Table 4.5), which identified both NADH and NADPH as growth limiting in StrpR and only NADH as growth limiting in ChlR. At molar growth yields this suggests that excess NADH yields are indeed responsible for the excess growth associated with the resistance to chloramphenicol, while both NADH and NADPH yields play a role in StrpR. The rigidity of the flux held through AKGDH and MDH reactions was restored, when these constraints were added. Experiments confirmed an increase in NADH levels (Figure 3.23) in the ChlR population. For the StrpR population the NAD levels go up, seen in the molar yield simulations that show a 2 fold increase in flux through the NADH16 reaction that is the quinone associated conversion of NADH to NAD.

#### 4.4. Conclusion

Model representing core metabolism of *C. violaceum* had 90% prediction accuracy and FBA related sensitivity parameters showed NADH and NADPH play a critical role in biomass yield. FVA showed reactions including AKGDH, MDH with forced flux in WT were redirected in case of ChlR and StrpR and failure to maintain a rigid core leads to re-sensitization. Also, a threshold of NADH/NAD is critical for survival and failure to compensate for cofactor imbalance results in killing of the resistant population under influence of certain metabolites in the medium. The results in this chapter are all under the condition for growth on glucose, where *C. violaceum* independent of susceptible or resistant population they grow optimally. To further extend the redox homeostasis to the candidate metabolites and elucidate many more hypothesis and predictions against the resistant population of *C. violaceum* as well as understand this opportunistic pathogen as a system itself there is a requirement for a genome scale metabolic model of *C. violaceum* that we will be discussing in the following chapter.

# Chapter 5

## Genome Scale Metabolic

## Reconstruction of *C. violaceum*

*“The ultimate test of understanding a simple cell, more than being able to build one, would be to build a computer model of the cell, because that really requires understanding at a deeper level”*

*-- C.A.Hutchison*

*“How often have I said to you that when you have eliminated the impossible, whatever remains, however improbable, must be the truth?”*

*- Sherlock Holmes*

### 5.1. Introduction

Understanding the complex relation between the genotype and phenotype of an organism is a fundamental part of systems biology research. Genome-scale reconstructions provide a mechanistic link between genotype and phenotype. This chapter includes genome scale mathematical representations of *C. violaceum* metabolism for analyzing and manipulating metabolism to understand the relationship between antibiotic resistance and metabolism using a systems approach along with all supporting experimental data generated so far and discussed in previous chapters of this thesis. Starting with a brief introduction to mathematical representation, the approaches and

steps involved for reconstruction of a genome-scale mathematical model with respect to metabolism have also been discussed. This chapter aims to identify genome wide metabolic features for *C. violaceum* and their correlation, if any to antibiotic resistance and re-sensitization using already existing antibiotics along with metabolite supplementation. How integration of the mathematical model along with experimental high throughput data proves to be beneficial for the overall quality of the model being applied for analyzing genotype to phenotype relationship and generate hypothesis to solve the serious problem of antibiotic resistance and been discussed in detail.

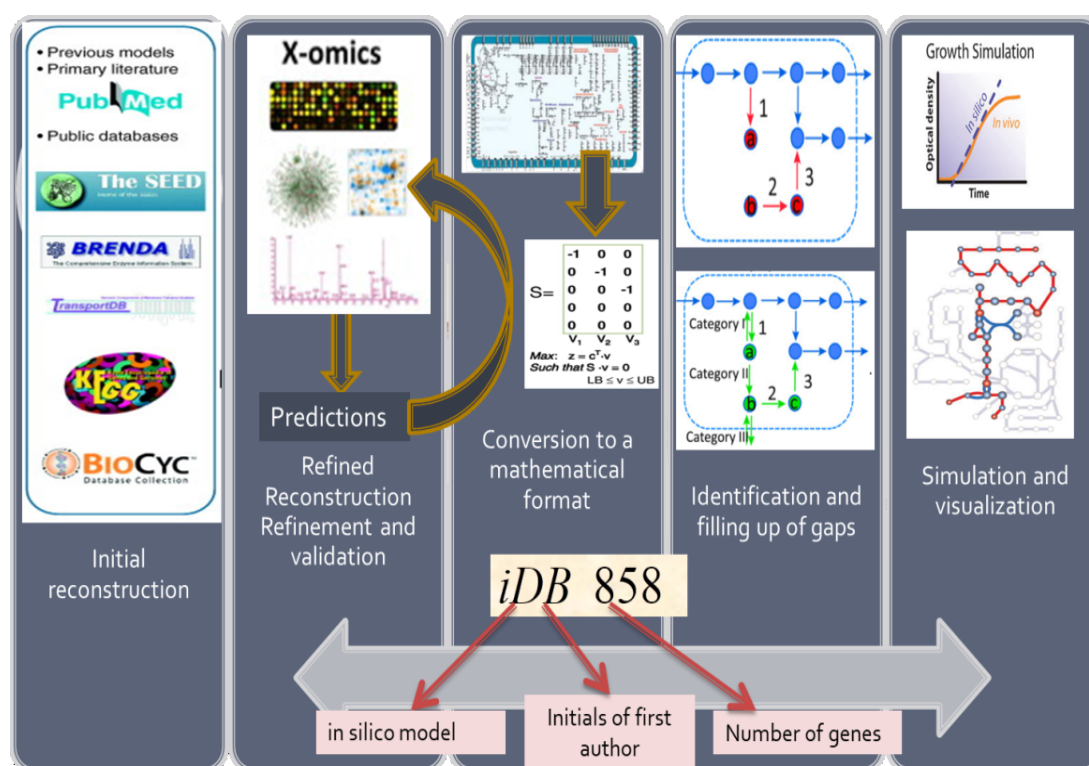


**Figure 5.1:** Reconstruction of genome scale metabolic model

As per the protocol for reconstruction of genome-scale metabolic models (GSMM) (Thiele, Ines; Palsson, 2010) it involves five-step process: (1) Initial reconstruction of a draft model built from gene annotation data coupled with information from databases that store various enzyme data such as ligand molecules (cofactors, substrates, products, inhibitors and activators), reaction formulae and metabolic pathways: KEGG, EXPASY, BRENDA, BioCyc, TIGR Microbial database, etc. and literature articles; (2)

Reconstruction of the model, and refinement and validation (iteratively) of the model through comparison of its predictions to in vivo or in vivo phenotypic information from literature references; (3) conversion of all the knowledge achieved to a mathematical representation (analyzed with a constraint-based approach); (4) Identification and filling up of gaps and (5) simulation and visualization of the predicted model. There has been a convention for naming GSMMs proposed by Reed et al. (2003), given as *i*DB858 (Figure 5.1) where 'i' refers to an in silico model; it is followed by the initials (DB) of the first author of the model; then the number of genes included in the model are indicated (858). Any lower-case letters following the number of genes indicate that slight modifications were made to the model.

Once a functional genome scale metabolic model for *C. violaceum* with quality prediction accuracy was generated it was further used for model simulations, hypothesis generation and other predictions. Some of the methods used for model simulations and predictions including FBA, FVA, dFBA, Pareto front analysis, etc. have already been discussed in the previous chapter so to avoid redundancy reference to sections in **Chapter 4 will be made** wherever required.

## 5.2. Materials and Methods

### 5.2.1. Genome Annotation

The complete genome sequence and annotation of *C. violaceum* ATCC 12472 (GenBank accession number) (Haselkorn et al., 2003) are freely available online at



**RAST** Rapid Annotation using Subsystem Technology version 4.0  
The NMPDR, SEED-based, prokaryotic genome annotation service.  
For more information about the SEED please visit <http://www.seeds.org>.

Home Your Jobs Manage Job #90421

**Job Details #90421**

- [Browse annotated genome in SEED Viewer](#)
- [View metabolic model](#)
- Available downloads for this job:
- [Share this genome with selected users](#)
- [Back to the Jobs Overview](#)

✓ Genome Upload has been successfully completed.

Genome ID - Name:	243365.12 - Chromobacterium violaceum ATCC 12472
Job:	#90421
User:	dl.das@ncbi.res.in
Date:	Wed May 15 05:48:30 2013
Sequencing method:	unknown
Coverage:	unknown
Number of contigs:	unknown
Read length:	
Genetic code:	11
Include into SEED:	no
Preserve gene calls:	no
Automatically fix errors:	yes
Fix frameshifts:	yes
Backfill gaps:	yes

✓ Rapid Propagation has been successfully completed.

✓ Quality Check has been successfully completed.

National Center for Biotechnology Information (NCBI) (<http://www.ncbi.nlm.nih.gov>). The genome sequence for *C. violaceum* was imported into the RAST server (<http://rast.nmpdr.org/>) for gene calling and annotation with subsequent manual inspection and curation (Figure 5.2). This information was used in the metabolic reconstruction and validation processes, as described in the following section.

**Figure 5.2:** Details of job submitted to RAST Server

### 5.2.2. Reconstruction of *C. violaceum* metabolic network

Figure 5.1 provides an overview of the genome-scale metabolic reconstruction pipeline of *C. violaceum*. The three major steps involved in developing a genome-scale metabolic model are (i) producing an initial draft reconstruction, (ii) manual curation and (iii) validation with experimentally observed results (Thiele, Ines; Palsson, 2010). The latter two steps are iteratively repeated in order to train the model to better describe the observed metabolic processes. We then identified and removed thermodynamically infeasible cycles (e.g. cycles resulting in free ATP production) and mass- and charge-balanced all reactions. The resulting model was then tested by comparing model predictions to available BIOLOG data (Lima-Bittencourt et al., 2011; Martin et al., 2007; Young et al., 2008) (amino acid requirement and carbohydrate utilization data). Reactions manually identified, were only added when sufficient evidence and information was available from experimental data, NCBI, KEGG, MetaCyc, BioCyc, BRENDA and SEED databases.

### 5.2.3. Initial Draft Reconstruction

Our reconstruction of a whole metabolism model for *C. violaceum* is based on an initial network obtained from the Model SEED server (<http://www.theseed.org/models/>) (Henry et al., 2010), an automated pipeline that generates genome-scale metabolic models directly from genome annotations. An initial draft genome-scale reconstruction of *C. violaceum* was built by submitting the whole genome sequence to the SEED Server. Genome-scale metabolic draft model was generated using the RAST server and the Model SEED database (Aziz et al., 2012; Henry et al., 2010). We modified the objective function of the SEED reconstruction to improve the biological interpretation of biomass as the objective function that in turn improves the solutions generated. After modifying the nutrient and biomass composition of the model to accurately capture the boundary conditions that define the overall phenotype, the internal network was curated.

### 5.2.4. Manual Curation for accurate biomass prediction

The initial draft reconstruction downloaded from Model SEED, was not able to generate biomass using minimal media or a richer chemically defined media. 27 precursors of biomass not forming *in silico* were identified through manual curation. The manually added reactions begin with “rDB” prefix in the model.

**Table 5.1:** Confidence score assigned during manual curation of the reconstruction obtained from SEED server

Score	Evidence	Type of Evidence
1.1	Gene is not present in CV but reaction essential for biomass production. Gene with known function is present in unrelated organism.	Homology in phylogenetically un-related organism
1.2	Enzyme not present in CV but indirect biochemical evidence of existence of the reaction is present. <30%.	Homology
1.3	Inferred from homology (as per UNIPROT data). Gene present in CV but very low match with other organism. 30% < 1.3 < 60%.	Homology
1.4	Gene present in CV and reaction essential for biomass production. Gene with known function present in related organism.	Homology in phylogenetically related organism
1.5	Gene present in CV and reaction essential for biomass production. Gene with known function present in well-known organism – <i>E. coli</i> , <i>Neisseria</i> , <i>franscisella</i> , <i>Pseudomonas</i> , <i>Ralstonia</i> , etc. >60%	Homology
1.6	Homology based evidence with a sequence homology =>95% with other protein with known crystal structure, function or biochemical evidence	Homology based Biochemical evidence
2.1	Physiological (phenotypic) evidence of utilization/uptake of the protein in CV (different structure growth, BIOLOG, etc.)	Physiological
2.2	Protein has been identified based on MS/ LC-MS/ MALDI. Evidence of uptake or utilization of compound, phenotypic evidence	Physiological
3.1	Cloning, expression and over-expression	Genetic evidence
3.2	Gene deletion studies	Genetic evidence
4.1	Biochemical evidence in very closely related species of CV. Ex: CV026.	Biochemical
4.2	Enzyme present and evidence of the reaction catalyzed in CV	Biochemical

### 5.2.5. Translation to BiGG database format and consistency check

There is a critical need for widely acceptable and clear standards for representing constraint-based models for extended applicability of such models and rapid improvement in the quality of reconstructed metabolic models (Ebrahim et al., 2015; Ravikrishnan and Raman, 2015). The SEED reactions and metabolites were matched with KEGG reaction IDs represented in KEGG database (<http://www.kegg.jp/>) or to the IDs available on BiGG database (<http://bigg.ucsd.edu/>). The gene and reaction annotations in KEGG were compared to that of the draft reconstructions and all the gene annotations were converted from peg IDs to the respective CV gene IDs. This process made it easy to compare the *C. violaceum* model with already existing BiGG Models, one of the major datasets of such models in the systems biology research community. Various consistency checks were also performed such as for directionality, occurrence of blocked genes, gaps, orphan metabolites as well as mass and charge balance.

### 5.2.6. Biomass composition

Biomass biosynthesis was set as a linear combination of the macromolecules protein, DNA, RNA, lipid, peptidoglycan and LPS, which were considered to account for the overall biomass composition. A detailed calculation of the biomass composition and its

assembly using legacy data is mentioned in Table 5.2 and available as Appendix 5.1. The breakup of the equation is given in Appendix 5.2

### 5.2.7. Flux Balance Analysis

Constraints based flux balance analysis (FBA) as described in **Chapter 4, section 4.2.2**, was used to simulate for growth (maximize biomass objective function) and violacein production.

### 5.2.8. Validation of the metabolic model

Validation of the metabolic model was performed in part by simulating for growth on metabolites that are potential carbon and nitrogen sources. The predictions were validated using published BIOLOG legacy data. The number of positive and negative predictions gives an insight into the predictive accuracy of the model. Additional simulation for 30 exogenous metabolites (Ex-mets) was predicted to check for model accuracy for growth, violacein and cyanide phenotype/production.

### 5.2.9. Metabolic model of WT, ChIR and StrpR population

A set of constraints that define the antibiotic susceptible WT and differentiated the evolved populations (ChIR and StrpR) were determined. The constraints used in different simulations included (i) Substrate (Glucose) uptake rates (ii) Growth yields (iii) Violacein secretion (iv) ATP maintenance costs associated with molar growth yields of each strain as discussed (Table 5.11). The specific growth rates were calculated using 1g biomass as the basis. The growth yields thus calculated were compared across the three strains. The goal of the simulations was to understand the flux distribution *in silico* and the sensitivity of growth yield to various precursors with specific reference to the cofactors NADH, NADPH and ATP.

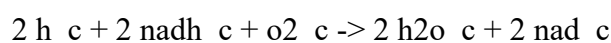
### 5.2.10. Flux variability analysis

To highlight the differences between the antibiotic sensitive and resistant populations, we classified reactions in the network based on their minimum and maximum flux values post FVA analysis and assigned categories that reflect their rigidity or flexibility as discussed in our earlier work (Banerjee et al., 2017) and in **Chapter 4, section 4.2.3**. Differences in unique forced fixed rates to variable or negligible rates in resistant populations as compared to wild type potentially indicate metabolic reprogramming.



### 5.2.12. NADH oxidase simulations to understand Redox homeostasis

The Pareto front, the set of Pareto optimal solutions were identified by constraining the glucose consumption rate, violacein secretion rate and the biomass production rate to experimental values and maximizing the fluxes through the generic ATPase (ATPM) and NADH oxidase reaction (NOX). Analysis of Pareto fronts and trade-off between ATP and NADH maintenance reactions (NADH oxidase, not generally present in *C. violaceum*) was performed to understand the effect of modulation of NADH/NAD ratios on growth of the three different population of *C. violaceum*. A reaction representing the NADH oxidase (water forming) with the right balance of protons and oxygen was added to the model based on a recent report that uses a NADH oxidase enzyme system to delineate the role of NADH imbalance and show decoupling of electron transfer via ETC and proton pumping for ATP synthesis (Titov et al., 2016). This reaction essentially acts as a drain if there is excess NADH in the system and is denoted in the model as “NADHox” represented as follows:



FVA analysis was performed in order to understand the influence of addition of NOX to the resistant population and how it may help ease the redox imbalance created as an effect of resistance to the antibiotic chloramphenicol and streptomycin respectively. Also, similar analysis was also performed by assigning the same ATP maintenance for all three populations and constraining NOX in order to attain the experimental biomass for ChlR and StrpR models.

### 5.2.13. Gene essentiality and Synthetic lethal genes in *C. violaceum*

Computationally single gene deletion study is performed by the function `singleGeneDeletion()` by deleting one gene at the time and then using the gene protein relationships (GPRs) to find the corresponding reactions and removing them. The removal of a reaction *i* from the network is performed by bounding the flux through that reaction to zero (i.e.,  $v_{i,\min} = v_{i,\max} = 0$ ) and optimizing for an objective function, often the biomass reaction. If the maximal value for biomass production is zero, then the gene is predicted to be lethal or essential for *C. violaceum*. *In silico* virulent genes are those that are non-essential for *C. violaceum* growth whereas essential genes will be deemed avirulent and attenuated genes would be those that result in lower growth than the wild

type (Raghunathan et al., 2009a). Deleting two genes simultaneously using the function `doubleGeneDeletion()` allows the determination of synthetic lethal genes. Using the relative growth rate data (growth rate ratio between the wild type and knockout) obtained, we identified synthetic lethal or synthetic sick interactions between genes in the model.

### 5.3. Results and Discussion

#### 5.3.1. Genome scale reconstruction and model statistics

The draft reconstruction was obtained from Model SEED based on genome sequence of ATCC 12472 strain submitted by the Brazilian National Genome Sequencing Consortium (Haselkorn et al., 2003) and contained 1303 reactions, 1144 metabolites and 892 genes. Of the 4407 protein coding genes only 61.3% could be assigned a putative function of which 20% were included in the draft model. It was transformed into a functional predictive genome scale model with 1255 reactions and 971 metabolites and 848 genes representing *C. violaceum* metabolism. The curation involved systematic literature mining for available information on *C. violaceum* metabolism. Data mining through PubMed search engine resulted in about 750 research articles (Figure 5.3) of that 472 papers provided direct or indirect evidence for gene protein reaction relationships and were utilized in the model curation process.

The SEED *in silico* *C. violaceum* was unable to produce twenty six out of 74 biomass precursors reported in literature (Creczynski-pasa and Antônio, 2004; Demoss and Happel, 1959) with glucose as the sole carbon source. A total of 69 reactions (Appendix 5.3) were added in order to have a functional biomass equation to represent growth in the GSM of *C. violaceum*.

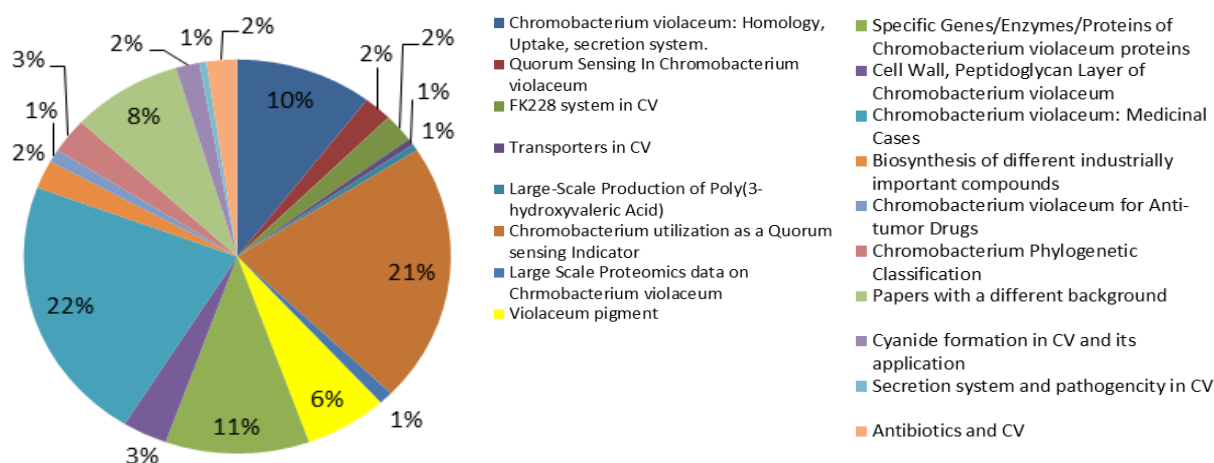


Figure 5.3. Literature mining for manual curation

Selected models and run FBA | Model construction | User models | Model statistics/Select | Flux Balance Results | About Model SEED

Complete and incomplete models currently owned by user:

export table

displaying 1 - 5 of 5

Name	Organism	Genes	Reactions	Source	Version	Status	Last update	Download links
<a href="#">Seed243365.1.102072</a>	Chromobacterium violaceum ATCC 12472	824	1110	PubSEED	0	Model created	7/18/2013	<a href="#">SBML format</a> <a href="#">Excel format</a> <a href="#">LP format</a>
<a href="#">Seed243365.4.102072</a>	Chromobacterium violaceum ATCC 12472	835	1108	PubSEED	0	Model created	7/18/2013	<a href="#">SBML format</a> <a href="#">Excel format</a> <a href="#">LP format</a>
<a href="#">Seed243365.12.102072</a>	Chromobacterium violaceum ATCC 12472	890	1184	RAST	0	Model reconstruction queued	7/18/2013	<a href="#">SBML format</a> <a href="#">Excel format</a> <a href="#">LP format</a>
<a href="#">Seed243365.13.102072</a>	Chromobacterium violaceum ATCC 12472	892	1184	RAST	0	Model reconstruction queued	7/18/2013	<a href="#">SBML format</a> <a href="#">Excel format</a> <a href="#">LP format</a>
<a href="#">Seed243365.14.102072</a>	Chromobacterium violaceum ATCC 12472	892	1184	RAST	0	Model reconstruction queued	7/18/2013	<a href="#">SBML format</a> <a href="#">Excel format</a> <a href="#">LP format</a>

Figure 5.4. The Model SEED server used to build the initial draft reconstruction

Seven reactions were added to lipopolysaccharide biosynthesis, 6 reactions were added to fatty acid metabolism and KDO2 lipid biosynthesis subsystems. Five reactions were added to four subsystems namely riboflavin metabolism, thiamine metabolism, folate biosynthesis and porphyrin metabolism. Purine metabolism, glyoxylate and dicarboxylate metabolism, nicotinate and nicotinamide metabolism needed four missing reactions in order to form biomass. Other subsystems that were missing one or two reactions and were gap filled included terpenoid biosynthesis, biotin metabolism, fatty acid biosynthesis, phenylalanine, tyrosine and tryptophan biosynthesis, urea cycle and

metabolism of amino groups, vitamin B6 metabolism, glycine, serine and threonine metabolism, TCA cycle, ubiquinone biosynthesis, glutathione metabolism, spermidine biosynthesis (urea cycle), glycolysis/ACP, aminosugar metabolism, lysine biosynthesis and peptidoglycan biosynthesis. Twenty two reactions were added to account for synthesis of the fatty acids and phosphoglycerides unique to *C. violaceum* in fatty acid biosynthesis and glycerolipid and glycerophospholipid metabolism subsystem in the model based on legacy data (Kampfer et al., 2009; Young et al., 2008). A total of 143 new reactions added with a prefix of “rDB” and 20 new metabolites were added with “mDB” prefix and the average confidence score for the model was 1.45. In order to account for all the constituents of biomass composition specific to *C. violaceum* and to replace components representing other organisms (for example *B. subtilis* cardiolipin) we modified the biomass formulation based on experimental evidence for *C. violaceum* and *N. meningitidis* wherever possible (Table 5.2 and Appendix 5.1 and 5.2). The model statistics for *i*DB858 is presented in Figure 5.6.

**Table 5.2:** Biomass composition of *C. violaceum*

Component	% Dry Weight	Organism
Protein <sup>1</sup>	41.33	<i>N.meningitidis</i>
RNA <sup>2</sup>	17.64	<i>C.violaceum</i>
DNA <sup>3</sup>	7.57	<i>C.violaceum</i>
Phospholipids <sup>1</sup>	6.64	<i>N.meningitidis</i>
Peptidoglycan <sup>3</sup>	0.06	<i>C.violaceum</i>
Lipopolysaccharide <sup>3</sup>	4.42	<i>C.violaceum</i>
Putrescine <sup>4</sup>	0.231	<i>C.violaceum</i>
Spermidine <sup>4</sup>	0.003	<i>C.violaceum</i>

### 5.3.2. *In silico* representation of metabolic genome features of *Chromobacterium violaceum*

In 2003, the *C. violaceum* ATCC 12472 genome sequencing project was executed by the Brazilian National Genome Sequencing Consortium that included 25 sequencing laboratories, 1 bioinformatics center, and 3 coordination laboratories spread across Brazil (Haselkorn et al., 2003). Of the 4407 protein coding genes only 61.3% could be assigned a putative function whereas 21.6% were identified as conserved hypothetical proteins and 17.1% other hypothetical proteins. On comparison with other sequenced organisms, *C.*

*violaceum* has been reported to be most similar to (17.4%) *Ralstonia solanacearum* (Haselkorn et al., 2003), a free living phytopathogen, similarities being in the Clusters of Orthologous Groups (COG) involved in environmental interactions such as inorganic ion transporters, that were absent in *Neisseria meningitidis* predicting *C. violaceum* to be free living rather than a commensal. *C. violaceum* genome was phylogenetically most similar to *N. meningitidis* serogroup A (9.75%), latter known to be a serious human pathogen capable of causing serious disease (Baart et al., 2007). Most of them belonged to COG from ribosomal structure, biogenesis and translation. *C. violaceum* was proposed to be well adapted to glucose, nitrogen, phosphate and amino acid starvation and is resistant to toxic agents such as hydrogen peroxide, arsenic (Carepo et al., 2004), UV radiation, oxidative damage due to presence of several ORFs that act in response to such stress like pho regulon, peptide utilization and heat shock related ORFs. Around 251 genes incorporated in the model had direct literature evidence. The model *i*DB858 was able to predict the physiology of *C. violaceum* as discussed in literature.

**Table 5.3:** Model characteristics

Model Feature	SEED	<i>i</i> DB858
Reactions	1303	1330
Internal Reactions	1185	966
Exchanges	118	189
Metabolites	1144	1004
Genes	892	858
Subsystems	306	72

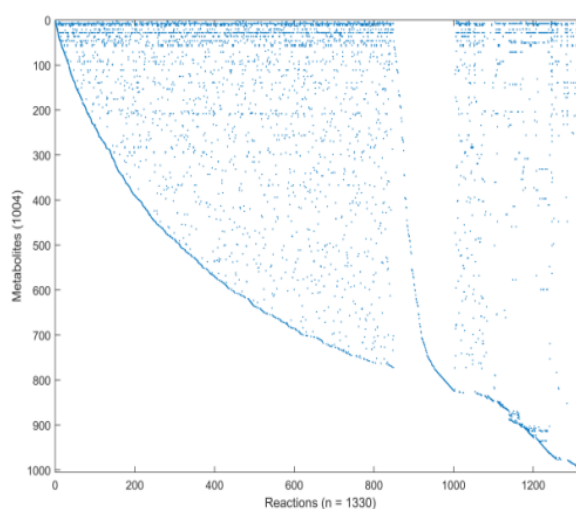


**Figure 5.5:** Stochiometric matrix for *i*DB858. Each nonzero value represented by a dot.

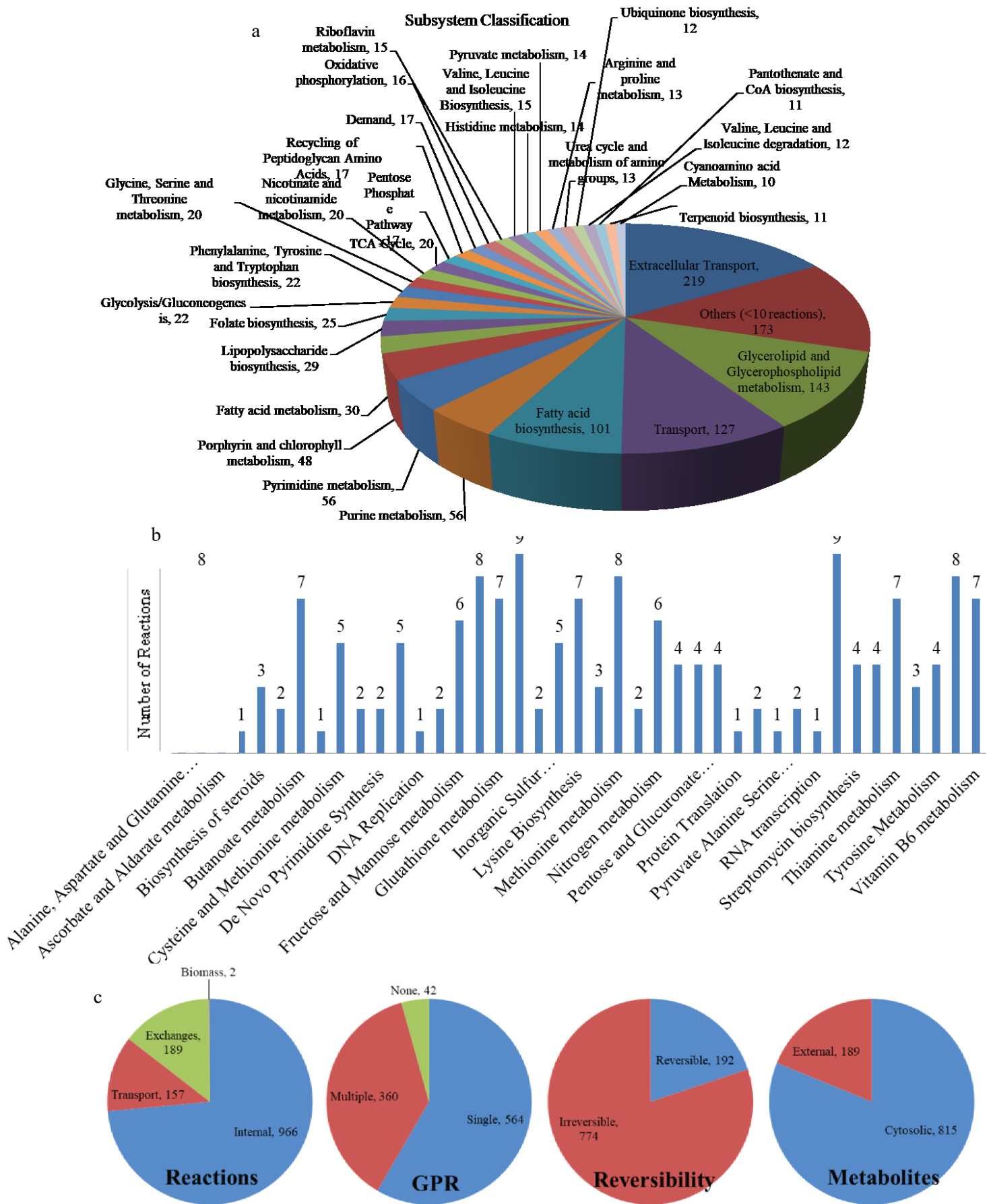


**Figure 5.6:** Model statistics and subsystem wise classification for *iDB858*

### 5.3.2.1. Central Carbon Metabolism

The *in silico* *C. violaceum*, *iDB858*, was able to synthesize all the necessary amino acids for its survival and was also able to synthesize cyanide (Michaels and Corpe, 1965). As previously reported (Banerjee et al., 2017) during aerobic growth on glucose it was able to use glycolysis, tricarboxylic acid and glyoxylate cycle to produce cellular energy required for cell survival. The model was able to utilize amino acids, lipids and acetonitrile as sole carbon sources (Chapatwale 1988). The latter was utilized by the presence of homologous nitrilase (CV\_2097) that allowed utilization of nitriles compounds such as indole acetonitrile, benzonitrile, phenylacetonitrile as suggested in literature (A. Acharya, 1997). All the genes required for nucleotide salvage pathway were accounted for in the model.

**Table 5.4:** Physiological characteristics successfully predicted by *iDB858*

Physiological function	<i>In silico</i>	Experimental Reference	
Lactate utilization	+	Ron Taylor 2009	
Acetonitrile utilization	+	Chapatwale 1988	
Glycerol utilization		In house	
Violacein production	+	Lichstein and Van de Sand 1945	
Cyanide production	Glucose	+	
	Succinate	+	Michaels and Corpe, 1965
	Glutamate	++	

In glycolysis *pck*, *agp*, *crr*, *ascF*, *eutG*, *pdc* genes were absent but *ppc* gene, CV\_0055 was present in addition to CV\_2491. In TCA *pfo*, *mgo*, *pck* genes were absent. In PPP *kdgK*, *ghrB*, *gnd*, *gcd*, genes were absent. Absence of *talB* (transaldolase) was compensated by *talC* (CV\_2247) transaldolase activity. In pyruvate metabolism *pck*, *mgo*, *pdc* (pyruvate decarboxylase), *aldA*, *hchA*, *ldhA*, *lldA* (lactate dehydrogenase, 1.1.2.3), *lldD*, *poxB*, *pfo*, *yccX*, *eutD*, *maeA*, *mhpF* (1.2.1.10, acetaldehyde-CoA dehydrogenase II, NAD-binding) genes were absent but CV\_2491 and *dld* (CV\_3027 – D-lactate dehydrogenase) were present and *adhE* (CV\_1137) replaced *mhpF* function in the model.

All the respiratory complexes (Complex I to V) were present in the model as reported in literature. Electrons entered the respiratory chain through NADH dehydrogenase (EC 1.6.5.3, 14 genes *nuoA* to *nuoN*) or succinate dehydrogenase (EC 1.3.5.1, *sdhA* to *sdhD*) and were transferred to the cytochrome bc1 or cytochrome c reductase (EC 1.10.2.2, *petA*, *petB* and *petC*) complex through ubiquinones. The quinone system in the model was

represented by ubiquinone Q-8 (Whistance et al., 1969). Two types of terminal cytochrome oxidase (EC 1.9.3.1) were reported (Creczynski-pasa and Antônio, 2004) in *C. violaceum*, SoxM was represented by *coxA* (CV\_0600), *coxB* (CV\_0599) and *coxC* (CV\_0603) whereas FixN was represented by CV\_1171, CV\_1172, CV\_1173 and CV\_1174 based on homology. SoxM type (aa3 type) worked under normal aerobic conditions whereas the FixN oxidases were involved under micro-aerophilic conditions (Castresana, 2001) that may allow colonization of oxygen-limited environments. Another terminal oxidase, cytochrome bd oxidase was also reported in *C. violaceum* known to play a role in oxidative stress and to create electrochemical membrane gradient for energetic requirements (Castresana, 2001). Cyanide formation in *C. violaceum* is a distinguishing feature among violacein producing bacteria. In general, cyanide binds with the respiratory electron chain molecule and inhibits respiration and kills the cells. Therefore, there must be an evolved respiratory system that is resistant to cyanide production as reported (Niven et al., 1975). *cioA* (CV\_3658), a cyanide insensitive terminal cytochrome oxidase in the respiratory electron transport (Tay et al., 2013) and *cioB* (CV\_3657) were genes present in *in silico* *C. violaceum* model homologous to the cytochrome bd (1.10.3.14) oxidases and may belong to cyanide insensitive oxidases (CIO) as observed in *Pseudomonas aeruginosa* (Zlosnik et al., 2006) suggesting terminal branching of the respiratory system in *C. violaceum* with one pathway resistant to cyanide inhibition (or azide, CO inhibition) while the other being sensitive (Niven et al., 1975). *C. violaceum* being a facultative anaerobe reactions involving nitrate (denitrification) or fumarate as terminal electron acceptors for growth under anaerobic conditions were present that convert glucose into acetic acid and formic acid under anaerobic condition (Creczynski-pasa and Antônio, 2004).

### 5.3.2.2. Cyanide Formation

Cyanide is produced by *C. violaceum* (Sneath, 1953) as a secondary metabolite that has application in pharmaceuticals industry to gold recovery from electronic scrap materials (Campbell et al., 2001; Carepo et al., 2004; Michaels and Corpe, 1965; Natarajan and Ting, 2014). Cyanide formation in *C. violaceum* is also used as a distinguishing feature among violacein producing bacteria. Culture conditions such as pH, temperature regulate cyanide production (Macadam and Knowles, 1984). <sup>14</sup>C studies have showed carbon atom of cyanide being derived from glycine (Brysk et al., 1969). *In silico* model of *C. violaceum* was able to produce small amounts of cyanide without any



additives in the media with either only glucose or succinate as carbon source and ammonium salts as nitrogen source. Glutamate on the other hand served as both carbon and nitrogen source with best cyanide yield (Michaels and Corpe, 1965) (refer to Table 5.4). The reactions involved in utilization of cyanide to form  $\beta$ -cyanoalanine (Brysk et al., 1969; Macadam and Knowles, 1984) and  $\beta$ -cyano- $\alpha$ -amino butyric acid were added to the model along with other reactions shown in Table 5.5. There is no inhibition of cytochrome c oxidase with the level of cyanide produced (Tay et al., 2013).

**Table 5.5:** Reaction information for the cyanide biosynthesis module

Reaction ID	Reaction Name	KEGG RID	Reaction Formula
rDB00166_c	glycine:acceptor oxidoreductase	R05704	gly_c + 2 nadph_c -> co2_c + 2 nadp_c + hcn_c
rDB00167_c	cyn_rxn2	R06614	HC00955_c <=> h2o_c + 3Aprop_c
rDB00168_c	$\gamma$ -Amino- $\gamma$ -cyanobutanoate aminohydrolase/nitrilase	R01887	2 h2o_c + acybut_c <=> glu__L_c + nh4_c
rDB00169_c	$\alpha$ -Aminopropionitrile aminohydrolase/Nitrilase	R03542	2 h2o_c + aprop_c <=> ala__L_c + nh4_c
rDB00170_c	cyn_rxn5	R01410	hcn_c -> aprop_c
rDB00171_c	cyn_rxn6	R01650	hcn_c -> acybut_c
rDB00172_c	cyn_rxn7	R03524	cys__L_c + hcn_c -> HC00955_c
rDB00173_c	cyn_rxn8	R01267	HC00955_c -> asn__L_c
rxn02792_c	(5-Glutamyl)-peptide:amino-acid 5-glutamyltransferase	R03971	h_c + glu__L_c + 3Aprop_c -> co2_c + h2o_c + HC01700_c
rxn02791_c	(5-Glutamyl)-peptide:amino-acid 5-glutamyltransferase	R03970	glu__L_c + HC00955_c <=> h2o_c + HC01577_c

### 5.3.2.3. Violacein biosynthesis

Violacein, an important bis-indole compound (indolocarbazole) obtained from bacteria with antioxidant activities has great potential as a drug exhibiting antibacterial, antitumoral, antiviral, trypanocidal and antiprotozoan properties (Durán et al., 2016). The main precursor metabolite for the synthesis of violacein is tryptophan (Demoss and Evans, 1959). Violacein biosynthetic pathway has a five gene vioABCDE operon structure (August et al., 2000; Balibar and Walsh, 2006; Hoshino, 2011; Sánchez et al., 2006; Shinoda et al., 2007). The operon is reported to be negatively regulated by VioS (Devescovi et al., 2017) and it is positively regulated by the CviI/R quorum sensing system. The first step is the oxidative dimerization of two molecules of tryptophan to indole-3-pyruvic acid (IPA) imine catalyzed by flavoenzyme L-tryptophan oxidase, VioA (CV\_3274) in presence of oxygen (Füller et al., 2016). This step is also critical for

biosynthesis of two other medically relevant bis-indole compounds rebeccamycin, an antiproliferative agent and staurosporine, a protein kinase inhibitor. IPA imine formed in the previous step described above, is converted to protodeoxyviolaceinic acid by VioB (CV\_3273) and VioE (CV\_3270). This is followed by the hydroxylation activity of VioD (CV\_3271) and VioC (CV\_3272) to form violacein and deoxyviolacein. In the reaction involving VioA,  $H_2O_2$  is formed that doesn't inhibit the functioning of the VioA rather stimulates higher production of protodeoxyviolacein. The flavin dependent oxygenases VioC and VioD work in simultaneous manner. In the presence of VioC, oxygen and NADPH, deoxyviolaceinic acid is formed from protodeoxyviolaceinic acid that is converted to deoxyviolacein in a non-enzymatic pathway in the presence of oxygen. If VioD acts on protodeoxyviolaceinic acid before VioC, in the presence of NADPH and molecular oxygen, then it forms protoviolaceinic acid. VioC synthesizes violaceinic acid which later gets converted into violacein by spontaneous oxidative decarboxylation. In the absence of VioC, VioD and NADPH, protodeoxyviolaceinic acid gets converted into prodeoxyviolacein in the presence of oxygen spontaneously. The reactions (Table 5.6) involved in the violacein biosynthesis as discussed above have been added to the model. The robustness analysis of different control reactions including oxygen uptake, NADPH demand, ATP demand and tryptophan demand were studied on two different objective functions biomass and violacein production as shown in Figure 5.7.

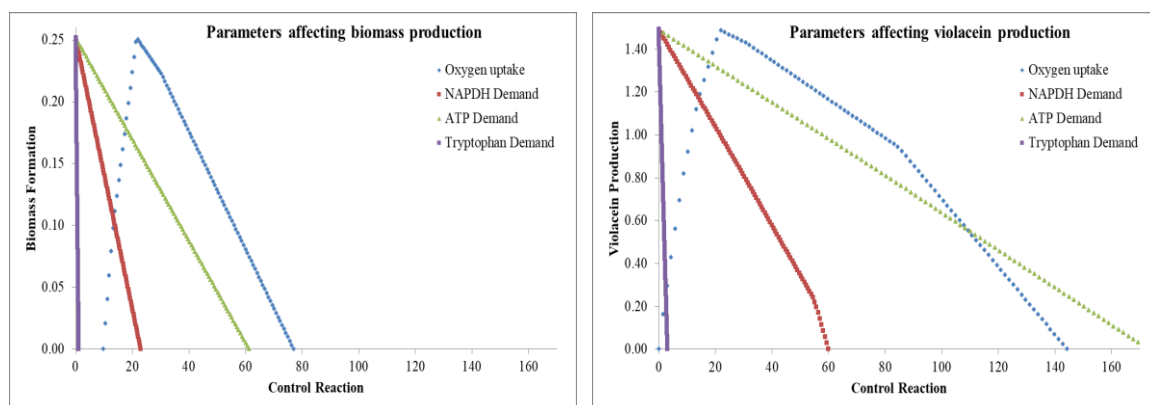


**Figure 5.7:** Robustness analysis to understand metabolite limitation on biomass and violacein formation in *iDB858* in glucose. Flux on the axes is represented as mmol/gDCW/hr and biomass is represented in grams.

The slope for different control reactions suggested that availability of the substrate amino acid tryptophan and the cofactor NADPH were the major bottlenecks in violacein biosynthesis pathway in *iDB858* as suggested in literature.

**Table 5.6:** Reaction information for the violacein biosynthesis module

Reaction ID	Reaction Name	KEGGID	Reaction Formula
rDB00091_c	Tryptophan 2-monooxygenase	R11119	$o2\_c + trp\_L\_c \rightarrow h\_c + h2o2\_c + mDB\_2i3ip\_c$
rDB00092_c	PDVnate synthesis	R11131	$2\ mDB\_2i3ip\_c \rightarrow co2\_c + nh4\_c + mDB\_pdvnate\_c$
rDB00093_c	Protodeoxyviolaceinate, NADPH:o2 oxidoreductase	R11134	$h\_c + nadph\_c + o2\_c + mDB\_pdvnate\_c \rightarrow h2o\_c + nadp\_c + mDB\_pvrate\_c$
rDB00094_c	Protoviolaceinate, NADPH:o2 oxidoreductase	R11135	$h\_c + nadph\_c + o2\_c + mDB\_pvrate\_c \rightarrow h2o\_c + nadp\_c + mDB\_vnate\_c$
rDB00095_c	Violacein spontaneous synthesis	R11136	$h\_c + o2\_c + mDB\_vnate\_c \rightarrow co2\_c + h2o\_c + mDB\_vio\_c$
rDB00096_c	Protodeoxyviolaceinate, NADPH:o2 oxidoreductase	R11374	$h\_c + nadph\_c + o2\_c + mDB\_pdvnate\_c \rightarrow h2o\_c + nadp\_c + mDB\_dvnate\_c$
rDB00097_c	Deoxyviolacein spontaneous synthesis	R11133	$h\_c + o2\_c + mDB\_dvnate\_c \rightarrow co2\_c + h2o\_c + mDB\_dvio\_c$
rDB00098_c	Prodeoxyviolacein spontaneous synthesis	None	$h\_c + o2\_c + mDB\_pdvnate\_c \rightarrow co2\_c + h2o\_c + mDB\_prodvio\_c$
rDB00099_c	Diffusion of violacein	None	$h\_c + mDB\_vio\_c \rightarrow h\_e + mDB\_vio\_e$
rDB00100_c	Diffusion of prodeoxyviolacein	None	$mDB\_prodvio\_c \rightarrow mDB\_prodvio\_e$
rDB00101_c	Diffusion of deoxyviolacein	None	$h\_c + mDB\_dvio\_c \rightarrow h\_e + mDB\_dvio\_e$
EX_vio_e	Violacein Exchange	None	$mDB\_vio\_e \rightleftharpoons$
EX_dvio_e	Deoxyviolacein Exchange	None	$mDB\_dvio\_e \rightleftharpoons$
EX_prodvio_e	Prodeoxyviolacein Exchange	None	$mDB\_prodvio\_e \rightleftharpoons$

#### 5.3.2.4. Macromolecular Biosynthesis

The cell envelope of *C. violaceum* similar to *N. meningitidis* and *E. coli* consists of an outer membrane, a peptidoglycan and a cytoplasmic (inner) membrane. The outer membrane has an asymmetrical organization in which the outside layer is primarily composed of lipopolysaccharide (LPS) (Wheat et al., 1963; Whiteside and Corpe, 1969) and proteins whereas the inside membrane contains phospholipids. Bacterial lipids in *C. violaceum* like in all gram negative bacteria including *S.marcescens*, *E. aerogenes* and *E. coli* contains phosphatidylethanolamine (PE) as the major phosphoglycerides, and lesser amounts of phosphatidylglycerol (PG), phosphatidic acid (PA) and diphosphatidylglycerol (cardiolipin, CL) (Randle et al., 1969). The overall phospholipid composition used in the model was 76.6% PE, and 17.9% PG, 4.6% CL and 0.9% PA based on legacy data (Kampfer et al., 2009; Randle et al., 1969). Metabolic reactions for lipids used for various cellular functions including triacylglycerol, phospholipids and

lipopolysaccharides were also included in the model. The fatty-acid biosynthesis subsystem in the model was curated using the template from *E. coli*. All genes, except for a homolog of the *E. coli*  $\beta$ -hydroxyacyl-acyl carrier protein (ACP) dehydrase FabA and FabB (3-oxoacyl-[acyl-carrier-protein] synthase I, 2.3.1.41), were present in the model in addition to CV\_2194, a hypothetical protein (enoyl-[acyl-carrier protein] reductase II, 1.3.1.9). Homologs to *E. coli* glycerol-3-phosphate acyltransferase (PlsB) were not found so absent in the model on the other hand PlsX homolog CV\_3417 and CV\_3688 homologous to PlsY were present in *iDB858*. The unique fatty acid compositions for *C. violaceum* containing cycloheptane rings (Kampfer et al., 2009; Young et al., 2008) were also added in the model. The glycerophospholipid and glycerolipid metabolism were modified accordingly using reactions from *E. coli* iAF1260 (Feist et al., 2007) and *Burkholderia* reconstructions (Bartell et al., 2014) based on gene sequence similarity.

The lipopolysaccharide (LPS) and peptidoglycan of *C. violaceum* are known to be responsible for activating host immune cells and the induction of inflammatory cytokines during bacterial infection, resulting in septic shock (Ghosh et al., 2014). Two type III secretion systems (T3SSs) encoded in three gene clusters (*Chromobacterium* pathogenicity islands Cpi-1, Cpi-1a and Cpi-2) are thought to be one of the most important virulent factors (Alves De Brito et al., 2004; Miki et al., 2010) and Cpi-1/-1a T3SS are involved in the formation of necrotic lesions in the liver (Miki et al., 2010). LPS consists of three parts: a lipid A part containing unique hydroxy fatty acid chains, a core oligosaccharide containing 3-deoxy-D-manno-octulosonate (KDO) and heptoses, and a specific polysaccharide (somatic O-antigen). *C. violaceum* lipid A has been reported to be structurally different compared to other *Enterobacteriaceae* like *Salmonella* and *E. coli* (Hase and Reitschel, 1977). In contrast to two phosphate groups that are largely free, in *C. violaceum* lipid A they are substituted each by a distinct, non-acylated, amino sugar. The glycosidically linked phosphate group was shown to be substituted by a glucosaminyl residue. This area, therefore, contains the structure of a glucosaminyl-1-phosphoryl-1-glucosaminide. The ester-linked phosphate group was found to be substituted by a 4-aminoarabinosyl residue. All genes involved in the biosynthesis of the lipid A of LPS are present in *iDB858* including *lpxB* (CV\_2209) and *lpxD* (CV\_2206) except for *lpxM* (myristoyl-acyl carrier protein (ACP)-dependent acyltransferase) that is absent in all betaproteobacteria (Opiyo et al., 2010). These genes are known to be related to virulence and pathogenicity in *C. violaceum* (Ghosh et al., 2014). The specific polysaccharide or O-antigen has been reported to be composed of D-glycero-D-mannoheptose and D-

fucosamine (Maclennan and Davies, 1957) along with galactose, glucose, glucosamine (Crumpton and Davies, 1958). Peptidoglycan degree of cross-linking and O-acetylation appeared to be associated with the genetic background of the strains and was found to be quite similar to *N. meningitidis*. The percentage of O-acetylation per disaccharide was on average 14.7% compared to 33% in *N. meningitidis* (Weadge et al., 2005). Other studies show that peptidoglycan structures are recognized by the innate immune system (Alves De Brito et al., 2004). Several studies have shown that a direct correlation exists between the extent of O- acetylation and susceptibility to lysozyme-catalyzed hydrolysis of peptidoglycan to protect the bacterium from a host immune response (Weadge et al., 2005). In our model genes including CV\_4346 and CV\_4349 were present that are known to be related to virulence and pathogenicity in the peptidoglycan biosynthesis subsystem.

*C. violaceum* has strong ability to adapt to stress condition due to presence of different types of transporter proteins. 25% of extracellular proteins have been reported to be involved in transport or metabolism (Ciprandi et al., 2013; Grangeiro et al., 2004).

### 5.3.3. SEED Draft model limitations

Although the genome of *C. violaceum* has no missing components in the biosynthetic pathways of all 20 amino acids and the purine/pyrimidine, the SEED reconstruction (<http://www.theseed.org/models/>) (Henry et al., 2010) did not reflect this feature. Pathways with gaps and missing reactions included lysine, phenylalanine, tyrosine and tryptophan biosynthesis and glycine, serine and threonine metabolism pathways. Biosynthesis and metabolism of all 20 amino acids along with purine pyrimidine nucleotides were found to be complete in *C. violaceum* genome. *C. violaceum* does not require any amino acids for its growth (Demoss and Happel, 1959). Many genes were not identified, annotated or miss-annotated. In case of lysine biosynthesis a lumped reaction had to be added for the conversion of L-aspartate semialdehyde to meso-2,6-diaminopimelate (rDB00050\_c) in order to form lysine in the reconstruction. For arginine biosynthesis reaction (rDB00003\_c) was added for formation of arginine (glutamate and 2acetamido-5-oxopentanoate to oxoglutarate and N-acetylornithine). Tryptophan metabolism in *C. violaceum* is unique as compared to other bacteria due to its oxidative conversion to natural bis-indole compound violacein (Duran, M., Alario A. F., 2010; Durán et al., 2016; Füller et al., 2016) through a five gene violacein operon (August et al., 2000; Balibar and Walsh, 2006; Hoshino, 2011) which will be discussed in another section. In the SEED reconstruction the reaction that converts chorismate to prephenate

(Chorismate mutase or prephenate dehydratase, CV\_2355, *pheA*) was missing (Figure 5.9) although indirect evidence (Ronau et al., 2013) supports its occurrence in the network for biosynthesis of phenylalanine, tyrosine and biomass formation. In case of glycine, serine threonine metabolism we added a reaction (rDB00029\_c) for linking 1-amino-2-propanol to aminoacetone. Synthesis of variety of cofactors and vitamins were also complete with the exception of pantothenate and biotin biosynthesis. Vitamin B12 was represented by Vitamin B12 coenzyme adenosylcobalamin (adocbl\_c) in the model and was synthesized by *i*DB858 and is also included in the biomass equation as suggested in literature to be important for cellular functioning (Demoss and Happel, 1959). This merely reiterates the fact that although automated draft reconstructions for metabolic models are a great starting point, detailed manual curation is a necessity for complete reconstructions that can be translated to models that can simulate cell function accurately.

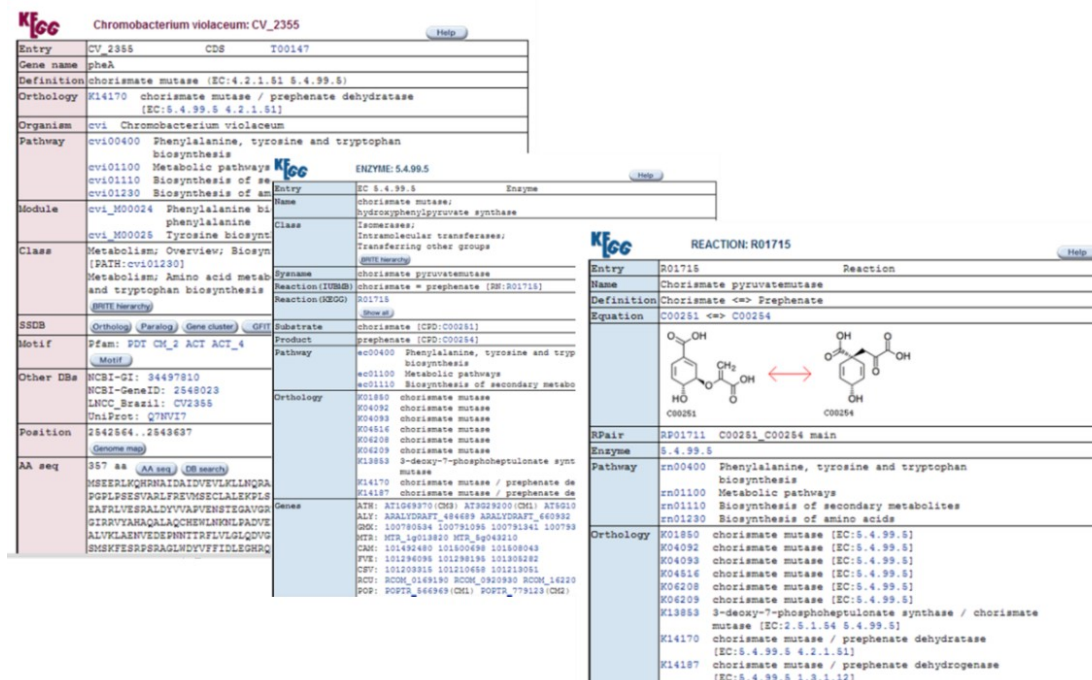
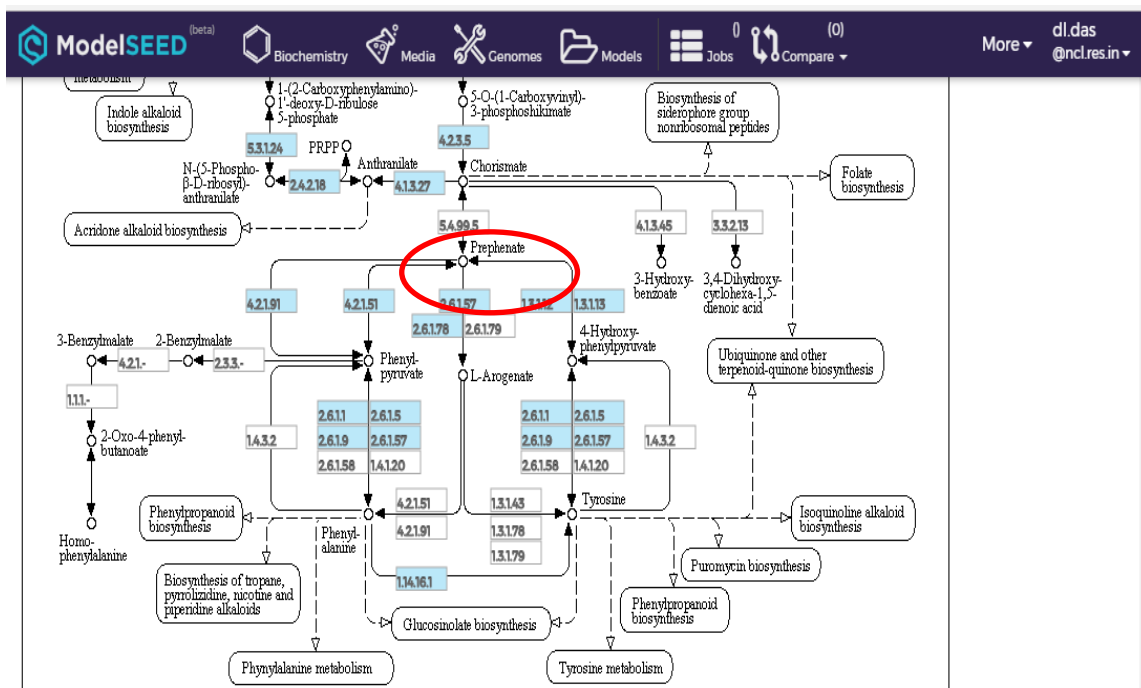


Figure 5.8. Gene, enzyme and reaction information of chorismate mutase as in KEGG database



**Figure 5.9.** Screen shot showing the missing chorismate mutase (red circle) in ModelSEED

### 5.3.4. Metabolic capacity validation of *i*DB858 based on BIOLOG GN2 plate phenotype

The metabolic reconstruction and modeling process as summarized in Figure 5.1 is an iterative process. With the biomass objective function, a genome-scale reconstruction model was converted into a model that could compute the growth/respiration phenotypes of *C. violaceum* in several C/N sources. We used the model to predict growth on different compounds used as sole carbon and nitrogen sources and compared the simulation results with high-throughput phenotypic microarray experimental data (Biolog<sup>TM</sup>) (Lima-Bittencourt et al., 2011; Martin et al., 2007; Young et al., 2008). Inconsistencies between simulation results and Biolog data were then used to refine the model by adding 36 missing reactions supported by literature; *i*DB858 was able to predict metabolic phenotypes of *C. violaceum* with a prediction accuracy of 89% (Table 5.7).

**Table 5.7:** BIOLOG *in silico* prediction accuracy

Total Substrates	95
Not in Model	38
Present in Model	57

True Positive	37	
True Negative	12	
False Positive	2*	*Glycerol and Formate
False Positive	4 <sup>#</sup>	<sup>#</sup> D-serine, Uridine, 2-Aminoethanol, Cis-aconitate
False Negative	2 <sup>#</sup>	<sup>#</sup> Leucine, Glucose-1-phosphate

\* Experimental evidence exists, # Conflicting literature evidence

**Table 5.8:** *In silico* prediction for the 57 BIOLOG GN2 plate substrates

Substrate	Lima-Bittencourt et al., 2011	Young et al., 2008	Martin et al., 2007	iDB858	Biomass
Sucrose	+		+	+	1.973
D-mannose	+	+		+	0.987
D-trehalose	+	+		+	1.973
L-phenylalanine	+	+		+	0.922
L-threonine	+	+		+	0.608
Inosine	+	+		+	0.689
Thymidine	+	+		+	0.888
D, L-a-glycerol phosphate	+	+		+	0.574
D-glucose-6-phosphate	+	+		+	1.051
N-acetyl-D-glucosamine	+			+	1.169
D-cellobiose	+			+	1.973
D-fructose	+			+	0.981
a-D-glucose	+			+	0.987
D, L-lactic acid	+			+	0.413
Succinic acid	+			+	0.472
D-alanine	+			+	0.383
L-alanine	+			+	0.440
L-alanyl-glycine	+			+	0.646
L-asparagine	+			+	0.467
L-aspartic acid	+			+	0.440
L-glutamic acid	+			+	0.432
Glycyl-L aspartic acid	+			+	0.675
Glycyl-L glutamic acid	+			+	0.657
L-histidine	+			+	0.440
a-Cyclodextrin	+			+	5.920
Dextrin	+			+	5.920
Glycogen	+			+	3.946
L-arabinose	+			+	0.614
D-arabitol	+			+	0.682



D-psicose	+		+	0.987
Turanose	+		+	1.973
L-ornithine	+		+	0.608
L-proline	+		+	0.564
L-serine	+		+	0.374
D-gluconic acid	+		+	0.860
b-Hydroxybutyric acid	+		+	0.525
Urocanic acid	+		+	0.485
D-serine	-	+	+	0.348
Uridine	-	+	+	0.679
2-Aminoethanol	-	+	+	0.334
Cis-aconitic acid	+	-	+	0.656
Formic acid*	-		+	0.054
Glycerol*	-		+	0.571
L-leucine#	+	-	-	0.000
Citric acid	-	-	+	0.000
a-D-glucose-1-phosphate#	-	+	-	0.000
a-Keto butyric acid	-		-	0.000
a-Keto glutaric acid	-	-	-	0.000
c-Amino butyric acid	-	-	-	0.000
Putrescine	-		-	0.000
D-galactose	-		-	0.000
m-Inositol	-		-	0.000
Maltose	-		-	0.000
D-mannitol	-		-	0.000
Acetic acid	-		-	0.000
D-sorbitol	-		-	0.000
Propionic acid	-		-	0.000

\* Experimental evidence exists, # Conflicting literature evidence

### 5.3.5. Growth prediction accuracy using *iDB858* based on in house Carbon Nitrogen source utilization phenotype

We also tested another 30 metabolites (Ex-mets) added in excess, *C. violaceum* was able to utilize 27 and did not utilize three substrates – citrate, oxoadipate and glyceraldehyde-3-phosphate. Growth for 24 out of the 27 exogenous metabolites tested were predicted successfully (88.9 % accuracy) using *iDB858* (Table 5.9). Five substrates were false negative (mannitol and sorbitol – contradicting legacy data, L-tryptophan, L-

valine and L-glutamine not working even at -1000 input of substrate). *C. violaceum* does not utilize citrate, oxalic acid and glyceraldehyde-3-phosphate.

**Table 5.9:** Overall in silico prediction accuracy of *i*DB858 for Ex-mets

Total Substrates		30
Not in Model		1
Present in Model		29
True Positive		22
True Negative		2
False Negative	5*	*Mannitol, Sorbitol, Tryptophan, Valine and Glutamine

In order to understand the behavior of *C. violaceum* we further simulated for growth and cyanide production using experimental data. Out of the 29 substrates, the model predicted growth on 20 substrates (ca. 69% prediction accuracy). Only four out of 29 substrates had less than 60% prediction accuracy (Table 5.10).

**Table 5.10:** In silico prediction accuracy of *i*DB858 for the 29 Ex-mets

Mets	Growth	Violacein	Cyanide	% Prediction Accuracy
Glc	0.967	0.0007	0.006	62.9
g6p	1.033	0.0007	0.006	95.6
g3p	0	0.0009	0.000	100.0
Fdp	1.082	0.0005	0.005	94.9
Fum	0.853	0.0005	0.005	54.9
Male	0.421	0.0009	0.009	69.8
D-Mal	0.827	0.0006	0.006	77.2
Succ	0.920	0.0008	0.008	91.9
2oxoadp	0.704	0.0022	0.021	85.6
MLO	0.561	0.0007	0.007	52.1
Pyr	0.667	0.0004	0.004	84.3
Cit	0.000	0.0005	0.000	100.0
Icit	1.292	0.0000	0.000	98.6
Lact	0.827	0.0007	0.007	83.4
Kga	0.258	0.0005	0.005	62.5
Ara	0.587	0.0004	0.004	66.5
m6p	1.033	0.0007	0.006	95.9
r5p	0.652	0.0007	0.007	75.5
3pg	0.397	0.0005	0.005	60.3
Trp	0.000	0.0007	0.000	0.0
Ala	0.419	0.0008	0.015	43.8
Val	0.000	0.0007	0.000	0.0

Asp	0.208	0.0007	0.013	89.2
Gln	0.000	0.0007	0.000	0.0
Glu	0.389	0.0005	0.009	30.4
Man	0.000	0.0006	0.000	0.0
Sbt	0.000	0.0007	0.000	0.0
Glyc	0.544	0.0006	0.006	69.8
Ascb	0.570	0.0006	0.006	70.4

### 5.3.6. Representing Antibiotic resistant populations of *C. violaceum*

Of the major constraints imposed on FBA models is synthesis of biomass of specific composition and thus involves tracking mass flow of elements (carbon, nitrogen, phosphorus, oxygen and sulfur) through the metabolic network. FBA also balances energy and reducing equivalents. Thus energy demands and maintenance costs need to be taken into account for accurate yield/flux predictions. Many of the energy-requiring transport reactions for substrate uptake necessary for growth (biomass synthesis) are included with defined ATP stoichiometry defined by the proton: ATP stoichiometry of the ATPases. There is also a cost of maintaining the instantaneous steady state, irrespective of whether the system is growing i.e, the non-growth associated ATP maintenance. Maintenance costs can be assessed for antibiotic resistant strains based on varying the flux of a generic ATPase in the model until the carbon consumed by the model matches that measured experimentally (Varma and Palsson, 1994; Poolman *et al.*, 2009). However, this method assumes that maintenance costs can be described entirely in terms of ATP expenditure, even though maintenance processes such as antioxidant metabolism and the re-synthesis of lipids require substantial amounts of reducing equivalents.

The maintenance requirement adds up the ATP energy requirements for biomass synthesis and violacein yields. The ATP maintenance requirements for the wildtype *C. violaceum* (WT) growing on glucose with violacein secretion decreased the maintenance costs (45%) for biomass synthesis from 12.59 to 6.96 ATP per g of biomass. As a consequence if the violacein demand decreases, the ATP maintenance costs would increase. For wild type and resistant strains (ChlR and StrpR) and experimental conditions described here (Table 5.11), the non-growth associated maintenance requirement was determined to be 6.96, 10.67 and 6.77 mmol of ATP per g of biomass respectively. This indicates lower violacein yields (as observed) for ChlR. Although StrpR had similar ATP maintenance costs, increased experimental yields of violacein indicate reprogramming of metabolism to account for that.

The model *iDB858* prediction of growth for WT was off by 19% (under-predicted) and over predicted for ChlR and StrpR at a single optimal oxygen uptake rate in all the three populations. Thus modulation of violacein yields and energy maintenance costs may be a metabolic signature of the action of these antibiotics.

**Table 5.11:** Experimental conditions used to define the three different population of *C.*

*violaceum*

Model	Glucose uptake rate <sup>#</sup>	Violacein secretion rate <sup>#</sup>	Molar growth yield <sup>#</sup>	ATPM	Biomass (in-silico)	Biomass (in-vitro) <sup>#</sup>	Oxygen uptake rate
WT	9.99	1.49	0.0312	6.96	0.25	0.31	21.58
ChlR	10.53	0.673	0.0314	10.67	0.68*	0.33	9.91
StrpR	12.78	0.702	0.0504	6.77	0.92*	0.64	17.03

# Experimental values

\*Constrain oxygen to lower the biomass predicted to match experimental biomass

Similarly the ATP maintenance requirements to achieve molar growth yields for *C. violaceum* wild type population in three other substrates pyruvate, succinate and D-malate under experimental conditions were calculated. The ATM maintenance scaled to the carbon equivalence for the substrates and was 3.62 for pyruvate, 4.94 for succinate and 2.6 for D-malate (Table 5.12).

**Table 5.12:** Experimental condition used to define wild type growth on different substrates

Substrate	Model	VSR*	ATPM <sup>#</sup>	Molar growth yield*	Oxygen uptake rate <sup>#</sup>
Pyruvate	WT	0.013	3.62	0.0092	1.927
Succinate	WT	0.019	4.94	0.0117	2.7222
D-malate	WT	0.027	2.6	0.0153	1.9392

\* Experimental values # determined *in silico*

**Table 5.13:** Experimental condition used to define resistant population growth on different substrates

Substrate	Model	VSR*	Molar growth yield*	Time of growth (hr)	ATPM <sup>#</sup>	<i>In silico</i> Molar growth yield <sup>#</sup>	Oxygen uptake rate <sup>#</sup>
Pyruvate	ChlR	0.013	0.0182	After 24	5.3	0.00027	2.2308
	StrpR	0.013	0.0157	<3	3.36	0.0106	1.8797
Succinate	ChlR	0.019	0.0160	<3	7.57	0	0
	StrpR	0.019	0.0150	<3	4.73	0.0128	2.6849
D-malate	ChlR	0.027	0.0282	0 – 24	3.99	0.0079	2.19

\* Experimental values # determined *in silico*

Using biomass, transport and maintenance costs as constraints allows one to predict the fluxes through central metabolism that provide carbon skeleton for biomass and also energy (ATP) and redox production. Although synthesis of biomass consumes energy, there are other substantial energy drains in the cell, including the cost of transporting ions, metabolites and macromolecules, and the cost of cell maintenance. Both of these costs are potentially higher in microbial systems evolved to antibiotics, and therefore also have a substantial effect on maintenance costs and potentially flux distributions in central metabolism.

Moreover, a comparison of CV cells evolved or adapted under antibiotic selection pressures conditions highlights substantial differences in the ATP and reducing equivalent costs of cell maintenance in these antibiotic resistant populations. This leads to the suggestion that antibiotic stress may be considered as a condition that leads to an increase in cell maintenance costs. Adding energy-linked transporters for nutrient uptake and for intracellular transport of metabolites, virulence factor violacein synthesis facilitated a more comprehensive analysis of the energy costs of biomass synthesis in the model.

### **5.3.7. Redox coupled metabolic flux redistribution a function of antibiotic perturbation**

Describing evolutionary situations requires optimal designs that often cope with interacting constraints like biomass/energy and redox. To give a good account of these selective forces, a Pareto or Multi Objective Optimization (MOO) approach can be useful. Previously (Banerjee *et al.*, 2017) flux variability analysis (FVA) was used to show two major features as a function of antibiotic perturbation. First being the rigid flux through overflow metabolism (acetate and formate) and second being flexible flux through reactions that maintained a rigid flux in case of the wild type population that were involved in redox and energy homeostasis. Changes between resistant and susceptible populations overall flux distribution indicated compensatory metabolic flux redistribution due to antibiotic selection pressure. In this study, as explained in the Methods section, we use FVA to answer two questions. First, whether the above features observed in a core metabolic model extended to a genome scale model and secondly, whether these features are a function of antibiotic or the resistance developed to the antibiotic or any other cause. Focus would mainly be on changes in flux space with respect to that in wild type model

(WT) either to a uniquely determined (i.e. if upper and lower boundaries coincide), negligible or a flexible flux through reactions.

#### **5.3.7.1. Effect of Antibiotic on *C. violaceum* metabolic network**

To understand the effect of the antibiotics chloramphenicol and streptomycin on *C. violaceum* cellular metabolism the flux distribution profiles of *i*DB858 were delineated using FVA. The perturbation in feasible metabolic flux distributions in the presence of chloramphenicol (WT+chl) and streptomycin (WT+strep) were analyzed (Table 5.14 and 5.15). Each scenario is limited by the experimental data reflecting growth limiting substrate and the growth yields in the presence of these antibiotics as discussed earlier.

The distinguishing features of altered metabolism in WT in presence of chloramphenicol include overflow metabolism via secretion of acetate and formate. The rewiring of pyruvate formate lyase (PFL) to act in a unidirectional manner potentially leads towards accumulation of formate. Fumarate reductase (FRD7), in the presence of chloramphenicol carries a very negligible flux (contrary to 2.5 fold reduction in WT+strep). Experimentally measured proton motive force (PMF) is 10 fold higher measured in Chapter 3 (Figure 3.27) in the presence of chloramphenicol through potential disruption of the lipid bilayer and increased proton pumping through formate and acetate (Páez *et al.*, 2013).

Fumarate reductase (FRD7) represents TCA as well as oxidative phosphorylation and is involved in relaying electrons towards cytochrome oxidase that would eventually create a PMF/ electrochemical membrane gradient for ATP synthesis. The failure of FRD7 to remain a control node in the presence of chloramphenicol indicates the continued use of O<sub>2</sub> as terminal electron acceptor. The corresponding ETC complex, represented by cytochrome oxidase bo3 carries a 12 fold lower flux compared to WT. Therefore the ATP synthesis is potentially less dependent on the conventional ETC-PMF and relies on substrate-level phosphorylation via glycolysis to pyruvate (and fermentation to acetate and formate). The turning on of AckA is known to increase proton pumping and membrane potential.

In the presence of streptomycin however, higher ammonia and cyanide are produced and siphoned off to make more glutamate and glycine as seen experimentally and varied folate metabolism (through increased PABA). Lysine, methionine, histidine correlated to the altered function (via mutation) of the PLP utilizing PabC. Glutamate efflux (experimental data & SOTA reaction directionality) has been implicated previously in

streptomycin induced decreased cell viability (Iscla *et al.*, 2014). ATP generation is almost three fold lower through the ETC-PMF route similar to that of WT. These results are validated by the metabolite profiling data.

The increased flux towards tetrahydrofolate synthesis with co-synthesis of formate (FTHFD) is potentially rechanneled through the folate pathway instead of formate secretion. The flux through these reactions and pathways are correlated with downstream urea cycle and cyano-amino metabolism indicating potential cyanide based respiration inhibition. Other metabolic processes related to electron transport chain are functional but decreased in the presence of streptomycin. The PMF in this scenario is 3-fold lower than in the absence of antibiotic.

Around 5% (68) of the total reactions including 11 redox coupled reactions spanning 16 different subsystems showed differential flux distribution for the antibiotic presence. These 11 redox coupled reactions (involving NADH/NADPH) show that there is increased accumulation of NADH in the presence of streptomycin as compared to chloramphenicol that was confirmed by experimental quantitation of NAD/NADH levels (Banerjee *et al.*, 2017). This could potentially lead to pseudo-hypoxia even in the presence of normal oxygen levels. These changes observed *in silico* as well as *in vitro*, confirms modulation of flux involving NADH. The PMF is a third of that observed in the wild type (Figure 3.27, Chapter 3) and correlates well to the 3 fold decrease in unique flux held by the cytochrome oxidase bo3 reaction.

**Table 5.14:** FVA analysis results to show the effect of chloramphenicol on WT

Subsystem	Reaction ID	Reaction Formula	WT	WT+chl
Glycolysis	PYK	adp_c + pep_c -> atp_c + pyr_c	0.0005	0.76
TCA Cycle	FRD7	succ_c + q8_c <=> fum_c + q8h2_c	5.13	-0.00039 to 0.00019
Oxidative phosphorylation	cytochrome oxidase bo3 ubiquinol-8	2.5 h_c + 0.5 o2_c + q8h2_c -> h2o_c + 2.5 h_e + q8_c	31.22	2.61
Pyruvate metabolism	PFL	accoa_c + for_c <=> coa_c + pyr_c	-10.84 to 0.23	-0.45
	PTAr	h_c + accoa_c + pi_c -> actp_c + coa_c	0.0001	1.53
	ACKr	actp_c + adp_c -> h_c + atp_c + ac_c	0.0001	1.53
	EX_for	for_e <=>	0.0001	0.45
	EX_ac	ac_e <=>	0.0001	1.53

**Table 5.15:** FVA analysis results to show the effect of streptomycin on WT

Subsystem	Reaction ID	Reaction Formula	WT	WT+strep
TCA Cycle	AKGDH	coa_c + nad_c + akg_c -> co2_c + nadh_c + succoa_c	0.05	1.10
	FUM	mal_L_c <=> fum_c + h2o_c	-5.31	-3.14
	MDH	nad_c + mal_L_c <=> h_c + nadh_c + oaa_c	5.72	2.04
Oxidative phosphorylation	cytochrome oxidase bo3 ubiquinol-8	2.5 h_c + 0.5 o2_c + q8h2_c -> h2o_c + 2.5 h_e + q8_c	31.22	10.03
Pyruvate metabolism	PFL	accoa_c + for_c <=> coa_c + pyr_c	-10.84 to 0.23	-1.88 to 1.1
	PPS	atp_c + h2o_c + pyr_c -> h_c + pi_c + pep_c + amp_c	0.0002	0.15
Purine metabolism	ATP carbamate phosphotransferase	atp_c + co2_c + nh4_c <=> h_c + adp_c + cbp_c	0.17	1.10
Folate biosynthesis	MTHFD	nadp_c + mlthf_c <=> nadph_c + methf_c	0.41	1.10
Glutamate metabolism	FTHFD	h2o_c + 10fthf_c -> h_c + for_c + thf_c	0.22	1.10
	ASPTA	asp_L_c + akg_c <=> oaa_c + glu_L_c	-0.63	-1.10
Glycine, Serine and Threonine metabolism	PSERT	akg_c + pser_L_c <=> glu_L_c + 3php_c	-3.54	-1.10
	GHMT	gly_c + h2o_c + mlthf_c <=> ser_L_c + thf_c	-0.46	-1.10
Arginine and proline metabolism	PRO1x	h_c + nadh_c + 1pyr5c_c -> nad_c + pro_L_c	0.35	0.002
	SOTA	akg_c + sucorn_c <=> sugsa_c + glu_L_c	4e-5	1.10
	SGSAD	h2o_c + nad_c + sugsa_c -> 2 h_c + nadh_c + sucglu_c	4e-5	1.10
	SGDS	h2o_c + sucglu_c <=> succ_c + glu_L_c	4e-5	1.10
	AST	arg_L_c + succoa_c -> h_c + coa_c + sucarg_c	4e-5	1.10
	ARGSL	argsuc_c -> fum_c + arg_L_c	0.07	1.10
	ARGSS_1	atp_c + asp_L_c + citr_L_c -> ppi_c + argsuc_c + amp_c	0.07	1.10
Urea cycle and metabolism of amino groups	AGGPR	nadph_c + acg5p_c -> pi_c + nadp_c + acg5sa_c	0.08	1.10
	OCBT	cbp_c + orn_c -> 2 h_c + pi_c + citr_L_c	0.07	1.10
	ORNTAC	glu_L_c + acorn_c <=> orn_c + acglu_c	0.08	1.10
	ACGK	h_c + atp_c + acglu_c -> adp_c + acg5p_c	0.08	1.10
	ACOTA	glu_L_c + acg5sa_c -> akg_c + acorn_c	0.08	1.10
Cyanoamino Metabolism	glycine:acceptor oxidoreductase	gly_c + 2 nadph_c -> co2_c + 2 nadp_c + hcn_c	0.28	1.10
	cyn_rxn6	hcn_c -> acybut_c	0.28	1.10
	NH4+ Exchange	nh4_e <=>	-6.28	1.09



### 5.3.7.2. Compensatory metabolic reprogramming as a survival strategy in resistant population: Rebalance Redox cofactors

The metabolic reprogramming associated with the impact of antibiotic selection pressures was analyzed by FVA using customized models to represent WT, ChlR and StrpR (Table 5.16 and 5.17). In case of ChlR, the three unique reactions that change direction were PFL, FRD7 and ICL. PFL, responsible for converting pyruvate and CoA to formate and AcCoA, had the ability to work reversibly in WT but resolves to unidirectional flux in ChlR model shifting the equilibrium towards accumulation of formate and offset overflow metabolism. ICL, the bifurcation point in TCA that results in flux through the glyoxylate shunt is non-functional. The TCA cycle is completely functional in ChlR with increased flux through regulatory control node ICDH, resulting in increased flux through SUCOAS increasing SuccoA and ADP and reduced succinate accumulation as reported earlier in LCMS data (Banerjee *et al.*, 2017). Thus, the flux through oxidative phosphorylation related cytochrome oxidase is reduced by 50%. This could potentially contribute to the reduction of membrane potential by half (Chapter 3 Figure 3.27) as captured by FACS analysis using the BacLight Kit. Lowering flux through MDH may redirect partly the flux to the malate pyruvate shuttle increasing the flux through acetate producing ACK and PTA reactions.

The iron related oxygen oxidoreductase reprogrammed to increase  $Fe^{+2}$  indicates higher use of the  $Fe^{+2}$  ion for pyruvate metabolism. Iron homeostasis or metabolism has been recently implicated as one of the mechanisms that play a critical role in the antibiotic mediated cell death as well as evolution of de novo antibiotic resistance (Yeom *et al.*, 2010; Martínez and Rojo, 2011; Méhi *et al.*, 2014). In our analysis we observed FeII oxygen oxidoreductase had a very low flux and in the opposite direction in both the resistant population when compared to WT. Fenton reaction will not be favored due to such shift in equilibrium towards  $Fe^{2+}$  and prevent further DNA damage and sequence changes.

StrpR had a uniquely determined flux through NADH producing reaction Acetaldehyde dehydrogenase (ACALD) as well as acetate metabolism (ACKA, PTAr). StrpR also shows accumulation of L-malate, succinate and small amounts of pyruvate. In the StrpR population *in silico*, the glyoxylate shunt (ICL, MALS) is potentially functional, albeit at a 10 fold lower rate as compared to WT. The upper half of the TCA is functional and the flux through the control node AKGDH is higher. Taken together this

indicates high levels of succinate as compared to wildtype as observed in previous LCMS data.

Differences in unique forced fixed rates in resistant and susceptible populations indicate compensatory metabolic reprogramming as a response to antibiotic perturbation at genome scale. Both the resistant populations resort on overflow metabolism towards acetate. ICL, the glyoxylate shunt enzyme implicated in pathogenesis and persistence in *Salmonella* and resistance in *Mycobacterium* (Dunn *et al.*, 2009) shunts isocitrate by bypassing part of the TCA cycle. The glyoxylate shunt functions in case of StrpR but TCA continues through oxidative branch in case of ChlR. In case of StrpR higher flux through pyrimidine metabolism is represented by cytidylate kinase (CYTK1) that correlated well with previously published LCMS data showing higher average relative abundance of cytosine and adenosine in StrpR (Banerjee *et al.*, 2017).

Since the flux through the cytochrome oxidase does not completely account for the increase in membrane potential, acetate metabolism may also contribute to the PMF in the StrpR population.

The lowered oxygen uptake rates and the increased flux towards NADH, represents a state of pseudohypoxia. In vitro phosphorylation of enzymes consuming PYR and ACE (PDH) is regulated by the NAD<sup>+</sup>/NADH ratio. Lower NAD<sup>+</sup>/NADH ratios increase PDH phosphorylation. In the presence of chloramphenicol, when the ChlR population was growing on glucose the resistant population maintained the NAD/NADH ratio at 0.28 while in the presence of streptomycin, the StrpR population maintained the NAD/NADH ratio at 2.47. This validates the prediction of increased overflow metabolism related to combined yields of acetate and formate in ChlR. Potentially, the PDH must be completely dephosphorylated in the ChlR as compared to StrpR to evoke such a response. The NAD/NADH ratios in the wildtype were around 0.25 for glucose and pyruvate, while it was 0.73 for succinate and oxoadipate. The ChlR strain shows major 7 fold reduction indicating high levels of NAD recycling provided by pyruvate. The fact that StrpR also has a similar NAD/NADH ratio as wildtype indicates, that some other factor coming into play apart from redox transfer of electrons. Concurrently, PMF/membrane potential are higher for the resistant populations in pyruvate as compared to the wildtype. This suggests potential incapability to maintain ATP homeostasis under these conditions and an eventually complete decoupling of electron transfer and ATP synthesis. Similar results were observed for succinate, maleate and 2-oxoadipate.

**Table 5.16:** FVA analysis results to show compensation in case of ChlR

Subsystem	Reaction ID	Reaction Formula	WT	ChlR
Glycolysis	PYK	$adp\_c + pep\_c \rightarrow atp\_c + pyr\_c$	0.001	1.44
	SUCOAS	$atp\_c + coa\_c + succ\_c \rightarrow adp\_c + pi\_c + succoa\_c$	4e-5	0.07
TCA	MDH	$nad\_c + mal\_L\_c \rightleftharpoons h\_c + nadh\_c + oaa\_c$	5.72	0.22
	ICDHyrb	$nadp\_c + icit\_c \rightleftharpoons h\_c + mDB\_oxasucc\_c + nadph\_c$	0.00005	0.0038
Oxidative phosphorylation	cytochrome oxidase bo3	$2.5 h\_c + 0.5 o2\_c + q8h2\_c \rightarrow h2o\_c + 2.5 h\_e + q8\_c$	31.22	14.42
	PTAr	$h\_c + accoa\_c + pi\_c \rightarrow actp\_c + coa\_c$	0.0001	11.78
Pyruvate metabolism	ACKr	$actp\_c + adp\_c \rightarrow h\_c + atp\_c + ac\_c$	0.0001	11.78
	PFL	$accoa\_c + for\_c \rightleftharpoons coa\_c + pyr\_c$	-10.84 to 0.23	-9.58
	PPC	$co2\_c + h2o\_c + pep\_c \rightarrow 2 h\_c + pi\_c + oaa\_c$	0.0001	0.60
Glyoxylate and dicarboxylate metabolism	ICL	$icit\_c \rightleftharpoons succ\_c + glx\_c$	5.09	-0.004
Purine metabolism	ADK2	$h\_c + amp\_c + pppi\_c \rightarrow ppi\_c + adp\_c$	0.0007	0.001
Pyrimidine metabolism	CYTK1	$atp\_c + cmp\_c \rightarrow adp\_c + cdp\_c$	0.06	0.08
Porphyrin and chlorophyll metabolism	FeII oxygen oxidoreductase	$4 h\_c + o2\_c + 4 fe2\_c \rightleftharpoons 2 h2o\_c + 4 fe3\_c$	0.00005	-0.0007
Extracellular Transport	EX_ac_e	$ac\_e \rightleftharpoons$	0.0001	11.82
	EX_for_e	$for\_e \rightleftharpoons$	0.0001	9.80

**Table 5.17:** FVA analysis results to show compensation in case of StrpR

Subsystem	Reaction ID	Reaction Formula	WT	StrpR
Glycolysis/Gluconeogenesis	PYK	$adp\_c + pep\_c \rightarrow atp\_c + pyr\_c$	0.001	1.61
TCA Cycle	AKGDH	$coa\_c + nad\_c + akg\_c \rightarrow co2\_c + nadh\_c + succoa\_c$	0.05	0.14
	MDH	$nad\_c + mal\_L\_c \rightleftharpoons h\_c + nadh\_c + oaa\_c$	5.72	1.58
Oxidative phosphorylation	cytochrome oxidase bo3 ubiquinol-8	$2.5 h\_c + 0.5 o2\_c + q8h2\_c \rightarrow h2o\_c + 2.5 h\_e + q8\_c$	31.22	28.42
	PTAr	$h\_c + accoa\_c + pi\_c \rightarrow actp\_c + coa\_c$	0.0001	11.76
	ACKr	$actp\_c + adp\_c \rightarrow h\_c + atp\_c + ac\_c$	0.0001	11.76
Pyruvate metabolism	ACALD	$acald\_c + coa\_c + nad\_c \rightleftharpoons h\_c + accoa\_c + nadh\_c$	0.0007	0.002
	PFL	$accoa\_c + for\_c \rightleftharpoons coa\_c + pyr\_c$	-10.84 to 0.23	-14.53 to 0.59
	MALS	$accoa\_c + h2o\_c + glx\_c \rightarrow h\_c +$	5.10	0.51

		$\text{coa\_c} + \text{mal\_L\_c}$		
	ME2	$\text{nadp\_c} + \text{mal\_L\_c} \rightarrow \text{co2\_c} + \text{nadph\_c} + \text{pyr\_c}$	4.69	0.00004
	PPC	$\text{co2\_c} + \text{h2o\_c} + \text{pep\_c} \rightarrow 2 \text{h\_c} + \text{pi\_c} + \text{oaa\_c}$	0.0001	0.54
Glyoxylate and dicarboxylate metabolism	ICL	$\text{icit\_c} \rightleftharpoons \text{succ\_c} + \text{glx\_c}$	5.09	0.50
Pyrimidine metabolism	CYTK1	$\text{atp\_c} + \text{cmp\_c} \rightarrow \text{adp\_c} + \text{cdp\_c}$	0.06	0.16
Porphyrin and chlorophyll metabolism	FeII oxygen oxidoreductase	$4 \text{h\_c} + \text{o2\_c} + 4 \text{fe2\_c} \rightleftharpoons 2 \text{h2o\_c} + 4 \text{fe3\_c}$	0.00005	-0.001
Extracellular Transport	EX_ac_e	$\text{ac\_e} \rightleftharpoons$	0.0001	11.85

### 5.3.8. Redox homeostasis critical for survival against antibiotics: NADH oxidase

Since the ETC performs two coupled functions (i) Redox transfer of electrons from NADH to molecular oxygen and (ii) conversion of the free energy of the electromotive force into a proton gradient. Involvement of the ETC as discussed in the previous sections could mean (i) an excess of reducing equivalents (termed reductive stress or pseudohypoxia, which includes stalling of NAD<sup>+</sup>-coupled reactions) or (ii) a reduced proton gradient (impairing pH and voltage- coupled processes, including ATP synthesis by the F1Fo-ATP synthase). Hence there is a need for dissecting the redox function of the ETC from its proton pumping function. If ETC is dysfunctional, glycolysis is capable of compensating for the lack of ATP production, but it is net redox-neutral. NAD<sup>+</sup> recycling is key for cell growth, because many biosynthetic pathways produce NADH as a by-product.

NADH oxidase or NOX has been reported to have a potential as a valuable tool for investigating redox metabolism (Vemuri *et al.*, 2006, 2007) and may allow for decoupling the role of redox imbalance and ATP synthesis deficiency in antibiotic resistance (Titov *et al.*, 2016). An *in silico* tool (H<sub>2</sub>O producing NADH Oxidase) as previously discussed (Banerjee *et al.*, 2017) was used to manipulate the NAD/NADH ratio in WT, ChlR and StrpR. Since converting NADH to NAD<sup>+</sup>, NOX also consumes protons and oxygen, Oxygen consumption (OUR) must increase in the presence of this oxidase. The flux through NOX indicates excess 13.2 and 10.31 mmol NADH per gDCW of biomass required to be recycled for redox balance in case of ChlR and StrpR respectively (Table 5.18). More flux through NOX for ChlR correlates to presence of more NADH for no change in growth rate coupled with no significant effect on the uptake of glucose. OUR in ChlR and StrpR strains increased by 170% and 86% respectively. In the absence of NOX, the reduced apparent OUR tend to indicate pseudo-hypoxia as reported in some systems

(Gomes *et al.*, 2013). Also it was observed that even though the ATPM for StrpR is quite similar to that of WT (6.77 compared to 6.96) it requires a significant amount of flux (10.31) through NOX in order to mimic experimental growth condition in StrpR at optimal oxygen. This suggests decoupled redox homeostasis and PMF, in case of StrpR.

To further investigate decoupled redox balance and ATP synthesis at genome scale level we looked at FVA in the three populations (WT, ChlR and StrpR) in presence of NOX. The results provided an insight into the NAD<sup>+</sup> recycling associated metabolic reprogramming in the resistant populations.

Based on the feasible flux distributions, the resistant populations behaved very similar to the wild type. Redox coupled reactions MDH and ME2 along with PPC, OAADC reactions that result in accumulation of OAA (Table 5.19, yellow) changed category in ChlR and StrpR towards NAD recycling through NOX addition similar to the surviving WT. Reactions (Table 5.19, bright red) that were unique to ChlR approached similar flux distribution similar to WT in the presence of NOX indicating once again a redox cycling as a mechanism for growth. This represents the reprogramming of metabolism in resistant populations to survive in the presence of antibiotic and grow like WT in the absence of the antibiotic.

Overflow metabolism was indicated yet again by PFL, formate transport and exchange, the glyoxylate shunt enzyme ICL, L-malate accumulating MALS, SucCoA accumulation through SUCOAS, accumulation of citrate through CS, oxidative phosphorylation by FRD7, and redox coupled AKGDH. In case of StrpR the introduction of NOX helps the model revert back to WT-like phenotype but for ChlR the ATPM as well as NOX play an important role. This again confirms our hypothesis of decoupled ETC and ATP synthesis in case of StrpR and not in ChlR scenario. No succinate accumulation in ChlR as compared to very high levels in StrpR contributed by a functional glyoxylate shunt. So there is an implicit requirement of pyruvate (also seen through directionality of PYK in both resistant populations) through acetate formate fermentation to promote cell growth by recycling NAD<sup>+</sup> from NADH.

Taken together, we show that attributing the cell maintenance costs to consumption of both ATP (ATPM) and reducing equivalents (NOX) has a substantial effect on the predicted flux distributions and allows one to account for experimentally determined fluxes for evolved antibiotic resistant populations. NAD recycling may thus be the key for increased cell growth in the resistant populations, because many of the biosynthetic

pathways utilized may produce NADH as a byproduct. ATP hydrolysis contributes to optimizing membrane potentials. These *in silico* constructs thus allow for dissection of the relative contributions of redox imbalance and ATP insufficiency to antibiotic resistance pointing towards reductive stress or pseudo- hypoxia and disruption of ATP homeostasis to kill them.

**Table 5.18:** Constrains used for NADH oxidase simulations for ChlR and StrpR

Model	Glucose uptake rate	Violacein secretion rate	ATPM	Biomass		Oxygen uptake rate	NOX
				(in-silico)	(in-vitro)		
ChlR	10.53	0.673	10.67	0.68	0.33	9.91	0
				0.68	0.33	26.53	13.2
StrpR	12.78	0.702	6.77	0.92	0.64	17.03	0
				0.92	0.64	31.7	10.31

**Table 5.19:** Selected reactions from Flux variability analysis post NADH oxidase addition to ChlR and StrpR models of *C. violaceum*

Subsystem	Reaction ID	WT	ChlR <sup>#</sup>	StrpR <sup>#</sup>	ChlR <sup>@</sup>	StrpR <sup>@</sup>	ChlR Nox <sup>#</sup>	StrpR Nox <sup>#</sup>	ChlR Nox <sup>@</sup>	StrpR Nox <sup>@</sup>
TCA Cycle	MDH	2	1	1	2	1	2	2	2	2
	CS	1	7d	1	7d	1	1	1	1	1
	SUCOAS	7d	1	7d	1	7d	7d	7d	7d	7d
	FRD7	2	8	2	8	2	2	2	2	2
	AKGDH	3	7d	3	7d	3	3	3	3	3
Pyruvate metabolism	ME2	3	7d	7d	7d	7d	3	3	3	3
	PPC	7d	1	1	2	1	7d	7d	7d	7d
	OAADC	3	7d	7d	7d	7d	3	3	3	3
Glyoxylate & dicarboxylate metabolism	PFL	8	5	8	5	8	8	8	8	8
	MALS	1	7d	1	7d	1	1	1	1	1
	ICL	1	4	1	4	1	1	1	1	1
Glutathione metabolism	AMPTASECG	7b	5	4	7b	4	4	4	7b	4
	glutathione hydralase	7b	5	4	7b	4	4	4	7b	4
Extracellular Transport	Ex_for_e	7d	1	7d	2	7d	7d	7d	7d	7d

# – using their respective ATPM values, @ – using the WT model ATPM. Yellow or red colors in the Reaction ID column signify common to ChlR and StrpR or unique to ChlR model respectively. Pale red indicates reactions when WT ATPM is used for ChlR model.

### 5.3.9. Gene Essentiality and Synthetic lethality

Single and double gene deletion analyses were performed to understand the effects of gene deletion or enzymopathies on the metabolic network of *C. violaceum* using the genome scale model *i*DB858 and classified into virulent, avirulent and attenuated genes depending on the essentiality towards growth of *C. violaceum* (Table 5.20). 191 virulent genes were minimally required for survival of *in silico* *C. violaceum* in glucose medium under aerobic condition that included *pabC*. A total of 644 genes were found to be avirulent and 23 attenuated genes that resulted in 36% to 98% reduction in growth. Gene essentiality for biomass precursors was also analyzed as shown in Figure 5.11a.

We identified conditional essential genes for *C. violaceum* in glucose and five other C-source metabolites (pyruvate, succinate, maleate, D-malate and 2-oxoadipate, Table 5.21). These metabolites also showed re-sensitization of the resistant population ChlR and StrpR to the respective antibiotic. A total of 191 genes were found to be essential for glucose as well as the other 5 substrates that belonged to different subsystems (Figure 5.10). Nine genes, essential for growth, were condition independent and were identified during growth on the five substrates (Table 5.21, Figure 5.11b). These included five genes from the glycolytic pathway and gene that supports anaplerotic replenishment of pyruvate. There were 3 additional genes essential for growth on 2-oxoadipate that belonged to TCA, tryptophan metabolism and valine, leucine and isoleucine degradation subsystem.

**Table 5.20:** Single gene deletion analysis for glucose under aerobic condition

Category	GR Ratio	Genes
Attenuated	0.36 to 0.98	23
Virulent genes	0	191
Avirulent genes	0.99 to 1	644

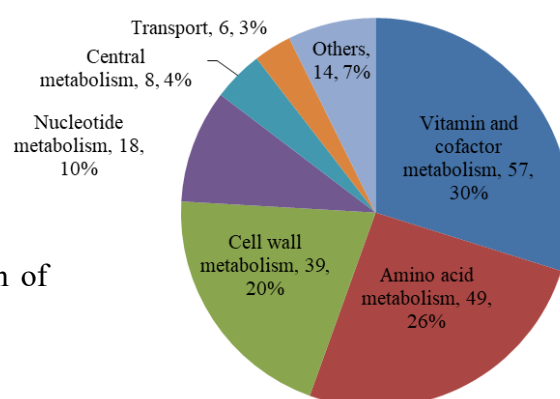


**Figure 5.10:** Subsystems wise classification of essential genes common to all the substrates

Double gene deletion (DGD) analysis (Figure 5.12) led to identification of 186 genes in 518 combinations resulting in synthetic lethal (SL) and sick (SS) interactions (Table 5.22). CV\_0939, *tpiA* had the highest interaction/connectivity. The analysis of the synthetic lethal and sick interactions predicted *in silico* showed that 101 genes involved only in synthetic lethal pairs belonged majorly to porphyrin metabolism, phenylalanine, tyrosine and tryptophan biosynthesis and purine metabolism. 39 genes involved uniquely in synthetic sick interactions belonged majorly to oxidative phosphorylation and TCA. Two of the SL pairs involved genes CV\_1071, *sucA*, 2-oxoglutarate dehydrogenase E1 component with CV\_1075 or CV\_1076 that are involved in SUCOAS reaction of TCA. CV\_1071 is involved in utilization of 2oxoadipate (2oxoADP) and involves NAD/NADH. This may explain 2oxoADP as a candidate metabolite for re-sensitization of ChlR and StrpR. This analysis would help in predicting drug targets that would otherwise be extremely challenging to test experimentally (possible pairs based on 858 genes - 7,36,164).

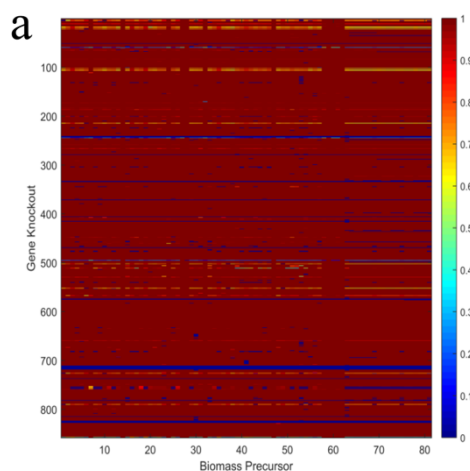


**Figure 5.11:** Single Gene deletion (SGD) analysis. a) Heat map for single gene deletion analysis for biomass precursors. b) Cluster heat map of conditionally essential genes for 5 candidate metabolites along with glucose.

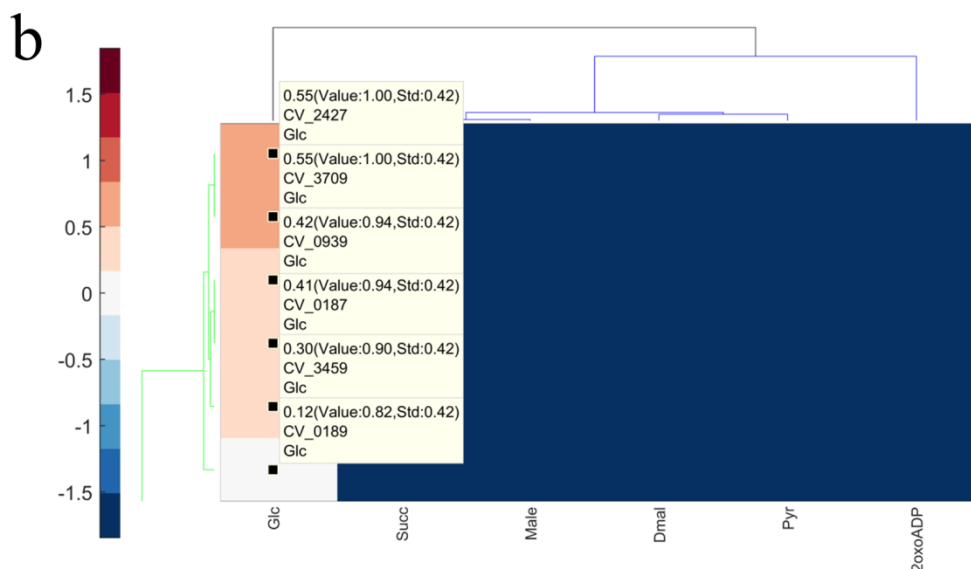




**Table 5.21:** Selected genes from single gene deletion analysis for six metabolites including glucose and candidate metabolites that re-sensitize ChlR and StrpR

Gene Deleted	Growth Rate Ratio (KO/WT)						Reaction ID	Subsystem
	Glc	Pyr	Succ	D-mal	2oxoADP	Male		
CV_0187	0.94	0	0	0	0	0	FBA	Glycolysis
CV_0189	0.82	0	0	0	0	0	PGK	
CV_2427	1	0	0	0	0	0	FBP	
CV_3459	0.90	0	0	0	0	0	ENO	
CV_0939	0.94	0	0	0	0	0	TPI	
CV_3709	1	0	0	0	0	0	PPS	Pyruvate metabolism
CV_1071	0.99	0.99	0.99	0.99	0	0.99	rxn00441	TCA Cycle
CV_3918	1	1	1	1	0	1	GLUTCOADH	Tryptophan metabolism
CV_2720	0.99	0.99	0.99	0.99	0	0.99	HACD9	Val, Leu and Ile degradation

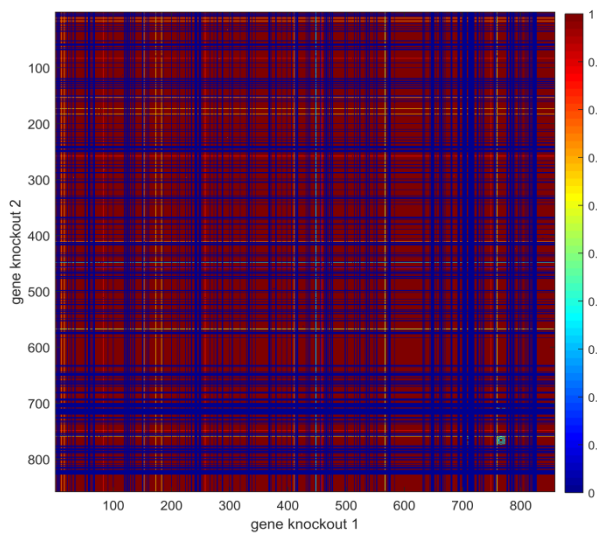


**Figure 5.12:** Heat map showing double gene deletion analysis on glucose under aerobic condition.

**Table 5.22:** Double gene deletion analysis for glucose under aerobic condition

Synthetic Lethal Pairs	101
SL genes	79
Synthetic Sick Pairs	158
SS Genes	57
Highest connectivity	6, 15
Lowest connectivity	1

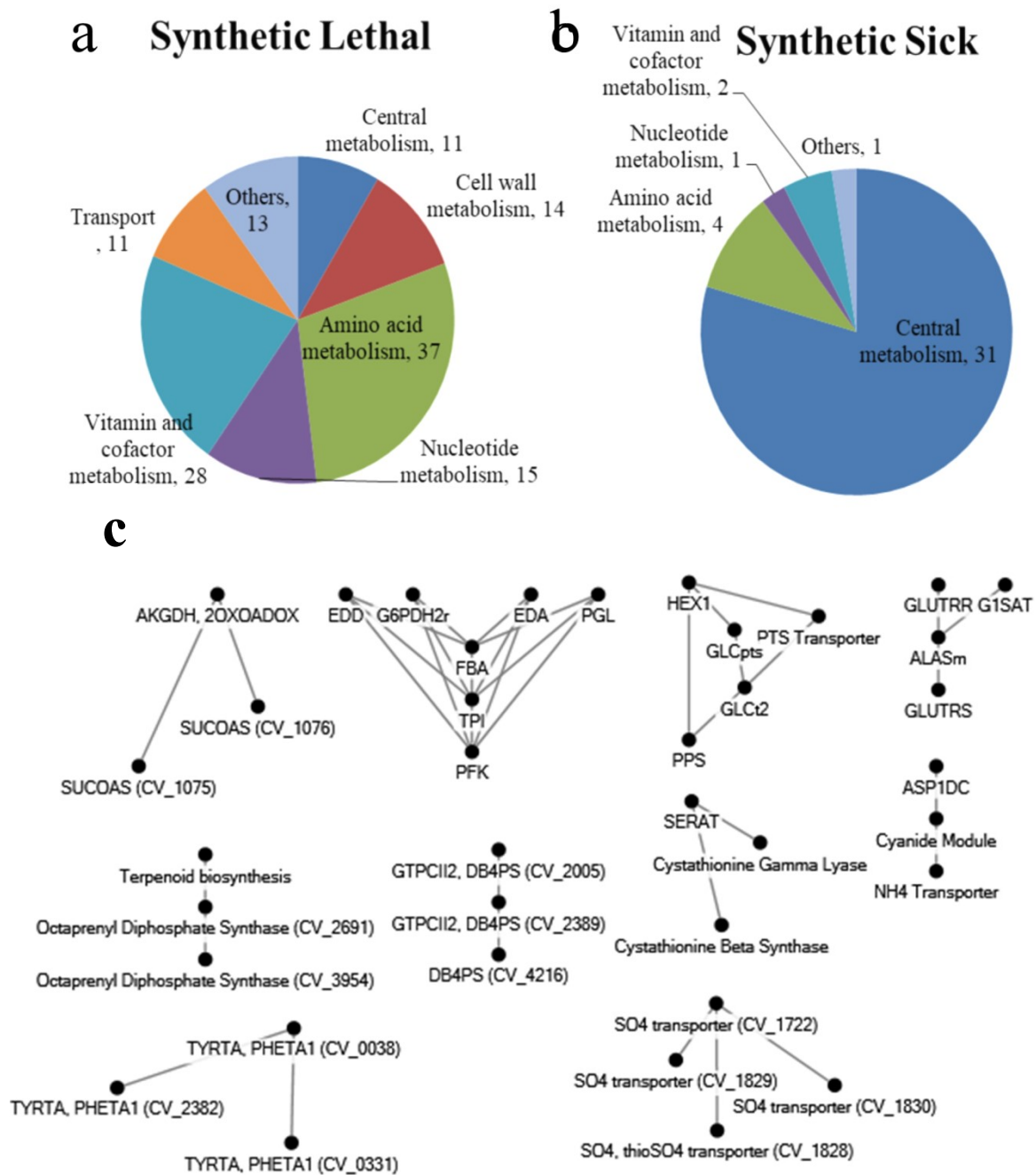


**Figure 5.13:** Double Gene deletion (DGD) analysis. a) Pie charts showing subsystem classification of unique genes involved in Synthetic Lethal (a) and Synthetic Sick pairs c) Synthetic lethal interactions for genes with 2 or more connectivity wherein dots represent the genes.

## 5.5. Conclusion

A whole genome-scale metabolic model of *Chromobacterium violaceum*, *i*DB858 was generated that predicted growth potential accurately (86% prediction accuracy) using a combination of in-house growth phenotyping and BIOLOG legacy data for validation.

Experimental growth yields were predicted accurately on glucose. Similar to a small model representing central metabolism (Chapter 4), FVA shed light on importance of redox balance. The impact of chloramphenicol on growth of WT highlights overflow metabolism whereas streptomycin results in some overflow in addition to ammonia, cyanide and glutamate production. There was increased accumulation of NADH in presence of streptomycin compared to that in presence of chloramphenicol that matched our experimental data discussed in Chapter 3, Section 3.3.3.6. In case of the resistant population ChlR and StrpR, both resort on overflow metabolism along with accumulation of malate, succinate and pyruvate in case of StrpR. The carbon flux through TCA is diverted through the glyoxylate shunt in case of StrpR but continues to oxidative branch in ChlR. Several redox coupled reaction carried unique values of flux pointing towards the critical role the redox homeostasis plays in maintaining viability and cellular function in the resistant population. The flux distributions in the presence of NOX in silico show that NAD<sup>+</sup> recycling may be the key for the survival of ChlR and StrpR.

Integration of heterogeneous data into such models would allow one to predict physiology. Thus, constraints-based flux balance analysis of genome-scale models can be used to understand emergent phenomena like antibiotic resistance.



# Chapter 6

## Antibiotic Resistance – A Public Health Perspective

*“Health care is vital to all of us some of the time, but public health is vital to all of us all of the time”*

- C. Everett Koop

*“The major reason we are seeing antibiotic resistance is overuse of antibiotics in the population for illnesses that don’t require antibiotics”*

-Bob Harrison

*"To live, to err, to fall, to triumph, to recreate life out of life."*

- James Joyce;

### 6.1. Introduction

Antimicrobial resistance is a global multifaceted phenomenon that necessitates stewardship and surveillance to control its spread even after emergence. It is one of the principal public health problems of the 21st century that threatens the effective prevention and treatment of an ever-increasing range of infections.

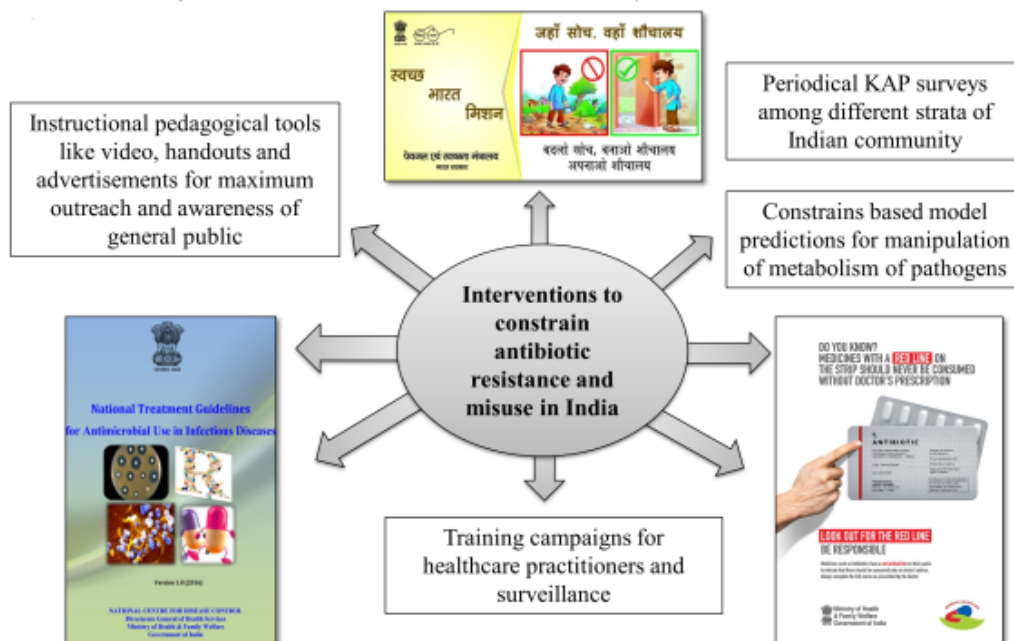


**Figure 6.1:** Interventions needed against antibiotic resistance, a multifactorial problem, in India. They not only include government enactment but also active participation of healthcare practitioners and general public.

The antibiotic era has been remarkably short and the miracle of these drugs is slipping away. Life without antibiotics is unimaginable in a world that has had cheap and plentiful supply since World War II. Antibiotics are societal drugs (Sarkar and Gould, 2006) and are used not only treat primary infections but are also a staple in modern medicine. Antimicrobial resistance is a threat that ranks along with climate change and terrorism (Laxminarayan et al., 2013). Antibiotic resistance occurs when an antibiotic has lost its ability to control bacterial growth effectively even in therapeutic concentrations. This phenomenon can turn back the clock on decades of progress into modern medicine and return us to a pre-antibiotic era. The WHO currently projects 700 deaths per day and predicts that by 2050, ten million deaths will be attributed to antimicrobial resistance alone, a number far greater than that for cancer (O’Neill, 2014). The portfolio management decisions of major pharmaceutical companies have also led to drying up of the antibiotic discovery pipeline (Butler et al., 2017) a catastrophe of huge proportions.

The World Health Assembly adopted a global action plan in 2015 on antimicrobial resistance that outlines five main objectives (<http://www.who.int/antimicrobial-resistance/global-action-plan/en/>). The scope of the threat necessitates action and solutions to be implemented at several levels of society.

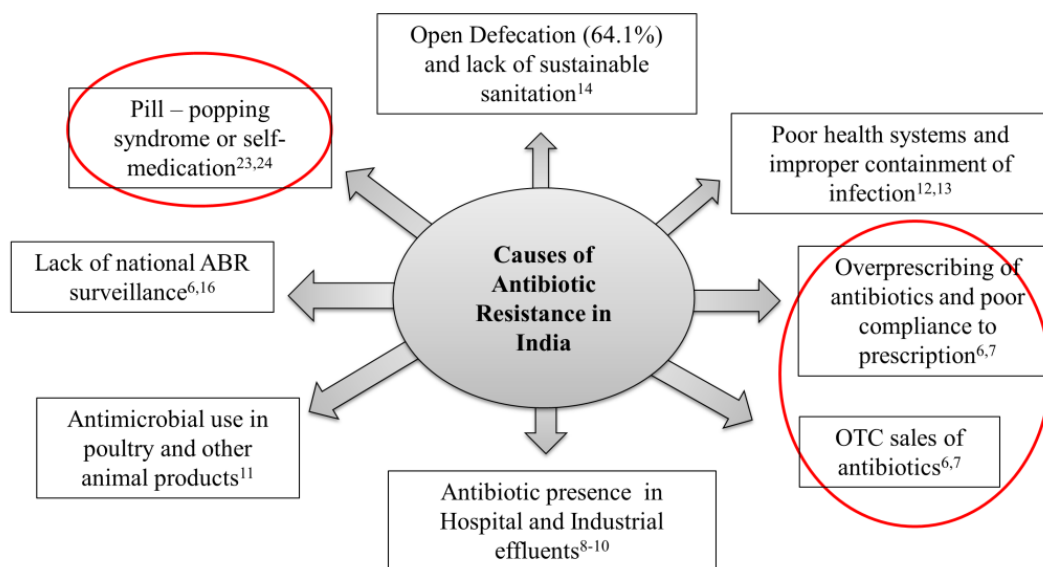


**Figure 6.2:** Causes of antibiotic resistance, a multifactorial problem, in India. This chapter focusses primarily on the ones encircled in red

Antimicrobial resistance is thus a multifactorial problem (Figure 6.2) and the social context in India plays a major role. Ranking high is the lack of regulation and policy with respect to the prescription, over-the counter (OTC) sales (Morgan et al., 2011; Reardon, 2014) and environmental disposal (Diwan et al., 2009; Fick et al., 2009; Gothwal and Shashidhar, 2015) of antibiotics. The situation is exacerbated by the uncontrolled use in livestock and animal products (Van Boeckel et al., 2015), poor health systems and lack of containment of infections (John et al., 2011; Kumar et al., 2013). Basic hygiene is also compromised by open defecation and lack of sustainable sanitation (Dasgupta et al., 2015). There seems to be an irrational antibiotic use in the country (Laxminarayan and Chaudhury, 2016), and a lack of any AMR surveillance (Reardon, 2014; WHO, 2014) at the local or national level. This can lead to prolonged sickness, extended treatment and unaffordable health care, among other problems.

Since 2011, major interventions have been put into action by the government at the community level to tackle the problem of antibiotic resistance. The Jaipur Declaration, ([http://www.searo.who.int/entity/world\\_health\\_day/media/2011/whd-11\\_amr\\_jaipur\\_declaration\\_.pdf](http://www.searo.who.int/entity/world_health_day/media/2011/whd-11_amr_jaipur_declaration_.pdf), 2011) signed in September 2011 followed by the Chennai Declaration (Ghafur et al., 2012) in August 2012, implement policies regulating

antibiotic use in India (Table 6.1). Before 2012, there was also no functioning national antibiotic policy to restrict OTC dispensing of antibiotics without prescription. March 2014 witnessed the adoption at the federal level of Schedule H1 in the Drugs and Cosmetics Act, which restricts the sale of 46 OTC drugs, including antibiotics and anti-TB drugs (Hazra, 2014). Among other actions taken by the government, “Medicines with the Red Line” media campaign was launched during the 3 day international conference on antimicrobial resistance in February 2016 (Travasso, 2016). Recently the first version of guidelines for standardized national treatment was issued by the National Centre for Disease Control, Government of India for the practitioners for rationalised use of currently available antibiotics and the effective management of patients for common infectious diseases (Dutta, 2017; *National Treatment Guidelines for Antimicrobial use in Infectious Diseases*, 2016). On the contrary, regulation of antibiotic residues in animal food produce remains in a grey area with standards existing for seafood and honey but not for poultry (Laxminarayan and Chaudhury, 2016).

There are many hurdles to overcome antimicrobial resistance. Firstly, India remains the world’s largest consumer of antibiotics amongst BRICS countries (Van Boeckel et al., 2014) (Brazil, Russia, India, China, and South Africa) with per capita usage increasing by 37% in the last decade (Ganguly et al., 2011; Laxminarayan and Chaudhury, 2016) (Figure 6.3). The need exists to impose a delicate balance in increasing access for appropriate indications and decreasing the excessive inappropriate use of antibiotics for coughs, colds, and diarrhoea (Chatterjee et al., 2015). Thus, amongst the many hurdles to overcome AMR, poor national surveillance (WHO, 2014) and a general lack of knowledge regarding rational use of antibiotics rank the highest in the Indian subcontinent.



**Table 6.1:** National Policies and Campaigns against Antibiotic misuse and Resistance

	Date	Features
Jaipur Declaration on Antimicrobial Resistance	6 September 2011	Health ministers of WHO’s South-East Asia urged to governments to develop national antibiotic policies and enforce regulations on the use of antimicrobial agents.
Chennai Declaration	August 2012	Indian Medical Societies including government policymakers, MCI, ICMR, the Drug Controller General of India, and WHO discussed a five year roadmap of actions critical to containing resistance domestically and to forge consensus around the necessary steps (Ghafur et al., 2012). March 2014 saw adoption at the federal level of the Schedule H1 to the Drugs and Cosmetics Act, which restricts the sale of 46 over-the-counter drugs including antibiotics.
“Medicines with the Red Line” public awareness campaign	February 2016	Indian Health Minister launched the campaign on identifying prescription drugs, now being marked with a red line and curb self-medication.
National Treatment Guidelines for Common Infectious Diseases, 1.0 Version	19 February 2016	National Centre for Disease Control under Ministry of Health and Family Affair, Government of India has published the 1 <sup>st</sup> version of national treatment guidelines to enhance appropriate usage of antimicrobials for common infectious diseases.

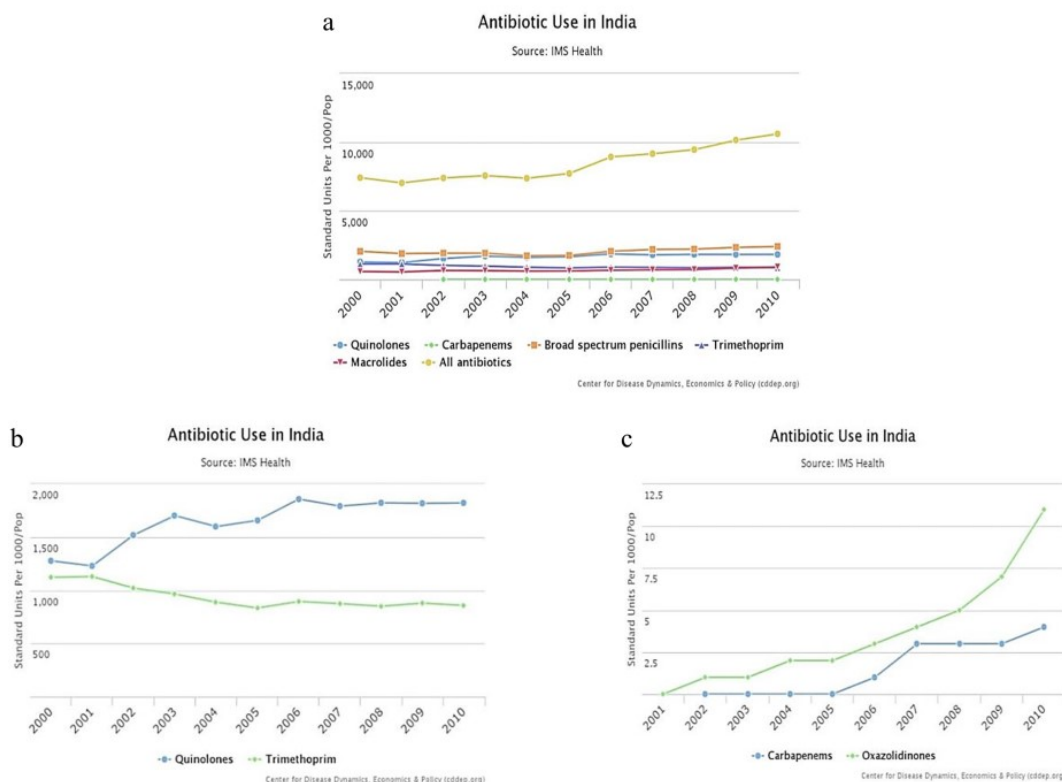


**Figure 6.3:** Trends in antibiotic consumption in India, 2000 – 2010. Source: CDDEP. ResistanceMap Washington DC: Center for Disease Dynamics, Economics & Policy; 2015 [August 20, 2015]. <http://www.resistancemap.org>.

The Knowledge, Attitude and Practice (KAP) survey tools were developed in the 1950s in the fields of family planning and population studies in third world countries (Vandamme, 2009). In the last five years, three studies that focused on the general population showed varied levels (13% (Kumar et al., 2015) to 100% (Ahmad et al., 2015)) of self-medication of which 32% were antimicrobials (Keshari et al., 2014). Antibiotic re-use and shared prescriptions were also high (ca. 30%) and more than half the cohort stopped taking the medicine once the symptoms subsided (Aishwaryalakshmi et al., 2012). The urban population was more aware (Ahmad et al., 2015) of the rational use of medicines, expiry dates and disposal mechanisms as opposed to rural populations (Shah et al., 2011). Most of the ignorance in the latter demographic was propagated due to lack of information and knowledge and non-availability of health care facilities (Phalke et al., 2006) rather than financial costs. Antibiotics (amoxicillin and co-amoxiclav, roxithromycin, azithromycin, ciprofloxacin, cefixime and levofloxacin) (Bhanwra, 2013; Chinnasami et al., 2016; Keshari et al., 2014; Parakh et al., 2013; Savkar et al., 2015) and paracetamol (Kasabe et al., 2015; Keshari et al., 2014) were commonly bought over the counter from chemists to get relief from fever, cold and cough. Only 20% of the pregnant women attending village clinics (Adhikari et al., 2013) used prescriptions to buy antibiotics. Only 20-30% of the population cohorts (Chinnasami et al., 2016) on an average were aware of the use of antibiotics in bacterial versus viral infections. A higher grade of education was correlated with high KAP score as 90% of postgraduates, 84.1% of graduates and only 67% of high school matriculates had the highest KAP score (Agarwal et al., 2015).

India, with a population of more than 1.34 billion (as of July 2017) marked by cultural diversity, and emerging from varied socio-economic backgrounds, requires assessments across different strata of the community. In this study we use a KAP survey as a tool for the educational diagnosis of antibiotic use and misuse within a select cohort of the Indian population to evaluate the public health issue of AMR.

## **6.2. Materials and methods**

### **6.2.1. Study Design and Population**

This study was a 7-week cross-sectional questionnaire based survey conducted in June - July 2016 as part of a CSIR 800 project. 504 respondents belonging to different demographic strata of Indian society were targeted that included but were not restricted to CSIR - NCL students, scientists, and other staff, chemists and businessmen. Individuals

less than 18 years and above 75 years of age were excluded along with those individuals who did not give verbal consent. Individuals who were unable to answer the questions due to some barriers were excluded along with pregnant women.

### 6.2.2. Study Questionnaire

A semi-structured questionnaire was developed following WHO guidelines (Wood and Tsu, 2008) on KAP survey focusing on antibiotic use and misuse. The questionnaire was modified to accommodate the current policies and campaigns started by the Indian government (Ghafur et al., 2012; Hazra, 2014; Travasso, 2016) and in order to suit the target population. The annual income stratification was done with the updated Kuppaswamy's socio-economic status scale (Oberoi, 2015). Stratification based on literacy included illiterates (no education at all), less than primary education (less than 8<sup>th</sup> class education), primary to secondary education (8<sup>th</sup> to 12<sup>th</sup> class education), undergraduates, graduates and postgraduates. The questionnaire included a total of 35 questions, 26 close-ended questions pertaining to the responders' knowledge, attitude and practices regarding the antibiotic use and self-medication. The knowledge section consisted of 14 questions followed by 5 questions pertaining to Attitude and finally 7 questions in the Practice section. Nine open-ended questions relating to the demographic details of the participants were also included. The questionnaire covered the following aspects a) standard demographic data to assess any correlation between respondent demographic characteristics and antibiotic use practices; b) the respondent's attitude and behavior towards regulated use of antibiotics and antibiotic resistance; c) self-medication; d) information about medicines given to them by pharmacists; e) obtaining prescriptions and having them filled. Response options included True/False, Yes/No and 5 point *Likert* scale (strongly disagree - disagree - undecided - agree - strongly agree) wherever appropriate and the first question had multiple choices.

The above mentioned pre-tested questionnaire was administered by two different approaches (Figure 6.4). The questionnaire was uploaded on Google forms and the link (<http://goo.gl/forms/wFi1VjfyHYbVo35I3>) was provided to the respondents through official emails or social media. The questionnaire was made available in English and Marathi to target the local population. The study was explained to the respondents and informed consent was obtained from each participant. Participants either filled in the questionnaire independently or were read the questions and answers were recorded for them. In order to achieve generalizability of the sample, a survey was performed using

members of the general public at different study sites (e.g. shopping malls, supermarkets, housing societies, CSIR – NCL reception, cafeteria, different departments, shopping complex, medical center, etc.). Please refer to questionnaire in Appendix 6.1. The received questionnaires were checked for completeness of data and satisfaction with the inclusion and exclusion criteria. Simple pedagogical tools and descriptive statistics were used to generate percentages and proportions.

### 6.2.3. Statistical Analysis

The data was analyzed by using simple descriptive statistics to generate frequencies, percentages and proportions. Data were further summarized by appropriate statistical tests using GraphPad Prism 6, version 6.01 for Windows, (GraphPad Software Inc., San Diego; 2007).

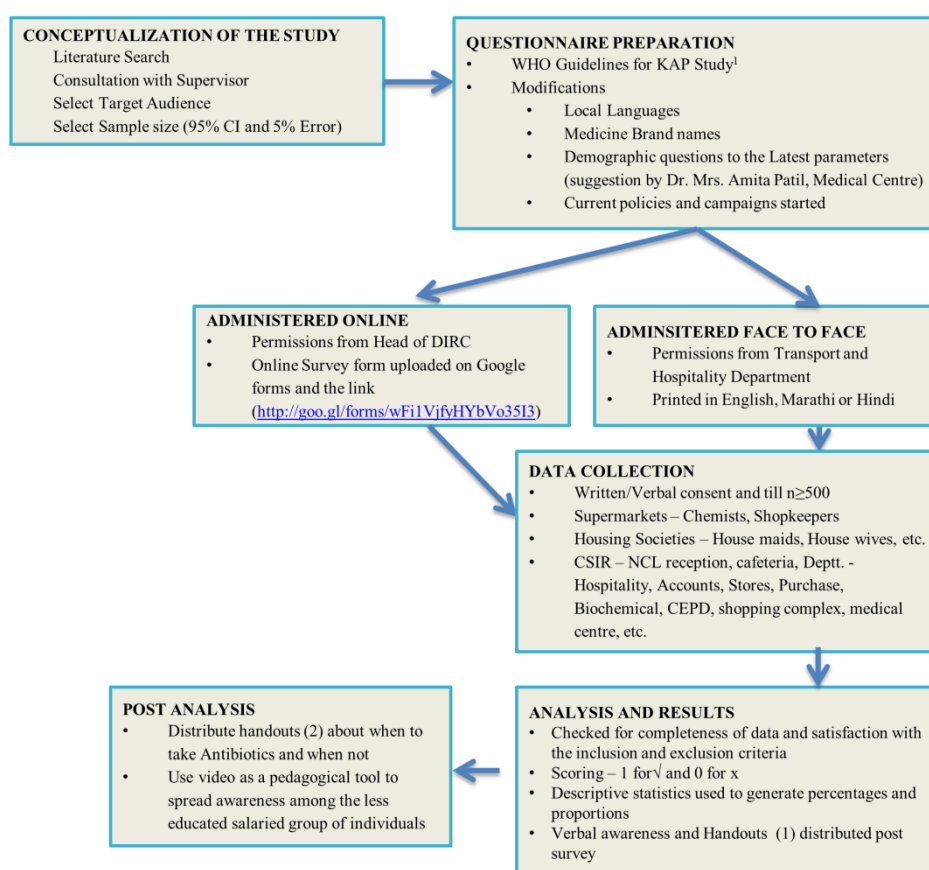


**Figure 6.4:** Methodology followed in this study.

### 6.3. Results and Discussion

This is the first of a kind study done with a moderate size dataset (>500) involving the general population of India and is comparable to two studies of similar sample sizes of around 500, conducted in rural areas of Maharashtra (Phalke et al., 2006) and another undertaken in households of the Sonipat city, Haryana (Kumar et al., 2015), which focused on reporting utilization practices in the households rather than antibiotic use. Although bigger data-sets have been reported they are in a certain subtype of population; e.g., 1121 dental and paramedical students (Tevatia et al., 2016), 872 parents (Agarwal et al., 2015) and 656 pregnant women visiting village clinics (Adhikari et al., 2013). No study exists on the general population or a cross section of society and hence a holistic sample set has been addressed in this study.

#### 6.3.1. Demographics

The demographics of the 504 respondents are presented in Table 6.2, where 66.5% belonged to Maharashtra. The age, education and professional/employment status was analysed. 98% of the study group was below the age of retirement (60 years). The dataset consisted of students and salaried individuals in similar ratio (~40%). Within the set there were 196 employed people of whom 40 are graduates, 75 postgraduates and among the professionals there were 7 chemists and 6 clinicians.

The overall results (Figure 6.5a) convey that of the 504 respondents, 8% of the respondents had the correct knowledge, 12% had the correct attitude and 23% followed the correct practice for rational antibiotic use. Only 4 (<1%) respondents had the correct knowledge, attitude and practice towards rational antibiotic use and AMR; they were all postgraduates (PG).

**Table 6.2:** Demographic details of all 504 respondents

Gender		Occupation	
Male	252 (50.0)	Student	200 (39.7)
Female	252 (50.0)	Salaried	196 (38.9)
Age		Business	24 (4.8)
18 – 20	21 (4.2)	Professional	43 (8.5)
21 – 30	286 (56.7)	House wife	12 (2.4)
31 – 40	114 (22.6)	Retired	9 (1.8)
41 – 50	34 (6.7)	Doctor	6 (1.2)
51 – 60	39 (7.7)	Others	14 (2.8)
61 – 75	10 (2.0)		

Educational Qualification		Annual Income (₹)	
Illiterate	13 (2.6)	Less than 20,000	36 (8.2)
		20,000 – 1,00,000	128 (29.0)
Less than Primary	28 (3.6)	1,00,000 – 5,00,000	172 (39.0)
		5,00,000 – 10,00,000	72 (16.3)
Undergraduate	34 (6.7)	More than 10,00,000	33 (7.5)
Graduate	94 (18.7)	Family member in health related field	
Postgraduate	288 (57.1)	Yes	129 (26.0)
		No	368 (74.0)
Others	19 (3.8)		

### 6.3.2. Knowledge

The respondents were tested on their knowledge of the use of antimicrobials in viral and bacterial infections, purchase of OTC and prescription drugs including the recently introduced red line drugs (Figure 6.5) and AMR were presented. Overall the correct knowledge about antibiotic use and resistance was observed only in 39 out of 504 individuals that included 33 postgraduates. With respect to profession, 19 students, 11 salaried and 4 professionals belonged to this group.

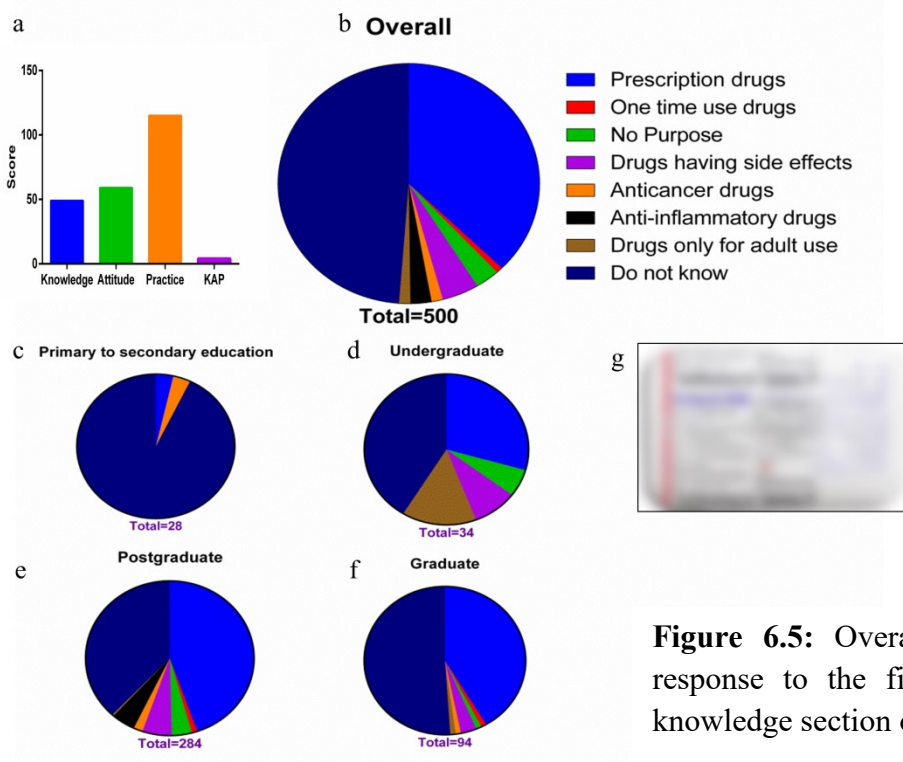


**Figure 6.5:** Overall KAP score and response to the first question of the knowledge section of the KAP survey.

The postgraduates had the highest score ( $13.6\pm 2.8$  out of 17) and illiterates (no education at all) had the lowest score ( $5.8\pm 3.1$ ). Students ( $13.4\pm 3$ ) outperformed other professionals. Out of 504 respondents, 15 individuals thought the red line on the medicine strip or package has no purpose, of which 11 belonged to the postgraduate community. Overall 63% respondents were unaware that the red line indicated prescription drugs that included 71% of undergraduates (UG), 58.5% of graduates (G) and 55% of postgraduates (PG). Overall 31% were unaware that bacterial infection is not the cause for common cold and cough, 28% of postgraduates and 38% graduates belonged to this group. Almost half of the respondents (47%) were unaware that antibiotics cannot cure viral infections but only bacterial infection. 55% of the graduates belong to this group along with 27% of postgraduates. 86% of respondents who received only school education were unaware of the same. 90% of the respondents who had only received school education lacked the knowledge about differences between commonly used antibiotics and OTC medicines along with 17% of postgraduates and 32% of graduates. Illiterates had no idea about the red line or about the specificity of antibiotics towards bacterial infection. They neither could differentiate between OTC and antibiotics, nor were aware about consequences of indiscriminate use of antibiotics. 69.2% of illiterates believed common cold and flu is caused by change in climate and more than 60% believed paracetamol is an antibiotic. None of the respondents who had received less than primary education were aware of the red line. Around half of the undergraduate respondents believed that antibiotics are prescribed to reduce pain and inflammation compared to 83.2% postgraduates who disagreed. On an average 61% of illiterates and school pass outs believed that antibiotics were prescribed for pain or inflammation. 22% of the 504 respondents either did not comment or disagreed that AMR is a serious problem posed by our society locally or globally. Six out of seven illiterates, three out of four school pass outs, one in ten postgraduates, one in five graduates and all undergraduates belonged to this group.

The knowledge of ineffectiveness of antibiotics on irrational use was least in undergraduates (51.5%) and highest in postgraduates (90.6%). The awareness about the medical cost burden was significantly higher (91%) compared to that of other repercussions associated with injudicious and indiscriminate use of antibiotics (55%) in the study group.

### 6.3.3. Attitude

The attitude (Figure 6.6) towards falling sick and the consumption/prescription of antibiotics defined the tendency of the population to contribute towards AMR. A total of 59 respondents (11%) showed the correct attitude; this included 41 postgraduates, 12 graduates and 2 undergraduates. Based on profession 28 students, 14 salaried respondents, 8 professionals and 4 businessmen belonged to this group. None of the illiterates were aware of their contribution to antibiotic resistance by consuming antibiotics. Postgraduates including businessmen once again had the highest average score ( $3.1 \pm 1.3$  out of 5) whereas lowest was ( $1.5 \pm 1.3$ ) for illiterates. More than 23% in each group disagreed that they contribute to AMR by taking antibiotics while more than 79% of illiterates and school pass outs remained undecided. One in five (PG) to one in four (G) of the highly educated group believed that skipping a dose does not contribute to AMR and was within the range documented in studies i.e. 21.3% – 31% (Rekha et al., 2014) but was far less than that documented in study performed in the rural areas of Maharashtra (Phalke et al., 2006), 36% of school pass outs believed the same whereas 62% illiterates remain undecided. One fourth of the study group believed that skipping a dose does not contribute to ABR that included 53.6% of those who had less than primary education, 36% respondents of primary to secondary educated individuals, 19.4% of postgraduates and 22% of graduates. Again the undecidedness of less educated respondents was highlighted through responses of 61.5% of illiterates and 36% of school pass outs being unaware of the consequences of skipping a dose.



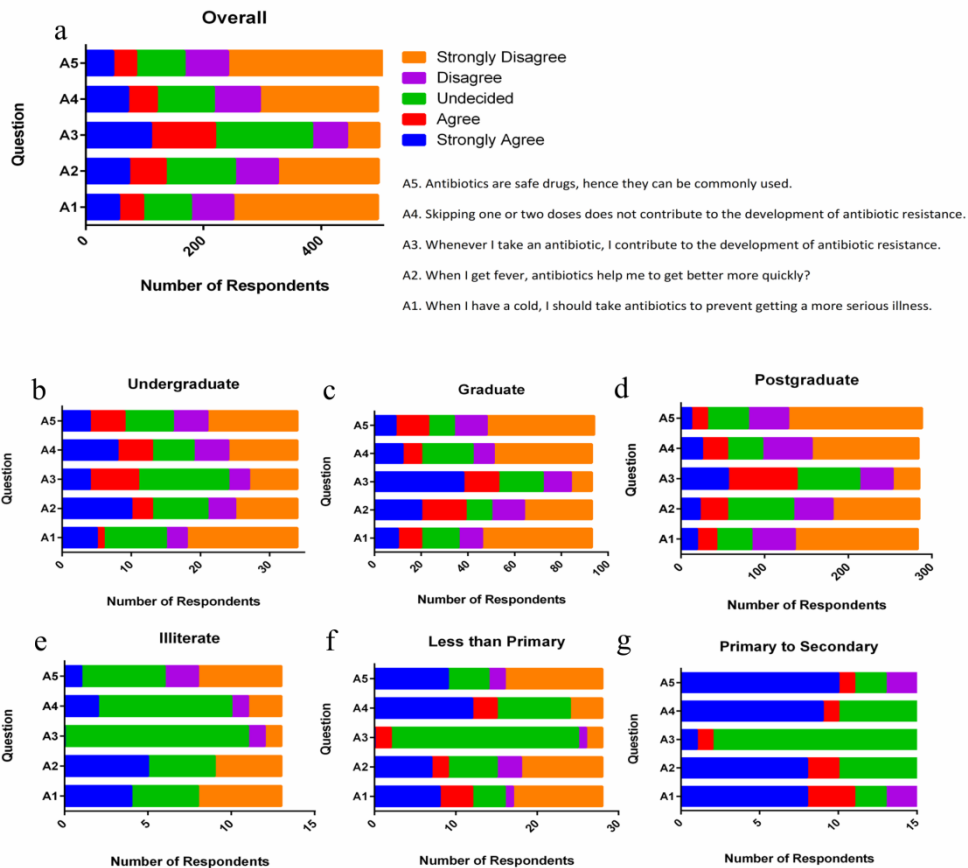


**Figure 6.6:** Responses to the attitude section of the KAP survey.

### 6.3.4. Practice

Practices (Figure 6.7 and 6.8) here measure the concrete action of popping pills in response to falling sick with or without consulting the doctor. Highest consumers of antibiotics (Figure 6.3) were the educated population. 58.8% of undergraduates, 75.5% of graduates and 69.1% of postgraduates belonged to this category compared to 30.8% of uneducated respondents. The average frequency of antibiotic use was 23% similar to statistics available for India (Morgan et al., 2011). Postgraduates had the highest average score ( $7.1 \pm 2.0$  out of 9) and illiterates had the lowest ( $4.3 \pm 1.4$ ). Retired respondents also reflected good practice with an average score of  $7.2 \pm 2.1$  compared to an average score of  $5.9 \pm 2.2$  for the salaried group of individuals. The 115 individuals who had the correct practice consisted of 89 postgraduates, 10 graduates, 7 undergraduates and one from each group that had received primary and secondary education respectively. This group included 66 students, 25 salaried, 7 professionals, 4 each of retired and doctors and 2 businessmen. One in four people in this study would stop taking antibiotics once they felt better and did not complete the full course (Figure 6.7), this proportion was higher for

illiterates (62%) and individuals with less than primary education (75%) along with 53.6% from the primary to secondary education group which concurred with the scores reported by Aishwaryalakshmi et. al.(Aishwaryalakshmi et al., 2012) Additionally, 16% of postgraduates and 24% each of undergraduates and graduates had the same practice and did not complete the full course. 11% of undergraduates and postgraduates saved antibiotics for future use.

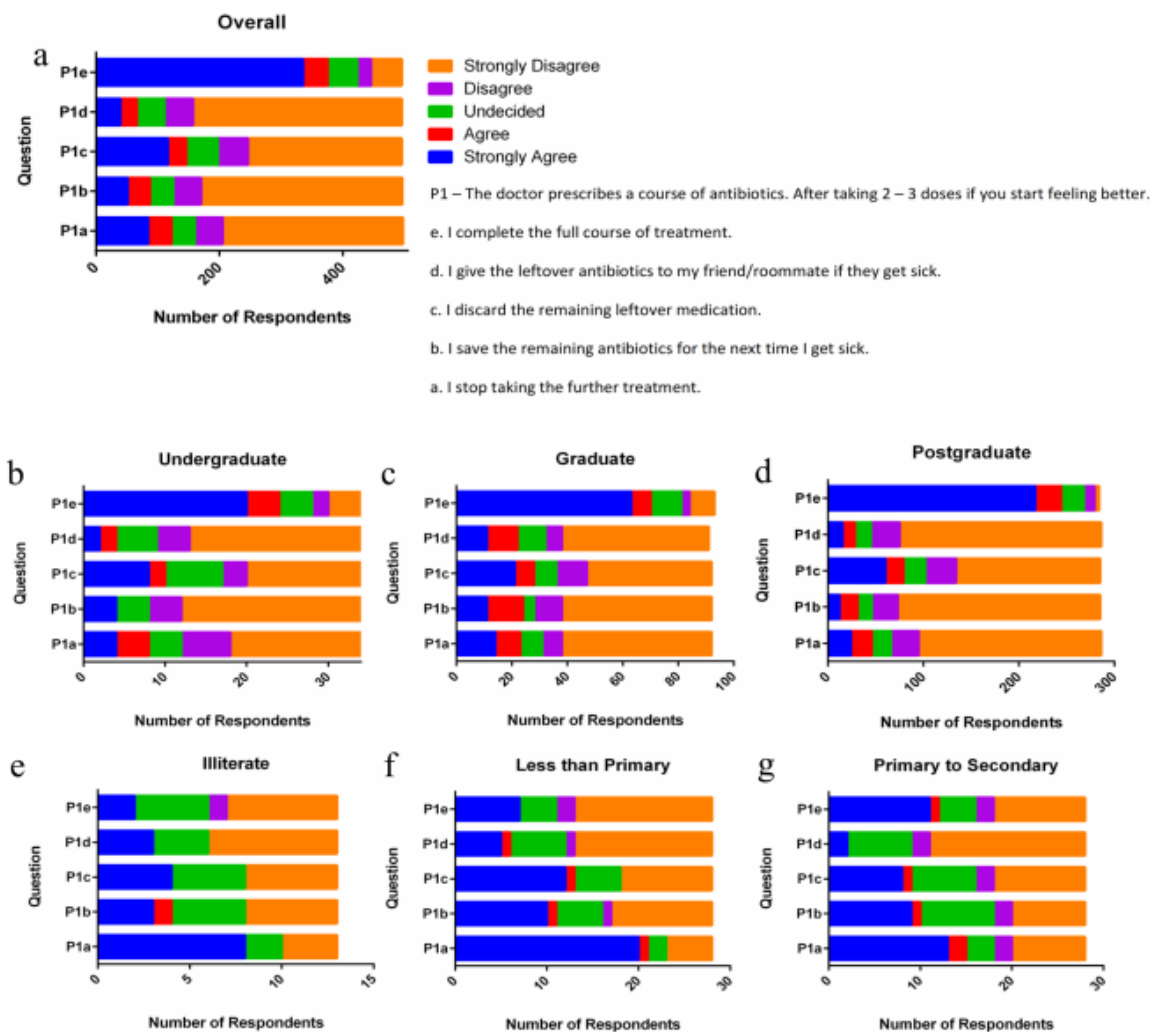


**Figure 6.7:** Responses to the practice section question 1 of the KAP survey.

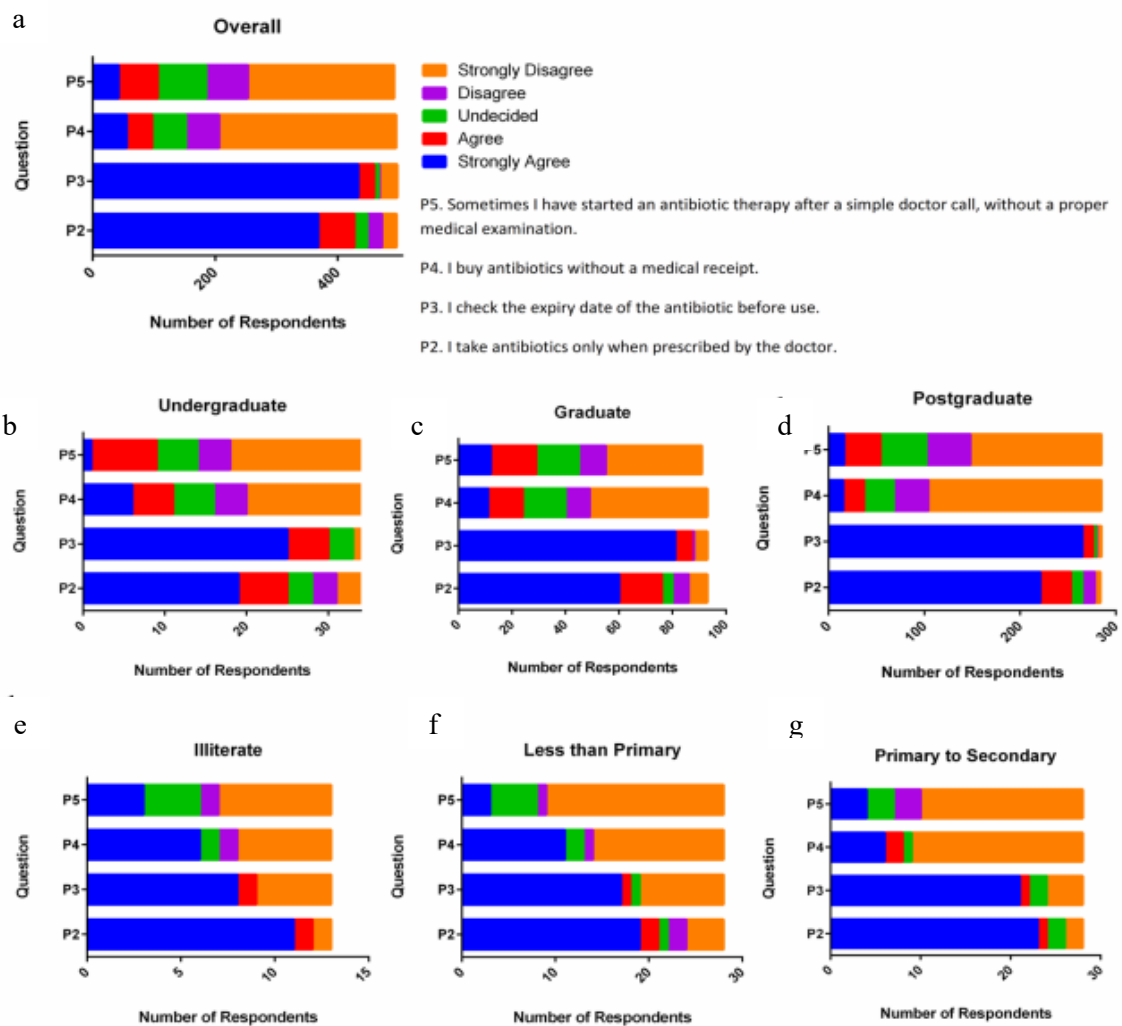


**Figure 6.8:** Responses to the practice section questions 2 to 5 of the KAP survey.

There wasn't any clear understanding of how unused antibiotics were disposed in the under educated population, which is consequently a major societal concern as reported previously (Shah et al., 2011). This calls for spreading awareness regarding appropriate disposal of unwanted medicines. Medicating friends or relatives was prevalent independent of the level of literacy as 23% of illiterates and graduates practiced sharing their medicines with friends or family along with 10% of postgraduates and 12% of undergraduates. In this study, 14.5% did not practice completion of the full course of prescribed medicines which is in accordance with Agarwal et. al. (Agarwal et al., 2015) This cluster of individuals included 54% of illiterates, 61% of individuals with less than

primary education, 6% of postgraduates and 15% of undergraduates and graduates. 9.7% individuals were found to self-medicate in this study that was relative to the proportions obtained by Kasabe et al. for the patients category in the Pune region (Kasabe et al., 2015). More than 7% of the illiterates, postgraduate, individuals with primary to secondary education belonged to this group along with 17.7% of undergraduates, 14% of graduates and 21% of individuals with less than primary education. 31.5% of illiterates and individuals with less than primary education along with 2% of postgraduates, 3% of undergraduates, 6.4% of graduates and 14.3% of individuals with schooling between primary and secondary education did not check the expiry date before consumption of antibiotics. One in five bought medicines without a medical receipt and tended to start an antibiotic course by calling a doctor without a proper medical examination (Figure 6.8). The 20% of respondents who bought antibiotic without a prescription consisted of 13% of postgraduates, 29% of undergraduates and graduates and 40% of individuals with less than primary education. 46% of illiterates agreed and the same proportion disagreed on buying antibiotics without prescriptions/medical receipts.

The percentage of the population buying antibiotics over the counter is alarming and shows severe laxity resulting in calls for stringent policies to restrict even the supply system of antibiotics from chemist to consumers as suggested in earlier reports (Kalra et al., 2015). The 22% of respondents who started antibiotic courses after calls to the doctor without a proper medical examination included 31.9% of graduates, 19% of postgraduates, 25% of illiterates and undergraduates, and 12.5% of school pass outs. 65.5% of respondents had consumed antibiotics in the last year similar to that reported in a 2016 study (Chinnasami et al., 2016).

In the KAP survey questionnaire, five questions (KQ1, KQ4, KQ11, AQ4 and PQ1e, Refer Appendix 6.1) critically decided the respondent's status towards antibiotic stewardship. None of the adults who had only received education in school knew the correct answer. Our study highlights the definitive influence of education on the prudent use of antibiotics, as the proportion of correct responses increased from 9% in undergraduates to 11% in graduates to 21% in postgraduates respectively.

The correlational statistics (Table 6.3) suggests that, if we categorize based on literacy, postgraduates had a moderate positive correlation ( $p$ -value  $\leq 0.0001$ ) whereas school pass outs had a weak to moderate negative correlation between Knowledge and Attitude (K-A). If categorization was based on profession, better correlation was observed between K-A, Knowledge and Practice (K-P) and Attitude and Practice (A-P) for salaried

individuals (strong for K-P) in comparison to students. House wives showed, moderate (if not statistically significant) negative correlation between K-A. Based on gender, males had a moderate positive correlation, better for A-P in contrast to females, who had a moderate positive correlation (better than males) for K-A and a strong positive correlation for K-P.

**Table 6.3:** Correlational Statistics for all 504 respondents

	Variable (n)	K-A	K-P	A-P
Based on Literacy	Illiterate (13)	0.030	0.077	0.199
	Less than Primary (28)	-0.183	0.150	0.295
	Primary to Secondary (28)	-0.270	0.128	0.041
	Undergraduate (34)	0.398 <sup>a</sup>	0.369 <sup>a</sup>	0.367 <sup>a</sup>
	Graduate (94)	0.277 <sup>b</sup>	0.203	0.316 <sup>b</sup>
	Postgraduate (288)	0.329 <sup>d</sup>	0.257 <sup>d</sup>	0.398 <sup>d</sup>
	Others (19)	0.477 <sup>a</sup>	0.576 <sup>b</sup>	0.223
Based on Profession	Student (200)	0.383 <sup>d</sup>	0.250 <sup>c</sup>	0.370 <sup>d</sup>
	Salaried (196)	0.488 <sup>d</sup>	0.505 <sup>d</sup>	0.441 <sup>d</sup>
	Business (24)	0.390	0.425 <sup>a</sup>	0.503 <sup>a</sup>
	Professional (43)	0.288	0.264	0.439 <sup>b</sup>
	House wife (12)	-0.331	0.214	0.546
	Retired (9)	0.385	0.127	0.476
	Doctor (6)	0.000	-0.114	-0.218
	Others (14)	-0.222	0.621 <sup>a</sup>	0.150
Gender	Male (252)	0.411 <sup>d</sup>	0.391 <sup>d</sup>	0.446 <sup>d</sup>
	Female (252)	0.444 <sup>d</sup>	0.510 <sup>d</sup>	0.395 <sup>d</sup>

Footnotes: <sup>a</sup>P ≤ 0.05, <sup>b</sup>P ≤ 0.01, <sup>c</sup>P ≤ 0.001 and <sup>d</sup>P ≤ 0.0001

Interpretation of findings from this survey should be done cautiously as there are limitations to the study including the size and location of the population. The study revealed a higher knowledge, awareness and practice in individuals that were educated at least till higher secondary level. The study also revealed unawareness amongst 30-40% of this cross section of society to the difference between bacterial and viral infections and the futility of using antibiotics for the latter. The majority didn't realize the problem with skipping a dose or incomplete courses of prescribed antibiotics. The red line was not identified by a majority of the population and neither could it identify the global threat posed by AMR. One in five believed antibiotic resistance was not a serious issue. One in

four individuals stopped taking the antibiotics once they felt better. One in ten people self-medicated on a regular basis; including one in five undergraduate and one in seven graduate degree holders.

**a**

**Medicines Banned in India Include**  
प्रतिबंधित दवाओं में शामिल  
भारतात बंदी घालण्यात आलेली औषधे खालील प्रमाणे आहेत



Not just Vicks 500 and Corex India has banned 344 drugs

Over The Counter (OTC) Medicines allowed in India Include  
भारत में अनुमति दी गई दवाओं में शामिल  
भारतात बंदी नसलेली औषधे खालील प्रमाणे आहेत



**b**



DO YOU KNOW? MEDICINES WITH A RED LINE ON THE STRIP SHOULD NEVER BE CONSUMED WITHOUT DOCTOR'S PRESCRIPTION

क्या आपको पता है? दवाओं की पर्ची पर एक लाइन रेखा प्रतीक है कि उन दवाओं का सेवन डॉक्टर की पर्ची के बिना कभी नहीं किया जाना चाहिए

तुम्हारा माहित आहे का? ज्या औषधांच्या कडवर वर लात रेखा आहे ती औषधे डाक्टरांच्या चिठ्ठी शिवाय विकत घेऊन घेतत व त्यांचे सेवन करू नये

**लाल रेखा पर ध्यान दें जिम्मेदार बनिएं**

पैठियायोजिक जेसे दवाडुली के पैक पर एक लात रेखा होती है जिसका संकेत है कि केवल डॉक्टर की सलाह पर उन दवाडुली का सेवन किया जाना चाहिए। हमेशा विक्रयक द्वारा निर्धारित कोर्स पूरा करें।

**LOOK OUT FOR THE RED LINE BE RESPONSIBLE**

Medicines such as antibiotics have a red vertical line on their packs to indicate that they should be consumed only on doctor's advice. Always complete the full course as prescribed by the doctor.

**लाल रेखा पाहो जबाबदार रहा**

पैठियायोजिक मारुपी औषधे पैक वर लाल रेखा चिन्हित की, ही औषधे केवल डाक्टरांच्या सल्लाहा नुसार व सेवन ब्रदरनीत मेहुनी डाक्टरानी सल्लाहाकेत ओषधांचा कोर्स पूरा करावा

Ministry of Health & Family Welfare Government of India

स्वास्थ्य और परिवार कल्याण मंत्रालय सरकार और परिवार कल्याण विभाग

डॉक्टरांच्या चिठ्ठी शिवाय खालील X H श्रेणी औषधे विकली जातात

डॉक्टर की पर्ची बिना बिक रही शेड्यूल एक्स एच की दवाएं

समाचार आलेख बातम्या लेख

A CSIR 800 Project Initiative, Issued in public interest, Circulated By Deepanwita Banerjee, July 14, 2016.  
सीएसआर 800 परियोजना, जनहित में जारी, दीपान्विता बॅनर्जी द्वारा परिचालित, मुंबयार, 14 जुलाई 2016.  
सीएसआर 800 प्रकल्प, मावजनिक हितार्थे जारी, दीपान्विता बॅनर्जी कडून प्रसारित, 14 जुलाई 2016.

A CSIR 800 Project Initiative, Issued in public interest, Circulated By Deepanwita Banerjee, July 14, 2016.  
सीएसआर 800 परियोजना, जनहित में जारी, दीपान्विता बॅनर्जी द्वारा परिचालित, मुंबयार, 14 जुलाई 2016.  
सीएसआर 800 प्रकल्प, मावजनिक हितार्थे जारी, दीपान्विता बॅनर्जी कडून प्रसारित, 14 जुलाई 2016.

FRONT SIDE

BACK SIDE

**Figure 6.9:** Handout distributed to the respondents post KAP study.

We strongly recommend implementation of educational programs for primary/secondary schools in the country. There is utmost need for proper statutory antibiotic control policies restricting availability of drugs to the public. Educational programs should make healthcare practitioners aware including pharmacists/chemists and consumers alike. Safe practices need to be reiterated. Students and salaried employees must be educated about dangers of self-medication and indiscriminate use of drugs.

Minor ailments can be relieved with OTC medications such as Paracetamol or with some other traditional or herbal medicines, without physician consultation. Instructional and educational campaigns among different classes of Indian society using short videos, printed handouts (Figure 6.9, were distributed after this study was conducted) and other pedagogical tools are critical. Private firms and pharmacists should be involved as partners for creating awareness among communities for rational use and resistance to antibiotics. Currently, there is a huge market and policy failure that allows the sale of drugs without a prescription. To address the threat of AMR, our study underscored the importance of education and prudent use of antibiotics in human medicine. It is critical to develop strategies comprising measures related to information, education and surveillance across the varied populations in India. Antibiotic stewardship activities in hospitals, clinics and nursing homes are critical along with imposition of good sanitation and hygiene. Coordination between the health sector and the animal husbandry/poultry sector is also essential. In any ecological system, including in the case of antibiotics, pressure causes evolution. In the light of resultant development of resistance and therapeutic failures, research programs to develop quick diagnostics and extending shelf life of existent antibiotics need to be funded. Government needs to formulate a comprehensive plan to deal with AMR and invest or find aid in state of the art diagnostics and new drugs. Non-adherence to such practices is a major public health issue.

#### **6.4. Conclusion**

In conclusion our study of 504 individuals is a first of a kind for the general population that sheds light on the knowledge, attitude and practices regarding antibiotic use and resistance among Indians belonging to varied income strata, different professions and educational background. The results brings to light the fact that the interventions and awareness campaigns should not be only educational but multipronged to tackle the serious societal issue of antibiotic resistance within the Indian society with special reference to its 800 million citizens. One needs to sound the alarm and educate each citizen about the scope and threat of AMR. Battling resistant bugs mandates the prudent use of antibiotics.





# Chapter 7

## Conclusion and Future Scope

*"I would rather have questions that can't be answered than answers that can't be questioned"*

*- Richard Feynman*

*"The significant problems we face cannot be solved at the same level of thinking with which we created them"*

*- Albert Einstein*

The genotype- phenotype relationship is fundamental to biological systems. The work described in this dissertation is a systems biology approach to studying *Chromobacterium violaceum* metabolism and its role in antibiotic resistance. This thesis explored the differential features of genotype and metabolic phenotype in response to antibiotics and antibiotic selection pressures. Dynamics of cell metabolism was shaped by cell architecture and environment and delineated using heterogeneous data types. Genome wide elucidation of DNA sequence, systemic phenotypes helped understand the molecular components and their interaction. Since biological systems are complex and more than the sum of their parts and new properties are known to emerge as an effect of interactions a model driven model-integrated approach was used. Constraints-based flux balance modeling identified the weakest link that can break the resistance phenotype. Thus, in this thesis I have advanced the current understanding of antibiotic resistance and

its connections to metabolism and developed scalable methods to identify candidates to re-sensitize resistant pathogens to antibiotics.

## 7.1. Recapitulation

A broad recap of some of the main concepts described and realized in this thesis is discussed here.

- Eight genetic variation in different levels of protein hierarchy resulted in acquired antibiotic resistance against two completely different antibiotics.
- Genetic variations were detected in genes including the local repressor of AcrAB drug efflux pump and S12 ribosomal protein *rpsL*.
- Phenotypic plasticity and metabolic reprogramming was identified in the resistant populations and the fitness costs associated results in re-sensitization using 4 different substrates.
- Nine fold higher growth rates and 1.3 fold increase in violacein point towards phenotypic plasticity of the evolved strains.
- Temporal variation of metabolites suggest metabolic reprogramming as a survival strategy against antibiotics Successful genotype to phenotype correlations were identified, some obvious but some non-obvious.
- *iDB147* shed light on the nature, flexibility and rigidity of the core metabolism and helped us understand redox homeostasis is critical for survival of *C. violaceum*.
- A genome scale model for *C. violaceum*, *iDB858* was developed that shed light on to the emergent properties including but not limited to restriction of flux through different reactions (*in silico* enzymopathies) and perturbation of the reducing equivalents and PMF resulting in re-sensitization of the resistant populations when supplemented with candidate metabolites that take advantage of these enzymopathies and redox imbalance.

Apart from the above, many different correlations emerged as a result of integrative analysis of the heterogeneous data types in the context of a small and large scale model. Firstly correlation was observed in case of the repressor of a multi drug efflux pump, *acrR* (**Chapter 2, section 2.**) with extracellular violacein and prodeoxyviolacein as

observed in metabolomics high resolution mass spectrometry data (**Chapter 3, section 3.3.3.3**). Secondly correlation was observed in between the variant of *rpsL* (**Chapter 2, section 2.**) that leads to hyper-accurate phenotype with longer lags observed for different substrates (Ex-mets) in case of StrpR that bears the mutation (**Chapter 3, section 3.3.2**). Thirdly, correlation of *pabC* variation that may result in diverting carbon flux towards more amino acid biosynthesis (Chapter 2 section 2.) with accumulation of methionine, ile/leu and alanine in StrpR compared to other two, amino acid pools are higher as observed in metabolomics high resolution mass spectrometry data (**Chapter 3, Figure 3.10 and 3.13**). Fourth correlation is between PCA analysis of metabolomics data (**Chapter 3, Figure 3.7 and 3.8**) proving WT and StrpR to be behaving similarly compared to ChlR with model driven predictions and analysis that show that StrpR behaves more like WT but ChlR shows a completely different ATPM as well as FVA distribution (**Chapter 4 and 5**). Fifth correlation observed was between FVA that showed accumulation of pyruvate, malate and succinate in case of StrpR FVA (**Chapter 5, Section 5.**) with LCMS metabolomics profiles showing accumulation of significant amounts of pyruvate, succinate and malate in case of StrpR in comparison to the other two population data (**Chapter 3, Figure 3.5**). Finally the emergent property of redox imbalance as a function of antibiotic resistance development and decoupling between ETC and PMF was observed using experiments (**Chapter 3, Figures 3.19 to 3.26**) and proved by model simulations and predictions as explained in **Chapter 4 and 5**.

## 7.2 Unknown Frontiers of Antibiotic resistance

Some of the more global questions that are addressed in this thesis and yet need answers are:

1. Will the post genomic era delay onset of the post-antibiotic era?
2. Can metabolic changes modulate susceptibility of bacteria towards antibiotics?
3. Is there a recipe of antibiotics and adjuvants that will treat infection without development of resistance?

The answers to these questions and subverting this global crisis lies inadvertently in our abilities to measure and readout MICs of drugs, genomic features at different levels of molecular hierarchy and growth substrate preferences of clinically isolated resistant pathogens. The precision of tailoring specific microenvironments of the pathogen localization would predominantly dictate the future of personalized medicine and individualized therapy in infectious disease.

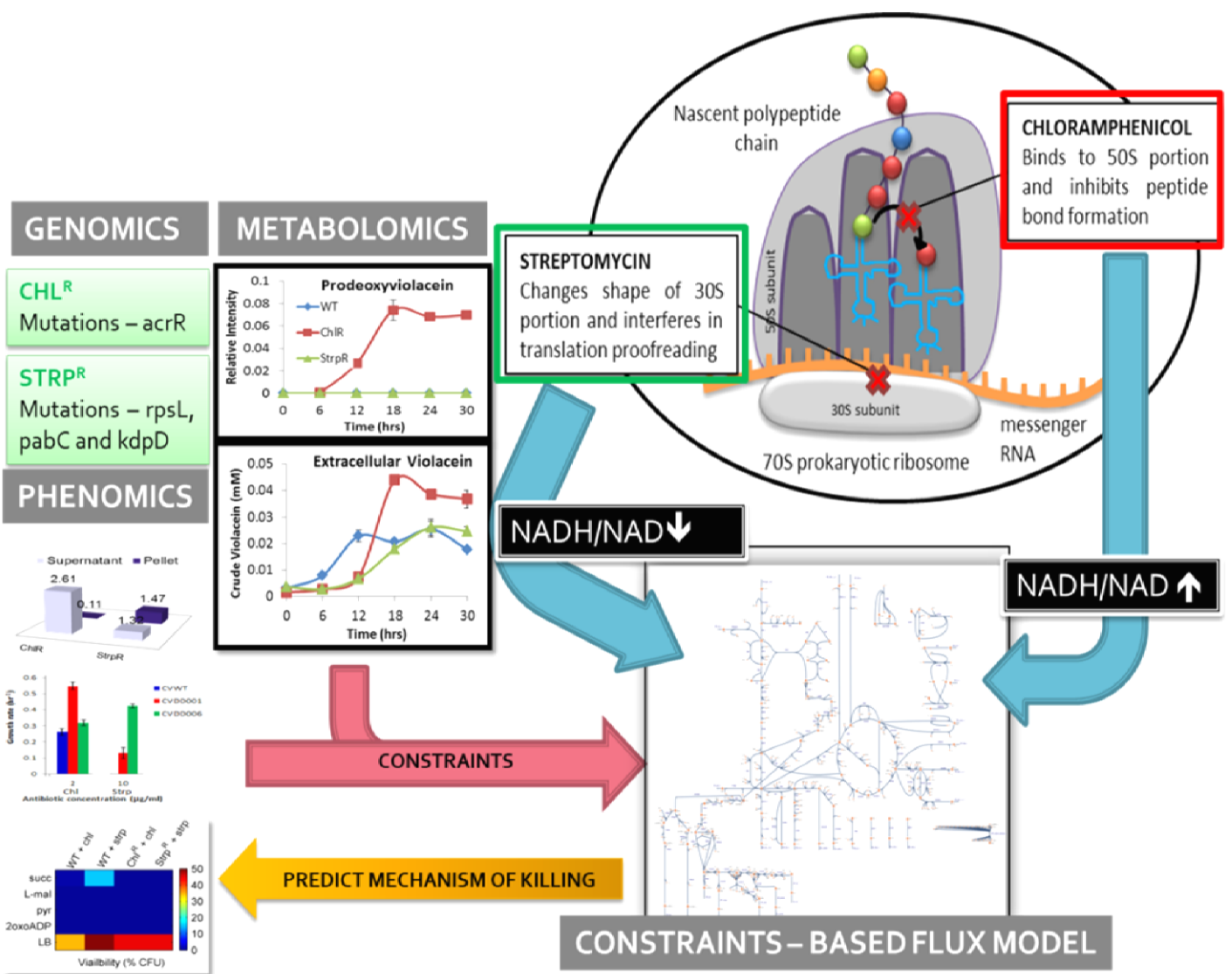


**Figure 7.1.** Emergent properties identified in this thesis work using a systems approach to counter antibiotic resistance

## 7.1.Future Scope and Directions

The common practice of self-medication and the availability of counterfeit drugs have exacerbated drug resistance in the developing world which leads to consequent treatment complications and increased healthcare costs. If resistance to treatment continues to spread, our interconnected, high-tech world may find itself back in the dark ages of medicine, before today's miracle drugs ever existed. The platform developed in this thesis may be used to identify and validate more candidate substrates for re-sensitization as well as used as a standard protocol for other pathogens in clinical settings. This will prove to be a scalable pipeline integrating growth, metabolite and MIC profiling and constraints-based flux balance models for clinical isolates and extend it to the ESKAPE (*Enterococcus faecium*, *Staphylococcus aureus*, *Klebsiella pneumoniae*, *Acinetobacter baumannii*, *Pseudomonas aeruginosa*, and *Enterobacter* species) pathogens. Such constraints-based models will help to understand differential dynamics of cell metabolism for susceptible and resistant bacteria and provide a systems level focus on mechanisms of resistance and open up novel avenues for personalized treatment and individualized therapy. In house OMICS data sets included in this thesis work can be further integrated with an additional layer of available gene expression data and ribosomal machinery information to predict other genotype- phenotype relationships under such conditions.



# References

- A. Acharya, A.J.D., 1997. Studies on utilization of acetonitrile by *Rhodococcus erythropolis* A10. *World J. Microbiol. Biotechnol.* 13, 175–178.
- Acevedo, A., Aroca, G., Conejeros, R., 2014. Genome-scale NAD(H/(+)) availability patterns as a differentiating feature between *Saccharomyces cerevisiae* and *Scheffersomyces stipitis* in relation to fermentative metabolism. *PLoS One* 9, e87494.  
doi:10.1371/journal.pone.0087494
- Adhikari, A., Ray, M., Banerjee, S., Debnath, P., Bhattacharya, S., Bhowal, T., Verma, S.K., 2013. Kap (Knowledge, Attitudes and Practices) Study on Medicine and Health Infrastructure Use in Pregnant Women of Rural Areas of Maharashtra, India: a Cross-Sectional Survey. *Int. J. Res. Ayurveda Pharm.* 4, 793–796. doi:10.7897/2277-4343.04602
- Agarwal, D., Gregory, S.T., O'Connor, M., 2011. Error-Prone and Error-Restrictive Mutations Affecting Ribosomal Protein S12. *J. Mol. Biol.* 410, 1–9.  
doi:10.1016/j.jmb.2011.04.068
- Agarwal, S., Yewale, V.N., Dharmapalan, D., 2015. Antibiotics use and misuse in children: A knowledge, attitude and practice survey of parents in India. *J. Clin. Diagnostic Res.* 9, SC21-SC24. doi:10.7860/JCDR/2015/14933.6819
- Ahmad, A., Khan, M.U., Srikanth, A.B., Kumar, B., Singh, N.K., Trivedi, N., Elnour, A.A., Patel, I., 2015. Evaluation of Knowledge, Attitude and Practice about Self-medication Among Rural and Urban North Indian Population. *Int. J. Pharm. Clin. Res.* 7, 326–332.
- Ahmetagic, A., Pemberton, J.M., 2011. Antibiotic resistant mutants of *Escherichia coli* K12 show increases in heterologous gene expression. *Plasmid* 65, 51–7.  
doi:10.1016/j.plasmid.2010.11.004
- Ahmetagic, A., Pemberton, J.M., 2010. Stable high level expression of the violacein indolocarbazole anti-tumour gene cluster and the *Streptomyces lividans* amyA gene in *E. coli* K12. *Plasmid* 63, 79–85. doi:10.1016/j.plasmid.2009.11.004
- Aishwaryalakshmi, K., Sasikala, B., Sreelalitha, N., Vigneshwaran, E., Yr, P., 2012.

- Assessment of Knowledge Perception and Attitudes on Medications in General Population. *Indian J. Pharm. Pract.* 5, 3–6.
- Allen, H.K., Donato, J., Wang, H.H., Cloud-Hansen, K.A., Davies, J., Handelsman, J., 2010. Call of the wild: antibiotic resistance genes in natural environments. *Nat. Rev. Microbiol.* 8, 251–259. doi:10.1038/nrmicro2312
- Allison, K.R., Brynildsen, M.P., Collins, J.J., 2011. Metabolite-enabled eradication of bacterial persisters by aminoglycosides. *Nature* 473, 216–220. doi:10.1038/nature10069
- Almaas, E., Oltvai, Z.N., Barabasi, A.L., 2005. The Activity Reaction Core and Plasticity of Metabolic Networks. *PLoS Comput. Biol.* 1, e68. doi:10.1371/journal.pcbi.0010068.eor
- Alonso, A., Martinez, J.L., 2000. Cloning and characterization of SmeDEF, a novel multidrug efflux pump from *Stenotrophomonas maltophilia*. *Antimicrob. Agents Chemother.* 44, 3079–3086. doi:10.1128/AAC.44.11.3079-3086.2000
- Alves De Brito, C.F., Carvalho, C.M.B., Santos, F.R., Gazzinelli, R.T., Oliveira, S.C., Azevedo, V., Teixeira, S.M.R., 2004. *Chromobacterium violaceum* genome: Molecular mechanisms associated with pathogenicity. *Genet. Mol. Res.* 3, 148–161. doi:ss11 [pii]
- Andersson, D.I., 2003. Persistence of antibiotic resistant bacteria. *Curr. Opin. Microbiol.* 6, 452–456. doi:10.1016/j.mib.2003.09.001
- Andrews, J.M., 2001. Determination of minimum inhibitory concentrations. *J. Antimicrob. Chemother.* 48, 5–16. doi:10.1093/jac/48.suppl\_1.5
- August, P.R., Grossman, T.H., Minor, C., Draper, M.P., MacNeil, I.A., Pemberton, J.M., Call, K.M., Holt, D., Osburne, M.S., 2000. Sequence analysis and functional characterization of the violacein biosynthetic pathway from *Chromobacterium violaceum*. *J. Mol. Microbiol. Biotechnol.* 2, 513–9. doi:11075927
- Aziz, R.K., Devoid, S., Disz, T., Edwards, R. a., Henry, C.S., Olsen, G.J., Olson, R., Overbeek, R., Parrello, B., Pusch, G.D., Stevens, R.L., Vonstein, V., Xia, F., 2012. SEED Servers: High-Performance Access to the SEED Genomes, Annotations, and Metabolic Models. *PLoS One* 7, e48053. doi:10.1371/journal.pone.0048053
- Baart, G.J.E., Zomer, B., de Haan, A., van der Pol, L. a, Beuvery, E.C., Tramper, J., Martens, D.E., 2007. Modeling *Neisseria meningitidis* metabolism: from genome to metabolic fluxes. *Genome Biol.* 8, R136. doi:10.1186/gb-2007-8-7-r136
- Balibar, C.J., Walsh, C.T., 2006. In Vitro Biosynthesis of Violacein from L -Tryptophan by the Enzymes VioA - E from *Chromobacterium V iolaceum* †. *Biochemistry* 45, 15444–15457.
- Banerjee, D., Parmar, D., Bhattacharya, N., Ghanate, A.D., Panchagnula, V., Raghunathan,



- A., 2017. A scalable metabolite supplementation strategy against antibiotic resistant pathogen *Chromobacterium violaceum* induced by NAD<sup>+</sup>/NADH<sup>+</sup> imbalance. *BMC Syst. Biol.* 11, 51. doi:10.1186/s12918-017-0427-z
- Barnard, a. M.L., Simpson, N.J.L., Lilley, K.S., Salmond, G.P.C., 2010. Mutations in *rpsL* that confer streptomycin resistance show pleiotropic effects on virulence and the production of a carbapenem antibiotic in *Erwinia carotovora*. *Microbiology* 156, 1030–1039. doi:10.1099/mic.0.034595-0
- Bartell, J.A., Blazier, A.S., Yen, P., Thøgersen, J.C., Jelsbak, L., Goldberg, J.B., Papin, J.A., 2017. Reconstruction of the metabolic network of *Pseudomonas aeruginosa* to interrogate virulence factor synthesis. *Nat. Commun.* 8, 14631. doi:10.1038/ncomms14631
- Bartell, J.A., Yen, P., Varga, J.J., Goldberg, J.B., Papin, J.A., 2014. Comparative Metabolic Systems Analysis of Pathogenic Burkholderia. *J. Bacteriol.* 196, 210–226. doi:10.1128/JB.00997-13
- Becker, S.A., Feist, A.M., Mo, M.L., Hannum, G., Palsson, B.O., Herrgard, M.J., 2007. Quantitative prediction of cellular metabolism with constraint-based models: the COBRA Toolbox. *Nat Protoc* 2. doi:10.1038/nprot.2007.99
- Becker, S.A., Feist, A.M., Mo, M.L., Hannum, G., Palsson, B.Ø., Herrgard, M.J., 2007. Quantitative prediction of cellular metabolism with constraint-based models: the COBRA Toolbox. *Nat. Protoc.* 2, 727–738. doi:10.1038/nprot.2007.99
- Bhanwra, S., 2013. A study of non-prescription usage of antibiotics in the upper respiratory tract infections in the urban population. *J. Pharmacol. Pharmacother.* 4, 60–62. doi:10.4103/0976-500X.107684
- Bhargava, P., Collins, J.J., 2015. Boosting Bacterial Metabolism. *Cell Metab.* 21, 154–155. doi:10.1016/j.cmet.2015.01.012
- Bhattacharya, N., Singh, A., Ghanate, A., Phadke, G., Parmar, D., Dhaware, D., Basak, T., Sengupta, S., Panchagnula, V., 2014. Matrix-assisted laser desorption/ionization mass spectrometry analysis of dimethyl arginine isomers from urine. *Anal. Methods* 6, 4602. doi:10.1039/c4ay00309h
- Bhubalan, K., Kam, Y.C., Yong, K.H., Sudesh, K., 2010. Cloning and expression of the PHA synthase gene from a locally isolated. *Malays. J. Microbiol.* 6, 81–90.
- Blosser, S., Gray, K.M., 2000. Extraction of violacein from *Chromobacterium violaceum* provides a new quantitative bioassay for N -acyl homoserine lactone autoinducers. *J. Microbiol. Methods* 40, 47–55.

- Bordbar, A., Feist, A.M., Usaite-Black, R., Woodcock, J., Palsson, B.O., Famili, I., 2011. A multi-tissue type genome-scale metabolic network for analysis of whole-body systems physiology. *BMC Syst. Biol.* 5, 180. doi:10.1186/1752-0509-5-180
- Brysk, M.M., Corpe, W. a., Hankes, L. V., 1969.  $\beta$ -Cyanoalanine Formation by *Chromobacterium violaceum*. *J. Bacteriol.* 97, 322–327.
- Burns, J.L., Hedin, L.A., Lien, D.M., 1989. Chloramphenicol resistance in *Pseudomonas cepacia* because of decreased permeability. *Antimicrob. Agents Chemother.* 33, 136–141. doi:10.1128/AAC.33.2.136
- Busse, J., Auling, G., 1988. Polyamine Pattern as a Chemotaxonomic Marker within the Proteobacteria. *Syst. Appl. Microbiol.* 11, 1–8. doi:10.1016/S0723-2020(88)80040-7
- Butler, M.S., Blaskovich, M.A., Cooper, M.A., 2017. Antibiotics in the clinical pipeline at the end of 2015. *J. Antibiot. (Tokyo).* 70, 3–24. doi:10.1038/ja.2016.72
- Campbell, S.C., Olson, G.J., Clark, T.R., McFeters, G., 2001. Biogenic production of cyanide and its application to gold recovery. *J. Ind. Microbiol. Biotechnol.* 26, 134–139. doi:10.1038/sj.jim.7000104
- Carepo, M.S.P., De Azevedo, J.S.N., Porto, J.I.R., Bentes-Sousa, A.R., Da Silva Batista, J., Da Silva, A.L.C., Schneider, M.P.C., 2004. Identification of *Chromobacterium violaceum* genes with potential biotechnological application in environmental detoxification. *Genet. Mol. Res.* 3, 181–194. doi:10.1002/chem.201002065
- Carter, A.P., Clemons, W.M., Brodersen, D.E., Morgan-warren, R.J., Wimberly, B.T., Ramakrishnan, V., 2000. Functional insights from the structure of the 30S ribosomal subunit and its interactions with antibiotics. *Nature* 407, 340–348.
- Castresana, J., 2001. Comparative genomics and bioenergetics. *Biochim. Biophys. Acta - Bioenerg.* 1506, 147–162. doi:10.1016/S0005-2728(01)00227-4
- Chatterjee, D., Begum, S., Adhikari, A., Sen, S., Hazra, A., Das, A., 2015. A questionnaire-based survey to ascertain the views of clinicians regarding rational use of antibiotics in teaching hospitals of Kolkata. *Indian J. Pharmacol.* 47, 105. doi:10.4103/0253-7613.150373
- Chavali, A.K., Whittemore, J.D., Eddy, J.A., Williams, K.T., Papin, J.A., 2008. Systems analysis of metabolism in the pathogenic trypanosomatid *Leishmania major*. *Mol Syst Biol* 4. doi:10.1038/msb.2008.15
- Cheung, C.Y.M., Williams, T.C.R., Poolman, M.G., Fell, D.A., Ratcliffe, R.G., Sweetlove, L.J., 2013. A method for accounting for maintenance costs in flux balance analysis improves the prediction of plant cell metabolic phenotypes under stress conditions. *Plant*

- J. 75, 1050–1061. doi:10.1111/tpj.12252
- Chico-Calero, I., Suárez, M., González-Zorn, B., Scortti, M., Slaghuis, J., Goebel, W., Vázquez-Boland, J.A., 2002. Hpt, a bacterial homolog of the microsomal glucose- 6-phosphate translocase, mediates rapid intracellular proliferation in *Listeria*. *Proc. Natl. Acad. Sci.* 99, 431–436. doi:10.1073/pnas.012363899
- Chinnasami, B., Sadasivam, K., Ramraj, B., Pasupathy, S., Chinnasami, B., Pediatr, J.C., 2016. Knowledge , attitude and practice of parents towards antibiotic usage and its resistance. *Int. J. Contemp. Pediatr.* 3, 256–261.
- Ciprandi, A., Da Silva, W.M., Santos, A.V., De Castro Pimenta, A.M., Carepo, M.S.P., Schneider, M.P.C., Azevedo, V., Silva, A., 2013. *Chromobacterium violaceum*: Important insights for virulence and biotechnological potential by exoproteomic studies. *Curr. Microbiol.* 67, 100–106. doi:10.1007/s00284-013-0334-5
- Control, N.C. for D., 2016. National Treatment Guidelines for Antimicrobial use in Infectious Diseases.
- Creczynski-pasa, T.B., Antônio, R. V, 2004. Energetic metabolism of *Chromobacterium violaceum*. *Genet. Mol. Res.* 3, 162–166.
- Crumpton, M.J., Davies, D. a. L., 1958. The isolation of d-fucosamine from the specific polysaccharide of *Chromobacterium violaceum* (NCTC 7917). *Biochem. J.* 70, 729–736.
- Daniels, C., Ramos, J.L., 2009. Adaptive drug resistance mediated by root-nodulation-cell division efflux pumps. *Clin. Microbiol. Infect.* 15, 32–36. doi:10.1111/j.1469-0691.2008.02693.x
- Dasgupta, S., Ramaswamy, D.R., Noronha, K., Rao, S., Seetharaman R, George, N., Singh, A., Singh, T., Dhiman, S., Bhol, A., 2015. Swachh Bharat: Industry Engagement – Scope & Examples. *Sci-Fi Sanit. Initiat. Res. Report. New Delhi Cent. Policy Res.*
- Datsenko, K.A., Wanner, B.L., 2000. One-step inactivation of chromosomal genes in *Escherichia coli* K-12 using PCR products. *Proc. Natl. Acad. Sci. U. S. A.* 97, 6640–5. doi:10.1073/pnas.120163297
- Davies, J., 1994. Inactivation of antibiotics and the dissemination of resistance genes. *Science* (80-. ). 264, 375–382.
- Dean, C.R., Narayan, S., Daigle, D.M., Dzink-Fox, J.L., Puyang, X., Bracken, K.R., Dean, K.E., Weidmann, B., Yuan, Z., Jain, R., Ryder, N.S., 2005. Role of the AcrAB-TolC efflux pump in determining susceptibility of *Haemophilus influenzae* to the novel peptide deformylase inhibitor LBM415. *Antimicrob. Agents Chemother.* 49, 3129–3135. doi:10.1128/AAC.49.8.3129-3135.2005

- Demirci, H., Wang, L., Iv, F.V.M., Murphy, E.L., Carr, J.F., Blanchard, S.C., Jogl, G., Dahlberg, A.E., Gregory, S.T., 2013. The central role of protein S12 in organizing the structure of the decoding site of the ribosome. *RNA* 19, 1791–1801.  
doi:10.1261/rna.040030.113.4
- Demoss, R.D., Evans, N.R., 1959. Physiological aspects of violacein biosynthesis in nonproliferating cells. *J. Bacteriol.* 78, 583–588.
- Demoss, R.D., Happel, M.E., 1959. Nutritional requirements of *Chromobacterium violaceum*. *J. Bacteriol.* 77, 137–141.
- Derewacz, D.K., Goodwin, C.R., McNeese, C.R., McLean, J.A., Bachmann, B.O., 2013. Antimicrobial drug resistance affects broad changes in metabolomic phenotype in addition to secondary metabolism. *Proc. Natl. Acad. Sci.* 110, 2336–2341.  
doi:10.1073/pnas.1218524110
- Devescovi, G., Kojic, M., Covaceuszach, S., Cámara, M., Williams, P., Bertani, I., Subramoni, S., Venturi, V., 2017. Negative Regulation of Violacein Biosynthesis in *Chromobacterium violaceum*. *Front. Microbiol.* 8, 1–11. doi:10.3389/fmicb.2017.00349
- Diwan, V., Tamhankar, A.J., Aggarwal, M., Sen, S., Khandal, R.K., Lundborg, C.S., 2009. Detection of antibiotics in hospital effluents in India. *Curr. Sci.* 97, 1752–1755.
- Dörries, K., Schlueter, R., Lalk, M., 2014. Impact of Antibiotics with Various Target Sites on the Metabolome of *Staphylococcus aureus*. *Antimicrob. Agents Chemother.* 58, 7151–7163.
- Dunn, M.F., Ramírez-Trujillo, J.A., Hernández-Lucas, I., 2009. Major roles of isocitrate lyase and malate synthase in bacterial and fungal pathogenesis. *Microbiology* 155, 3166–3175. doi:10.1099/mic.0.030858-0
- Duran, M., Alario A. F., D.N., 2010. *Chromobacterium violaceum* and Its Important Metabolites – review. *Folia Microbiology* 55, 535–547.
- Durán, N., Justo, G.Z., Durán, M., Brocchi, M., Cordi, L., Tasic, L., Castro, G.R., Nakazato, G., 2016. Advances in *Chromobacterium violaceum* and properties of violacein-Its main secondary metabolite: A review. *Biotechnol. Adv.* doi:10.1016/j.biotechadv.2016.06.003
- Durán, N., Menck, C.F., 2001. *Chromobacterium violaceum*: a review of pharmacological and industrial perspectives. *Crit. Rev. Microbiol.* 27, 201–222.  
doi:10.1080/20014091096747
- Dutta, S.S., 2017. India launches strategy to curb antimicrobial resistance. *BMJ* 357, j2049.  
doi:10.1136/bmj.j2049
- Dwyer, D.J., Belenky, P.A., Yang, J.H., MacDonald, I.C., Martell, J.D., Takahashi, N., Chan,

- C.T.Y., Lobritz, M.A., Braff, D., Schwarz, E.G., Ye, J.D., Pati, M., Vercruyse, M., Ralifo, P.S., Allison, K.R., Khalil, A.S., Ting, A.Y., Walker, G.C., Collins, J.J., 2014. Antibiotics induce redox-related physiological alterations as part of their lethality. *Proc. Natl. Acad. Sci. U. S. A.* 111, E2100-9. doi:10.1073/pnas.1401876111
- Ebrahim, A., Almaas, E., Bauer, E., Bordbar, A., Burgard, A.P., Chang, R.L., Drager, A., Famili, I., Feist, A.M., Fleming, R.M., Fong, S.S., Hatzimanikatis, V., Herrgard, M.J., Holder, A., Hucka, M., Hyduke, D., Jamshidi, N., Lee, S.Y., Le Novere, N., Lerman, J.A., Lewis, N.E., Ma, D., Mahadevan, R., Maranas, C., Nagarajan, H., Navid, A., Nielsen, J., Nielsen, L.K., Nogales, J., Noronha, A., Pal, C., Palsson, B.O., Papin, J.A., Patil, K.R., Price, N.D., Reed, J.L., Saunders, M., Senger, R.S., Sonnenschein, N., Sun, Y., Thiele, I., 2015. Do genome-scale models need exact solvers or clearer standards? *Mol. Syst. Biol.* 11, 831–831. doi:10.15252/msb.20156157
- Edgar, R., Friedman, N., Shahar, M.M., Qimron, U., 2012. Reversing bacterial resistance to antibiotics by phage-mediated delivery of dominant sensitive genes. *Appl. Environ. Microbiol.* 78, 744–751. doi:10.1128/AEM.05741-11
- Edwards, J.S., Covert, M., Palsson, B., 2002. Metabolic modelling of microbes: The flux-balance approach. *Environ. Microbiol.* 4, 133–140. doi:10.1046/j.1462-2920.2002.00282.x
- Edwards, J.S., Palsson, B.O., 2000. The *Escherichia coli* MG1655 in silico metabolic genotype: its definition, characteristics, and capabilities. *Proc. Natl. Acad. Sci. U. S. A.* 97, 5528–5533. doi:10.1073/pnas.97.10.5528
- Edwards, J.S., Palsson, B.O., 1999. Systems properties of the *Haemophilus influenzae* Rd Metabolic Genotype. *Cell Biol. Metab.* 274, 17410–17416.
- Elkins, C. a., Mullis, L.B., Lacher, D.W., Jung, C.M., 2010. Single nucleotide polymorphism analysis of the major tripartite multidrug efflux pump of *Escherichia coli*: Functional conservation in disparate animal reservoirs despite exposure to antimicrobial chemotherapy. *Antimicrob. Agents Chemother.* 54, 1007–1015. doi:10.1128/AAC.01126-09
- Fani, F., Leprohon, P., Légaré, D., Ouellette, M., 2011. Whole genome sequencing of penicillin-resistant *Streptococcus pneumoniae* reveals mutations in penicillin-binding proteins and in a putative iron permease. *Genome Biol.* 12, R115. doi:10.1186/gb-2011-12-11-r115
- Fantinatti-Garboggini, F., Almeida, R. De, Portillo, V.D.A., Barbosa, T. a P., Trevilato, P.B., Neto, C.E.R., Coêlho, R.D., Silva, D.W., Bartoletti, L.A., Hanna, E.S., Brocchi, M.,

- Manfio, G.P., 2004. Drug resistance in *Chromobacterium violaceum*. *Genet. Mol. Res.* 3, 134–147.
- Farrar, W.E., O'dell, N.M., 1976. beta-Lactamase activity in *Chromobacterium violaceum*. *J. Infect. Dis.* 134, 290–3.
- Federowicz, S., Kim, D., Ebrahim, A., Lerman, J., Nagarajan, H., Cho, B., Zengler, K., Palsson, B., 2014. Determining the control circuitry of redox metabolism at the genome-scale. *PLoS Genet.* 10, e1004264. doi:10.1371/journal.pgen.1004264
- Feist, A.M., Henry, C.S., Reed, J.L., Krummenacker, M., Joyce, A.R., Karp, P.D., Broadbelt, L.J., Hatzimanikatis, V., Palsson, B.Ø., 2007. A genome-scale metabolic reconstruction for *Escherichia coli* K-12 MG1655 that accounts for 1260 ORFs and thermodynamic information. *Mol. Syst. Biol.* 3. doi:10.1038/msb4100155
- Feist, A.M., Herrgard, M.J., Thiele, I., Reed, J.L., Palsson, B.O., 2009. Reconstruction of biochemical networks in microorganisms. *Nat Rev Microbiol* 7.
- Fernández, M., Conde, S., De La Torre, J., Molina-Santiago, C., Ramos, J.L., Duque, E., 2012. Mechanisms of resistance to chloramphenicol in *Pseudomonas putida* KT2440. *Antimicrob. Agents Chemother.* 56, 1001–1009. doi:10.1128/AAC.05398-11
- Fick, J., Söderström, H., Lindberg, R.H., Phan, C., Tysklind, M., Larsson, D.G.J., 2009. Contamination of Surface, Ground, and Drinking Water From Pharmaceutical Production. *Environ. Toxicol. Chem.* 28, 2522. doi:10.1897/09-073.1
- Forster, J., 2003. Genome-Scale Reconstruction of the *Saccharomyces cerevisiae* Metabolic Network. *Genome Res.* 13, 244–253. doi:10.1101/gr.234503
- Freeman, Z.N., Dorus, S., Waterfield, N.R., 2013. The KdpD/KdpE Two-Component System: Integrating K<sup>+</sup> Homeostasis and Virulence. *PLoS Pathog.* 9, e1003201. doi:10.1371/journal.ppat.1003201
- Fuhrer, T., Sauer, U., 2009. Different Biochemical Mechanisms Ensure Network-Wide Balancing of Reducing Equivalents in Microbial Metabolism □ †. *J. Bacteriol.* 191, 2112–2121. doi:10.1128/JB.01523-08
- Fuhrer, T., Sauer, U., 2009. Different Biochemical Mechanisms Ensure Network-Wide Balancing of Reducing Equivalents in Microbial Metabolism. *J. Bacteriol.* 191, 2112–2121. doi:10.1128/JB.01523-08
- Füller, J.J., Röpke, R., Krausze, J., Rennhack, K.E., Daniel, N.P., Blankenfeldt, W., Schulz, S., Jahn, D., Moser, J., 2016. Biosynthesis of Violacein, Structure and Function of l-Tryptophan Oxidase VioA from *Chromobacterium violaceum*. *J. Biol. Chem.* 291, 20068–20084. doi:10.1074/jbc.M116.741561

- Ganguly, N.K., Arora, N.K., Chandy, S.J., Fairoze, M.N., Gill, J.P.S., Gupta, U., Hossain, S., Joglekar, S., Joshi, P.C., Kakkar, M., Kotwani, A., Rattan, A., Sudarshan, H., Thomas, K., Wattal, C., Easton, A., Laxminarayan, R., 2011. Rationalizing antibiotic use to limit antibiotic resistance in india. *Indian J. Med. Res.* 134, 281–294. doi:IndianJMedRes\_2011\_134\_3\_281\_85559 [pii]
- Ghafur, A., Mathai, D., Muruganathan, A., Jayalal, J. a, Kant, R., Chaudhary, D., Prabhash, K., Abraham, O.C., Gopalakrishnan, R., Ramasubramanian, V., Shah, S.N., Pardeshi, R., Huilgol, A., Kapil, A., Gill, J., Singh, S., Rissam, H.S., Todi, S., Hegde, B.M., Parikh, P., 2012. The Chennai Declaration: a roadmap to tackle the challenge of antimicrobial resistance. *Indian J. Cancer* 50, 71–3. doi:10.4103/0019-509X.104065
- Ghisalberti, D., Masi, M., Pagès, J.-M., Chevalier, J., 2005. Chloramphenicol and expression of multidrug efflux pump in *Enterobacter aerogenes*. *Biochem. Biophys. Res. Commun.* 328, 1113–1118. doi:10.1016/j.bbrc.2005.01.069
- Ghosh, R., Tiwary, B.K., Kumar, A., Chakraborty, R., 2014. Guava leaf extract inhibits quorum-sensing and *Chromobacterium violaceum* induced lysis of human hepatoma cells: whole transcriptome analysis reveals differential gene expression. *PLoS One* 9, e107703. doi:10.1371/journal.pone.0107703
- Global action plan on antimicrobial resistance [WWW Document], n.d. URL <http://www.who.int/antimicrobial-resistance/global-action-plan/en/>
- Gomes, A.P., Price, N.L., Ling, A.J.Y., Moslehi, J.J., Montgomery, M.K., Rajman, L., White, J.P., Teodoro, J.S., Wrann, C.D., Hubbard, B.P., Mercken, E.M., Palmeira, C.M., de Cabo, R., Rolo, A.P., Turner, N., Bell, E.L., Sinclair, D.A., 2013. Declining NAD<sup>+</sup> Induces a Pseudohypoxic State Disrupting Nuclear-Mitochondrial Communication during Aging. *Cell* 155, 1624–1638. doi:10.1016/j.cell.2013.11.037
- Gothwal, R., Shashidhar, T., 2015. Antibiotic Pollution in the Environment: A Review. *CLEAN - Soil, Air, Water* 43, 479–489. doi:10.1002/clen.201300989
- Grangeiro, T.B., Jorge, D.M.D.M., Bezerra, W.M., Vasconcelos, a. T.R., Simpson, a. J.G., 2004. Transport genes of *Chromobacterium violaceum*: An overview. *Genet. Mol. Res.* 3, 117–133.
- Green, J.M., Merkel, W.K., Nichols, B.P., 1992. Characterization and sequence of *Escherichia coli* pabC, the gene encoding aminodeoxychorismate lyase, a pyridoxal phosphate-containing enzyme. *J. Bacteriol.* 174, 5317–5323.
- Han, H.S., Nam, H.Y., Koh, Y.J., Hur, J., Jung, J.S., 2003. Molecular Bases of High-Level Streptomycin Resistance in *Pseudomonas marginalis* and *Pseudomonas syringae* pv .

- actinidiae. *J. Microbiol.* 41, 16–21.
- Hase, S., Reitschel, E.T., 1977. The chemical structure of the lipid A component of lipopolysaccharides from *Chromobacterium violaceum* NCTC 9694. *Eur. J. Biochem.* 75, 23–34.
- Haselkorn, R., Artur, L., Bataus, M., Batista, S., Teno, C., 2003. The complete genome sequence of *Chromobacterium violaceum* reveals remarkable and exploitable bacterial adaptability. *Proc. Natl. Acad. Sci. U. S. A.* 100, 11660–11665.  
doi:10.1073/pnas.1832124100
- Hazra, A., 2014. Schedule H1: hope or hype? *Indian J. Pharmacol.* 46, 361–362.  
doi:10.4103/0253-7613.135945
- Heinken, A., Sahoo, S., Fleming, R.M.T., Thiele, I., 2013. Systems-level characterization of a host-microbe metabolic symbiosis in the mammalian gut. *Gut Microbes* 4, 28–40.  
doi:10.4161/gutm.22370
- Henry, C.S., DeJongh, M., Best, A. a, Frybarger, P.M., Linsay, B., Stevens, R.L., 2010. High-throughput generation, optimization and analysis of genome-scale metabolic models. *Nat. Biotechnol.* 28, 977–982. doi:10.1038/nbt.1672
- Hoshino, T., 2011. Violacein and related tryptophan metabolites produced by *Chromobacterium violaceum*: Biosynthetic mechanism and pathway for construction of violacein core. *Appl. Microbiol. Biotechnol.* 91, 1463–1475. doi:10.1007/s00253-011-3468-z  
[http://www.searo.who.int/entity/world\\_health\\_day/media/2011/whd-11\\_amr\\_jaipur\\_declaration\\_.pdf](http://www.searo.who.int/entity/world_health_day/media/2011/whd-11_amr_jaipur_declaration_.pdf), 2011. Jaipur declaration on antimicrobial resistance. World Health Organization.
- Hu, B., Yang, Y.-M., Beck, D.A.C., Wang, Q.-W., Chen, W.-J., Yang, J., Lidstrom, M.E., Yang, S., 2016. Comprehensive molecular characterization of *Methylobacterium extorquens* AM1 adapted for 1-butanol tolerance. *Biotechnol. Biofuels* 9, 84.  
doi:10.1186/s13068-016-0497-y
- Ibarra, R.U., Edwards, J.S., Palsson, B.O., 2002. *Escherichia coli* K-12 undergoes adaptive evolution to achieve in silico predicted optimal growth. *Nature* 420, 20–23.  
doi:10.1038/nature01195.1.
- Iscla, I., Wray, R., Wei, S., Posner, B., Blount, P., 2014. Streptomycin potency is dependent on MscL channel expression. *Nat. Commun.* 5, 4891. doi:10.1038/ncomms5891
- Jahn, L.J., Munck, C., Ellabaan, M.M.H., Sommer, M.O.A., 2017. Adaptive Laboratory Evolution of Antibiotic Resistance Using Different Selection Regimes Lead to Similar



- Phenotypes and Genotypes. *Front. Microbiol.* 8, 1–14. doi:10.3389/fmicb.2017.00816
- Jamshidi, N., Palsson, B.Ø., 2007. Investigating the metabolic capabilities of *Mycobacterium tuberculosis* H37Rv using the in silico strain iNJ661 and proposing alternative drug targets. *BMC Syst. Biol.* 1, 26. doi:10.1186/1752-0509-1-26
- Jerby, L., Ruppin, E., 2012. Predicting drug targets and biomarkers of cancer via genome-scale metabolic modeling. *Clin. Cancer Res.* 18, 5572–5584. doi:10.1158/1078-0432.CCR-12-1856
- John, T.J., Dandona, L., Sharma, V.P., Kakkar, M., 2011. Continuing challenge of infectious diseases in India. *Lancet* 377, 252–269. doi:10.1016/S0140-6736(10)61265-2
- Kaczmarek, F.S., Gootz, T.D., Dib-Hajj, F., Shang, W., Hallowell, S., Cronan, M., 2004. Genetic and molecular characterization of beta-lactamase-negative ampicillin-resistant *Haemophilus influenzae* with unusually high resistance to ampicillin. *Antimicrob. Agents Chemother.* 48, 1630–9.
- Kalra, D.D., Kini, P. V, Kalra, R.D., Jathanna, V.R., 2015. Assessment of self - medication among dental students in Pune city , Maharashtra : A cross - sectional survey. *J. Indian Assoc. Public Heal. Dent.* 13, 318–323. doi:10.4103/2319-5932.165283
- Kampfer, P., Busse, H.-J., Scholz, H.C., 2009. *Chromobacterium piscinae* sp. nov. and *Chromobacterium pseudoviolaceum* sp. nov., from environmental samples. *Int. J. Syst. Evol. Microbiol.* 59, 2486–2490. doi:10.1099/ijs.0.008888-0
- Kasabe, G.H., Tiwari, S.A., Ghongane, B.B., 2015. A survey of knowledge, attitude and practices of self medication in Pune region. *Int. J. Med. Res. Heal. Sci.* 4, 811. doi:10.5958/2319-5886.2015.00161.7
- Kenney, T.J., Churchward, G., 1994. Cloning and sequence analysis of the *rpsL* and *rpsG* genes of *Mycobacterium smegmatis* and characterization of mutations causing resistance to streptomycin. *J. Bacteriol.* 176, 6153–6156.
- Keshari, S.S., Kesarwani, P., Mishra, M., 2014. Prevalence and Pattern of Self-medication Practices in Rural Area of Barabanki. *Indian J. Clin. Pract.* 25, 636–639. doi:10.4103/0975-2870.148828
- Kim, D.E., Chivian, D., Baker, D., 2004. Protein structure prediction and analysis using the Robetta server. *Nucleic Acids Res.* 32, W526–W531. doi:10.1093/nar/gkh468
- Kim, T.Y., Sohn, S.B., Kim, Y. Bin, Kim, W.J., Lee, S.Y., 2012. Recent advances in reconstruction and applications of genome-scale metabolic models. *Curr. Opin. Biotechnol.* 23, 617–623. doi:10.1016/j.copbio.2011.10.007
- Kohanski, M.A., Dwyer, D.J., Hayete, B., Lawrence, C.A., Collins, J.J., 2007. A Common

- Mechanism of Cellular Death Induced by Bactericidal Antibiotics. *Cell* 130, 797–810. doi:10.1016/j.cell.2007.06.049
- Kohanski, M. a, Dwyer, D.J., Collins, J.J., 2010. How antibiotics kill bacteria: from targets to networks. *Nat. Rev. Microbiol.* 8, 423–435. doi:10.1038/nrmicro2333
- Kolibachuk, D., Miller, A., Dennis, D., 1999. Cloning , Molecular Analysis , and Expression of the Polyhydroxyalkanoic Acid Synthase ( phaC ) Gene from *Chromobacterium violaceum* Cloning , Molecular Analysis , and Expression of the Polyhydroxyalkanoic Acid Synthase ( phaC ) Gene. *Appl. Environ. Microbiol.* 65, 3561–3565.
- Kothari, V., Sharma, S., Padia, D., 2017. Recent research advances on *Chromobacterium violaceum*. *Asian Pac. J. Trop. Med.* 1–9. doi:10.1016/
- Kumar, R., Goyal, A., Chhokar, S., Gilhotra, N., 2015. A Cross Sectional Study on Medicines Utilization Practices of Kabirpur in Haryana , India. *Int. J. Pharma Res. Heal. Sci.* 3, 592–600.
- Kumar, S.G., Adithan, C., Harish, B., Roy, G., Malini, A., Sujatha, S., 2013. Antimicrobial resistance in India: A review. *J. Nat. Sci. Biol. Med.* 4, 286. doi:10.4103/0976-9668.116970
- Laxminarayan, R., Chaudhury, R.R., 2016. Antibiotic Resistance in India: Drivers and Opportunities for Action. *PLoS Med.* 13, e1001974. doi:10.1371/journal.pmed.1001974
- Laxminarayan, R., Duse, A., Wattal, C., Zaidi, A.K.M., Wertheim, H.F.L., Sumpradit, N., Vlieghe, E., Hara, G.L., Gould, I.M., Goossens, H., Greko, C., So, A.D., Bigdeli, M., Tomson, G., Woodhouse, W., Ombaka, E., Peralta, A.Q., Qamar, F.N., Mir, F., Kariuki, S., Bhutta, Z.A., Coates, A., Bergstrom, R., Wright, G.D., Brown, E.D., Cars, O., 2013. Antibiotic resistance-the need for global solutions. *Lancet Infect. Dis.* 13, 1057–1098. doi:10.1016/S1473-3099(13)70318-9
- Lázár, V., Pal Singh, G., Spohn, R., Nagy, I., Horváth, B., Hrtyan, M., Busa-Fekete, R., Bogos, B., Méhi, O., Csörgő, B., Pósfai, G., Fekete, G., Szappanos, B., Kégl, B., Papp, B., Pál, C., 2013. Bacterial evolution of antibiotic hypersensitivity. *Mol. Syst. Biol.* 9, 700. doi:10.1038/msb.2013.57
- Lee, D.-H., Palsson, B.O., 2010. Adaptive Evolution of *Escherichia coli* K-12 MG1655 during Growth on a Nonnative Carbon Source, L-1,2-Propanediol. *Appl. Environ. Microbiol.* 76, 4158–4168. doi:10.1128/AEM.00373-10
- Letisse, F., Lindley, N.D., 2000. An intracellular metabolite quantification technique applicable to polysaccharide-producing bacteria. *Biotechnol. Lett.* 22, 1673–1677. doi:10.1023/A:1005663526753

- Levin, B.R., Perrot, V., Walker, N., 2000. Compensatory Mutations, Antibiotic Resistance and the Population Genetics of Adaptive Evolution in Bacteria. *Genetics* 154, 985–997.
- Li, M., Gu, R., Su, C., Routh, M.D., Harris, K.C., Jewell, S., Mcdermott, G., Yu, E.W., 2008. Crystal structure of the transcriptional regulator AcrR from *Escherichia coli*. *J. Mol. Biol.* 374, 591–603.
- Lima-Bittencourt, C.I., Astolfi-Filho, S., Chartone-Souza, E., Santos, F.R., Nascimento, A.M. a, 2007. Analysis of *Chromobacterium* sp. natural isolates from different Brazilian ecosystems. *BMC Microbiol.* 7, 58. doi:10.1186/1471-2180-7-58
- Lima-Bittencourt, C.I., Costa, P.S., Hollatz, C., Raposeiras, R., Santos, F.R., Chartone-Souza, E., Nascimento, A.M. a, 2011. Comparative biogeography of *Chromobacterium* from the neotropics. *Antonie Van Leeuwenhoek* 99, 355–370. doi:10.1007/s10482-010-9501-x
- Liu, J., Gao, Q., Xu, N., Liu, L., 2013. Genome-scale reconstruction and in silico analysis of *Aspergillus terreus* metabolism. *Mol. Biosyst.* 9, 1939–48. doi:10.1039/c3mb70090a
- Livermore, D.M., 2003. Bacterial resistance: origins, epidemiology, and impact. *Clin. Infect. Dis.* 36, S11-23. doi:10.1086/344654
- Lobritz, M. a., Belenky, P., Porter, C.B.M., Gutierrez, A., Yang, J.H., Schwarz, E.G., Dwyer, D.J., Khalil, A.S., Collins, J.J., 2015. Antibiotic efficacy is linked to bacterial cellular respiration. *Proc. Natl. Acad. Sci.* 112, 8173–8180. doi:10.1073/pnas.1509743112
- Maarleveld, T.R., Khandelwal, R.A., Olivier, B.G., Teusink, B., Bruggeman, F.J., 2013. Basic concepts and principles of stoichiometric modeling of metabolic networks. *Biotechnol. J.* 8, 997–1008. doi:10.1002/biot.201200291
- Macadam, A.M., Knowles, C.J., 1984. Purification and Properties of Beta-cyano-L-alanine Synthase from the Cyanide-producing Bacterium, *Chromobacterium Violaceum*. *Biochim. Biophys. Acta* 786, 123–132. doi:10.1016/0167-4838(84)90081-5
- Maclennan, a P., Davies, D. a, 1957. The isolation of D-glycero-D-galactoheptose and other sugar components from the specific polysaccharide of *Chromobacterium violaceum* (BN). *Biochem. J.* 66, 562–567.
- Mahadevan, R.Ã., Schilling, C.H., 2003. The effects of alternate optimal solutions in constraint-based genome-scale metabolic models. *Metab. Eng.* 5, 264–276. doi:10.1016/j.ymben.2003.09.002
- Mahadevan, R., Henson, M.A., 2012. Genome-Based Modeling and Design of Metabolic Interactions in Microbial Communities. *Comput. Struct. Biotechnol. J.* 3, e201210008. doi:10.5936/csbj.201210008

- Majewski, R.A., Domach, M.M., 1990. Simple constrained-optimization view of acetate overflow in *E. coli*. *Biotechnol. Bioeng.* 35, 732–738. doi:10.1002/bit.260350711
- Martin, P.A.W., Gundersen-Rindal, D., Blackburn, M., Buyer, J., 2007. *Chromobacterium subtsugae* sp. nov., a betaproteobacterium toxic to Colorado potato beetle and other insect pests. *Int. J. Syst. Evol. Microbiol.* 57, 993–999. doi:10.1099/ijms.0.64611-0
- Martínez, J.L., Rojo, F., 2011. Metabolic regulation of antibiotic resistance. *FEMS Microbiol. Rev.* 35, 768–89. doi:10.1111/j.1574-6976.2011.00282.x
- Mcclean, K.H., Winson, M.K., Fish, L., Taylor, A., Chhabra, S.R., Camara, M., Daykin, M., John, H., Swift, S., Bycroft, B.W., Stewart, G.S. a B., Williams, P., 1997. Quorum sensing and *Chromobacterium violaceum*: exploitation of violacein production and inhibition for the detection of N-acyl homoserine lactones. *Microbiology* 143, 3703–3711. doi:10.1099/00221287-143-12-3703
- Méhi, O., Bogos, B., Csörgő, B., Pál, F., Nyerges, Á., Papp, B., Pál, C., 2014. Perturbation of Iron Homeostasis Promotes the Evolution of Antibiotic Resistance. *Mol. Biol. Evol.* 31, 2793–2804. doi:10.1093/molbev/msu223
- Meyer, H., Liebeke, M., Lalk, M., 2010. A protocol for the investigation of the intracellular *Staphylococcus aureus* metabolome. *Anal. Biochem.* 401, 250–259. doi:10.1016/j.ab.2010.03.003
- Michaels, R., Corpe, W.A., 1965. CYANIDE FORMATION BY CHROMOBACTERIUM VIOLACEUM. *J. Bacteriol.* 89, 106–12.
- Miki, T., Iguchi, M., Akiba, K., Hosono, M., Sobue, T., Danbara, H., Okada, N., 2010. *Chromobacterium* pathogenicity island 1 type III secretion system is a major virulence determinant for *Chromobacterium violaceum*-induced cell death in hepatocytes. *Mol. Microbiol.* 77, 855–872. doi:10.1111/j.1365-2958.2010.07248.x
- Montero, C.I., Johnson, M.R., Chou, C.J., Connors, S.B., Geouge, S.G., Tachdjian, S., Nichols, J.D., Kelly, R.M., 2007. Responses of wild-type and resistant strains of the hyperthermophilic bacterium *Thermotoga maritima* to chloramphenicol challenge. *Appl. Environ. Microbiol.* 73, 5058–5065. doi:10.1128/AEM.00453-07
- Morgan, D.J., Okeke, I.N., Laxminarayan, R., Perencevich, E.N., Weisenberg, S., 2011. Non-prescription antimicrobial use worldwide: A systematic review. *Lancet Infect. Dis.* 11, 692–701. doi:10.1016/S1473-3099(11)70054-8
- Morohoshi, T., Fukamachi, K., Kato, M., Kato, N., Ikeda, T., 2010. Regulation of the violacein biosynthetic gene cluster by acylhomoserine lactone-mediated quorum sensing in *Chromobacterium violaceum* ATCC 12472. *Biosci. Biotechnol. Biochem.* 74, 2116–

2119. doi:10.1271/bbb.100385

- Morohoshi, T., Kato, M., Fukamachi, K., Kato, N., Ikeda, T., 2008. N -Acylhomoserine lactone regulates violacein production in *Chromobacterium violaceum* type strain ATCC 12472. *FEMS Microbiol. Lett.* 279, 124–130. doi:10.1111/j.1574-6968.2007.01016.x
- Mosher, R.H., Camp, D.J., Yang, K., Brown, M.P., Shaw, W. V, Vining, L.C., 1995. Inactivation of Chloramphenicol by O-Phosphorylation: A NOVEL RESISTANCE MECHANISM IN *STREPTOMYCES VENEZUELAE* ISP5230, A CHLORAMPHENICOL PRODUCER. *J. Biol. Chem.* 270, 27000–27006. doi:10.1074/jbc.270.45.27000
- Nagrath, D., Avila-Elchiver, M., Berthiaume, F., Tilles, A.W., Messac, A., Yarmush, M.L., 2007. Integrated energy and flux balance based multiobjective framework for large-scale metabolic networks. *Ann. Biomed. Eng.* 35, 863–885. doi:10.1007/s10439-007-9283-0
- Nagrath, D., Bequette, W.W., Cramer, S.M., Messac, A., 2005. Multiobjective optimization strategies for linear gradient chromatography. *AIChE J.* 51, 511–525. doi:10.1002/aic.10459
- Nandakumar, M., Nathan, C., Rhee, K.Y., 2014. Isocitrate lyase mediates broad antibiotic tolerance in *Mycobacterium tuberculosis*. *Nat. Commun.* 5, 1–10. doi:10.1038/ncomms5306
- Natarajan, G., Ting, Y.P., 2014. Pretreatment of e-waste and mutation of alkali-tolerant cyanogenic bacteria promote gold biorecovery. *Bioresour. Technol.* 152, 80–85. doi:10.1016/j.biortech.2013.10.108
- Niven, D.F., Collins, P. a, Knowles, C.J., 1975. The respiratory system of *Chromobacterium violaceum* grown under conditions of high and low cyanide evolution. *J. Gen. Microbiol.* 90, 271–285. doi:10.1099/00221287-90-2-271
- O'Neill, J., 2014. Review on Antimicrobial Resistance: Antimicrobial Resistance: Tackling a Crisis for the Health and Wealth of Nations. London Wellcome Trust.
- O'Rourke, P.E.F., Eadsforth, T.C., Fyfe, P.K., Shepherd, S.M., Hunter, W.N., 2011. *Pseudomonas aeruginosa* 4-amino-4-deoxychorismate lyase: Spatial conservation of an active site tyrosine and classification of two types of enzyme. *PLoS One* 6. doi:10.1371/journal.pone.0024158
- Oberhardt, M.A., Goldberg, J.B., Hogardt, M., Papin, J.A., 2010. Metabolic network analysis of *Pseudomonas aeruginosa* during chronic cystic fibrosis lung infection. *J. Bacteriol.* 192, 5534–5548. doi:10.1128/JB.00900-10
- Oberhardt, M. a, Puchałka, J., Fryer, K.E., Martins dos Santos, V. a P., Papin, J. a, 2008.

- Genome-scale metabolic network analysis of the opportunistic pathogen *Pseudomonas aeruginosa* PAO1. *J. Bacteriol.* 190, 2790–2803. doi:10.1128/JB.01583-07
- Oberoi, S., 2015. Updating income ranges for Kuppaswamy's socio-economic status scale for the year 2014. *Indian J. Public Health* 59, 156. doi:10.4103/0019-557X.157540
- Okusu, H., Nikaido, H., 1996. AcrAB efflux pump plays a major role in the antibiotic resistance phenotype of *Escherichia coli* Multiple-Antibiotic-Resistance (Mar) mutants. *J. Antibiot. (Tokyo)*. 178, 306–308.
- Olliver, A., Vallé, M., Chaslus-Dancla, E., Cloeckert, A., 2004. Role of an *acrR* mutation in multidrug resistance of in vitro-selected fluoroquinolone-resistant mutants of *Salmonella enterica* serovar Typhimurium. *FEMS Microbiol. Lett.* 238, 267–272. doi:10.1016/j.femsle.2004.07.046
- Opiyo, S.O., Pardy, R.L., Moriyama, H., Moriyama, E.N., 2010. Evolution of the Kdo2-lipid A biosynthesis in bacteria. *BMC Evol. Biol.* 10, 362. doi:10.1186/1471-2148-10-362
- Orth, J.D., Thiele, I., Palsson, B.Ø., 2010. What is flux balance analysis? *Nat Biotechnol* 28, 245–248. doi:10.1038/nbt.1614
- Österlund, T., Nookaew, I., Bordel, S., Nielsen, J., 2013. Mapping condition-dependent regulation of metabolism in yeast through genome-scale modeling. *BMC Syst. Biol.* 7, 36. doi:10.1186/1752-0509-7-36
- Panecka, J., Mura, C., Trylska, J., 2014. Interplay of the Bacterial Ribosomal A-Site, S12 Protein Mutations and Paromomycin Binding: A Molecular Dynamics Study. *PLoS One* 9, e111811. doi:10.1371/journal.pone.0111811
- Parakh, R., Sharma, N., Kothari, K., Parakh, R., 2013. Self-medication practice among engineering students in an engineering college in North India. *J. Phytopharm.* 2, 30–36.
- Parish, T., Smith, D.A., Kendall, S., Casali, N., Bancroft, G.J., Stoker, N.G., 2003. Deletion of two-component regulatory systems increases the virulence of *Mycobacterium tuberculosis*. *Infect. Immun.* 71, 1134–40.
- Paulander, W., Maisnier-Patin, S., Andersson, D.I., 2009. The fitness cost of streptomycin resistance depends on *rpsL* mutation, carbon source and RpoS ( $\sigma^S$ ). *Genetics* 183, 539–546. doi:10.1534/genetics.109.106104
- Peng, B., Su, Y., Li, H., Han, Y., Guo, C., Tian, Y., Peng, X., 2015. Exogenous Alanine and / or Glucose plus Kanamycin Kills Antibiotic-Resistant Bacteria Article Exogenous Alanine and / or Glucose plus Kanamycin Kills Antibiotic-Resistant Bacteria. *Cell Metab.* 21, 249–261. doi:10.1016/j.cmet.2015.01.008
- Perkins, A.E., Nicholson, W.L., 2008. Uncovering new metabolic capabilities of *Bacillus*

- subtilis using phenotype profiling of rifampin-resistant *rpoB* mutants. *J. Bacteriol.* 190, 807–14. doi:10.1128/JB.00901-07
- Phalke, V.D., Phalke, D.B., Durgawale, P.M., 2006. Self-Medication Practices in Rural Maharashtra. *Indian J. Community Med.* 31, 34–35.
- Poolman, M.G., Miguët, L., Sweetlove, L.J., Fell, D.A., 2009. A Genome-Scale Metabolic Model of Arabidopsis and Some of Its Properties. *PLANT Physiol.* 151, 1570–1581. doi:10.1104/pp.109.141267
- Pradel, E., Pagès, J., Page, J., 2002. The AcrAB-TolC Efflux Pump Contributes to Multidrug Resistance in the Nosocomial Pathogen *Enterobacter aerogenes* The AcrAB-TolC Efflux Pump Contributes to Multidrug Resistance in the Nosocomial Pathogen *Enterobacter aerogenes* 46. doi:10.1128/AAC.46.8.2640
- Price, N.D., Reed, J.L., Palsson, B.O., 2004. Genome-scale models of microbial cells: evaluating the consequences of constraints. *Nat Rev Microbiol* 2. doi:10.1038/nrmicro1023
- Puchałka, J., Oberhardt, M. a., Godinho, M., Bielecka, A., Regenhardt, D., Timmis, K.N., Papin, J. a., Martins Dos Santos, V. a P., 2008. Genome-scale reconstruction and analysis of the *Pseudomonas putida* KT2440 metabolic network facilitates applications in biotechnology. *PLoS Comput. Biol.* 4. doi:10.1371/journal.pcbi.1000210
- Puppe, W., 1995. Membrane Topology Analysis of the Sensor Kinase KdpD of *Escherichia coli*. *J. Biol. Chem.* 270, 28282–28288. doi:10.1074/jbc.270.47.28282
- Quail, M.A., Smith, M., Coupland, P., Otto, T.D., Harris, S.R., Connor, T.R., Bertoni, A., Swerdlow, H.P., Gu, Y., 2012. A tale of three next generation sequencing platforms : comparison of Ion Torrent , Pacific Biosciences and Illumina MiSeq sequencers. *BMC Genomics* 13, 341. doi:10.1186/1471-2164-13-341
- Raghunathan, A., Reed, J., Shin, S., Palsson, B., Daefler, S., 2009a. Constraint-based analysis of metabolic capacity of *Salmonella typhimurium* during host-pathogen interaction. *BMC Syst. Biol.* 3, 38. doi:10.1186/1752-0509-3-38
- Raghunathan, A., Reed, J., Shin, S., Palsson, B., Daefler, S., 2009b. Constraint-based analysis of metabolic capacity of *Salmonella typhimurium* during host-pathogen interaction. *BMC Syst. Biol.* 3, 38. doi:10.1186/1752-0509-3-38
- Raghunathan, A., Shin, S., Daefler, S., 2010. Systems approach to investigating host-pathogen interactions in infections with the biothreat agent *Francisella*. Constraints-based model of *Francisella tularensis*. *BMC Syst. Biol.* 4, 1–19. doi:10.1186/1752-0509-4-118

- Randle, C.L., Albro, P.W., Dittmer, J.C., 1969. The phosphoglyceride composition of gram-negative bacteria and the changes in composition during growth. *Biochim. Biophys. Acta - Lipids Lipid Metab.* 187, 214–220. doi:10.1016/0005-2760(69)90030-7
- Ravikrishnan, A., Raman, K., 2015. Critical assessment of genome-scale metabolic networks: the need for a unified standard. *Brief. Bioinform.* 16, 1057–1068. doi:10.1093/bib/bbv003
- Reardon, S., 2014. Antibiotic resistance sweeping developing world. *Nature* 509, 141–142.
- Reed, J.L., Famili, I., Thiele, I., Palsson, B.O., 2006. Towards multidimensional genome annotation. *Nat. Rev. Genet.* 7, 130–141. doi:10.1038/nrg1769
- Reed, J.L., Vo, T.D., Schilling, C.H., Palsson, B.O., 2003. An expanded genome-scale model of *Escherichia coli* K-12 (iJR904 GSM/GPR). *Genome Biol.* 4, R54. doi:10.1186/gb-2003-4-9-r54
- Rekha, M.S., Khan A K, Bagewadi, H.G., Venkatadri, T. V, 2014. A study of Knowledge, Attitude, Perceptions and Practices regarding Antimicrobial Resistance and usage among third and fourth year medical students. *Int. J. Pharmacol. Ther.* 4, 32–37.
- Renzoni, A., Andrey, D.O., Jouselin, A., Barras, C., Monod, A., Vaudaux, P., Lew, D., Kelley, W.L., 2011. Whole genome sequencing and complete genetic analysis reveals novel pathways to glycopeptide resistance in *Staphylococcus aureus*. *PLoS One* 6, e21577. doi:10.1371/journal.pone.0021577
- Riedel, S., Neoh, K.M., Eisinger, S.W., Dam, L.M., Tekle, T., Carroll, K.C., 2014. Comparison of Commercial Antimicrobial Susceptibility Test Methods for Testing of *Staphylococcus aureus* and Enterococci against Vancomycin, Daptomycin, and Linezolid. *J. Clin. Microbiol.* 52, 2216–2222. doi:10.1128/JCM.00957-14
- Riemer, S., Rex, R., Schomburg, D., 2013. A metabolite-centric view on flux distributions in genome-scale metabolic models. *BMC Syst. Biol.* 7, 33. doi:10.1186/1752-0509-7-33
- Ronau, J. a., Paul, L.N., Fuchs, J.E., Corn, I.R., Wagner, K.T., Liedl, K.R., Abu-Omar, M.M., Das, C., 2013. An additional substrate binding site in a bacterial phenylalanine hydroxylase. *Eur. Biophys. J.* 42, 691–708. doi:10.1007/s00249-013-0919-8
- Rothberg, J.M., Hinz, W., Rearick, T.M., Schultz, J., Mileski, W., Davey, M., Leamon, J.H., Johnson, K., Milgrew, M.J., Edwards, M., Hoon, J., Simons, J.F., Marran, D., Myers, J.W., Davidson, J.F., Branting, A., Nobile, J.R., Puc, B.P., Light, D., Clark, T. a, Huber, M., Branciforte, J.T., Stoner, I.B., Cawley, S.E., Lyons, M., Fu, Y., Homer, N., Sedova, M., Miao, X., Reed, B., Sabina, J., Feierstein, E., Schorn, M., Alanjary, M., Dimalanta, E., Dressman, D., Kasinskas, R., Sokolsky, T., Fidanza, J. a, Namsaraev, E., McKernan,



- K.J., Williams, A., Roth, G.T., Bustillo, J., 2011. An integrated semiconductor device enabling non-optical genome sequencing. *Nature* 475, 348–352.  
doi:10.1038/nature10242
- Rothenbücher, M.C., Facey, S.J., Kiefer, D., Kossmann, M., Kuhn, A., 2006. The Cytoplasmic C-Terminal Domain of the Escherichia coli KdpD Protein Functions as a K<sup>+</sup> + Sensor. *J. Bacteriol.* 188, 1950–1958. doi:10.1128/JB.188.5.1950
- Ruppin, E., Papin, J.A., Figueiredo, L.F. De, Schuster, S., 2010. Metabolic reconstruction , constraint-based analysis and game theory to probe genome- scale metabolic networks theory to probe genome-scale metabolic networks. *Curr. Opin. Biotechnol.* 21, 1–9.  
doi:10.1016/j.copbio.2010.07.002
- Ryan, K.S., Balibar, C.J., Turo, K.E., Walsh, C.T., Drennan, C.L., 2008. The violacein biosynthetic enzyme VioE shares a fold with lipoprotein transporter proteins. *J. Biol. Chem.* 283, 6467–6475. doi:10.1074/jbc.M708573200
- Sánchez, C., Braña, A.F., Méndez, C., Salas, J. a., 2006. Reevaluation of the violacein biosynthetic pathway and its relationship to indolocarbazole biosynthesis. *ChemBioChem* 7, 1231–1240. doi:10.1002/cbic.200600029
- Sandberg, T.E., Pedersen, M., LaCroix, R.A., Ebrahim, A., Bonde, M., Herrgard, M.J., Palsson, B.O., Sommer, M., Feist, A.M., 2014. Evolution of Escherichia coli to 42 °C and Subsequent Genetic Engineering Reveals Adaptive Mechanisms and Novel Mutations. *Mol. Biol. Evol.* 31, 2647–2662. doi:10.1093/molbev/msu209
- Sarkar, P., Gould, I.M., 2006. Antimicrobial Agents are Societal Drugs. *Drugs* 66, 893–901.  
doi:10.2165/00003495-200666070-00001
- Savkar, M.K., Manu, G., Bhat, N.P., Nagashree, B.N., Deepika, G., 2015. Knowledge, Attitude and Practice (KAP) of Self-medication among Engineers working in BGSIT, B G Nagar, Mandya, Karnataka. *Int. J. Curr. Pharm. Clin. Res.* 5, 177–180.
- Schellenberger, J., Que, R., Fleming, R.M.T., Thiele, I., Orth, J.D., Feist, A.M., Zielinski, D.C., Bordbar, A., Lewis, N.E., Rahmanian, S., Kang, J., Hyduke, D.R., Palsson, B.O., 2011. Quantitative prediction of cellular metabolism with constraint-based models: the COBRA Toolbox v2.0. *Nat. Protoc.* 6, 1290–1307. doi:10.1038/nprot.2011.308
- Schneiders, T., Amyes, S.G.B., Levy, S.B., 2003. Role of AcrR and RamA in Fluoroquinolone Resistance in Clinical Klebsiella pneumoniae Isolates from Singapore. *Antimicrob. Agents Chemother.* 47, 2831–2837. doi:10.1128/AAC.47.9.2831
- Schuetz, R., Zamboni, N., Zampieri, M., Heinemann, M., Sauer, U., 2012. Multidimensional Optimality of Microbial Metabolism. *Science (80-. )*. 336, 601–604.

doi:10.1126/science.1216882

- Schwarz, S., Kehrenberg, C., Doublet, B., Cloeckaert, A., 2004. Molecular basis of bacterial resistance to chloramphenicol and florfenicol. *FEMS Microbiol. Rev.* 28, 519–42.  
doi:10.1016/j.femsre.2004.04.001
- Scortti, M., Lacharme-Lora, L., Wagner, M., Chico-Calero, I., Losito, P., Vázquez-Boland, J.A., 2006. Coexpression of virulence and fosfomycin susceptibility in *Listeria*: molecular basis of an antimicrobial in vitro–in vivo paradox. *Nat. Med.* 12, 515.
- Sebek, O.K., 1965. Microbiological method for the determination of L-tryptophan. *J. Bacteriol.* 90, 1026–31.
- Sergeev, G., Roy, S., Jarek, M., Zapolskii, V., Kaufmann, D.E., Nandy, R.K., Tegge, W., 2014. High-throughput screening and whole genome sequencing identifies an antimicrobially active inhibitor of *Vibrio cholerae*. *BMC Microbiol.* 14, 49.  
doi:10.1186/1471-2180-14-49
- Shah, A., Parmar, S., Ramkishan, A., Mehta, A., 2011. Knowledge, attitude and practice (KAP) survey regarding the safe use of medicines in rural area of Gujarat. *Adv. Trop. Med. Public Heal. Int.* 1, 66–70.
- Shinoda, K., Hasegawa, T., Sato, H., Shinozaki, M., Kuramoto, H., Takamiya, Y., Sato, T., Nikaidou, N., Watanabe, T., Hoshino, T., 2007. Biosynthesis of violacein: a genuine intermediate, protoviolaceinic acid, produced by VioABDE, and insight into VioC function. *Chem. Commun. (Camb).* 4140–4142. doi:10.1039/b705358d
- Smith, A.L., Erwin, A.L., Kline, T., Unrath, W.C.T., Nelson, K., Weber, A., Howald, W.N., 2007. Chloramphenicol is a substrate for a novel nitroreductase pathway in *Haemophilus influenzae*. *Antimicrob. Agents Chemother.* 51, 2820–9. doi:10.1128/AAC.00087-07
- Smith CA, O’Maille G, Want EJ, Qin C, Trauger SA, Brandon TR, Custodio DE, Abagyan R, S.G., 2005. METLIN: a metabolite mass spectral database. *Ther Drug Monit* 27, 747–751.
- Springer, B., Kidan, Y.G., Prammananan, T., Ellrott, K., Bottger, E.C., Sander, P., 2001. Mechanisms of Streptomycin Resistance: Selection of Mutations in the 16S rRNA Gene Conferring Resistance. *Antimicrob. Agents Chemother.* 45, 2877–2884.  
doi:10.1128/AAC.45.10.2877-2884.2001
- Sreevatsan, S., Pan, X.I., Stockbauer, K.E., Williams, D.L., Kreiswirth, B.N., Musser, J.M., 1996. Characterization of rpsL and rrs Mutations in Streptomycin- Resistant *Mycobacterium tuberculosis* Isolates from Diverse Geographic Localities. *Antimicrob. Agents Chemother.* 40, 1024–1026.

- Stauff, D.L., Bassler, B.L., 2011. Quorum Sensing in *Chromobacterium violaceum*: DNA Recognition and Gene Regulation by the CviR Receptor. *J. Bacteriol.* 193, 3871–3878. doi:10.1128/JB.05125-11
- Steinbüchel, A., Schmack, G., 1995. Large-scale production of poly(3-hydroxyvaleric acid) by fermentation of *Chromobacterium violaceum*, processing, and characterization of the homopolyester. *J. Environ. Polym. Degrad.* 3, 243–258. doi:10.1007/BF02068679
- Stoesser, N., Batty, E.M., Eyre, D.W., Morgan, M., Wyllie, D.H., Del Ojo Elias, C., Johnson, J.R., Walker, a S., Peto, T.E. a, Crook, D.W., 2013. Predicting antimicrobial susceptibilities for *Escherichia coli* and *Klebsiella pneumoniae* isolates using whole genomic sequence data. *J. Antimicrob. Chemother.* 68, 2234–44. doi:10.1093/jac/dkt180
- Strohalm, M., Hassman, M., Košata, B., Kodíček, M., 2008. mMass data miner: an open source alternative for mass spectrometric data analysis. *Rapid Commun. Mass Spectrom.* 22, 905–908. doi:10.1002/rcm.3444
- Su, Y., Peng, B., Han, Y., Li, H., Peng, X., 2015. Fructose Restores Susceptibility of Multidrug-Resistant *Edwardsiella tarda* to Kanamycin. *J. Proteome Res.* 150220103905001. doi:10.1021/pr501285f
- Suzuki, S., Horinouchi, T., Furusawa, C., 2014. Prediction of antibiotic resistance by gene expression profiles. *Nat. Commun.* 5, 1–12. doi:10.1038/ncomms6792
- Swem, L.R., Swem, D.L., O’Loughlin, C.T., Gatmaitan, R., Zhao, B., Ulrich, S.M., Bassler, B.L., 2009. A Quorum-Sensing Antagonist Targets Both Membrane-Bound and Cytoplasmic Receptors and Controls Bacterial Pathogenicity. *Mol. Cell* 35, 143–153. doi:10.1016/j.molcel.2009.05.029
- Tay, S.B., Natarajan, G., Rahim, M.N.B.A., Tan, H.T., Chung, M.C.M., Ting, Y.P., Yew, W.S., 2013. Enhancing gold recovery from electronic waste via lixiviant metabolic engineering in *Chromobacterium violaceum*. *Sci. Rep.* 3, 2236. doi:10.1038/srep02236
- Taylor, R., 2009. Beta Proteobacteria, in: *Current Protocols in Microbiology*. John Wiley & Sons, Inc., Hoboken, NJ, USA, pp. 575–922. doi:10.1002/9780471729259.mc0400s15
- Tevatia, S., Chaudhry, S., Rath, R., Dodwad, V., 2016. A Questionnaire based survey on Knowledge, Attitude and Practice of Antibiotics among Dental and Paramedical students - A cross sectional survey. *World J. Pharm. Pharm. Sci.* 5, 1205–1216. doi:10.20959/wjpps20165-6726
- Thiele, Ines; Palsson, B., 2010. A protocol for generating a high quality genome scale metabolic reconstruction. *Nat Protoc* 5, 93–121. doi:10.1038/nprot.2009.203.A
- Timms, A.R., Steingrimsdottir, H., Lehmann, A.R., Bridges, B.A., 1992. Mutant sequences in

- the rpsL gene of Escherichia coli B/r: mechanistic implications for spontaneous and ultraviolet light mutagenesis. *Mol. Gen. Genet.* 232, 89–96.
- Titov, D. V, Cracan, V., Goodman, R.P., Peng, J., Grabarek, Z., Mootha, V.K., 2016. Complementation of mitochondrial electron transport chain by manipulation of the NAD<sup>+</sup>/NADH ratio. *Science* (80-. ). 352, 231–235. doi:10.1126/science.aad4017
- Toivonen, J.M., Boocock, M.R., Jacobs, H.T., 1999. Modelling in Escherichia coli of mutations in mitoribosomal protein S12: novel mutant phenotypes of rpsL. *Mol. Microbiol.* 31, 1735–1746. doi:10.1046/j.1365-2958.1999.01307.x
- Toprak, E., Veres, A., Michel, J.-B., Chait, R., Hartl, D.L., Kishony, R., 2012. Evolutionary paths to antibiotic resistance under dynamically sustained drug selection. *Nat. Genet.* 44, 101–5. doi:10.1038/ng.1034
- Travasso, C., 2016. India draws a red line under antibiotic misuse. *BMJ* 1202, i1202. doi:10.1136/bmj.i1202
- Van Boeckel, T.P., Brower, C., Gilbert, M., Grenfell, B.T., Levin, S.A., Robinson, T.P., Teillant, A., Laxminarayan, R., 2015. Global trends in antimicrobial use in food animals. *Proc. Natl. Acad. Sci.* 112, 5649–5654. doi:10.1073/pnas.1503141112
- Van Boeckel, T.P., Gandra, S., Ashok, A., Caudron, Q., Grenfell, B.T., Levin, S.A., Laxminarayan, R., 2014. Global antibiotic consumption 2000 to 2010: An analysis of national pharmaceutical sales data. *Lancet Infect. Dis.* 14, 742–750. doi:10.1016/S1473-3099(14)70780-7
- Vandamme, E., 2009. Concepts and challenges in the use of Knowledge-Attitude-Practice surveys: Literature review., Strategic Network on Neglected Diseases and Zoonoses.
- Varma, A., Palsson, B.O., 1994. Stoichiometric Flux Balance Models Quantitatively Predict Growth and Metabolic By product secretion in wild type Escherichia coli W3110. *Appl. Environ. Microbiol.* 60, 3724–3731. doi:PMC201879
- Varma, A., Palsson, B.O., 1993. Metabolic Capabilities of Escherichia coli II. Optimal Growth Patterns. *J. Theor. Biol.* 165, 503–522. doi:10.1006/jtbi.1993.1203
- Vo, T.D., Greenberg, H.J., Palsson, B.O., 2004. Reconstruction and Functional Characterization of the Human Mitochondrial Metabolic Network Based on Proteomic and Biochemical Data. *J. Biol. Chem.* 279, 39532–39540. doi:10.1074/jbc.M403782200
- Walderhaug, M.O., Polarek, J.W., Voelkner, P., Daniel, J.M., Hesse, J.E., Altendorf, K., Epstein, W., 1992. KdpD and KdpE, proteins that control expression of the kdpABC operon, are members of the two-component sensor-effector class of regulators. *J. Bacteriol.* 174, 2152–9.

- Wang, H., Dzik-Fox, J., 2001. Genetic Characterization of Highly Fluoroquinolone-Resistant Clinical *Escherichia coli* Strains from China: Role of *acrR* Mutations. *Antimicrob. agents ...* 45, 1515–1521. doi:10.1128/AAC.45.5.1515
- Wang, Z., Wu, J., Zhu, L., Zhan, X., 2016. Activation of glycerol metabolism in *Xanthomonas campestris* by adaptive evolution to produce a high-transparency and low-viscosity xanthan gum from glycerol. *Bioresour. Technol.* 211, 390–397. doi:10.1016/j.biortech.2016.03.096
- Wass, M.N., Kelley, L. a., Sternberg, M.J.E., 2010. 3DLigandSite: Predicting ligand-binding sites using similar structures. *Nucleic Acids Res.* 38, 469–473. doi:10.1093/nar/gkq406
- Weadge, J.T., Pfeffer, J.M., Clarke, A.J., 2005. Identification of a new family of enzymes with potential O-acetylpeptidoglycan esterase activity in both Gram-positive and Gram-negative bacteria. *BMC Microbiol.* 5, 49. doi:10.1186/1471-2180-5-49
- Webber, M. a, Talukder, A., Piddock, L.J. V, 2005. Contribution of mutation at amino acid 45 of *AcrR* to *acrB* expression and ciprofloxacin resistance in clinical and veterinary *Escherichia coli* isolates. *Antimicrob. Agents Chemother.* 49, 4390–2. doi:10.1128/AAC.49.10.4390-4392.2005
- Wheat, R.W., Rollins, E.L., Leatherwood, J.M., Barnes, R.L., 1963. Studies on the cell wall of *Chromobacterium violaceum*: the separation of lipopolysaccharide and mucopeptide by phenol extraction of whole cells. *J. Biol. Chem.* 238, 26–9.
- Whistance, G.R., Dillon, J.F., Threlfall, D.R., 1969. The nature, intergeneric distribution and biosynthesis of isoprenoid quinones and phenols in gram-negative bacteria. *Biochem. J.* 111, 461–472.
- Whiteside, T.L., Corpe, W. a., 1969. Effect of enzymes on the composition and structure of *Chromobacterium violaceum* cell envelopes. *J. Bacteriol.* 97, 1449–59.
- WHO, 2014. Antimicrobial resistance. Global Report on Surveillance. *Bull. World Health Organ.* 61, 383–94. doi:10.1007/s13312-014-0374-3
- Wiegand, I., Hilpert, K., Hancock, R.E.W., 2008. Agar and broth dilution methods to determine the minimal inhibitory concentration (MIC) of antimicrobial substances. *Nat. Protoc.* 3, 163–175. doi:10.1038/nprot.2007.521
- Wodke, J. a H., Pucha, J., Lluch-Senar, M., Marcos, J., Yus, E., Puchałka, J., Godinho, M., Gutiérrez-Gallego, R., dos Santos, V. a P.M., Serrano, L., Klipp, E., Maier, T., 2013. Dissecting the energy metabolism in *Mycoplasma pneumoniae* through genome-scale metabolic modeling. *Mol. Syst. Biol.* 9, 653. doi:10.1038/msb.2013.6
- Wood, S., Tsu, V., 2008. A guide to developing knowledge , attitude and practice surveys.

WHO Libr. Cat. Data 1–68.

- Xu, Z., Fang, X., Wood, T.K., Huang, Z.J., 2013. A Systems-Level Approach for Investigating *Pseudomonas aeruginosa* Biofilm Formation. *PLoS One* 8, 1–14. doi:10.1371/journal.pone.0057050
- Yang, C.-H., Li, Y.-H., 2011. *Chromobacterium violaceum* infection: a clinical review of an important but neglected infection. *J. Chin. Med. Assoc.* 74, 435–41. doi:10.1016/j.jcma.2011.08.013
- Ye, Q.Z., Liu, J., Walsh, C.T., 1990. p-Aminobenzoate synthesis in *Escherichia coli*: purification and characterization of PabB as aminodeoxychorismate synthase and enzyme X as aminodeoxychorismate lyase. *Proc. Natl. Acad. Sci. U. S. A.* 87, 9391–5. doi:10.1073/pnas.87.23.9391
- Yeom, J., Imlay, J.A., Park, W., 2010. Iron Homeostasis Affects Antibiotic-mediated Cell Death in *Pseudomonas* Species \* □ S. doi:10.1074/jbc.M110.127456
- Young, C.-C., Arun, a B., Lai, W.-A., Chen, W.-M., Chou, J.-H., Shen, F.-T., Rekha, P.D., Kämpfer, P., 2008. *Chromobacterium aquaticum* sp. nov., isolated from spring water samples. *Int. J. Syst. Evol. Microbiol.* 58, 877–880. doi:10.1099/ijs.0.65573-0
- Zlosnik, J.E.A., Tavankar, G.R., Bundy, J.G., Mossialos, D., O’Toole, R., Williams, H.D., 2006. Investigation of the physiological relationship between the cyanide-insensitive oxidase and cyanide production in *Pseudomonas aeruginosa*. *Microbiology* 152, 1407–1415. doi:10.1099/mic.0.28396-0
- Zwietering, M.H., Jongenburger, I., Rombouts, F.M., van ’t Riet, K., 1990. Modeling of the bacterial growth curve. *Appl. Environ. Microbiol.* 56, 1875–1881. doi:10.1111/j.1472-765X.2008.02537.x

## List of Publications

- Banerjee, D., Parmar, D., Bhattacharya, N., Ghanate, A.D., Panchagnula, V., Raghunathan, A., 2017. A scalable metabolite supplementation strategy against antibiotic resistant pathogen *Chromobacterium violaceum* induced by NAD<sup>+</sup>/NADH<sup>+</sup> imbalance. BMC Syst. Biol. 11, 51. doi:10.1186/s12918-017-0427-z
- Banerjee, D. and Raghunathan, A. Knowledge, Attitude and Practice of Antibiotic Use and Antimicrobial Resistance: A Case Study Post the “Red Line” Initiative, Accepted in Current Science 2018, Volume 114.
- Immanuel, S.R.C., Banerjee, D., Rajankar, M.P. and Raghunathan, A. Integrated Constraints Based Analysis Of An Engineered Violacein Pathway In *Escherichia coli*. Submitted
- Banerjee, D. and Raghunathan, A. Genome Scale Metabolic Model Of *Chromobacterium violaceum*, Submitted
- Immanuel, S.R.C., Sadhukhan, P.P., Banerjee, D., Mohole, M.S., Parmar, D. Ghanate, A.D., Panchagnula, V. and Raghunathan., A. Constraints-based Flux Balance Model Predicts System-wide Differential Phenotypes In Drug Resistant And Sensitive Glioblastoma Cancer Cells, In preparation

### CONFERENCE PRESENTATIONS

- Banerjee, D. et. al. Integrating metabolomics data as constraints in flux balance models to understand antibiotic resistance. Poster presentation delivered at 11th Annual International Conference, Metabolomics, CA, USA, June – July 2015.
- Banerjee, D. et al. Metabolic Inquiry and Cellular Engineering: A Systems Approach. Poster presentation delivered at NNMCB National Meeting on Mathematical and Computational Biology at CSIR-NCL and IISER Pune, India, December 2015.
- Raghunathan, A. and Banerjee, D. Towards A Genetic Basis for Antibiotic Resistance in *Chromobacterium violaceum*. Oral presentation delivered at AIChE Annual Meeting, CA, USA, November 2013.

# Appendices

**Appendix 1.1.** Minimum inhibitory concentration reported for *C. violaceum* in literature

<b>Antibiotics</b>	<b>Concentration (<math>\mu\text{g/ml}</math>)</b>	<b>Susceptibility*</b>
Ampicillin	>1024	Resistant
Amikacin	<2	Susceptible
Amoxicillin-clavulanic acid	256	Resistant
Cefepime	<2	Susceptible
Cefotaxime	>128	Resistant
Chloramphenicol	10	Susceptible
Ciprofloxacin	0.006	Susceptible
Co-trimoxazole	25	Susceptible
Erythromycin	15	Susceptible
Gentamicin	<2	Susceptible
Imipenem	1	Susceptible
Kanamycin	4	Susceptible
Nalidixic Acid	<2	Susceptible
Neomycin	10	Susceptible
Norfloxacin	10	Susceptible
Penicillin	>32	Resistant
Piperacillin/tazobactam	3	Susceptible
Rifampicin	32	Intermediate
Streptomycin	16	Susceptible
Tetracycline	<2	Susceptible
Ticarcillin/clavulanate	32	Intermediate
Trimethoprim/sulfamethoxazole	0.094	Susceptible
Vancomycin	30	Intermediate

\*(Kothari et al., 2017; Lima-Bittencourt et al., 2011, 2007), (Xan et al., 2008)



**Appendix 1. 2: *C. violaceum* infection cases in India**

	Year	Location	Age/Sex	Clinical presentation	Antibiotics given	Outcome	Reference
1	1979	Andhra Pradesh	4/M	Septicemia Meningitis		Fatal	Annapurna et al., 1979
2	1987	Karnataka	NB/M	Meningitis		Fatal	Shetty et al., 1987
3	2000	Karnataka	2yr 10 months/F	Diarrhea		Recovered	Ballal et al., 2000
4	2002	Karnataka	2months/F	Pustules, Ear Discharge, Septicemia and Meningitis		Fatal	Chattopadhyay et al., 2002
5	2002	Karnataka	8 days	Pustules, Septicemia, Meningitis and Multiple abscesses		Fatal	Shenoy et al., 2002
6	2002	Chandigarh	6.5/M	Septicemia, Pustules		Recovered	Ray et al., 2004
7	2003	West Bengal	24/M	Abscess Leg		Recovered	Dutta et al., 2003
8	2008	Kerala	6months/M	Septicemia, Skin Pustules, Broncho pneumonia		Recovered	Vijayan et al., 2009
9	2012	Vellore	40/M		PTZ later changed to meropenem	Fatal	Karthik et al., 2012
10	2012	Mumbai	11/F	Multiple liver & splenic abscesses with skin lesions & cardiogenic shock	PTZ and Gent; Ciprofloxacin later stages	Recovered	Saboo et al., 2012
11	2012	Tamil Nadu	42/M	Infection at the site of sutured scalp	Gentamycin	Recovered	Kumar, 2012
12	2013	Navi Mumbai	10/M	Septicemia	Ceftriaxone, Amikacin and Metronidazole	Fatal	Kar et al., 2013
13	2014	Orissa	19/M	UTI	Ciprofloxacin	Recovered	Swain et al., 2014
14	2015	South India	53/F	Septicemia	Imipenem, Ciprofloxacin, PTZ	Recovered	Madi et al., 2015
15	2016	Kerala	11month/M	Septicemia		Fatal	Kamjarakkal et al., 2016

16	2016	Kerala	2.5/M	Respiratory Distress, Hypotension, Shock		Fatal	
17	2016	Kerala	12/F			Recovered	
18	2016	Kerala	55/F	Catheter related blood stream infection	PTZ	Recovered	Balarama et al., 2016
19	2017	Kerala	73/M	UTI		Recovered	Vincent et al., 2017
20	2017	Madhya Pradesh	2/M	Chest abscess and ulceration	Ceftriaxone, Amikacin, Meropenem		Ahmed et al., 2017

## Appendix 2.1: Summary of variants confirmed using Sanger sequencing post whole genome sequencing

S.N.	Gene locus	Gene name	Nucleotide change	Type	Amino acid change	GENE STRETCH	Gene detail	
1	CV_0436	<i>acrR</i>	G179T <sup>a</sup>	SNP	R60L	456,438 -> 457,085, 648 bp / 215 AA	Transcription repressor of multidrug efflux pump	
			G375GAT <sup>a</sup>	INS	Premature termination, 141 AA	acrAB operon, TetR (AcrR) family		
2	CV_4365	<i>marC</i>	C4648G	SNP	No Change	708,719 -> 4,709,366	multiple drug resistance protein	
3	CV_4191	<i>rpsL</i>	G117T <sup>b</sup>	SNP	R86S	4,519,516 <- 4,519,887, 372 bp / 123 AA	30S ribosomal protein S12	
4	CV_3410	<i>pabC</i>	A147deletion <sup>b</sup>	DEL	Premature termination, 226 AA	3,703,561 <- 3,704,373, 813 bp / 270 AA	4-amino-4-deoxychorismate lyase	
5	CV_1596	<i>kdpD</i>	G167deletion <sup>b</sup>	DEL	Premature termination, 682 AA	1,719,330 <- 1,722,017, 2688 bp / 895 AA	2 component regulatory protein sensor kinase. Osmosensitive K <sup>+</sup> channel histidine kinase KdpD (EC 2.7.3.)	
6	CV_0066	CV_0066	G655C*	SNP	P219A	75,121 <- 76,422, 1302 bp / 433 AA	Hypothetical protein	
7	Nt CDS	nt cds	1263524*	SNP		between CV_1197 and tRNA Ser	Cv_1197 - polysaccharide/polyol phosphate ABC transporter ATPase	
8	CV_0464	CV_0464	A4273C*	SNP				
			G4274A*	SNP				
			T4276A*	SNP				
			C4277G*	SNP	Synonymous		478,148 -> 483,712, 5565 bp / 1854 AA	Hypothetical protein, Homologous to Fibronectin type III domain protein
			G4278C*	SNP				
			C4344G*	SNP				

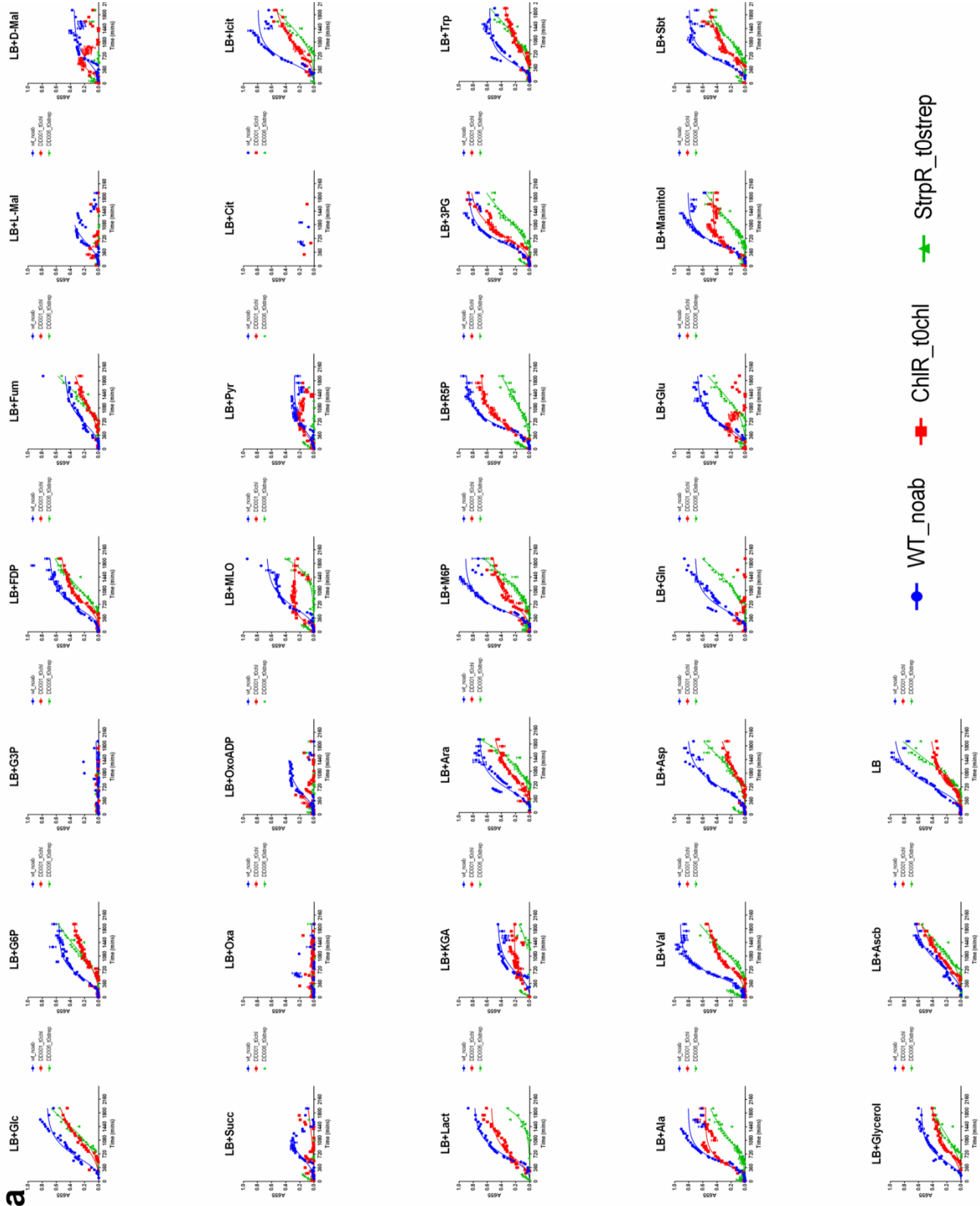
**Appendix 2.2.** List of primers used for confirmation of variants after whole genome sequencing. Abbreviations: Tm - Melting temperature; GC% - Percentage GC content; FW - Forward Primer; REV - Reverse Primer; ncX\_FW - Non Coding Region Forward Primer numberX, ncX\_REV - Non Coding Region Reverse Primer number X.

S.NO	Sequence Name	Sequence	No.Of Bases	Tm	GC%	amplicon size (base pairs)
1	0066_FW	CTGTTCTCCCGCTCCG	17	59.44	70.59	452
2	0066_REV	TCAACGCCGACACGCTG	17	60.73	64.71	
3	0112_FW	TGATTGATGTCGCGCCGTAT	20	60.25	50	489
4	0112_REV	GGTAGTCGAGGCGATGAAGG	20	59.97	60	
5	0189_FW	CATTATCCCCGATGGCGCTT	20	60.61	55	431
6	0189_REV	CAAGAACGTGGCGGAAGTG	19	59.43	57.89	
7	0436_FW	GTTTCAGCGAGCAGGGC	16	57.92	68.75	428
8	0436_REV	CCACCGCCACTTCGTCC	17	60.42	70.59	
9	0464_FW	GGACGGCAAGACCAGCAATA	20	60.39	55	427
10	0464_REV	GTAGGTGGTGGCGTTGAGAG	20	60.39	60	
11	nc1_FW	CGGAAGTGAAGAGCCTGGTG	20	60.67	60	427
12	nc1_REV	AAGTGCCGTTGCCATCCTT	19	60.23	52.63	
13	0570_FW	GAGGTCAGGTTGGATGCGAT	20	59.82	55	567
14	0570_REV	GCAGGATACGGGACAGGAAA	20	59.46	55	
15	nc2_FW	GACGGGATGTTGCGGACTAT	20	59.9	55	536
16	nc2_REV	CATCGTGGTGGGACTCTTGG	20	60.39	60	
17	0740_FW	TCGAAGGAGAAATCGACGCC	20	60.18	55	386
18	0740_REV	CACTACATGGGCACCTCCAC	20	60.39	60	
19	0877_FW	CGCTGGAAATGACCGACGTG	20	61.96	60	410
20	0877_REV	CATCATCTGGCGGTAGTCCC	20	59.97	60	
21	nc3nd4_FW	CGTGAAAGGGCGGTGTTCTA	20	60.32	55	477
22	nc3nd4_REV	CGATGAAGGGCGGAATGGG	19	60.89	63.16	
23	1080_FW	GCCCCGAGACCAAGGACAAG	19	60.38	63.16	329
24	1080_REV	CGGTATTCGCCACTTGCTTC	20	59.63	55	
25	nc5_FW	CAGAGCACCGAGTCCATCAA	20	59.75	55	301
26	nc5_REV	CCTCCTGGCTGGGAAACATC	20	60.39	60	
27	nc6_FW	GCGTCATTCATCGTTCGGG	20	59.97	55	332
28	nc6_REV	GGCTGCCTTCGGAACAAAAC	20	60.32	55	
29	1199_FW	AACACGCTCTTGGGGATGG	19	60	57.89	372
30	1199_REV	TATCTCTTCCGTCAGCACGC	20	59.9	55	
31	1261_FW	CTGCTTGACCCGAGGCTAAT	20	59.82	55	516
32	1261_REV	GAAATTCTCGTCCAGGCGCT	20	60.74	55	
33	nc7_FW	CAGGGACGGGGAGGAT	17	59.66	70.59	396
34	nc7_REV	CAGGCGATTGGTCAGGGAAA	20	60.32	55	
35	1296_FW	GGCAATGGCGAGGACTTC	18	58.5	61.11	403
36	1296_REV	TGCCAGATGATGGTTCCGAC	20	60.11	55	
37	1301_FW	TGGACAGTGGCAGCAAGG	18	59.89	61.11	488
38	1301_REV	AGTCGTGTAATAAGGCAGCAC	21	58.38	47.62	
39	nc8_FW	TGGTTAGAGCACACCTTGAC	21	59.93	52.38	504
40	nc8_REV	GAACAGCTCCTTGACGGCAT	20	60.67	55	
41	1596_FW	CGCCTCGTCTGTATGGA	18	58.48	61.11	492
42	1596_REV	GCCAAGGTGATGCTGTTTCAT	20	58.82	50	
43	nc9_FW	CGTCCTCGATGGCTGTACG	19	60.3	63.16	486
44	nc9_REV	GTCTGCTCCAGCTCGGTATG	20	60.25	60	
45	1872_FW	TGGGCGTGTGATCTCTGG	20	60.32	55	419
46	1872_REV	ACCTCTGCTGTTCAAGACTCG	21	60	52.38	
47	1994_FW	TTCGTCTACCCGATGTTCCG	20	59.55	55	413
48	1994_REV	ACGCTCCACAGCCACATATC	20	60.18	55	
49	nc10_FW	TGCTTTCGGCATTCTTGTGG	20	59.4	50	512
50	nc10_REV	TTGAGCGAGGTCACCTTCCC	20	59.97	55	
51	2377_FW	CGAGGGGCTGGAAATCAG	18	57.45	61.11	405
52	2377_REV	TTAGTAGGCAGGGCGAAGTC	20	59.18	55	
53	2560_FW	AACGAGGAAACCGACGACAA	20	59.9	50	465
54	2560_REV	GAAGAACGAGTACCACGGCA	20	60.04	55	

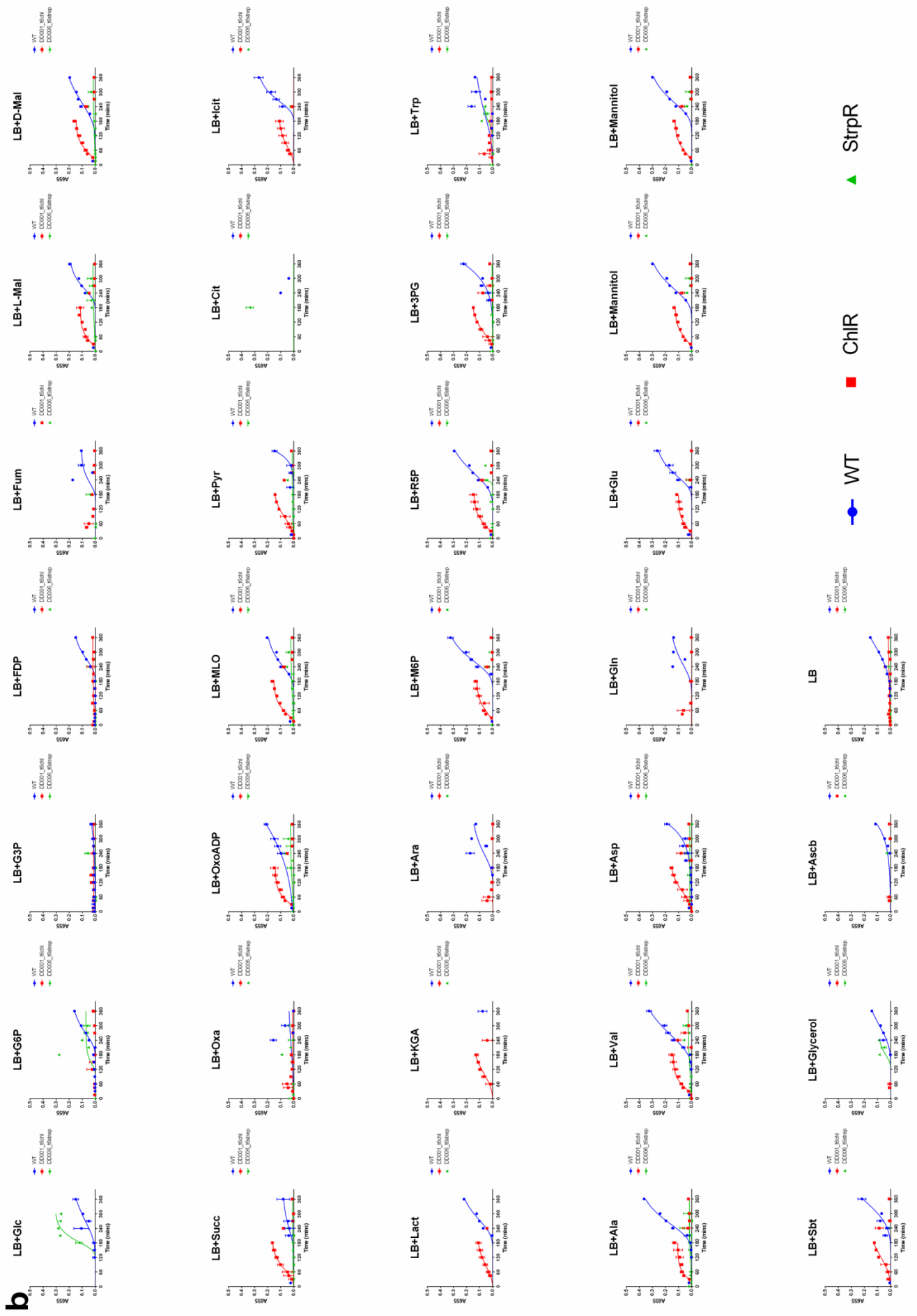
55	nc11_FW	GCCATTTTCAGGTGCGTCATC	20	59.9	55	471
56	nc11_REV	AATGCGCTGGCGAAGTTTTT	20	59.97	45	
57	2789_FW	CCGCCCTGCATCAACAAGTA	20	60.68	55	478
58	2789_REV	CCACGTAGTTCACACCAGG	20	60.32	60	
59	nc13_FW	AGTTGATGCACGAAACAAAGC	21	58.27	42.86	512
60	nc13_REV	TTGTGGCAAGACCCTGCG	18	60.59	61.11	
61	nc14_FW	TATCAGCCACAGACCAAGCC	20	59.75	55	545
62	nc14_REV	GGTATCGGAAGAGGAGAGCG	20	59.41	60	
63	3076_FW	ACATACTGGCGGATCACTCG	20	59.61	55	498
64	3076_REV	CAACACCCACACGGTAATCG	20	59.21	55	
65	3101_FW	TGCCAGGACATCAATACCCG	20	59.82	55	383
66	3101_REV	TCCAGCACATAGGCGTGT	18	58.61	55.56	
67	3351_FW	TTACTCCCCGAAACCACAGA	20	58.28	50	294
68	3351_REV	CTGTTCAACGACGACCAGAT	20	57.93	50	
69	3458_FW	GAGCACGCCAACAAATACCCT	20	60.68	55	554
70	3458_REV	CCTTCACCAGCAGCGAGTT	19	60.3	57.89	
71	nc15_FW	GCGATGTACCAGGCCAAGAT	20	60.18	55	463
72	nc15_REV	CAAGGAAGCGGACAGGAAGT	20	59.96	55	
73	3519_FW	GATCCGAACCGCCTCACC	18	60.2	66.67	453
74	3519_REV	GATGAATTGCTGGTTGGCCG	20	60.18	55	
75	3561_FW	GAGGTGGGTTTCGACGATGAC	20	60.46	60	461
76	3561_REV	GGGTGTCTGCCTCGTAGATG	20	59.9	60	
77	nc16_FW	GGTCCCCCAGAAATACCTGC	20	60.11	60	475
78	nc16_REV	GGCTACCTGAACGGTGTGA	20	59.97	55	
79	4028_FW	ATGGAGATGTGGGCTGCAA	20	59.96	50	305
80	4028_REV	TCGTGGTGGTTCAAAGCGAT	20	60.25	50	
81	4102_FW	GCTCTGGAACACGGTATGC	19	58.62	57.89	563
82	4102_REV	GGAGGAAAGGCGGTGGATTT	20	60.32	55	
83	4129_FW	CTATGGTGTTCAGCACGAAGC	21	59.61	52.38	418
84	4129_REV	ACCTGAGTACCGAATGACCG	20	59.18	55	
85	4192_FW	CGGTCACTTCGTTCGGTCT	18	59.05	61.11	415
86	4192_REV	ATCGCCGCCAGTCCAT	17	61.19	64.71	
87	4384_FW	CGTGCGTGAAGCCGTATC	20	60.25	55	471
88	4384_REV	TTGTTCGTCATCTCGTCCAG	20	59.47	55	
89	4284_FW	CAGGAGCCTTACTTCGGCAA	20	60.04	55	404
90	4284_REV	AAGGTTTCGGTGTGGTCGTT	20	60.11	50	
91	0464b_FW	CAGCGTGTCTCCTCGTATG	20	60.86	60	402
92	0464b_REV	CTGCTGGCGGTGGTGTGTC	17	60.74	70.59	
93	4010_FW	CGATACGCCTGAACCCATCA	20	59.9	55	485
94	4010_REV	CGCACTCCAGCAGATTGAAG	20	59.27	55	
95	nc17_FW	AGCTGACTTCACTGCCAAGC	20	60.89	55	416
96	nc17_REV	AGATCGACCCCAATCTGTGC	20	59.82	55	
97	nc18_FW	TCCTGTCTGTCTCGCTTG	18	60.05	61.11	402
98	nc18_REV	ATTCCAGCGTCCCAGCTTAC	20	60.11	55	
99	1137_FW	GTCGAGGATGTAACGGCTCC	20	60.25	60	421
100	1137_REV	GCAGGTCTTCTCGTCCTTGT	20	59.68	55	
101	0662_FW	ACTCCAACCACAAGAAAACCAC	22	59.24	45.45	402
102	0662_REV	GCCAGATTGACGACGGTG	18	58.53	61.11	
103	3410_FW	AAAGGCGAAGGCGTCCAGAT	20	62.19	55	305
104	3410_REV	GATCCGGCGATACAGGAAGG	20	60.04	60	
105	2590_FW	CTGCAATTCTGGGGATGGA	20	59.74	55	409
106	2590_REV	GCATGAGCGGTAAGTACGGT	20	60.18	55	
107	1471_FW	GCTTCCGCTTCCAGATCCTT	20	60.11	55	420
108	1471_REV	CCTATCGCACTGAGCCTGTT	20	59.82	55	
109	1071_FW	GCTGGATTACCGCATGACCT	20	60.18	55	389
110	1071_REV	GCAGCGTGGTGAACCTTGTC	19	59.72	57.89	
111	1144_FW	ATGTACCAGCCGTCCAGCTC	20	61.96	60	433
112	1144_REV	TGAACAACATCCAGAAAGGCG	21	59.12	47.62	

113	1962_FW	GTACTCGTCGCCAACCTG	19	60.45	63.16	372
114	1962_REV	ACGTCCTCGCAGTGTTTCAG	20	60.6	55	
115	1063_FW	GGACGATGGAATATCCGACCA	21	59.38	52.38	415
116	1063_REV	ACATGCCGAGAACTCCCTG	20	60.04	55	
117	nc19_FW	TTCGATGTACGTTGCTGTCA	20	57.57	45	583
118	nc19_REV	CAAGTTTGTATGCTGGAGCGG	20	59.83	55	
119	nc20_FW	CGACGGCCTGTTGCAGA	17	60.01	64.71	369
120	nc20_REV	CTGGTCTACCTGTGCTACGC	20	60.18	60	
121	nc21_FW	ATCTGCGACGAACCTGGGC	18	60.13	61.11	449
122	nc21_REV	GGGGTGTTCTGCTGGTC	18	59.97	66.67	
123	4309_FW	CGGGTAAAAGCAAGCGGC	18	59.82	61.11	400
124	4309_REV	CTGGCGCTGACCGAGATG	18	60.58	66.67	
125	0962_FW	GGTTCAGCCATTGCAGCTT	20	61.54	55	469
126	0962_REV	TTCAGACCAAGACCGCTCAG	20	59.68	55	
127	1470_FW	CGCTACTGGACAGCGTCAC	19	60.8	63.16	443
128	1470_REV	CAACGCCAAAACCGTCTCG	19	60.08	57.89	
129	4191_FW	GATTACTTGGGACGCTTGGC	20	59.27	55	424
130	4191_REV	TTTCTGGAGGCGTGTGCTT	20	60.47	50	
131	0004nc22_FW	CGACGTGTAAGGGGTAGGG	20	59.83	60	462
132	0004nc22_REV	GGGGTGCAGCTCTTTCTGAT	20	60.03	55	
133	0560_FW	CTTGACCGTGGAGCTGGAG	19	60.08	63.16	412
134	0560_REV	GCGACACCAAGACCTCGAT	19	59.78	57.89	
135	0772_FW	AGCTTTTCATCGCCTCCAGT	20	59.67	50	419
136	0772_REV	GCTGATTGCCCGTTTCAAGC	20	60.73	55	
137	0816_FW	CCACCGAGGACGAGCAGTA	19	61.04	63.16	400
138	0816_REV	GGGATTTCTATCATCGCGCC	20	58.92	55	
139	0821_FW	CGCCCGACATGGAGGAT	17	58.76	64.71	491
140	0821_REV	GCCAGCCTCGACTACGC	17	60.26	70.59	
141	nc23_FW	CGATTTTCGTTCCAAGGCTATCTG	22	59.2	50	411
142	nc23_REV	AAAGCGAACAAGCTGTCCCA	20	60.47	50	
143	1114_FW	CTTTCAGCTCCTCCACCAGC	20	60.68	60	415
144	1114_REV	AAGAATCGTGGGACGGCTAC	20	59.82	55	
145	nc24_FW	GTTGGCTTGATGCGGTTGC	19	60.73	57.89	440
146	nc24_REV	AAGTGGGAAGGCGAGTTGAAG	21	60.54	52.38	
147	nc25_FW	ACTACGGCTACTACATCGTGC	21	59.67	52.38	423
148	nc25_REV	CAAGGTGGACAGCTATTCCG	20	58.34	55	
149	1299_FW	TTCCGCCTTCATCTTCAGGA	20	58.72	50	407
150	1299_REV	GCCGCAAGTACACCTTCCTC	20	61.02	60	
151	0304_FW	GTAAGCTGGGACGCTGGAAT	20	60.11	55	990
152	0304_REV	CGGGATGGCCGTTTTTCTTT	20	59.4	50	
153	0700_FW	CAATCATGCCCCTCGCACTA	20	60.18	55	1272
154	0700_REV	GCCCAGTTTCGGCATTTCATCA	20	59.68	55	
155	2729_FW	TCTCCTCCTCCCGTCAACTT	20	59.89	55	880
156	2729_REV	CTGAGCGGGCTGGAAAAATG	20	59.83	55	
157	1455_FW	GCCAGTCCAGATTGTTTCGGA	20	60.04	55	607
158	1455_REV	GAGGAAAGGCGGAAAAATCGC	20	59.9	55	
159	4365_FW	AAGCCTCTACAATCTGCGGG	20	59.82	55	722
160	4365_REV	TGTGGCAGAAATGGGGTTTCG	20	60.89	55	

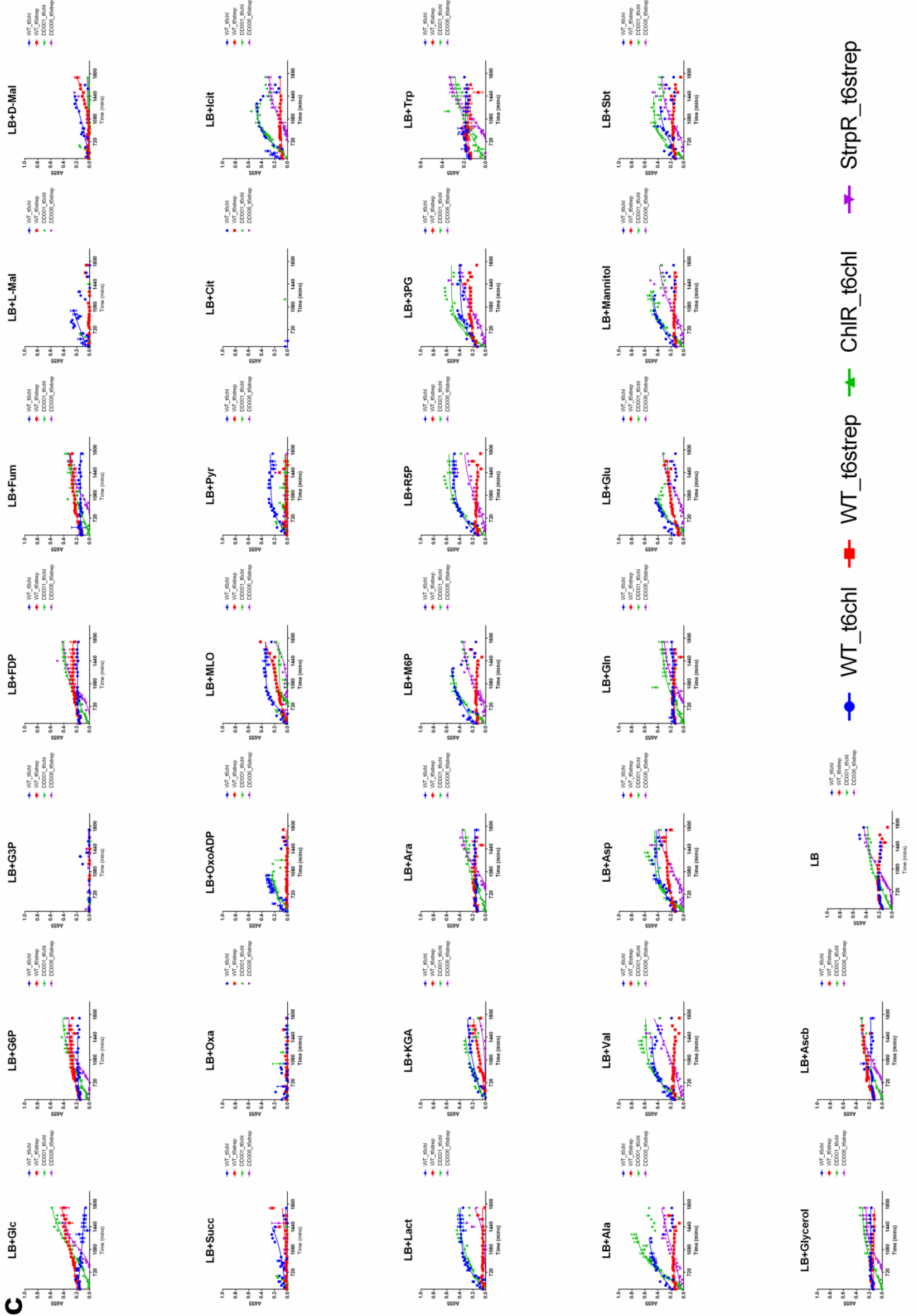
**Appendix 3.1.** Growth profiles for WT, ChIR and StrpR using 30 different C/N substrates (Ex-mets). a) Antibiotic added to media from the beginning ( $t_0$ ). b) No antibiotic added and c) Antibiotic added after 6 hours ( $t_6$ ) showing WT with chloramphenicol and streptomycin, (WT\_t6chl and WT\_t6strep, respectively), ChIR with chloramphenicol added to the media and StrpR with streptomycin added to the media. Plots made using GraphPad Prism v6.01 and  $n = 3$ .



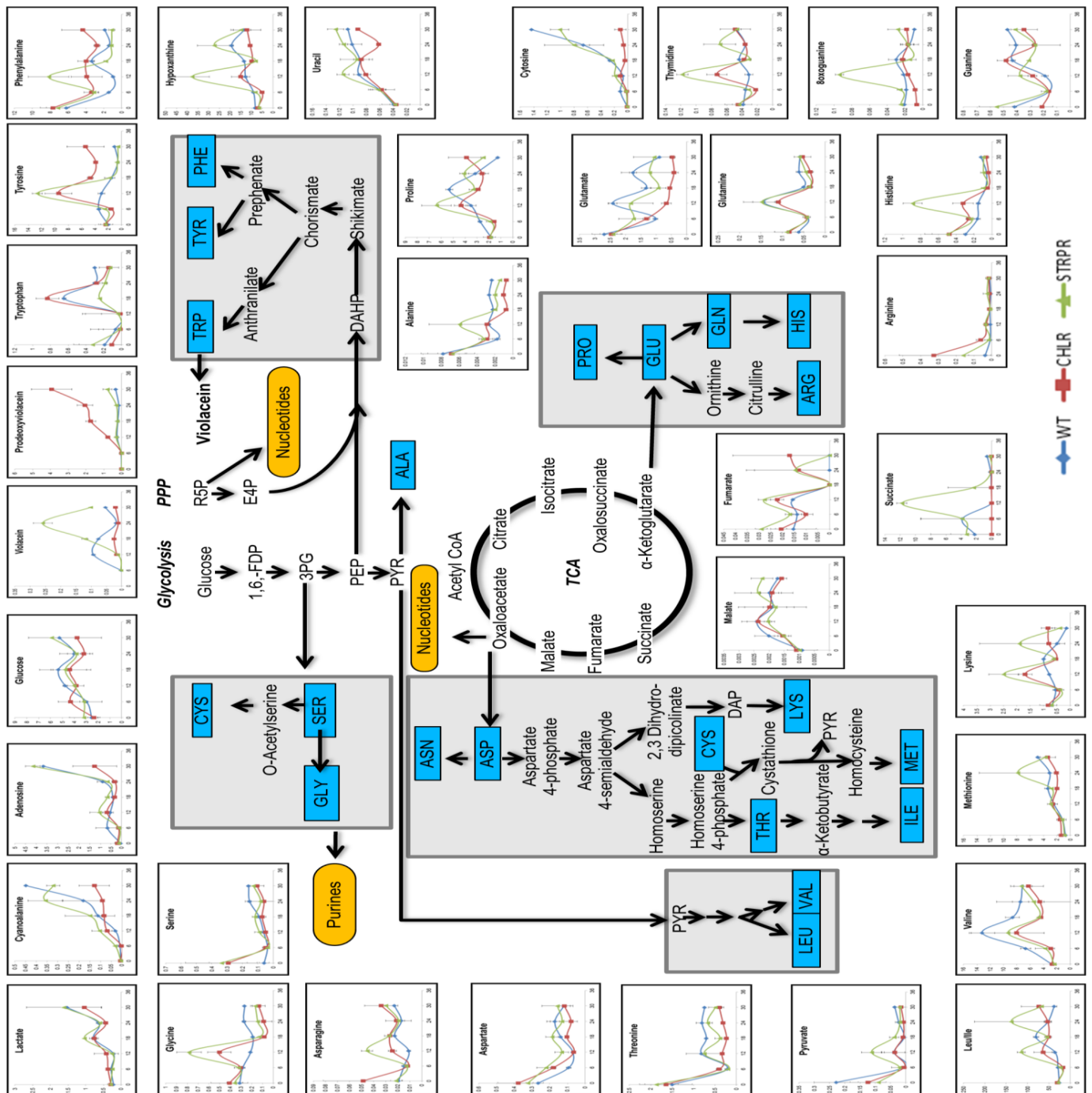
**b**



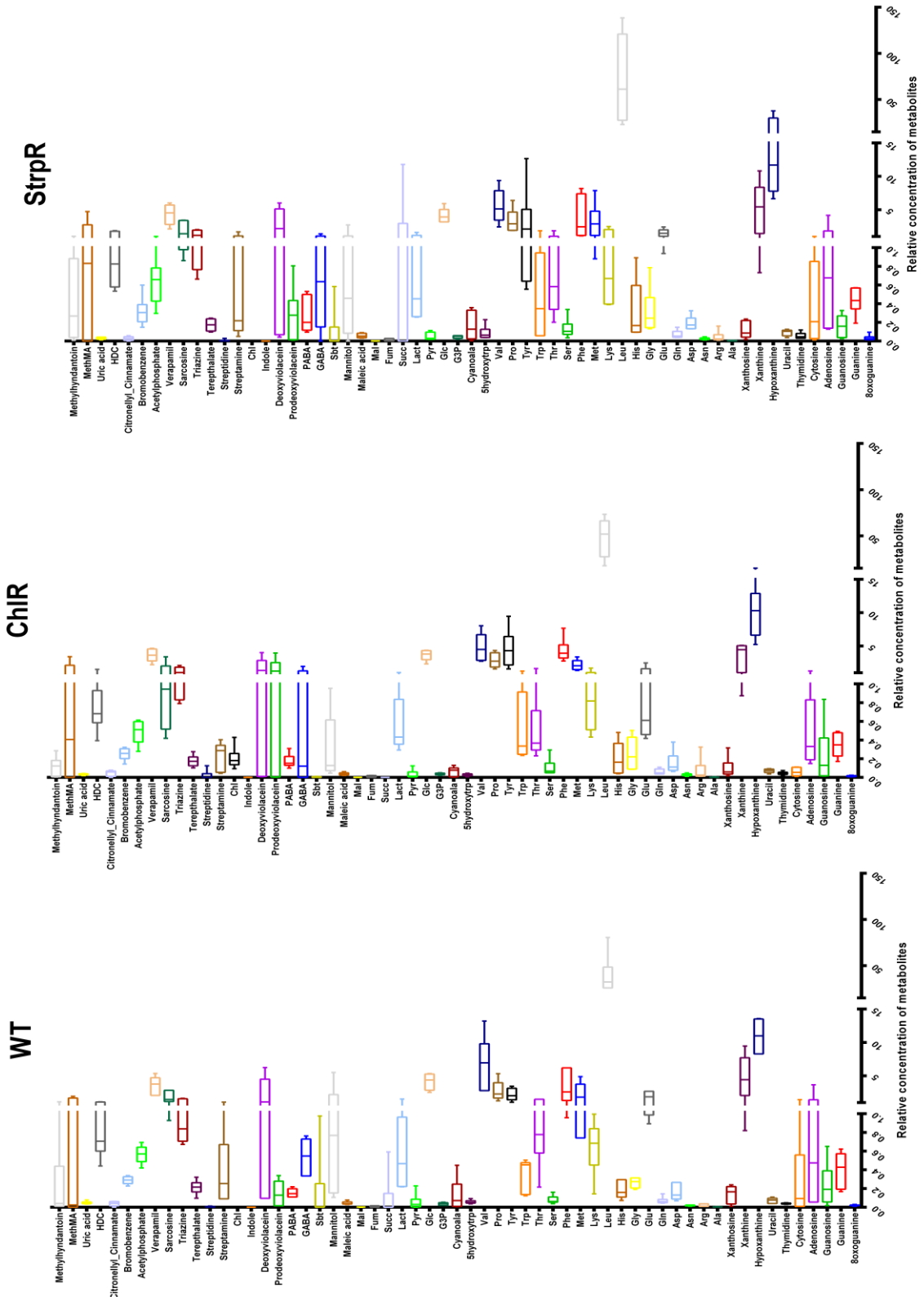


**C**

**Appendix 3.2:** Metabolic time profiles for the three population of *C. violaceum* showing oscillatory or linear behavior with varying amplitude, period and phase lag during growth on glucose across sensitive and resistant populations. The central carbon metabolism network is drawn for quick correlation. Solid blue squares show all amino acids. Yellow rounded rectangles show nucleotides. Fructose-1,6-biphosphate (1,6-FDP), D-ribose-5-phosphate (R5P), D-erythrose-4-phosphate (E4P), glycerate-3P (3PG), phosphoenolpyruvate (PEP), pyruvate (PYR). All the values were normalized to the internal standard (Refer material and methods for details). Graph legends: Blue – WT, Red – ChlR, Green – StrpR. Means  $\pm$  S.D and  $n \geq 2$ .



**Appendix 3.3:** To understand the spread and skewness of the metabolomic data obtained for the three different populations, we have made box and whiskers plots. gives us a lot of information about the data ranging from differential spread, three orders of magnitudes, etc.



## Appendix 5.1: Calculation of biomass composition using legacy data

### Overall Composition

Component	% Dry Weight	Reference	Notes
Protein	71	(Baart et al., 2007)	Using <i>Neisseria</i> values as no clear literature found for <i>C.violaceum</i> .
RNA	30.3	(Herbert, 1961)	Exponential cells of c. violaceum in complex medium contains RNA % as 30.3.
DNA	13	(Wheat et al., 1963)	
Phospholipids	11.4	(Baart et al., 2007)	Using neisseria values as no clear literature found for <i>C.violaceum</i> .
Peptidoglycan	0.1	(Wheat et al., 1963)	
Lipopolysaccharide	7.6	(Crumpton and Davies, 1958; Wheat et al., 1963)	Average values between 7.61 and 7 %
PHB	38	(Kolibachuk et al., 1999)	98% PHB formed with the yield of 38% of dry weight with glucose as carbon source
Putrescine	0.4	(Busse and Auling, 1988)	<i>C. violaceum</i> values
Spermidine	0.004	(Busse and Auling, 1988)	<i>C. violaceum</i> values
Energy (mmol ATP/gDCW)	59.81	(Feist et al., 2007)	<i>E. coli</i> values

Component	% Dry Weight	Organism (Reference)
Protein	<b>41.33</b>	<i>N.meningitidis</i>
RNA	<b>17.64</b>	<i>C.violaceum</i>
DNA	<b>7.57</b>	<i>C.violaceum</i>
Phospholipids	<b>6.64</b>	<i>N.meningitidis</i>
Peptidoglycan	<b>0.06</b>	<i>C.violaceum</i>
Lipopolysaccharide	<b>4.42</b>	<i>C.violaceum</i>
PHB	<b>22.12</b>	<i>C.violaceum</i>
Putrescine	<b>0.231</b>	<i>C.violaceum</i>
Spermidine	<b>0.003</b>	<i>C.violaceum</i>
Total	<b>100</b>	

### DNA Composition

Reference - Haselkorn R, Artur L, Bataus M, Batista S, Teno C: The complete genome sequence of *Chromobacterium violaceum* reveals remarkable and exploitable bacterial adaptability. *Proc Natl Acad Sci U S A* 2003, 100:11660–11665.

DNA	% Prevalence	MW (g/mol)	Relative Weight/mol	% (by weight)	mmol/gDW
dATP	17.6	487.151	85.74	17.75	<b>0.028</b>
dGTP	32.4	503.15	163.02	33.75	<b>0.051</b>
dTTP	17.6	478.136	84.15	17.42	<b>0.028</b>
dCTP	32.4	463.125	150.05	31.07	<b>0.051</b>
	Total		Sum of Rel Weight/mol	Total	
	100		482.96	100	

---

**Explanation:**

The 64.8% GC content is split evenly between dGTP and dCTP. MWs taken from ChEBI website. The relative weights/mol are the % prevalances multiplied by the molecular weights.

% by weight is calculated by dividing the relative weights/mol by the sum of the relative weights/mol.

mmol/gDW is calculated by:

$(\% \text{ by weight}/100) * (X \text{ grams of DNA/gDW}) * (1/\text{molecular weight}) * (1000 \text{ mmol/mol})$

**RNA Composition**

Reference - ORF DNA sequences (proxy for RNA) for *C. violaceum* used from Haselkorn et. al 2004

---

RNA	% Prevalence	MW (g/mol)	Relative weight/mol	% (by weight)	mmol/gDW
ATP	18.00	503.15	90.57	18.24	<b>0.064</b>
GTP	32.00	519.149	166.13	33.46	<b>0.114</b>
UTP	18.00	480.108	86.42	17.41	<b>0.064</b>
CTP	32.00	479.124	153.32	30.88	<b>0.114</b>
	Total		Sum of Rel Weight/mol	Total	
	100		496.43	100	

---

**Explanation**

MWs taken from ChEBI website. The relative weights/mol are the % prevalances multiplied by the molecular weights. % by weight is calculated by dividing the relative weights/mol by the sum of the relative weights/mol.

mmol/gDW is calculated by:

$(\% \text{ by weight}/100) * (X \text{ grams of RNA/gDW}) * (1/\text{molecular weight}) * (1000 \text{ mmol/mol})$

**Protein Composition**

Protein sequence for *C. violaceum* ATCC 12472 was downloaded from Uniprot Proteome ID - UP000001424

---

Amino Acid	Count	% Prevalence	MW (g/mol)	Relative Weight/mol	% (by weight)	mmol/gDW
Alanine (A)	174329	12.49	89.09	11.13	8.77	<b>0.407</b>
Arginine (R)	95825	6.87	175.212	12.03	9.48	<b>0.224</b>
Asparagine (N)	40011	2.87	132.12	3.79	2.98	<b>0.093</b>
Aspartic acid (D)	75976	5.44	132.1	7.19	5.67	<b>0.177</b>
Cysteine (C)	14379	1.03	121.16	1.25	0.98	<b>0.034</b>
Glutamate (E)	75054	5.38	146.12	7.86	6.19	<b>0.175</b>
Glutamine (Q)	61225	4.39	146.14	6.41	5.05	<b>0.143</b>
Glycine (G)	117225	8.40	75.06	6.31	4.97	<b>0.274</b>
Histidine (H)	30530	2.19	155.15	3.39	2.67	<b>0.071</b>
Isoleucine (I)	61630	4.42	131.17	5.79	4.56	<b>0.144</b>
Leucine (L)	160400	11.49	131.17	15.08	11.88	<b>0.374</b>
Lysine (K)	50092	3.59	146.19	5.25	4.13	<b>0.117</b>
Methionine (M)	34257	2.45	149.21	3.66	2.89	<b>0.080</b>

---

Phenylalanine (F)	48018	3.44	165.19	5.68	4.48	<b>0.112</b>
Proline (P)	69184	4.96	115.13	5.71	4.50	<b>0.161</b>
Serine (S)	78774	5.65	105.09	5.93	4.67	<b>0.184</b>
Threonine (T)	59258	4.25	119.19	5.06	3.99	<b>0.138</b>
Tryptophan (W)	20482	1.47	204.22	3.00	2.36	<b>0.048</b>
Tyrosine (Y)	34649	2.48	181.19	4.50	3.54	<b>0.081</b>
Valine (V)	94136	6.75	117.15	7.90	6.23	<b>0.220</b>
	Sum	Total		Sum of Rel Weight/mol	Total	
	1395434	100		126.93	100	

#### Explanation

MWs taken from ChEBI website. The relative weights/mol are the % prevalances multiplied by the molecular weights. % by weight is calculated by dividing the relative weights/mol by the sum of the relative weights/mol. mmol/gDW is calculated by:

$(\% \text{ by weight}/100) * (X \text{ grams of protein/gDW}) * (1/\text{molecular weight}) * (1000 \text{ mmol/mol})$

#### Polyamine Composition

Reference - Busse J, Auling G: Polyamine Pattern as a Chemotaxonomic Marker within the Proteobacteria. Syst Appl Microbiol 1988, 11:1–8.

			MW	
Polyamine	umol/gDW	mmol/gDW	(g/mol)	% dry weight
Putrescine	44.1	0.0441	90.2	<b>0.397782</b>
Spermidine	0.3	0.0003	148.32	<b>0.00445</b>
Cadaverine	7.3	0.0073	104.23	<b>0.076088</b>
1,3-diaminopropane	5.6	0.0056	74.15	<b>0.041524</b>
2 hydroxyputrescine	23.2	0.0232	104.18	<b>0.241698</b>
			Total	<b>0.761541</b>

#### Peptidoglycan Composition

Peptidoglycan	% dry weight	MW (g/mol)	mmol/gDW
n subunit	0.06	1983.21	<b>0.000293</b>
n-1 subunit	0.06	993.12	<b>0.000586</b>

#### Model Information

Code	Name	Charged Formula	MW
cpd15665_c	Peptidoglycan polymer (n subunits)	C80H125N16O42R	1983.21
cpd15666_c	Peptidoglycan polymer (n-1 subunits)	C40H63N8O21R	993.12

## Lipopolysaccharide Composition

Reference - Hase S, Reitschel ET: The chemical structure of the lipid A component of lipopolysaccharides from *Chromobacterium violaceum* NCTC 9694. Eur J Biochem 1977, 75:23–34.

Lipid A is the representative component of LPS in the E. coli model. We have done the same here.

New_metabolite	<i>C. violaceum</i> Lipid A	C91H165N4O33P2	
		MW (g/mol)	
C	91	12.01	1092.91
H	165	1.01	166.65
N	4	14.01	56.04
O	33	16	528
P	2	30.97	61.94
			1905.54
Lipopolysaccharide	% dry weight	MW (g/mol)	mmol/g DW
LPS	4.42	1905.54	<b>0.023215</b>

## Fatty Acid Composition Part 1

Reference - Kämpfer P, Busse HJ, Scholz HC. Int J Syst Evol Microbiol 2009 and Young C-C, Arun a B, Lai W-A, Chen W-M, Chou J-H, Shen F-T, Rekha PD, Kämpfer P. Int J Syst Evol Microbiol 2008

	Fatty acid	C	H	O	MW (g/mol)	% Prevalence of Total FA in <i>C. violaceum</i>	% Overall Prevalence	Weighted MW (g/mol)	
Unsaturated fatty acid	16:1	16	29	0.5	229.408	35.8	36.95	84.75529928	Palmitoleate
	18:1	18	33	0	249.462	15	15.48	38.61640867	omega-7-cis-octadecenoic acid
	12:0	12	23	0	167.316	5.6	5.78	9.669448916	dodecanoic acid
Saturated fatty acid	14:0	14	27	0	195.37	1.7	1.75	3.42754386	tetradecanoic acid or myristic acid
	16:0	16	31	0	223.424	23.9	24.66	55.1066419	hexadecanoic acid or palmitic acid
Cyclopropane fatty acid	17:0cyc	17	31	0	235.435	1.7	1.75	4.130438596	Cycloheptadecanoic acid
B-hydroxy FA (only LPS)	10:0-3OH	10	19	1	155.261	5.2	5.37	8.331859649	3-hydroxydecanoate
	12:0-2OH	12	23	1	183.315	3	3.10	5.675386997	2-hydroxydodecanoate
	12:0-3OH	12	23	1	183.315	5	5.16	9.458978328	3-hydroxydodecanoate
Sum						96.9	100	Average Fatty Acid MW	

Lipids	% Prevalence	Specific Lipids	% Prevalence	Overall % Prevalence	Number of C	Number of H	Number of O	Number of P	Number of N	Number of FA	MW (g/mol)	Relative Weight/mol	% by weight	mmol/g DW
Phospholipids	100	PE	76.6	76.60	1791	3001	432	50	50	2	34135.7	2614 7.9	73.42	<b>0.001427</b>
		PG	17.9	17.90	1841	3001	532	50	0	2	35635.8	6378. 8	17.91	<b>0.000334</b>
		CLPN (DPG)	4.6	4.60	3532	6547	882	100	0	4	67107.4	3086. 94	8.67	<b>8.57E-05</b>
		PA	0.9	0.90										
Total			100	Total							Sum 3561	Total 100		
	100			99.10								3.7	100	

### Fatty Acid Composition Part 2

Reference - Kämpfer P, Busse HJ, Scholz HC. Int J Syst Evol Microbiol 2009 and Young C-C, Aruna B, Lai W-A, Chen W-M, Chou J-H, Shen F-T, Rekha PD, Kämpfer P. Int J Syst Evol Microbiol 2008

Lipids	% Prevalence	Head Group	% Prevalence	MW (g/mol)	Number of Fatty Acids	Fatty Acid	% Prevalence	Overall % Prevalence	MW (g/mol)	Relative MW/mol	% by weight	mmol/g DW
Phospholipids	100	phosphatidylethanolamine (PE)	76.6	269.15	2	PE 12:0	6.69	5.12	603.78	30.94	4.11	<b>0.0045</b>
						PE 14:0	2.03	1.56	659.89	10.27	1.36	<b>0.0014</b>
						PE 16:0	28.55	21.87	716.00	156.61	20.79	<b>0.0193</b>
						PE 16:1	42.77	32.76	727.97	238.50	31.67	<b>0.0289</b>
						PE 18:1	17.92	13.73	768.07	105.44	14.00	<b>0.0121</b>
		PE 17:0cy	2.03	1.56	740.02	11.51	1.53	<b>0.0014</b>				
		phosphatidylglycerol (PG)	17.9	300.16	2	PG 12:0	6.69	1.20	634.79	7.60	1.01	<b>0.0011</b>
						PG 14:0	2.03	0.36	690.90	2.51	0.33	<b>0.0003</b>
						PG 16:0	28.55	5.11	747.01	38.18	5.07	<b>0.0045</b>
						PG 16:1	42.77	7.66	758.98	58.11	7.72	<b>0.0067</b>
PG 18:1	17.92					3.21	799.08	25.63	3.40	<b>0.0028</b>		



				PG							
				17:0cy	2.03	0.36	771.03	2.80	0.37	<b>0.0003</b>	
				c							
				CLPN	6.69	0.31	1177.4	3.62	0.48	<b>0.0003</b>	
				12:0			8				
				CLPN	2.03	0.09	1289.7	1.20	0.16	<b>0.0001</b>	
				14:0			0				
				CLPN	28.55	1.31	1401.9	18.41	2.44	<b>0.0012</b>	
				16:0			2				
cardiolip	4.6	508.22	4	CLPN	42.77	1.97	1425.8	28.05	3.72	<b>0.0017</b>	
in				16:1			5				
(CLPN)				CLPN	17.92	0.82	1506.0	12.42	1.65	<b>0.0007</b>	
				18:1			7				
				CLPN	2.03	0.09	1449.9	1.35	0.18	<b>0.0001</b>	
				17:0cy			6				
				c							
				small							
	99.1			% of	300.0						
				other	0					<b>Sum</b>	
				FAs							
						99.1		753.1			
								8			

### Appendix 5.2: Biomass equation of iDB858

	Mets	Type of Met		Coefficient
1	thr_L_c	AA	L-Threonine	0.16293
2	gly_c	AA	Glycine	0.31790
3	atp_c	NUC	ATP	59.81000
4	dctp_c	NUC	dCTP	0.07863
5	coa_c	VIT&CO	Coenzyme A	0.003097
6	arg_L_c	AA	L-Arginine	0.26227
7	h2o_c	Ions	H2O	59.81000
8	nad_c	VIT&CO	NAD	0.003097
9	dttp_c	NUC	dTTP	0.04423
10	met_L_c	AA	L-Methionine	0.09140
11	ala_L_c	AA	L-Alanine	0.47288
12	nadp_c	VIT&CO	NADP	0.003097
13	val_L_c	AA	L-Valine	0.25432
14	mg2_c	Ions	Magnesium	0.003097
15	mqn8_c	VIT&CO	Menaquinone 8	0.003097
16	gtp_c	NUC	GTP	0.17558
17	ribflv_c	VIT&CO	Riboflavin	0.003097
18	glu_L_c	AA	L-Glutamate	0.20266
19	dgtp_c	NUC	dGTP	0.07863
20	lys_L_c	AA	L-Lysine	0.13511
21	asp_L_c	AA	L-Aspartate	0.20664
22	ser_L_c	AA	L-Serine	0.21458
23	sheme_c	VIT&CO	Siroheme	0.003097
24	fe2_c	Ions	Fe2+	0.003097
25	ctp_c	NUC	CTP	0.17558
26	pro_L_c	AA	L-Proline	0.18677
27	k_c	Ions	Potassium	0.003097
28	zn2_c	Ions	Zinc	0.003097
29	udcpdp_c	PEPTIDO	Bactoprenyl diphosphate	0.00059
30	peptido_CV_c	PEPTIDO	Peptidoglycan polymer (n subunits)	0.00059
31	cys_L_c	AA	L-Cysteine	0.03974
32	so4_c	Ions	Sulfate	0.003097
33	q8_c	VIT&CO	Ubiquinone-8	0.003097
34	gln_L_c	AA	L-Glutamine	0.16690
35	datp_c	NUC	dATP	0.04423
36	gthrd_c	VIT&CO	GSH	0.003097
37	spmd_c	POLYNH2	Spermidine	0.00030
38	leu_L_c	AA	L-Leucine	0.43712
39	tyr_L_c	AA	L-Tyrosine	0.09537
40	thf_c	VIT&CO	5,6,7,8-Tetrahydrofolate	0.003097
41	his_L_c	AA	L-Histidine	0.08345
42	fad_c	VIT&CO	Flavin adenine dinucleotide oxidized	0.003097
43	amet_c	VIT&CO	S-Adenosyl-L-methionine	0.003097
44	5mthf_c	VIT&CO	5-Methyltetrahydrofolate	0.003097
45	utp_c	NUC	UTP	0.09876
46	10fthf_c	VIT&CO	10-Formyltetrahydrofolate	0.003097
47	cobalt2_c	Ions	Co2+	0.003097

48	asn_L_c	AA	L-Asparagine	0.10729
49	ptrc_c	POLYNH2	Putrescine	0.04410
50	trp_L_c	AA	L-Tryptophan	0.05563
51	pydx5p_c	VIT&CO	Pyridoxal 5-phosphate	0.003097
52	phe_L_c	AA	L-Phenylalanine	0.13114
53	adocbl_c	VIT&CO	Adenosylcobalamin	0.003097
54	thmpp_c	VIT&CO	Thiamine diphosphate	0.003097
55	ile_L_c	AA	L-Isoleucine	0.16690
56	pheme_c	VIT&CO	Protoheme	0.003097
57	2dmmq8_c	VIT&CO	2-Demethylmenaquinone 8	0.003097
58	fe3_c	Ions	Fe3+	0.003097
59	cl_c	Ions	Chloride	0.003097
60	mn2_c	Ions	Mn2+	0.003097
61	cu2_c	Ions	Cu2+	0.003097
62	ca2_c	Ions	Calcium	0.003097
63	colipa_c	LPS	core oligosaccharide lipid A	0.02321
64	pe120_c	PLIPID	Dodecanoylphosphatidylethanolamine	0.00452
65	pe140_c	PLIPID	Tetradecanoylphosphatidylethanolamine	0.00137
66	pe160_c	PLIPID	Phosphatidylethanolamine_dihexadecanoyl	0.01927
67	pe161_c	PLIPID	Phosphatidylethanolamine_dihexadec-9-enoyl	0.02886
68	pe181_c	PLIPID	Phosphatidylethanolamine_dioctadec-11-enoyl	0.01209
69	pe170cyc_c	PLIPID	pe170cyc	0.00137
70	pg120_c	PLIPID	Phosphatidylglycerol_didodecanoyl	0.00106
71	pg140_c	PLIPID	Phosphatidylglycerol_ditetradecanoyl	0.00032
72	pg160_c	PLIPID	Phosphatidylglycerol_dihexadecanoyl	0.00450
73	pg161_c	PLIPID	Phosphatidylglycerol_dihexadec-9-enoyl	0.00675
74	pg181_c	PLIPID	Phosphatidylglycerol_dioctadec-11-enoyl	0.00283
75	pg170cyc_c	PLIPID	pg170cyc	0.00032
76	clpn120_c	PLIPID	clpn120	0.00027
77	cpd15792_c	PLIPID	clpn140	0.00008
78	cpd15791_c	PLIPID	clpn160	0.00116
79	clpn161_c	PLIPID	clpn161	0.00173
80	clpn181_c	PLIPID	clpn181	0.00073
81	clpn170cyc_c	PLIPID	clpn170cyc	0.00008
1	ppi_c	Ions	Diphosphate	0.4846
2	h_c	Ions	H+	59.81000
3	adp_c	NUC	ADP	59.81000
4	pi_c	Ions	Phosphate	59.81000

**Appendix 5.3:** List of reactions added to iDB858 in order to form biomass

Reaction ID	Reaction name	GPR
rDB00002_c	Chorismate mutase/prephenate dehydratase	(CV_2355)
rDB00003_c	Acetylornithine aminotransferase	(CV_1496) or (CV_2256)
rDB00004_c	erythronate-4-phosphate dehydrogenase	(CV_3789)
rDB00005_c	(E)-4-hydroxy-3-methylbut-2-enyl-diphosphate synthase	(CV_3538)
rDB00006_c	Isoprenyl transferase	(CV_2691) or (CV_2200)
rDB00007_c	GAP filling rxn in Riboflavin metabolism	"
rDB00008_c	Acid phosphatase	(CV_3525) or (CV_4286)
rDB00009_c	Exopolyphosphatse	(CV_1262)
rDB00010_c	Non-canonical purine NTP pyrophosphatase	(CV_0926)
rDB00011_c	oxidoreductase protein	(CV_3210)
rDB00012_c	GMP synthase	(CV_3465) or (CV_3746)
rDB00013_c	Hydroxymethylpyrimidine kinase	(CV_0151)
rDB00014_c	Hydroxymethylpyrimidine kinase	(CV_0151)
rDB00015_c	Dihydrofolate reductase	(CV_1028)
rDB00016_c	formyltetrahydrofolate synthetase	(CV_1925)
rDB00017_c	phosphoribosylglycinamide formyltransferase	(CV_3616)
rDB00018_c	Aminomethyltransferase	(CV_3431)
rDB00019_c	5-methyltetrahydrofolate-homocysteine S-methyltransferase	(CV_3429) and (CV_0528 or CV_1074 or CV_2037) and (CV_3431)
rDB00020_c	glycoaldehyde dehydrogenase	"
rDB00021_c	glycolate dehydrogenase	(CV_1724)
rDB00022_c	glycerate dehydrogenase	(CV_3789 or CV_1724)
rDB00023_c	phosphoglycerate dehydrogenase	(CV_1724)
rDB00024_c	Pimeloyl-acp methyl ester esterase	"
rDB00025_c	Pimeloyl-acp methyl ester esterase	(CV_4380)
rDB00026_c	precorrin-3B synthase	"
rDB00027_c	precorrin-6A synthase	(CV_1565)
rDB00028_c	Cobalt-precorrin-7 (C5)-methyltransferase	(CV_1562)
rDB00029_c	threonine-phosphate decarboxylase	(CV_2728)
rDB00030_c	ATP: L-threonine O-phosphotransferase	(CV_1537)
rDB00031_c	Riboflavin kinase	(CV_3570)
rDB00032_c	quinolinate synthetase	(CV_3678)
rDB00033_c	nicotinamiae-nucleotide amidase	(CV_2370)
rDB00034_c	NADP pyrophosphate	(CV_2905)
rDB00035_c	ATP: NMN adenylyltransferase	(CV_0519)
rDB00036_c	2-oxoglutarate synthase	(CV_1071) and (CV_0528 or CV_1074 or CV_2037) and (CV_1072)
rDB00037_c	Lumped rxn for menaquinone formation	"
rDB00038_c	glutamate-cysteine ligase	(CV_4276)
rDB00039_c	Carboxynospermidine synthase	"

rDB00040_c	pyruvate decarboxylase	(CV_0586) or (CV_0587) or (CV_3889)
rDB00041_c	oleoyl-ACP hydrolase	"
rDB00042_c	Palmitoyl-CoA : electron-transfer flavoprotein 2, 3-oxidoreductase	(CV_1785) or (CV_2723) or (CV_3816)
rDB00043_c	Myristoyl-CoA : electron-transfer flavoprotein 2, 3-oxidoreductase	(CV_1785) or (CV_2723) or (CV_3816)
rDB00044_c	Lauroyl-CoA : electron-transfer flavoprotein 2, 3-oxidoreductase	(CV_1785) or (CV_2723) or (CV_3816)
rDB00045_c	Decanoyl-CoA : electron-transfer flavoprotein 2, 3-oxidoreductase	(CV_1785) or (CV_2723) or (CV_3816)
rDB00046_c	Octanoyl-CoA : electron-transfer flavoprotein 2, 3-oxidoreductase	(CV_1785) or (CV_2723) or (CV_3816)
rDB00047_c	Hexanoyl-CoA : electron-transfer flavoprotein 2, 3-oxidoreductase	(CV_1785) or (CV_2723) or (CV_3816)
rDB00048_c	N-acetyl-D-glucosamine 1-phosphate 1,6-phosphomutase	(CV_3795)
rDB00049_c	oleoyl-ACP hydrolase	"
rDB00050_c	lumped rxn for lysine biosynthesis	"
rDB00051_c	phophomethylpyrimidine synthase	(CV_0235)
rDB00052_c	Thiamine Kinase	"
rDB00053_c	GAP filling rxn in Peptidoglycan biosynthesis	(CV_0834) and (CV_2562) and (CV_3586) and (CV_4360) and (CV_4349) and (CV_1125 or CV_3094)
rDB00054_c	UDP-3-O-acyl-GlcNAc deactylase	(CV_4337)
rDB00055_c	UDP-3-O-acyl-glucosamine N-acyltransferase	(CV_2206)
rDB00056_c	UDP-2, 3-diacylglucosamine hydrolase	(CV_3186)
rDB00057_c	KDO transferase	(CV_0225)
rDB00058_c	KDO transferase	(CV_0225)
rDB00059_c	GAP filling rxn in lipopolysaccharide biosynthesis	"
rDB00060_c	D-glycero-alpha-D-manno-heptose 1, 7-bisphosphate 7-phosphatase	(CV_1657)
rDB00061_c	GAP filling rxn in lipopolysaccharide biosynthesis	"
rDB00062_c	GAP filling rxn in lipopolysaccharide biosynthesis	"
rDB00063_c	GAP filling rxn in lipopolysaccharide biosynthesis	"
rDB00064_c	GAP filling rxn in lipopolysaccharide biosynthesis	(CV_3880)
rDB00065_c	glycosyltransferase	(CV_0817)
rDB00066_c	GAP filling rxn in lipopolysaccharide biosynthesis	"
rDB00067_c	Hydrogenobyrate-acid-a, c-diamide : cobalt cobalt-ligase	(CV_1571)
rDB00068_c	Oxygen insensitive nadph nitro reductase/ FMN reductase	(CV_3500)
rDB00069_c	Sink needed for 4-Hydroxy-benzylalcohol to leave system	"
rDB00133_c	5,6-dimethylbenzimidazole synthase	CV_1555

**Appendix 5.4:** Selected reactions showing changes in FVA of WT in absence of antibiotic (WT) and presence of chloramphenicol (WT+chl) for *C. violaceum*

SUBSYSTEM	BIGGID	CHEMICAL FORMULA	WT	WT+chl	
Glycolysis or Gluconeogenesis	HEX1	atp_c + glc_D_c -> adp_c + g6p_c	1	7d	
	PYK	adp_c + pep_c -> atp_c + pyr_c	7d	1	
	AKGDH	coa_c + nad_c + akc_c -> co2_c + nadh_c + succoa_c	3	7d	
TCA Cycle	FRD7	succ_c + q8_c <=> fum_c + q8h2_c	2	7c	
	FUM	mal_L_c <=> fum_c + h2o_c	4	7b	
	MDH	nad_c + mal_L_c <=> h_c + nadh_c + oaa_c	2	7a	
	CS	accoa_c + h2o_c + oaa_c -> h_c + coa_c + cit_c	1	7d	
Oxidative phosphorylation	cytochrome oxidase bo3 ubiquinol-8 2.5 protons	2.5 h_c + 0.5 o2_c + q8h2_c -> h2o_c + 2.5 h_e + q8_c	2	1	0.08
	PFL	accoa_c + for_c <=> coa_c + pyr_c	8	5	0.1
Pyruvate metabolism	MALS	accoa_c + h2o_c + glx_c -> h_c + coa_c + mal_L_c	1	7d	
	ME2	nadp_c + mal_L_c -> co2_c + nadph_c + pyr_c	3	7d	
	PTAr	h_c + accoa_c + pi_c -> actp_c + coa_c	7d	1	
	ACKr	actp_c + adp_c -> h_c + atp_c + ac_c	7d	1	
	OAADC	h_c + oaa_c -> co2_c + pyr_c	3	7d	
Purine metabolism	ADK1	atp_c + amp_c -> 2 adp_c	2	1	0.0005
	ATP carbamate phosphotransferase	atp_c + co2_c + nh4_c <=> h_c + adp_c + cbp_c	1	7a	
Pyrimidine metabolism	NDPK8	atp_c + dadp_c -> adp_c + datp_c	3	7d	
	NDPK2	atp_c + udp_c -> adp_c + utp_c	2	7a	
Folate biosynthesis	MTHFD	nadp_c + mlthf_c <=> nadph_c + methf_c	1	7a	
	FTHFD	h2o_c + 10fthf_c -> h_c + for_c + thf_c	1	7a	
Glutamate metabolism	ASPTA	asp_L_c + akc_c <=> oaa_c + glu_L_c	4	7b	
Glycine, Serine and Threonine metabolism	PSERT	akc_c + pser_L_c <=> glu_L_c + 3php_c	4	4	0.0005
	GHMT	gly_c + h2o_c + mlthf_c <=> ser_L_c + thf_c	4	7b	
Arginine and proline metabolism	PRO1x	h_c + nadh_c + 1pyr5c_c -> nad_c + pro_L_c	3	7d	
	P5CR	h_c + nadph_c + 1pyr5c_c -> nadp_c + pro_L_c	3	7d	
Glyoxylate and dicarboxylate metabolism	ICL	icit_c <=> succ_c + glx_c	1	7c	
Nitrogen metabolism	Carbonic acid hydro-lyase	co2_c + h2o_c -> h_c + hco3_c	1	7a	
	ARGSL	argsuc_c -> fum_c + arg_L_c	1	7a	
Urea cycle and metabolism of amino groups	ARGSS_1	atp_c + asp_L_c + citr_L_c -> ppi_c + argsuc_c + amp_c	1	7a	
	AGGPR	nadph_c + acg5p_c -> pi_c + nadp_c + acg5sa_c	1	7a	
	OCBT	cbp_c + orn_c -> 2 h_c + pi_c + citr_L_c	1	7a	
	ORNTAC	glu_L_c + acorn_c <=> orn_c + acglu_c	1	7a	

	ACGK	$h\_c + atp\_c + acglu\_c \rightarrow adp\_c + acg5p\_c$	1	7a
	ACOTA	$glu\_L\_c + acg5sa\_c \rightarrow akg\_c + acorn\_c$	1	7a
	glycine:acceptor oxidoreductase	$gly\_c + 2\ nadph\_c \rightarrow co2\_c + 2\ nadp\_c + hcn\_c$	1	7a
Cyanoamino Metabolism	$\gamma$ -Amino- $\gamma$ -cyanobutanoate aminohydrolase/nitrilase	$2\ h2o\_c + acybut\_c \rightleftharpoons glu\_L\_c + nh4\_c$	1	7a
	cyn_rxn6	$hcn\_c \rightarrow acybut\_c$	1	7a
	G3PD	$glyc3p\_c + fad\_c \rightarrow dhap\_c + fadh2\_c$	3	7d
Glycerolipid and Glycerophospholipid metabolism	sn-Glycerol-3-phosphate NADP 2-oxidoreductase	$h\_c + nadph\_c + dhap\_c \rightarrow glyc3p\_c + nadp\_c$	3	7d
	sn-Glycerol-3-phosphate NAD 2-oxidoreductase	$h\_c + nadh\_c + dhap\_c \rightarrow nad\_c + glyc3p\_c$	3	7d
Transport via ABC	Orthophosphate-ABC transport	$atp\_c + h2o\_c + pi\_e \rightarrow h\_c + adp\_c + 2\ pi\_c$	1	7a
Extracellular Transport	Exchange	$for\_e \rightleftharpoons$	7d	1
	EX_ac_e	$ac\_e \rightleftharpoons$	7d	1

**Appendix 5.5:** Selected reactions showing changes in FVA of WT in absence of antibiotic (WT) and presence of streptomycin (WT+strep) for *C. violaceum*

SUBSYSTEM	BIGGID	CHEMICAL FORMULA	WT	WT+strep	
TCA Cycle	AKGDH	$coa\_c + nad\_c + akg\_c \rightarrow co2\_c + nadh\_c + succoa\_c$	3	3	20.73
	FUM	$mal\_L\_c \rightleftharpoons fum\_c + h2o\_c$	4	5	0.59
	MDH	$nad\_c + mal\_L\_c \rightleftharpoons h\_c + nadh\_c + oaa\_c$	2	2	0.36
Oxidative phosphorylation	cytochrome oxidase bo3 ubiquinol-8 2.5 protons	$2.5\ h\_c + 0.5\ o2\_c + q8h2\_c \rightarrow h2o\_c + 2.5\ h\_e + q8\_c$	2	1	0.32
Pyruvate metabolism	PFL	$accoa\_c + for\_c \rightleftharpoons coa\_c + pyr\_c$	8	8	0.27
	PPS	$atp\_c + h2o\_c + pyr\_c \rightarrow h\_c + pi\_c + pep\_c + amp\_c$	7d	1	
Purine metabolism	ATP carbamate phosphotransferase	$atp\_c + co2\_c + nh4\_c \rightleftharpoons h\_c + adp\_c + cbp\_c$	1	1	6.63
Folate biosynthesis	MTHFD	$nadp\_c + mlthf\_c \rightleftharpoons nadph\_c + methf\_c$	1	1	2.67
	FTHFD	$h2o\_c + 10fthf\_c \rightarrow h\_c + for\_c + thf\_c$	1	1	5
Glutamate metabolism	ASPTA	$asp\_L\_c + akg\_c \rightleftharpoons oaa\_c + glu\_L\_c$	4	5	1.75
Glycine, Serine and Threonine metabolism	PSERT	$akg\_c + pser\_L\_c \rightleftharpoons glu\_L\_c + 3php\_c$	4	5	0.31
	GHMT	$gly\_c + h2o\_c + mlthf\_c \rightleftharpoons ser\_L\_c + thf\_c$	4	5	2.39
Arginine and proline	PRO1x	$h\_c + nadh\_c + 1pyr5c\_c \rightarrow nad\_c +$	3	3	0.005

metabolism		pro_L_c			
	SOTA	akg_c + sucorn_c <=> sucgsa_c + glu_L_c	7d	1	
	SGSAD	h2o_c + nad_c + sucgsa_c -> 2 h_c + nadh_c + sucglu_c	7d	1	
	SGDS	h2o_c + sucglu_c <=> succ_c + glu_L_c	7d	1	
	AST	arg_L_c + succoa_c -> h_c + coa_c + sucarg_c	7d	1	
	N2-succinyl-L-arginine iminohydrolase decarboxylating	2 h_c + 2 h2o_c + sucarg_c -> co2_c + sucorn_c + 2 nh4_c	7d	1	
	ARGSL	argsuc_c -> fum_c + arg_L_c	1	1	16.65
	ARGSS_1	atp_c + asp_L_c + citr_L_c -> ppi_c + argsuc_c + amp_c	1	1	16.65
Urea cycle and metabolism of amino groups	AGGPR	nadph_c + acg5p_c -> pi_c + nadp_c + acg5sa_c	1	1	14.25
	OCBT	cbp_c + orn_c -> 2 h_c + pi_c + citr_L_c	1	1	16.65
	ORNTAC	glu_L_c + acorn_c <=> orn_c + acglu_c	1	1	14.26
	ACGK	h_c + atp_c + acglu_c -> adp_c + acg5p_c	1	1	14.25
	ACOTA	glu_L_c + acg5sa_c -> akg_c + acorn_c	1	1	14.25
Cyanoamino Metabolism	glycine:acceptor oxidoreductase	gly_c + 2 nadph_c -> co2_c + 2 nadp_c + hcn_c	1	1	4
	cyn_rxn6	hcn_c -> acybut_c	1	1	4
Extracellular Transport	NH4+ Exchange	nh4_e <=>	4	1	

**Appendix 5.6:** Selected reactions from Flux variability analysis for WT, ChlR and StrpR at experimental constraints

Subsystem	Reaction ID	Reaction Formula	ChlR		StrpR		
			WT	Fold change	Fold change		
Glycolysis or Gluconeogenesis	HEX1	atp_c + glc_D_c -> adp_c + g6p_c	1	7d			
	PYK	adp_c + pep_c -> atp_c + pyr_c	7d	1			
	AKGDH	coa_c + nad_c + akg_c -> co2_c + nadh_c + succoa_c	3	7d	3	2.56	
	SUCOAS	atp_c + coa_c + succ_c -> adp_c + pi_c + succoa_c	7d	1	7d		
TCA Cycle	FRD7	succ_c + q8_c <=> fum_c + q8h2_c	2	8	2	0.12	
	MDH	nad_c + mal_L_c <=> h_c + nadh_c + oaa_c	2	1	0.04	1	0.28
	CS	accoa_c + h2o_c + oaa_c -> h_c + coa_c + cit_c	1	7d		1	0.1
	ICDHyrb	nadp_c + icit_c <=> h_c + mDB_oxasucc_c + nadph_c	7d	1		7d	
	ICDHyra	h_c + mDB_oxasucc_c -> co2_c + akg_c	7d	1		7d	



Oxidative phosphorylation	cytochrome oxidase bo3	$2.5 h_c + 0.5 o2_c + q8h2_c \rightarrow h2o_c + 2.5 h_e + q8_c$	2	1	0.46	1	0.91
	ubiquinol-8 cytochrome oxidase bd	$2 h_c + mql8_c + 0.5 o2_c \rightarrow h2o_c + mqn8_c + 2 h_e$	3	7d		7d	
	PTAr	$h_c + accoa_c + pi_c \rightarrow actp_c + coa_c$	7d	1		1	
	ACKr	$actp_c + adp_c \rightarrow h_c + atp_c + ac_c$	7d	1		1	
	ACALD	$acald_c + coa_c + nad_c \rightleftharpoons h_c + accoa_c + nadh_c$	7a	2		1	
Pyruvate metabolism	PFL	$accoa_c + for_c \rightleftharpoons coa_c + pyr_c$	8	5	0.27	8	1.37
	MALS	$accoa_c + h2o_c + glx_c \rightarrow h_c + coa_c + mal_L_c$	1	7d		1	0.1
	ME2	$nadp_c + mal_L_c \rightarrow co2_c + nadph_c + pyr_c$	3	7d		7d	
	PPC	$co2_c + h2o_c + pep_c \rightarrow 2 h_c + pi_c + oaa_c$	7d	1		1	
	OAADC	$h_c + oaa_c \rightarrow co2_c + pyr_c$	3	7d		7d	
Pyruvate Alanine Serine Interconversions	D-Amino acid dehydrogenase	$h2o_c + fad_c + ala_D_c \rightleftharpoons pyr_c + nh4_c + fadh2_c$	7b	7b		4	
Glyoxylate and dicarboxylate metabolism	ICL	$icit_c \rightleftharpoons succ_c + glx_c$	1	4		1	0.1
Glutathione metabolism	AMPTASE CG	$h2o_c + cgly_c \rightleftharpoons gly_c + cys_L_c$	7b	5		4	
	glutathione hydralase	$h2o_c + gthrd_c \rightleftharpoons glu_L_c + cgly_c$	7b	5		4	
Purine metabolism	ADK2	$h_c + amp_c + pppi_c \rightarrow ppi_c + adp_c$	7a	2		1	
Pyrimidine metabolism	CYTK1	$atp_c + cmp_c \rightarrow adp_c + cdp_c$	1	2	1.3	2	2.56
Porphyrin and chlorophyll metabolism	FeII oxygen oxidoreductase	$4 h_c + o2_c + 4 fe2_c \rightleftharpoons 2 h2o_c + 4 fe3_c$	7a	7b		4	
Reductive carboxylate cycle (CO2 fixation)	ACS	$h_c + atp_c + ac_c + coa_c \rightarrow ppi_c + accoa_c + amp_c$	1	7d		7d	
Extracellular Transport	EX_ac_e	$ac_e \rightleftharpoons$	7d	1		1	
	EX_for_e	$for_e \rightleftharpoons$	7d	1		7d	

## Appendix 6.1: KAP study questionnaire distributed to the respondents

### Knowledge माहिती

1. The red line as shown on the medicine package picture, indicates that  
औषध पॅकेज वर लाल line काय दर्शवते ?
- |   |   |
|---|---|
| a. Anticancer drugs<br>कर्करोग औषधे                 | e. Drugs only for adult use<br>प्रौढ वापरासाठी औषधे       |
| b. Anti-inflammatory drugs<br>दाह औषधे              | f. Drugs having side effects<br>साइड इफेक्ट्स देणारे औषधे |
| c. One time use drugs<br>एक वेळ वापर औषधे           | g. No Purpose<br>काही अर्थ नाही                           |
| d. Prescription drugs<br>डॉक्टरांनी सांगितलेली औषधे | h. Do not know<br>नाही माहिती                             |

True  
False  
सत्य  
असत्य

- |  |                          |                          |
|--|--------------------------|--------------------------|
| 2. If taken too often, antibiotics are less likely to work in the future.<br>खूप वेळा घेतले तर, antibiotics भविष्यात काम करण्याची शक्यता कमी आहे | <input type="checkbox"/> | <input type="checkbox"/> |
| 3. Antibiotics can cure bacterial infection.<br>Antibiotics जिवाणू infection बरा करू शकतात.  | <input type="checkbox"/> | <input type="checkbox"/> |
| 4. Antibiotics can cure viral infections.<br>Antibiotics व्हायरल इन्फेक्शन्स बरा करू शकतात.  | <input type="checkbox"/> | <input type="checkbox"/> |
| 5. Bacteria are germs that cause cold and flu.<br>Bacteria मुळे सर्दी आणि खोकला होतो.  | <input type="checkbox"/> | <input type="checkbox"/> |
| 6. Penicillin and Azithromycin are antibiotics.  | <input type="checkbox"/> | <input type="checkbox"/> |
| 7. Aspirin (Disprin) is an antibiotic.   | <input type="checkbox"/> | <input type="checkbox"/> |
| 8. Paracetamol is an antibiotic.   | <input type="checkbox"/> | <input type="checkbox"/> |
| 9. Antibiotics are indicated to reduce any kind of pain and inflammation.<br>Antibiotics कोणत्याही प्रकारचे वेदना आणि दाह कमी करतात.             | <input type="checkbox"/> | <input type="checkbox"/> |
| 10. Antibiotics can kill "good bacteria" present in our body.<br>Antibiotics "good bacteria" आपल्या शरीरातील चांगले जीवाणू नष्ट करू शकतात.       | <input type="checkbox"/> | <input type="checkbox"/> |

(Rate between 1 to 5, Strongly agree, somewhat agree, undecided, disagree and strongly disagree)

(1 ते 5 दरम्यान दर, ठामपणे, सहमत निर्णय घेतलेला नाही, थोडी सहमत, न जुळणे आणि जोरदार असहमत)

11. Antibiotic resistance is an important and serious public health issue faced by the world

Antibiotic resistance या जगासाठी एक महत्वाची सार्वजनिक आरोग्य समस्या आहे

--	--	--	--	--	--

12. Antibiotic resistance is an important and serious public health issue in our country

Antibiotic resistance आपल्या देशात एक महत्वाची सार्वजनिक आरोग्य समस्या आहे

--	--	--	--	--	--

13. Antibiotic resistance is an important and serious public health issue faced in Maharashtra

Antibiotic resistance महाराष्ट्रात एक महत्त्वपूर्ण आणि गंभीर सार्वजनिक समस्या आहे

14. Indiscriminate and injudicious use of antibiotics can lead to

False

True

अति आणि अवैचारिक Antibiotics वापराचे काय होऊ शकते  
असत्य

सत्य

a. Ineffective treatment

कुचकामी उपचार

b. Increased antibiotic efficacy

वाढलेली Antibiotic गुण

c. Emergence of bacterial resistance

Bacterial resistance उदय

d. Additional burden of medical cost to the patient

रुग्णाला अतिरिक्त वैद्यकीय खर्च भार

### Attitude दृष्टिकोन

(Rate between 1 to 5, Strongly agree, somewhat agree, undecided, disagree and strongly disagree)

(1 ते 5 दरम्यान दर, ठामपणे, सहमत निर्णय घेतलेला नाही, थोडी सहमत, न जुळणे आणि जोरदार असहमत)

1. When I have a cold, I should take antibiotics to prevent getting a more serious illness.

मला सर्दी आहे, तेव्हा मी एक अधिक गंभीर आजार टाळण्यासाठी Antibiotics घ्यावे.

2. When I get fever, antibiotics help me to get better more quickly.

मला ताप असेल तेव्हा antibiotics मला लवकर बर चांगले होण्यासाठी मदत करतात.

3. Whenever I take an antibiotic, I contribute to the development of antibiotic resistance.

जेव्हा पण antibiotic घेतो तेव्हा antibiotic resistance वाढतो .

4. Skipping one or two doses does not contribute to the development of antibiotic resistance.

एक किंवा दोन डोस नाही घेतल्याने काही फरक पडत नाही.

5. Antibiotics are safe drugs, hence they can be commonly used.

Antibiotics सुरक्षित औषधे आहेत, म्हणून ते सामान्यतः वापरू शकता.

### Practice सराव

(Rate between 1 to 5, Strongly agree, somewhat agree, undecided, disagree and strongly disagree)

(1 ते 5 दरम्यान दर, ठामपणे, सहमत निर्णय घेतलेला नाही, थोडी सहमत, न जुळणे आणि जोरदार असहमत)

1. The doctor prescribes a course of antibiotics. After taking 2 – 3 doses I start feeling better.

डॉक्टरांनी antibiotic कोर्स दिली आहे. 2 - 3 डोस नी मला बरं वाटायला लागय.

a. I stop taking the further treatment?

मी आणखी उपचार थांबवतो.

b. I save the remaining antibiotics for the next time I get sick.

उर्वरित antibiotics पुढील आजारा साठी सुरक्षित ठेवतो.

c. I discard the remaining leftover medication.

मी उर्वरित औषधे फेकून देतो.

d. I give the leftover antibiotics to my friend/roommate if they get sick.

मी उर्वरित औषधे आपल्या मित्रांना त्यांचा आजारा साठी देतो.

e. I complete the full course of treatment.

मी उपचाराचा पूर्ण कोर्स करतो.

2. I take antibiotics only when prescribed by the doctor.

जेव्हा डॉक्टर लिहून देतात, तेव्हाच मी antibiotics घेतो.

3. I check the expiry date of the antibiotic before use.  
वापरण्या पूर्वी मी expiry date तपासतो.
4. I buy antibiotics without a medical receipt.  
मी डॉक्टरांच्या पावती शिवाय antibiotics खरेदी करतो.
5. I have, at times started an antibiotic therapy after a simple doctor call, without a proper medical examination.  
योग्य तपासणी न करता, फक्त फोन वर डॉक्टर शी बोलल्यावर antibiotic therapy सुरू केली.
6. Have you used antibiotics in the last year?  Yes  No  
मी गेल्या वर्षी प्रतिजैविक वापर केला आहे.  होय  नाही
7. If yes, how many times?  
होय, किती वेळा?
- 1-2  
 3-5  
 > 5

1. Name \_\_\_\_\_

नाव

2. Age

वय

3. Sex

लिंग

4. Marital Status

वैवाहिक स्थिती

5. Employment

रोजगार

6. Educational Qualification

शैक्षणिक पात्रता

7. Annual Income (Rs.)

वार्षिक उत्पन्न (रुपये)

Less than 20,000

20,000 कमी जास्त

More than 20,000 to 1,00,000

20,000 पेक्षा जास्त, 1,00,000 हून कमी

More than 1,00,000 to 5,00,000

1,00,000 पेक्षा जास्त, 5,00,000 हून कमी

More than 5,00,000 to 10,00,000

5,00,000 पेक्षा जास्त, 10,00,000 हून कमी

More than 10,00,000

10,00,000 पेक्षा अधिक

8. Place (City)

स्थान (शहर)

9. At least one family member (parents, children, husband or wife) works in a

No

health related field

किमान एक कुटुंब सदस्य (आई, वडील, मुले, पती किंवा पत्नी) एक आरोग्य क्षेत्रात कार्य करते

नाही

Yes

होय

10. Signature

स्वाक्षरी

# DEEPANWITA BANERJEE

dipsiii@gmail.com

Chemical Engineering Division, CSIR – NCL, Pune - 411008, Maharashtra, India

## Education

---

Ph. D., DST – INSPIRE Fellow, CSIR - National Chemical Laboratory, Pune, Maharashtra, India  
Expected May 2018

M.Tech. Biotechnology, NIT, Rourkela, Orissa, India, 2009, 9.09 CGPA

B. Tech. Biotechnology, MDU, Rohtak, Haryana, India, 2007, 75.6%

GATE 2007

## Skills

---

- ◆ Constraint Based modeling and Flux Balance Analysis (FBA)
- ◆ Whole genome scale reconstruction of bacteria, its curation and analysis
- ◆ NGS (Ion Torrent) data analysis and primer designing for PCR and sequencing
- ◆ Knocking out genes in *E. coli*, Cloning and Genotyping
- ◆ Animal cell culture, MTT Assay, BIOLOG phenotypic microarray
- ◆ Basic Biochemical, Microbiological, Molecular Biology and Bioinformatics Techniques

## Past Research Experience

---

- ◆ BCIL Trainee in Molecular Diagnostics, AUROPROBE Laboratories 2009 – 2010  
Sponsored by BIP, DBT, Government of India
- ◆ Project Staff – School of Medical Science and Technology, IIT Kharagpur 2009

## Teaching and Mentoring Experience

---

- ◆ Lovely Professional University, Punjab, India 2010 – 2011  
Assistant Professor – Department of Biotechnology

## Conference Presentations

---

**Banerjee, D.** et. al. Integrating metabolomic data as constraints in flux balance models to understand antibiotic resistance. Poster presentation delivered at 11th Annual International Conference, Metabolomics, CA, USA, June – July 2015.

**Banerjee, D.** et al. Metabolic Inquiry and Cellular Engineering: A Systems Approach. Poster presentation delivered at NNMCB National Meeting on Mathematical and Computational Biology at CSIR-NCL and IISER Pune, India, December 2015.

Raghunathan, A. and **Banerjee, D.** Towards A Genetic Basis for Antibiotic Resistance in *Chromobacterium violaceum*. Oral presentation delivered at AIChE Annual Meeting, CA, USA, November 2013.

## Publications

---

**Banerjee, D.**, Parmar, D., Bhattacharya, N., Ghanate, A.D., Panchagnula, V., Raghunathan, A., 2017. A scalable metabolite supplementation strategy against antibiotic resistant pathogen *Chromobacterium violaceum* induced by NAD<sup>+</sup>/NADH<sup>+</sup> imbalance. BMC Syst. Biol. 11, 51. doi:10.1186/s12918-017-0427-z

**Banerjee, D.** and Raghunathan, A. Knowledge, Attitude and Practice of Antibiotic Use and Antimicrobial Resistance: A Study Post the “Red Line” Initiative, Curr. Sci. 114(9), 10 May 2018. doi: 10.18520/cs/v114/i09/1866-1877

Immanuel, S.R.C., **Banerjee, D.**, Rajankar, M.P., Deshmukh P. and Raghunathan, A. Synthetic Metabolic Engineering Of Violacein Biosynthesis In *Escherichia Coli*: Accessing Yield Space Through Gene And Environmental Design. *In Review*

- Banerjee, D.** and Raghunathan, A. Genome Scale Metabolic Model Of *Chromobacterium violaceum*, *In Preparation*
- Immanuel, S.R.C., Sadhukhan, P.P., **Banerjee, D.**, Mohole, M.S., Parmar, D. Ghanate, A.D., Panchagnula, V. and Raghunathan., A. Constraints-based Flux Balance Model Predicts System-wide Differential Phenotypes In Drug Resistant And Sensitive Glioblastoma Cancer Cells, *In preparation*